



**HAL**  
open science

# Greffage par polymérisation radicalaire par transfert d'atome d'une écorce hydrophile à la surface de particules de latex fonctionnalisées

Virginie Chabrol

► **To cite this version:**

Virginie Chabrol. Greffage par polymérisation radicalaire par transfert d'atome d'une écorce hydrophile à la surface de particules de latex fonctionnalisées. Other. Université Claude Bernard - Lyon I, 2012. English. NNT : 2012LYO10157 . tel-01012004

**HAL Id: tel-01012004**

**<https://theses.hal.science/tel-01012004>**

Submitted on 25 Jun 2014

**HAL** is a multi-disciplinary open access archive for the deposit and dissemination of scientific research documents, whether they are published or not. The documents may come from teaching and research institutions in France or abroad, or from public or private research centers.

L'archive ouverte pluridisciplinaire **HAL**, est destinée au dépôt et à la diffusion de documents scientifiques de niveau recherche, publiés ou non, émanant des établissements d'enseignement et de recherche français ou étrangers, des laboratoires publics ou privés.



N° d'ordre 157-2012



Année 2012

THESE DE L'UNIVERSITE DE LYON  
Délivrée par  
L'UNIVERSITE CLAUDE BERNARD LYON 1

ECOLE DOCTORALE MATERIAUX

DIPLOME DE DOCTORAT  
(arrêté du 7 août 2006)

soutenue publiquement le 5 Octobre 2012

par

**Virginie CHABROL**

**Functionalized latex particles as substrates  
for metal-mediated radical polymerization**

Directeur de thèse : Pr. Bernadette CHARLEUX

JURY :	Pr. Didier LEONARD	Université Claude Bernard Lyon I	Président de jury
	Pr. Bernadette CHARLEUX	Université Claude Bernard Lyon I	Directrice de thèse
	Dr. Sagrario PASCUAL	Université du Maine	Rapporteur
	Dr. Maud SAVE	Université de Pau et des Pays de l'Adour	Rapporteur
	Dr. Julien NICOLAS	Université Paris-Sud 11	Examineur
	Dr. Franck D'AGOSTO	Université Claude Bernard Lyon I	Co-encadrant
	Dr. Bernd RECK	BASF	Co-encadrant









N° d'ordre 157-2012



Année 2012

THESE DE L'UNIVERSITE DE LYON  
Délivrée par  
L'UNIVERSITE CLAUDE BERNARD LYON 1

ECOLE DOCTORALE MATERIAUX

DIPLOME DE DOCTORAT  
(arrêté du 7 août 2006)

soutenue publiquement le 5 Octobre 2012

par

**Virginie CHABROL**

**Functionalized latex particles as substrates  
for metal-mediated radical polymerization**

Directeur de thèse : Pr. Bernadette CHARLEUX

JURY :	Pr. Didier LEONARD	Université Claude Bernard Lyon I	Président de jury
	Pr. Bernadette CHARLEUX	Université Claude Bernard Lyon I	Directrice de thèse
	Dr. Sagrario PASCUAL	Université du Maine	Rapporteur
	Dr. Maud SAVE	Université de Pau et des Pays de l'Adour	Rapporteur
	Dr. Julien NICOLAS	Université Paris-Sud 11	Examineur
	Dr. Franck D'AGOSTO	Université Claude Bernard Lyon I	Co-encadrant
	Dr. Bernd RECK	BASF	Co-encadrant

# UNIVERSITE CLAUDE BERNARD - LYON 1

## Président de l'Université

Vice-président du Conseil d'Administration

Vice-président du Conseil des Etudes et de la Vie Universitaire

Vice-président du Conseil Scientifique

Secrétaire Général

**M. François-Noël GILLY**

M. le Professeur Hamda BEN HADID

M. le Professeur Philippe LALLE

M. le Professeur Germain GILLET

M. Alain HELLEU

## ***COMPOSANTES SANTE***

Faculté de Médecine Lyon Est – Claude Bernard

Directeur : M. le Professeur J. ETIENNE

Faculté de Médecine et de Maïeutique Lyon Sud – Charles Mérieux

Administrateur provisoire : M. le Professeur G. KIRKORIAN

UFR d'Odontologie

Directeur : M. le Professeur D. BOURGEOIS

Institut des Sciences Pharmaceutiques et Biologiques

Directeur : Mme la Professeure C. VINCIGUERRA.

Institut des Sciences et Techniques de la Réadaptation

Directeur : M. le Professeur Y. MATILLON

Département de formation et Centre de Recherche en Biologie Humaine

Directeur : M. le Professeur P. FARGE

## ***COMPOSANTES ET DEPARTEMENTS DE SCIENCES ET TECHNOLOGIE***

Faculté des Sciences et Technologies

Directeur : M. le Professeur F. De MARCHI

Département Biologie

Directeur : M. le Professeur F. FLEURY

Département Chimie Biochimie

Directeur : Mme le Professeur H. PARROT

Département GEP

Directeur : M. N. SIAUVE

Département Informatique

Directeur : M. le Professeur S. AKKOUCHE

Département Mathématiques

Directeur : M. le Professeur A. GOLDMAN

Département Mécanique

Directeur : M. le Professeur H. BEN HADID

Département Physique

Directeur : Mme S. FLECK

Département Sciences de la Terre

Directeur : Mme la Professeure I. DANIEL

UFR Sciences et Techniques des Activités Physiques et Sportives

Directeur : M. C. COLLIGNON

Observatoire de Lyon

Directeur : M. B. GUIDERDONI

Polytech Lyon

Directeur : M. P. FOURNIER

Ecole Supérieure de Chimie Physique Electronique

Directeur : M. G. PIGNAULT

Institut Universitaire de Technologie de Lyon 1

Directeur : M. C. VITON

Institut Universitaire de Formation des Maîtres

Directeur : M. R. BERNARD

Institut de Science Financière et d'Assurances

Directeur : Mme la Professeure V. MAUME-DESCHAMPS







## Remerciements

Les remerciements constituent sans doute la partie la plus lue d'une thèse et peut-être la plus intéressante. C'est pourquoi, je vais dans ces prochaines lignes me livrer à cet exercice de style et remercier toutes les personnes qui ont collaboré à cette thèse car la thèse n'est pas le fruit du dur labeur (ça si) d'une seule et unique personne (ça non).

Mes premiers remerciements s'adressent à Bernadette CHARLEUX, directrice du laboratoire C2P2, membre de l'IFU, IMUST, vice-présidente de l'école doctorale de chimie, mais aussi, titre un peu moins prestigieux, ma directrice de thèse. Bernadette, 7 années se sont écoulées entre le premier cours de polymères et la fin de cette thèse. Et pendant 7 ans, toujours de bons conseils, une grande disponibilité et de bonne humeur. Merci également de m'avoir accordé ta confiance ainsi que la grande liberté que tu m'as laissée pour réaliser ce travail. Bizarre de poursuivre l'aventure des polymères sans toi, mais je suis très fière de compter parmi tes anciens élèves.

Merci également à Franck D'AGOSTO pour avoir co-encadré cette thèse. Pas toujours évident de supporter mon sale caractère et mon obstination ! Je te suis reconnaissante, d'avoir non seulement fait avec, mais aussi et surtout d'avoir réussi à m'inculquer un peu de ta rigueur.

Ich wollte mich auch bei der Firma BASF bekanken, die dieses Projekt finanziert hat. Besonders möchte ich Bernd RECK und Matthias ZORN bekanken für ihre Geduld und für ihre wertvollen Ratschlägen danken, Sie haben mir geholfen, diese Doktorarbeit durchzuziehen. Je souhaite aussi remercier Caroline PETIGNY de BASF France pour toute l'aide administrative ainsi que pour le grand intérêt porté à ce projet.

Je tiens aussi à remercier Alexandre TERRENOIRE, initiateur de ce projet. Merci de m'avoir encouragée et écoutée depuis mon master 1 à BASF. Aurais-tu deviné que la petite stagiaire française deviendrait Dr. ?

Je voudrais remercier Sagrario PASCUAL et Maud SAVE d'avoir accepté de relire cette thèse et d'en avoir été les rapporteurs. Je remercie aussi à Julien NICOLAS pour avoir également accepté de juger ce travail. Leur lecture attentive et leurs avis sur ce projet ont suscité un échange scientifique que j'ai particulièrement apprécié.

Je tiens à exprimer mes plus vifs remerciements à Didier LEONARD pour avoir présidé mon jury et pour avoir tout simplement sauvé cette thèse. Je te dois beaucoup pour l'ensemble des résultats

obtenus par ToF-SIMS. Et il y en avait tant ! Grâce à ta bonne humeur et ta patience, j'ai pris un très grand plaisir à apprendre et à collaborer avec toi.

Hertzlichen Dank an Antje POLENTZ und Christina LAUE, die einen wichtigen Beitrag zum Gelingen meiner Doktorarbeit geleistet haben. Ja, Antje, ich bin endlich vertig nach 10 Jahren Studium ! Ich möchte auch dem BASF Laboranten-team (Arnold, Bianca, Felix, Michael, Myriam, Stephanie..) bedanken. Es hat mir Spaß gemacht mit Euch zu arbeiten aber es hat mir noch mehr Spaß gemacht mit Euch in die Rheingalerie oder zum Inder zu gehen !

Je remercie aussi tout le staff technique du C2P2. Merci à Olivier BOYRON pour les analyses GPC (la « boucheuse de colonne » s'en va enfin). Merci à Pierre-Yves DUGAS pour la cryo-TEM, pour le support informatique (oui, je ne suis vraiment pas douée pour ça). Je ne risque pas d'oublier ton rire... particulier... Merci aussi à Jean-Pierre BROYER, mon dealer de biblio, pour ton aide, tes cours de bricolage. Merci à Christine LUCAS de m'avoir tenu compagnie lors de mes séances (longues et nombreuses) de RMN. Et très grand merci à Nath, aussi bien pour m'avoir simplifié la paperasserie administrative, mais aussi pour nos « matins papote » et nos séances shopping (allez, la prochaine aura lieu à Londres).

Je remercie toutes les personnes rencontrées lors de nombreuses collaborations développées au cours de ces 3 ans. Merci à Beatrice BURDIN et Xavier JAURAND du CTμ pour leur support technique en microscopie. Merci à l'équipe de LASIM, plus particulièrement à Rodolphe ANTOINE et Tristan DOUSSINEAU pour les analyses d'électrospray. Je voudrais aussi remercier Nicole JAFFREZIC pour les analyses d'électrochimie.

Je souhaiterais aussi remercier François STOFFELBACH. Bien que tu n'aies pas collaboré directement à cette thèse, tu as cependant contribué à ce travail lorsque celui-ci n'en était qu'au stade de stage de master, en me formant et en débroussaillant le sujet, soit les parties les moins drôles. J'en profite pour remercier les autres « Parisiens » Chloé, Thanh, Stéphanie, Jutta, Marion C, Hugo et plus particulièrement Ben (Grand). C'est appréciable d'avoir du soutien moral... et je ne parle pas que du demi à la terrasse place Polytechnique... Merci aussi à l'ancienne Parisienne Lisa. J'ai particulièrement apprécié tes conseils avisés d'ancienne thésarde. Et puis c'était agréable de retrouver une compatriote à Ludwigshafen. Merci à Marion T d'avoir eu le courage de cohabiter avec une thésarde en pleine fin de rédaction. Ton dynamisme et ta bonne humeur m'ont beaucoup aidée à tenir le coup. Merci aussi à Francis et Lin pour m'avoir particulièrement aidée lorsque j'ai débarqué sur Lyon et merci pour la découverte des restos asiatiques de Lyon. Je n'oublie pas non plus Ségolène, l'ancienne Parisienne, puis Lyonnaise et Philadelphienne mais toujours disponible pour un

tchat pour m'écouter me lamenter. Généralement, mon moral remontait en flèche après avoir écouté tes péripéties... Comme quoi, il y a toujours plus « poisseux » que soit !

Je tenais aussi à remercier Roger SPITZ pour son aide concernant les complexes métalliques. Merci également à Sir Vincent MONTEIL aussi pour son aide et pour l'intérêt porté à l'étude des métaux. J'ai particulièrement aimé nos nombreuses discussions scientifiques ou autres, parce que je ne suis pas curieuse, mais j'aime tout savoir. Merci aussi à Elodie pour m'avoir accueillie au LCPP ainsi que pour les nombreux conseils apportés sur les colloïdes.

Petite dédicace à mes collègues du LCPP à qui je souhaite un bon courage pour la suite à savoir ; Amélie (Lyon or St Etienne, telle est la question. Fais le détour par Londres à l'occasion), Ana, ex-colloc (boa sorte !), Aurélie (oui, j'y pense à arrêter de fumer), Benoît (en effet, pas crédible quand tu es sérieux), Cath (j'ai FORT apprécié de te connaître aussi and we will keep in touch), Delphine (je te souhaite aussi plein de bonnes choses pour la suite), Edgard, le Croix-Roussien mexicain (merci pour m'avoir fait découvrir la vraie cuisine mexicaine. Prends soin des meubles !), Guilhem (viel Spaß), Julien (bon courage, collègue synthomer), Nico (on l'a finie notre TDM), Seb (fini les bouffées d'air frais), le club asiatique (Xuewei, Wenjing, Quiao, Linn)

And at last but not the least... Je remercie ma famille qui a vécu et surtout subi cette thèse. Merci pour leur soutien, leurs encouragements. Je leur suis redevable de tous les efforts qu'ils ont fournis et à ce titre, je leur dédie ce travail.



*Les questions ne sont pas obligées d'avoir du sens [...]. Mais les réponses, si.*

Terry Pratchett *Procrastination*



## Résumé

### **Introduction et état de l'art**

La polymérisation en émulsion consiste à polymériser par voie radicalaire un ou plusieurs monomères hydrophobes dans un milieu dispersé à phase continue aqueuse en présence de tensio-actifs. Elle permet la formation de latex, soit une suspension aqueuse stable de particules de (co)polymère idéalement sphériques de taille nanométrique. Depuis environ 60 ans, cette technique de polymérisation est largement exploitée dans l'industrie pour des raisons économiques, techniques (vitesse de polymérisation élevée, hautes conversions et masses molaires obtenues, faibles viscosités et toxicités, mise en œuvre simple...), mais aussi en raison des conditions de polymérisation et d'utilisation en phase avec les principes de la chimie verte.

Malgré ces nombreux avantages, la polymérisation radicalaire en émulsion souffre des limitations intrinsèques à la polymérisation radicalaire, soit un contrôle limité de la structure des polymères à l'échelle moléculaire.

Les dernières années ont cependant connu un renouvellement considérable des concepts de la polymérisation en émulsion à travers le développement des techniques de polymérisation radicalaire contrôlée (PRC). En contrôlant efficacement la structure et les architectures macromoléculaires, ces méthodes sont capables de donner naissance à de nouvelles morphologies de particules inaccessibles jusqu'alors.

Parmi les différentes morphologies accessibles par polymérisation en émulsion, les particules « cœur-écorce », possédant un cœur hydrophobe et une couronne hydrophile, ont connu un intérêt grandissant de par leurs propriétés de surface, élargissant ainsi leurs domaines d'utilisation (liants, revêtements, reconnaissance biologique, etc...).

En introduisant judicieusement à la surface des particules des fonctions chimiques capables de jouer le rôle d'amorceurs ou d'agents de contrôle et grâce aux méthodes de PRC, il est alors possible de greffer des chaînes de polymère par la méthode de greffage «à partir de» (*Figure 1*).



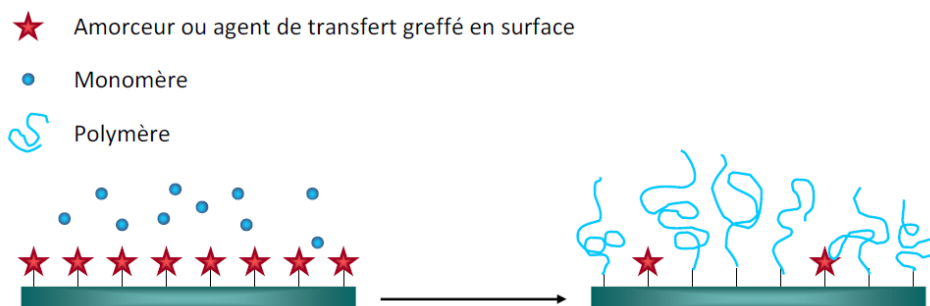


Figure 1. Principe du greffage « à partir de ».

Généralement, la méthode SI-ATRP (Surface-Initiated Atom Transfer Radical Polymerization) est la polymérisation radicalaire contrôlée la plus employée pour le greffage «à partir de». Cette technique assure le contrôle de la polymérisation par l'emploi d'un complexe de métal de transition de bas degré d'oxydation en combinaison avec un halogénure d'alkyle. Ce complexe, capable de subir une oxydation à un électron par abstraction de l'halogène de l'halogénure d'alkyle, permet un équilibre entre une espèce active (radical propageant) du polymère et une forme inactive du polymère (forme dormante) par un processus d'oxydation-réduction réversible (Figure 2).

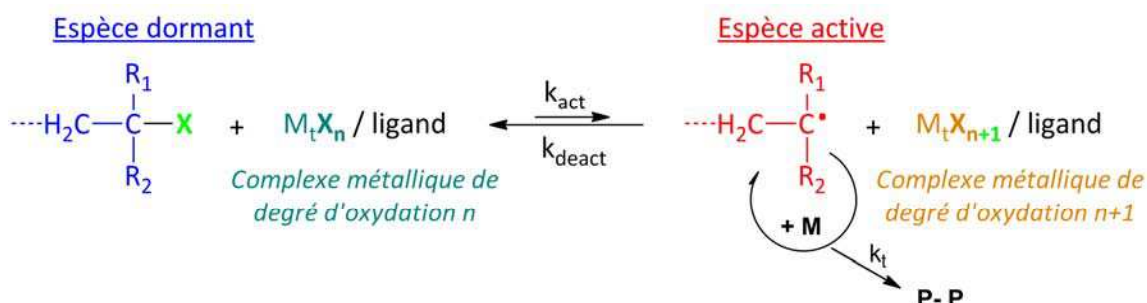


Figure 2. Schéma de l'équilibre de terminaison réversible en ATRP.

Bien que largement utilisée pour le greffage de particules inorganiques telles que la silice, cette méthode, SI-ATRP, n'a été que très peu employée à partir de particules organiques.

L'utilisation de latex fonctionnalisés comme supports pour le greffage de polymère par la méthode SI-ATRP a été décrite pour la première fois par l'équipe du professeur Charleux<sup>1</sup> en 2000. Ces travaux ont été par la suite repris par d'autres équipes, en particulier celle du

<sup>1</sup> Manuszak-Guerrini, M.; Charleux, B.; Vairon, J.P. *Macromolecular Rapid Communications* **2000**, 21, 669-674

professeur Brooks<sup>2</sup> et celle du professeur Morbidelli<sup>3</sup>. La procédure généralement employée consiste, dans une première étape, à fonctionnaliser la surface des particules de latex en copolymérisant un inimère (monomère porteur d'une fonction halogénure d'alkyle et capable de jouer le rôle d'amorceur dans l'étape de greffage). Ainsi, les particules de latex fonctionnalisées servent de support à la polymérisation en phase aqueuse de monomères hydrosolubles conduisant ainsi à la formation d'une écorce hydrophile greffée de manière covalente (Figure 3). Par cette voie, un bon contrôle des caractéristiques de la couronne de polymère formée est obtenu en ajustant la concentration de surface des fonctions qui amorcent ainsi que la concentration du monomère hydrophile. La densité de greffage, la longueur des chaînes greffées ainsi que leur structure et leur fonctionnalité chimique peuvent aussi être modulées. Cependant, ces différents travaux ont été conduits dans des conditions de synthèse que l'on pourrait qualifier d'idéales (faibles taux de solide et purification poussée des latex avant l'étape de greffage, utilisation de procédés sans tensio-actifs).

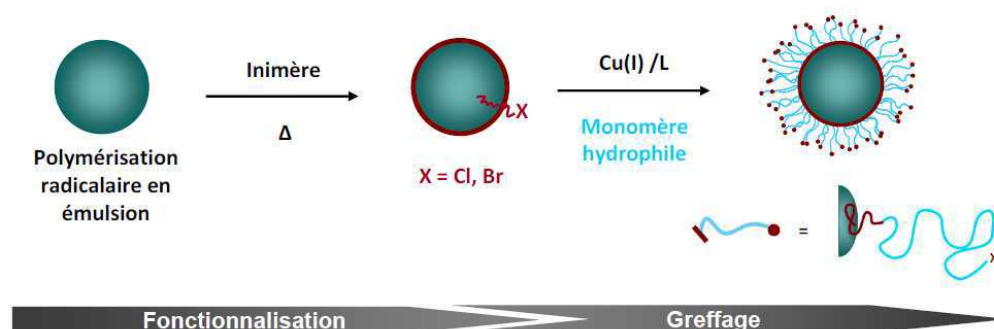


Figure 3. Principe général de la fonctionnalisation et du greffage de particules de latex par SI-ATRP.

Le sujet de cette thèse consiste à développer cette méthode de greffage afin de la rendre compatible avec les contraintes industrielles. Les principaux objectifs sont donc à : (i) fonctionnaliser l'extrême surface des particules selon un procédé industriel (procédé semi-continu, formulation industrielle de latex) ; (ii) mettre au point des conditions de greffage en présence de tensio-actifs et d'amorceur résiduel et cela à haut taux de solide.

<sup>2</sup> Jayachandran, K. N.; Takacs-Cox, A.; Brooks, D. E.. *Macromolecules* **2002**, 35, 4247-4257 (suivi de toute une série d'articles très détaillés)

<sup>3</sup> Mittal, V.; Matsko, N.B.; Butté, A.; Morbidelli, M. *European Polymer Journal* **2007**, 43, 4868-4881

Au regard des différents critères précédemment définis, l'utilisation de l'ATRP est, parmi les techniques de polymérisation radicalaire contrôlée, la plus adaptée car elle permet de fonctionnaliser facilement les particules de latex par simple copolymérisation de l'inimère, celui-ci n'interférant pas dans l'étape de polymérisation radicalaire en émulsion. De plus, la structure chimique de l'inimère peut être facilement modulée, élargissant ainsi la gamme des amorceurs potentiels pour le greffage. Lors de l'étape de greffage, la polymérisation par SI-ATRP peut être conduite à température ambiante, et donc permet de s'affranchir d'une quelconque contribution de l'amorceur thermique résiduel.

Cependant, l'inconvénient majeur de l'ATRP provient de la sensibilité à l'air du métal de bas degré d'oxydation, Cu(I), qui s'oxyde facilement en présence d'oxygène pour former du Cu(II). A cela s'ajoutent les fortes concentrations en complexe de cuivre (Cu/L) nécessaires pour conduire de façon contrôlée la polymérisation, et contaminant de ce fait les produits. Afin de pallier ces problèmes, de nouveaux procédés d'activation catalytique ont été développés.

Une de ces méthodes, développée par l'équipe du professeur Matyjaszewski<sup>4</sup> utilise comme catalyseur le Cu(II) qui est réduit *in situ* en Cu(I) par un agent réducteur tel que l'acide ascorbique ou le Cu(0). Dérivée de l'ATRP, cette technique, connue sous le nom activateur (ré)généré par transfert d'électron pour la polymérisation radicalaire par transfert d'atome (A(R)GET ATRP) permet de conduire la réaction en présence d'oxygène ainsi que de diminuer considérablement la quantité de catalyseur (*Figure 4*).

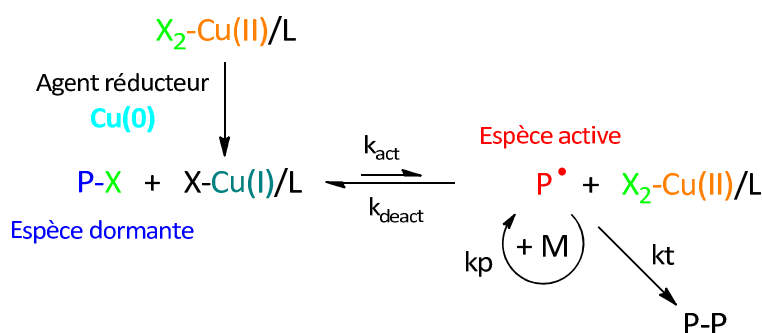


Figure 4. Mécanisme réactionnel de la polymérisation radicalaire contrôlée par la méthode de l'activateur (ré)généré par transfert d'électron (A(R)GET ATRP).

<sup>4</sup> Matyjaszewski, K.; Jakubowski, W.; Min, K.; Tang, W.; Huang, J. Y.; Braunecker, W. A.; Tsarevsky, N. V. *Proceedings of the National Academy of Sciences* **2006**, 103, 15309-15314



## Chapitre 2 : Etudes préliminaires

Une étude a été menée au préalable en solution afin de vérifier si les protocoles de MMRP étaient viables dans l'eau et si l'amorçage de la polymérisation se déroulait bien à partir de la fonction halogénure d'alkyle en présence du complexe de cuivre.

Pour cela, les polymérisations de monomères hydrophiles tel que le NAM (N-acryloylmorpholine), l'HEA (acrylate de 2-hydroxyéthyle) et le MAPEG (methacrylate de polyéthylène glycol) ont été menées dans l'eau avec seulement une partie du système catalytique. Dans ces conditions, aucune polymérisation n'a été observée à température ambiante prouvant de ce fait que la présence de l'amorceur et du système catalytique dans sa totalité (Cu(0) sous la forme d'un fil/PMDETA (Pentaméthylédiéthylènetriamine, ligand)/CuBr<sub>2</sub>) est nécessaire pour le bon déroulement de la réaction.

D'autres expériences de contrôle ont été conduites dans l'eau sans amorceur bromé mais en présence de tensio-actif (Dodécylsulfate de sodium, SDS) ou d'un amorceur thermique tel que le persulfate de potassium (KPS), le persulfate de sodium (NaPS), l'acide 4,4'-azobis(4-cyanopentanoïque) (ACPA) et de Cu(0)/PMDETA/CuBr<sub>2</sub>. Si aucun amorçage n'a eu lieu en présence de tensio-actif, une polymérisation du NAM a été observée en présence du catalyseur et de KPS ou NaPS. La réaction se déroulant à température ambiante, l'amorçage de la polymérisation a été imputé à une réaction entre le catalyseur et l'amorceur de type peroxyde. En présence d'un amorceur azoïque (ACPA), aucune polymérisation n'a eu cours, rendant donc possible la réaction de greffage des latex en présence de celui-ci.

Suite à ces expériences de contrôle, une série de polymérisations a été réalisée afin d'optimiser les conditions expérimentales dans l'eau pour les transposer directement à la réaction de greffage. Pour cela, différents paramètres ont été étudiés, comme la concentration des différents composants du système catalytique (CuBr<sub>2</sub>, PMDETA) et la nature de l'halogénure d'alkyle.

De façon générale, les polymérisations menées dans l'eau ont présenté une courte période de conversion rapide en monomère (~1h) puis un arrêt de la polymérisation. Une dépendance entre la conversion finale et la concentration en CuBr<sub>2</sub> a été observée ;

l'augmentation de la concentration en  $\text{CuBr}_2$  entraîne une baisse de la conversion finale ainsi que de la masse molaire finale du polymère.

A l'inverse, l'augmentation de la concentration en PMDETA entraîne une augmentation de la conversion finale mais abaisse la masse molaire finale du polymère.

La nature de l'halogénure d'alkyle influence aussi fortement le déroulement de la polymérisation. Les amorceurs de type bromure d'alkyle se sont présentés comme de bons amorceurs des monomères de type acrylate et acrylamide mais mauvais amorceurs pour les méthacrylates. Les chlorures d'alkyle sont quant à eux mieux adaptés pour les méthacrylates. Bien que la conversion des acrylates et acrylamides soit plus élevée en présence du chlorure d'alkyle, il est apparu que les masses molaires étaient élevées et que la distribution des masses molaires était large lorsque le couple  $\text{R-Cl/CuCl}_2$  était utilisé par rapport au couple  $\text{R-Br/CuBr}_2$ , à conditions expérimentales identiques.

Au regard des résultats obtenus dans cette étude, différents paramètres ont été fixés pour les transposer à la réaction de greffage. Pour un meilleur compromis entre conversion et concentration en catalyseur, un ratio molaire de 0,5/0,1 en  $\text{PMDETA/CuBr}_2$  par rapport à l'amorceur a été choisi. De même, l'amorceur bromé a été retenu afin d'obtenir des chaînes de polymère avec de petites masses molaires.

### **Chapitre 3 : Synthèse des latex fonctionnalisés**

Les particules cœurs employées dans cette étude sont toutes des particules de poly(méthacrylate de méthyle-co-acrylate de butyle), poly(MMA-co-nBA), synthétisées par polymérisation radicalaire en émulsion par un procédé semi-continu, à 40% de taux de solide, stabilisées par du SDS et l'ACPA a été employé en tant qu'amorceur thermique.

La majeure partie de l'étude concerne des particules réticulées. Celles-ci présentent l'avantage de maintenir leur intégrité, les rendant plus maniables lors des différentes étapes d'analyses. Cependant, des particules non réticulées ainsi que des particules obtenues à

partir de semence de PS ont aussi fait l'objet d'études. De façon générale ces modifications n'ont que très peu affecté la synthèse du latex, ou l'étape de fonctionnalisation.

Afin d'obtenir des particules de latex fonctionnalisées aptes au greffage, les fonctions brome doivent être localisées à l'extrême surface des particules et doivent être réparties de façon homogène. De ce fait, la copolymérisation de l'inimère doit s'effectuer à la surface de la particule et non dans la phase aqueuse, risquant de générer ainsi une population secondaire de particules, ni au cœur des particules.

Le protocole général de synthèse des particules de latex s'est déroulé en deux temps. Les particules de latex ont été obtenues par polymérisation radicalaire en émulsion par procédé semi-continu. Avant la consommation totale des monomères rentrant dans la composition du cœur, soit 90% de conversion, un mélange comprenant du MMA, de l'acrylate de 2(2-bromopropionyloxy) éthyle (BPEA, *Figure 6*) et du réticulant dans le cas des particules réticulées, a été introduit en semi-continu dans le milieu réactionnel. Le MMA, monomère relativement polaire, favorise la copolymérisation en surface des particules et la rapide propagation des chaînes favorise l'absorption des oligo-radicaux, évitant ainsi une nucléation secondaire.

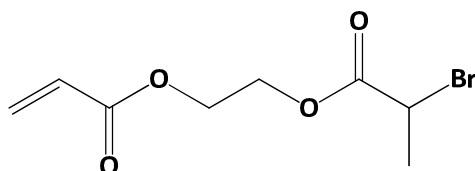


*Figure 6. Structure chimique de l'acrylate de 2(2-bromopropionyloxy) éthyle (BPEA).*

Suivant ce protocole, des latex fonctionnalisés stables à 40% de taux de solide ont été obtenus. De hautes conversions en BPEA (>95%) ont été mesurées par chromatographie en phase gazeuse. Le diamètre moyen des particules est de l'ordre de 110 nm pour les particules réticulées et 140 nm pour les non réticulées. Aucune population secondaire n'a été observée par microscopie électronique à balayage ou par diffusion dynamique de la lumière (*Figure 7*).

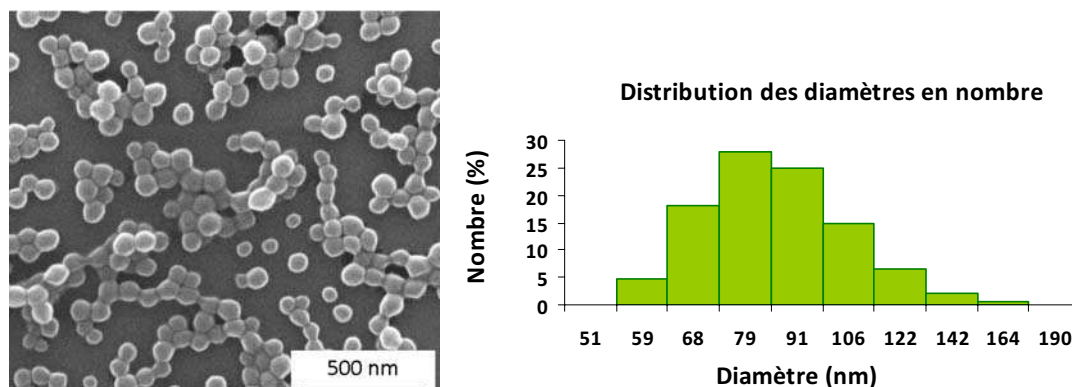


Figure 7. Cliché de microscopie électronique à balayage et diagramme des distributions des diamètres en nombre pour le latex réticulé fonctionnalisé (Latex 41).

La localisation des fonctions brome en surface des particules a pu être mise en évidence grâce aux mesures de ToF-SIMS (Time-of-Flight Secondary Ion Mass Spectrometry). Cette méthode d'analyse permet la détection des ions atomiques et moléculaires, sur une faible profondeur d'échantillon (environ 2 nm). De plus, cette analyse est sensible à des concentrations allant du ppm au ppb.

Pour tous les latex fonctionnalisés et dialysés, l'atome de brome ( $m/z = 78,913$ ) a pu être détecté ainsi qu'un fragment moléculaire ( $m/z = 178,981$ ) correspondant au groupe bromopropionyloxy (Figure 8).

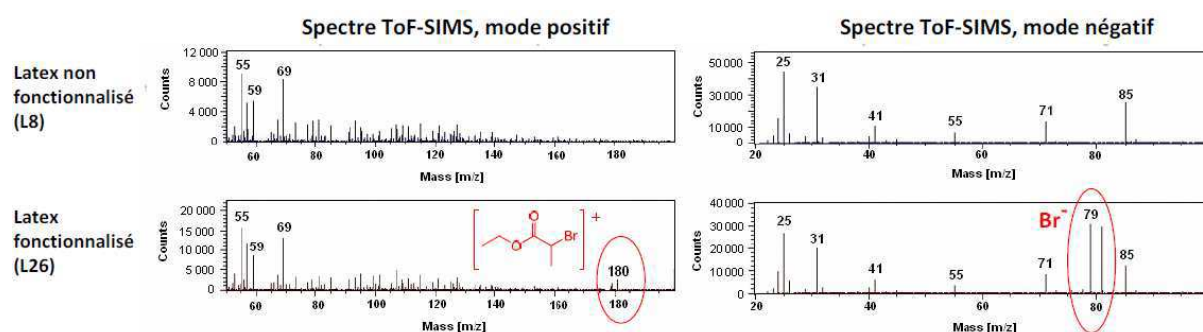


Figure 8. Spectre ToF-SIMS en mode positif et négatif des latex non fonctionnalisé (L8) et fonctionnalisé (L26)

La quantification absolue du brome et des fonctions à base de brome n'a pas pu être réalisée par l'analyse ToF-SIMS. Cependant, une quantification relative a pu être faite en comparant les intensités normalisées des pics relatifs au brome des différents latex fonctionnalisés à différents taux de BPEA. Par cette étude, nous avons vu une augmentation de l'intensité des pics relatifs au brome pour les latex fonctionnalisés avec une concentration de BPEA allant



de  $1,5 \times 10^{-6}$  à  $3,9 \times 10^{-5}$  mol/g<sub>latex</sub>. Au delà de cette concentration, les intensités ne varient plus, indiquant un recouvrement maximal de la surface par les fonctions à base de brome (Figure 9).

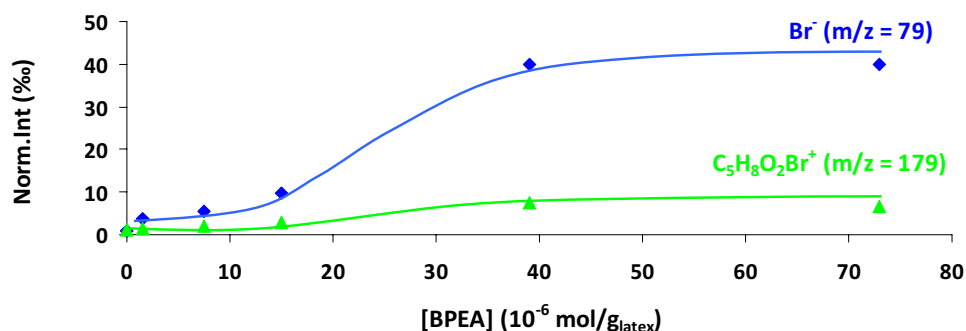


Figure 9. Variation de l'intensité normalisée des pics relatifs au brome en fonction de la concentration en BPEA utilisée lors de la fonctionnalisation des latex.

Les latex fonctionnalisés ont été mis en présence de Cu(0) et CuCl<sub>2</sub>/PMDETA afin de tester l'accessibilité des fonctions bromées ainsi que leur habilité à la réaction de transfert d'halogène. Après cette réaction, les latex ont été dialysés puis analysés par ToF-SIMS. La présence d'atome de chlore non présent initialement a été mise en évidence, prouvant de ce fait que l'atome de brome était en surface des particules de latex et que la fonction le contenant était apte à amorcer la réaction de greffage (Figure 10).

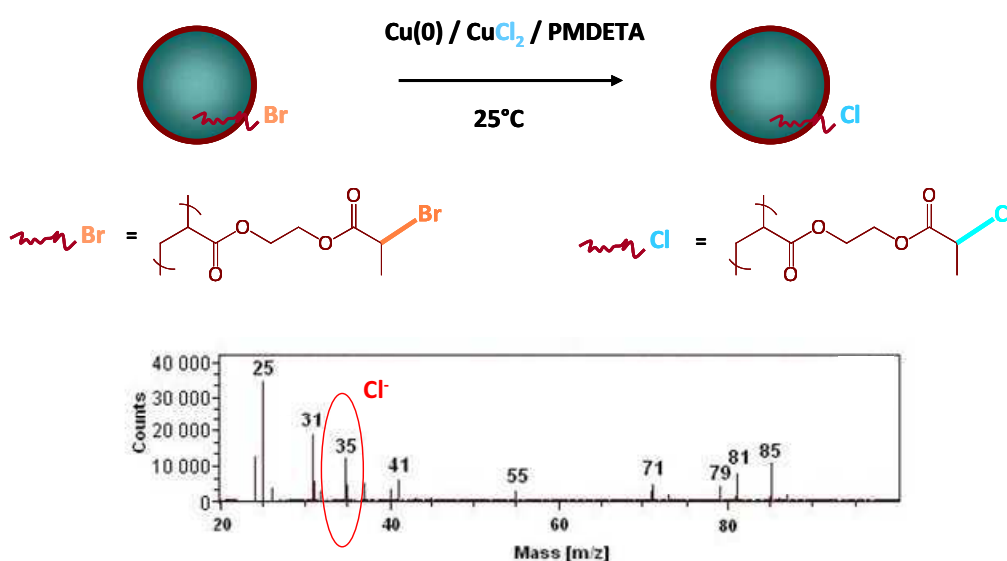


Figure 10. Schéma de la réaction de transfert d'halogène et spectre ToF-SIMS, mode négatif du latex obtenu après réaction de transfert d'halogène.

#### Chapitre 4 : Greffage des particule de latex

Le greffage des particules a été mené à température ambiante à partir des latex non purifiés à des taux de solide allant de 20 à 38%. Les conditions expérimentales ont été directement adaptées à partir des polymérisations menées dans l'eau. Le NAM a été sélectionné comme monomère, Cu(0) a été utilisé sous forme de fil et un ratio molaire par rapport au BPEA de 0,5/0,1 en PMDETA/CuBr<sub>2</sub> a été utilisé.

Généralement, de hautes conversions en NAM ont été obtenues après 2-3h de réaction. Cependant, il a été observé que la concentration en fonctions à base de brome influence fortement la conversion. A des concentrations en brome inférieures à  $7,3 \times 10^{-6}$  mol/g<sub>Latex</sub>, de faibles conversions finales (<50%) ont été obtenues, alors qu'une conversion supérieure à 70% a été atteinte pour des concentrations en brome supérieures à  $10^{-5}$  mol/g<sub>Latex</sub> (Figure 11). En corrélation avec la conversion, une augmentation du diamètre des particules a été observée pouvant aller de 10 nm à 100 nm. Cette variation est fortement influencée par la concentration en brome de surface et par la concentration en NAM.

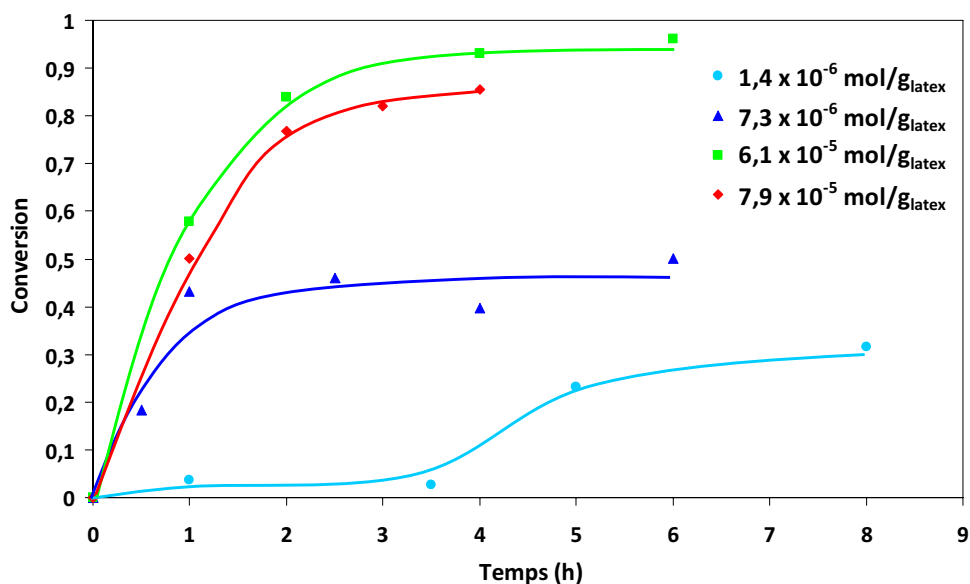


Figure 11. Conversion en NAM en fonction du temps pour le greffage de latex à différentes concentrations de BPEA (mol/g<sub>Latex</sub>) en présence de Cu(0)/PMDETA/CuBr<sub>2</sub>.

Sous certaines conditions, un gel a été formé par réactions de couplage inter-particulaires. Ces réactions ont été favorisées à faible concentration de CuBr<sub>2</sub>, quand la désactivation n'est pas assez efficace pour maintenir une faible concentration en radical propageant. De plus,

lorsque le greffage s'effectue en présence d'un grand ratio monomère/Br, l'épaisseur de la couronne augmente. De ce fait, la distance entre les particules diminue fortement, augmentant aussi les réactions de couplage inter-particulaires.

La preuve du greffage a pu être démontrée à partir des latex dialysés par la mise en évidence de la présence du groupe amide caractéristique du NAM par FT-IR et par ToF-SIMS.

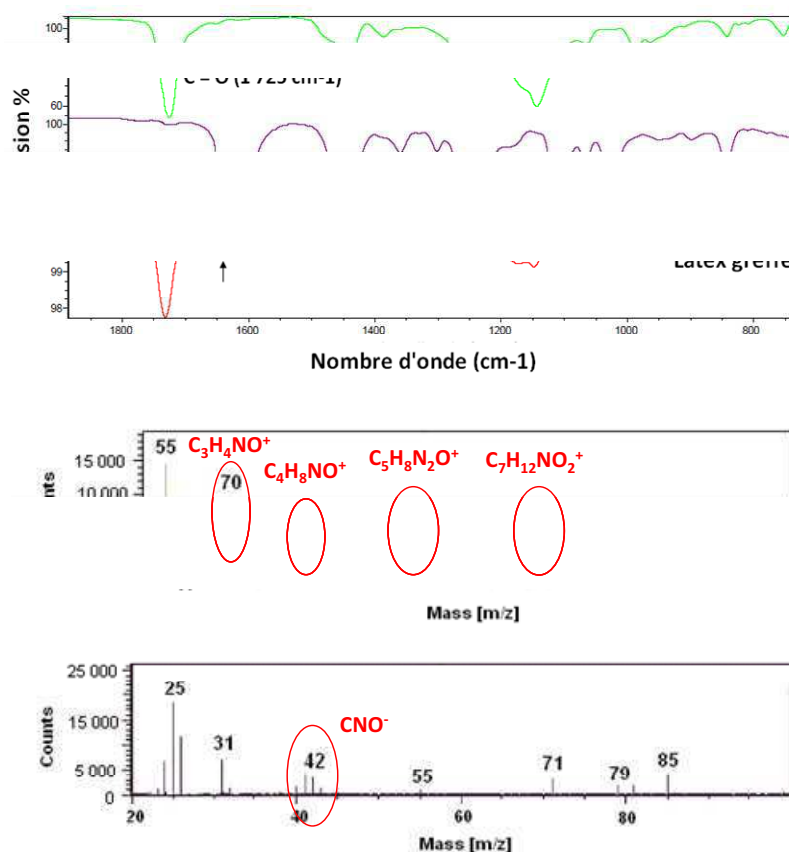


Figure 12. Spectre FT-IR et spectre ToF-SIMS en mode positif et négatif d'un latex greffé avec du poly(NAM).

La présence d'une couronne hydrophile à la surface des particules confère à celles-ci une très bonne stabilité colloïdale par stabilisation stérique. C'est pourquoi, la stabilité des latex a été mesurée en présence d'une solution concentrée en CaCl<sub>2</sub> ainsi que par un test de gel/dégel. Il a été constaté que les latex greffés étaient stables au cycle de gel/dégel ainsi que sous force ionique élevée confirmant le greffage d'une couronne de poly(NAM) à la surface des particules (Figure 13).



Figure 13. Tests de stabilité des latex greffés à la force ionique et au cycle gel/dégel.

Suite à ces résultats, l'étude du greffage s'est étendue à d'autres monomères hydrophiles tels que l'HEA, le (M)APEG, le PAM 100, le NIPAM, et l'AMPS. Bien que les résultats en termes de conversion et stabilité colloïdale obtenus avec ces monomères étaient moins bons que ceux obtenus avec le NAM, il a pu être démontré que cette méthode de greffage pouvait s'appliquer à une grande gamme de monomères hydrophiles.

Dans une autre étude, différents métaux ont été utilisés pour le greffage des particules. Tout en gardant les mêmes conditions expérimentales, Cu(0) a été remplacé par Fe(0), Zn(0) et Al(0).

En présence de Fe(0), seulement 13% de conversion ont été atteints. Les latex obtenus présentent alors des diamètres finaux proches des diamètres initiaux et une faible stabilité à la force ionique. Tous ces résultats indiquent un faible greffage.

Un bon greffage du poly(NAM) a été induit par Zn(0), donnant des résultats similaires à ceux obtenus avec Cu(0) dans les mêmes conditions : conversion >90%, augmentation du diamètre des particules comprise entre 20 à 40 nm, bonne stabilité en présence d'une solution de CaCl<sub>2</sub> à 2,25M.

Parmi les différents métaux testés, Al(0) n'appartient pas au groupe des métaux de transition. Cependant, grâce à un potentiel rédox très favorable, Al(0) réduit CuBr<sub>2</sub> pour générer Cu(I), activateur de la polymérisation. Par ce mécanisme, un bon greffage du poly(NAM) a été obtenu avec l'Al(0) (hautes conversions, augmentation du diamètre des particules, bonne stabilité en présence d'une solution de CaCl<sub>2</sub> à 2,25M).

## Conclusion

L'objectif de cette thèse consistait à développer une méthode de greffage des particules de latex en utilisant la polymérisation radicalaire contrôlée par transfert d'atome induite par les métaux, dans des conditions acceptables industriellement.

Afin de mieux maîtriser cette technique une étude a été menée en solution. Celle-ci nous a permis de vérifier et d'optimiser les protocoles de polymérisation radicalaire contrôlée par le cuivre dans l'eau.

Le système MePEG-Br/PMDETA/CuBr<sub>2</sub> de rapport molaire 1/0,5/0,1 a été retenu. Bien que sous ces conditions le contrôle de la polymérisation n'ait pas été atteint, la réaction a été suffisamment efficace (hautes conversions, faibles masses molaires et faible concentration en complexe de cuivre) pour justifier ce choix.

L'avantage de cette technique repose sur le fait que l'amorçage de la réaction ne se déroule qu'à partir de l'amorceur halogéné par un mécanisme de transfert d'halogène en présence du catalyseur. Ainsi, la réaction de greffage des particules ne peut être amorcée qu'à partir des fonctions halogénées de surface.

La fonctionnalisation des particules a été menée par polymérisation radicalaire en émulsion en utilisant un protocole en adéquation avec ceux employés dans l'industrie (procédé semi-continu, hauts taux de solide, présence de tensio-actif). La présence des fonctions brome à la surface des particules a été mise en évidence grâce aux analyses ToF-SIMS. Par cette même technique, l'accessibilité ainsi que l'habilité des ces fonctions à la réaction de transfert d'halogène ont été testées.

L'étape de greffage des particules fonctionnalisées a été menée selon les critères précédemment définis : haut taux de solide, présence de tensio-actifs et d'amorceur résiduels.

A partir des conditions préalablement définies lors des polymérisations menées dans l'eau (rapport molaire R-Br/PMFETA/CuBr<sub>2</sub> de 1/0,5/0,1), un bon greffage du poly(NAM) a été obtenu (hautes conversions, augmentation de la taille des particules, augmentation de la

stabilité colloïdale). Grâce aux différents tests de greffage, des critères à respecter afin d'obtenir un greffage efficace ont pu être définis. Une concentration de surface en brome suffisante est nécessaire pour atteindre des conversions élevées à des vitesses de polymérisation également élevées. Une concentration minimum en  $\text{CuBr}_2$  et un faible ratio monomère/Br sont indispensables pour limiter/supprimer les réactions de couplage inter-particulaires responsables de la formation de gels.

Si la plupart des greffages concernaient le poly(NAM), la méthode a été étendue avec succès à d'autres monomères hydrophiles. D'autres métaux tels que  $\text{Al}(0)$ ,  $\text{Zn}(0)$  ont aussi permis d'amorcer la réaction de greffage.

Au terme de ce travail, un système robuste de greffage a été mis en place. Bien que des améliorations soient encore à fournir, les conditions de greffage définies sont conciliables avec les contraintes industrielles. A la suite de ces travaux, une généralisation du protocole pourrait être envisagée afin qu'à partir d'un protocole « universel » une large gamme de monomères puissent être greffés à la surface des particules, élargissant ainsi les potentiels domaines d'applications.



## Abstract

Core-shell particles with a hydrophobic polymer core and a hydrophilic polymer shell are the subject of many works as they can find a wide range of applications. Various strategies to incorporate a hydrophilic polymer shell have been employed but there has been a growing interest in the “grafting from” method with the development of controlled/living radical polymerization (CRP) techniques and more particularly atom transfer radical polymerization (ATRP).

The general principle of the “grafting from” strategy consists in introducing initiating groups at the particle surface and in activating them to grow polymer chains via CRP. Due to fast initiation and simultaneous growth of the chains, CRP allows grafting density and brush thickness to be well-controlled.

In this context, the aim of this work was to incorporate a hydrophilic polymer shell at the surface of polymer particles obtained from emulsion polymerization by post-synthesis modification, using a “grafting from” approach based on aqueous metal-mediated radical polymerization

The starting latexes were synthesized via classical radical emulsion copolymerization of *n*-butyl acrylate and methyl methacrylate and were functionalized at their surface by a comonomer bearing a Br-functional group (the so-called inimer). The latter was introduced to play the role of the initiator in the grafting reaction, in the presence of the Cu(0)/CuBr<sub>2</sub>/PMDETA catalytic system.

Conditions for which the grafting step could be performed at room temperature, using high particle concentration in the presence of surfactant and initiator remaining from the emulsion polymerization were identified. As far as we know, this is the first time such grafting conditions have been applied with success from “real latexes”.





## List of Abbreviations

ACPA	4,4'-Azobis(4-cyanopentanoic acid)
AGET	Activators generated by electron transfer
AMPS	2-Acrylamido-2-methylpropane sulfonic acid
APEG	Poly(ethylene glycol) acrylate
ARGET	Activators regenerated by electron transfer
ATRA	Atom transfer radical addition
ATRP	Atom transfer radical polymerization
BDDA	1,4-butanediol diacrylate
BPEA	2(2-Bromopropionyloxy) ethyl acrylate
bipy	Bipyridine
Conc.	Concentration
Conv.	Conversion
CRP	Controlled radical polymerization
Cu(0)MP	Copper(0) mediated polymerization
D	Particle diameter
Disponil FES77	Sodium lauryl ether sulfate
DLS	Dynamic light scattering
DMF	Dimethyl formamide
DMSO	Dimethylsulfoxide
DP <sub>n</sub>	Number average degree of polymerization
DSC	Differential scanning calorimetry
ECD-MS	Electrospray charge-detection mass spectroscopy
ESR	Electron spin resonance
Et <sub>3</sub> N	Triethylamine
FRP	Free radical polymerization
FT-IR	Fourier transform infra-red
GC	Gas chromatography
HEA	2-hydroxyethyl acrylate
HEMA	2-hydroxyethyl methacrylate
ICAR	Initiators for continuous activators regeneration
k <sub>act</sub>	Activation rate constant
k <sub>deact</sub>	Deactivation rate constant
k <sub>p</sub>	Propagation rate constant
KPS	Potassium persulfate
LRP	Living radical polymerization
MA	Methyl acrylate
MePEG-OH	Poly(ethylene glycol) methyl ether
Me <sub>6</sub> TREN	Tris(2-dimethylaminoethyl)amine
MMA	Methyl methacrylate
MMC(R)P	Metal mediated controlled (radical) polymerization
M <sub>n</sub>	Number average molar mass
M <sub>w</sub>	Weight average molar mass
M <sub>w</sub> /M <sub>n</sub>	Molar mass dispersity
NaA	Sodium acrylate
NaHCO <sub>3</sub>	Sodium hydrogen carbonate

---

<i>NAM</i>	<i>N-acryloylmorpholine</i>
<i>NaMA</i>	<i>Sodium methacrylate</i>
<i>NaPS</i>	<i>Sodium persulfate</i>
<i>NaSS</i>	<i>Sodium 4-vinylbenzenesulfonate</i>
<i>nBA</i>	<i>nButyl acrylate</i>
<i>NIPAM</i>	<i>N-isopropylacrylamide</i>
<i>NMR</i>	<i>Nuclear magnetic resonance</i>
<i>NMP</i>	<i>Nitroxide mediated polymerization</i>
<i>OSET</i>	<i>Outer-sphere electron transfer</i>
<i>PAM 100</i>	<i>Phosphate esters of poly(ethylene glycol) monomethacrylate</i>
<i>PDI</i>	<i>Polydispersity index</i>
<i>PEG</i>	<i>Poly(ethylene glycol)</i>
<i>PEGMA</i>	<i>Poly(ethylene glycol) methacrylate</i>
<i>PMDETA</i>	<i>N,N,N',N',N''-pentamethyldiethylenetriamine</i>
<i>Poly(HEA)</i>	<i>Poly(2-hydroxyethyl acrylate)</i>
<i>PRE</i>	<i>Persistent radical effect</i>
<i>PS</i>	<i>Polystyrene</i>
<i>RAFT</i>	<i>Reversible addition-fragmentation chain transfer</i>
<i>RT</i>	<i>Room temperature</i>
<i>R-X</i>	<i>Alkyl halide</i>
<i>SARA</i>	<i>Supplemental activator and reducing agent</i>
<i>SDS</i>	<i>Sodium dodecyl sulfate</i>
<i>SEC</i>	<i>Size exclusion chromatography</i>
<i>SEM</i>	<i>Scanning electron microscopy</i>
<i>SET</i>	<i>Single electron transfer</i>
<i>SET-LRP</i>	<i>Single electron transfer living radical polymerization</i>
<i>SI-ATRP</i>	<i>Surface Initiated Atom Transfer Radical Polymerization</i>
<i>SI-P</i>	<i>Surface initiated polymerization</i>
<i>SN&amp;NI</i>	<i>Simultaneous reverse and normal initiation</i>
<i>TEM</i>	<i>Transmission electron microscopy</i>
<i>Tg</i>	<i>Glass transition temperature</i>
<i>ToF-SIMS</i>	<i>Time-of-Flight Secondary Ion Mass Spectrometry</i>

## [Table of contents](#)

<b>Introduction</b> .....	1
<b>Chapter 1: Literature review</b>	
<b>Introduction</b> .....	5
<b>1.1. Metal-mediated radical controlled polymerization</b> .....	9
1.1.a. Historical development.....	9
1.1.b. Components of the system.....	11
1.1.b.i. Initiator.....	11
1.1.b.ii. Monomer.....	12
1.1.b.iii. Metal.....	13
1.1.b.iv. Ligand.....	14
1.1.c. Metal-mediated polymerization developments.....	15
1.1.c.i. Reverse/Simultaneous Reverse and Normal Initiation and activators generated by electron transfer ATRP.....	16
1.1.c.ii. Activators regenerated by electron transfer ATRP and initiators for continuous activator regeneration.....	19
1.1.d. Zero valent metal mediated polymerization.....	21
1.1.d.i. Single-electron transfer living radical polymerization.....	22
1.1.d.ii. SARA ATRP.....	23
1.1.d.iii. Outer sphere Vs inner sphere electron transfer.....	24
1.1.d.iv. Various metal used.....	26
1.1.e. Metal mediated polymerization in water solution.....	27
1.1.e.i. ATRP in water solution.....	27
1.1.e.i. SET-LRP in water and in polar solvent.....	30
<b>1.2. Core-shell particle via surface initiated polymerization</b> .....	33
1.2.a. Introduction.....	33
1.2.b. Core-shell particles synthesis by conventional free radical polymerization.....	35
1.2.c. Surface-photoinitiated polymerization.....	36
1.2.d. Surface-initiated by metal mediated polymerization.....	37
1.1.d.i. Latex functionalization.....	39
1.1.d.ii. SI-ATRP in water solution.....	40
1.1.d.iii. SI-SET-LRP.....	44
1.2.e. Core-shell properties.....	46
<b>1.3. Conclusion</b> .....	48
<b>1.4. References</b> .....	50

**Chapter 2: Copper mediated polymerization in water**

<b>Introduction</b>	63
<b>2.1. Control experiments in water at room temperature</b>	66
2.1.a. A true multicomponent system	66
2.1.b. Side-initiation in presence of the components present in the latex	67
<b>2.2. Model system in water</b>	69
2.2.a. Influence of the $\text{CuBr}_2$ concentration	69
2.2.b. Influence of the ligand	73
2.2.b.i. Nature of the ligand	73
2.2.b.ii. Influence of the PMDETA concentration	74
2.2.c. Influence of the type of monomer	76
2.2.d. Influence of the type of initiator	78
<b>2.3. Conclusion</b>	84
<b>2.4. Experimental part</b>	86
2.4.a. Materials	86
2.4.b. Synthesis of the initiators	87
2.4.c. Copper mediated polymerization in water	88
<b>2.5. References</b>	88

**Chapter 3: Latex Functionalization**

<b>Introduction</b>	91
<b>3.1. Functionalized latex synthesis</b>	93
3.1.a. Synthesis of poly(MMA-co-nBA) crosslinked functionalized latexes	93
3.1.b. Kg scale transfer	94
3.1.c. Synthesis of poly(MMA-co-nBA) non-crosslinked functionalized latex particles	95
<b>3.2. Particle surface analysis by ToF-SIMS</b>	97
<b>3.3. Halogen transfer ability</b>	101
<b>3.4. Conclusion</b>	105
<b>3.5. Experimental part</b>	106
3.5.a. Materials	106
3.5.b. BPEA synthesis	106
3.5.c. Synthesis of poly(MMA-co-nBA) crosslinked latex	107
3.5.d. Synthesis of poly(MMA-co-nBA) crosslinked latex with PS seed	107
3.5.e. Synthesis of poly(MMA-co-nBA) non-crosslinked latex with PS seed	108
3.5.f. Halogen transfer mediated by $\text{Cu(0)/CuCl}_2$ /PMDETA	108
3.5.g. Latex references	109
<b>3.6. References</b>	110

## Chapter 4: Surface-initiated Polymerization

<b>Introduction</b>	111
<b>4.1. Control experiments</b>	113
<b>4.2. Surface initiated polymerization of NAM in presence of Cu(0)</b>	114
4.2.a. Surface-initiated polymerization at different BPEA concentrations	114
4.2.a.i. Core shell latex synthesis	114
4.2.a.ii. Stability test and viscosity analysis	116
4.2.a.iii. FT-IR analysis	119
4.2.a.iv. ToF-SIMS analysis	120
4.2.a.v. Electrospray charge-detection mass spectroscopy	123
4.2.a.vi. Serum analysis	125
4.2.b. Surface-initiated polymerization with different cores	126
4.2.c. Surface-initiated polymerization at different copper complex concentrations	128
4.2.d. Two-step grafting reaction	130
<b>4.3. Surface-initiated polymerization of different hydrophilic monomers in presence of Cu(0)</b>	137
<b>4.4. Surface-initiated polymerization of NAM in presence of different metals</b>	139
4.4.a. Surface-initiated polymerization	139
4.4.b. Removal of the copper salt	142
<b>4.5. Conclusion</b>	144
<b>4.6. Experimental part</b>	147
4.6.a. Materials	147
4.6.b. Surface initiated by copper mediated polymerization	147
4.6.c. Surface initiated polymerization from grafted poly(NAM) particle	148
4.6.d. Stability tests	148
4.6.e. . Electrospray charge-detection mass spectroscopy (ECD-MS)	148
<b>4.7. References</b>	149

<b>Conclusion</b>	151
-------------------	-----

### Annexes:

#### Characterization techniques

A.1. <sup>1</sup> H NMR	157
A.2. SEC	158
A.3. DLS	158
A.4. GC	158
A.5. DSC	159
A.6. TEM	159

A.7. SEM.....	159
A.8. ToF-SIMS.....	159
A.9. FT-IR.....	160
A.10. Viscosity measurement.....	160
A.11. Stability test.....	160
A.12. Electrospray charge-detection mass spectroscopy (ECD-MS).....	161
<b>Publications</b> .....	<b>163</b>
<b>Copyright: Permission/licence</b> .....	<b>175</b>

## **Introduction**

### **Latex noun, pl latexes or latices**

*1. The colorless or milky sap of certain trees and plants, such as the milkweed and the rubber tree, that hardens when exposed to the air. Latex usually contains gum resins, waxes, and oils, and sometimes toxic substances.*

*2. A manufactured emulsion of synthetic rubber or plastic droplets in water that resembles the latex of plants. It is used in paints, adhesives, and synthetic rubber products.*

*The American Heritage® Science Dictionary Copyright © 2005 by Houghton Mifflin Company.*

More than 10 million metric tons of latex are produced per year by emulsion polymerization and they are used in a wide range of applications as adhesives, paints, binders, additives for paper, textiles, construction materials. Acrylic latexes remain the leading emulsion polymer product type.

Polymers produced by emulsion polymerization, particularly emulsions in waterborne paints and coatings, have been of growing interest since the adoption of more stringent environmental regulations concerning the emission of volatil organic compounds (VOCs). Due to the increasing competition and public sensitivity to environmental issues, emulsion polymer producers are forced to achieve an efficient production of high-quality materials, via a safe and environmentally friendly process.



The latex surface modification offers a rather easy way to introduce new functionality or to improve latex properties onto existing polymers. One of these possible modifications is to bind covalently a polymer or a functional molecule using a surface-initiated reaction. In the last decade, grafted particles or core-shell particles have been particularly investigated. There has also been a growing interest in the “grafting from” method with the development of Controlled/living Radical Polymerization (CRP) techniques. Due to fast initiation and simultaneous growth of the chains, CRP allows grafting density and brush thickness to be well-controlled. However, only a few examples of grafted latexes have been developed in the industry, probably due to the difficulty to transpose such techniques at the industrial scale.

In this context, the aim of this work is to incorporate a polymer shell at the surface of polymer particles prepared via radical emulsion polymerization by post-synthesis modification, using a “grafting from” approach based on aqueous CRP. The use of a single type of functionalized particles as a platform to grow any kind of polymers with tailor-made characteristics would allow targeting different applications from the same starting latex recipe.

The choice of the CRP method used in the grafting step requires a procedure to introduce the functionality at the particle surface and the use of “as-synthesized” concentrated latexes, without elimination of the surfactant and of the remaining initiator, in the grafting step. To fulfill both criteria, Surface-Initiated Atom Transfer Radical Polymerization (SI-ATRP) was selected as it offers a versatile method to introduce the functionality via an inimer (i.e. a monomer bearing an alkyl halide group able to serve as an initiator in ATRP) at the particle surface. The latter can be polymerized by classical radical emulsion polymerization without interference with the initiating and propagating radicals. Finally, the grafting reaction by SI-ATRP can be performed at room temperature, hence preventing unwanted initiation by the remaining radical initiator. All those criteria impede the use of others CRP methods such as nitroxide-mediated polymerization (requiring elevated temperature) and reversible addition-fragmentation chain transfer (in which the reactive group of the functional monomer will react during the functionalization step).

However, a drawback of ATRP is the need for large quantities of catalyst (in particular copper(I) halide), which contaminate the final product and are difficult to remove. Since a few years, the use of copper metal has been particularly investigated because it is easier to handle than Cu(I) or Cu(II) salts. The role of Cu(0) in the mechanism of copper-mediated polymerization is not fully understood and still under debates, but this will not be the focus of this work since the main target of this project is the synthesis of new materials rather than the kinetic study. It nevertheless offers an easy way to proceed and allows to decrease the amount of copper complex which is of interest for potential industrial applications. The couple Cu(0)/Cu(II) was thus employed as a catalyst for our grafting reactions from latex particles in aqueous media at room temperature.

The general procedure is displayed on *Figure 1*, where, firstly the core particles are prepared by conventional radical emulsion polymerization. At the end of this step, the latex particles are covered with a thin layer of a polymer derived from an inimer (monomer with a halogen atom which is able to initiate the ATRP). Finally, the functionalized particles are used as substrates for copper-mediated polymerization in order to graft (from the surface) a functional (controlled polymer) shell.

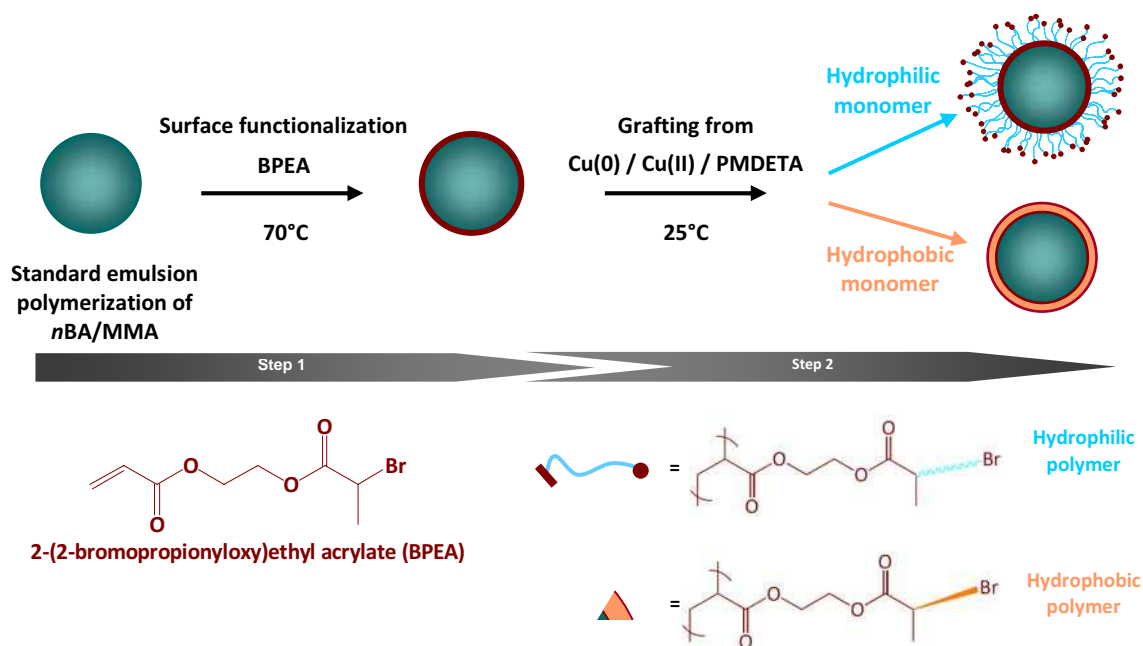


Figure 1. General principle of the Cu(0)-mediated surface-initiated radical polymerization use in this work.

The present study will be arranged in four chapters and will start with a literature review concerning the recent progresses in the area of Metal-Mediated Controlled Radical Polymerization (MMCRP). Then, the synthesis of polymer particles exhibiting a hydrophilic shell created via surface-initiated radical polymerization will be developed.

The second chapter will be devoted to metal mediated CRP in aqueous solution, from a soluble ATRP initiator, as a model reaction for grafting reaction. This preliminary work aims at defining the best conditions to be transposed to the grafting reaction.

The latex functionalization will be presented in the first part of chapter 3, followed by a thorough surface analysis.

The surface-initiated polymerization will be described in chapter 4. The study will demonstrate the success of the synthesis of a hydrophilic shell using metal-mediated radical polymerization via chemical characterization and evolution of the latex final properties.

# Chapter 1

## Literature review

### Introduction

100 million tons of polymers are produced annually under free radical polymerization (FRP) conditions. However, as FRP is a chain growth polymerization method dominated by termination and chain transfer events, precise tailoring of the macromolecular architecture is difficult to achieve.

Therefore, living radical polymerization (LRP) also called controlled radical polymerization (CRP) has received a growing interest in the polymer chemistry field as it allows the production of new polymers with precise molecular architecture.

The concept of living polymerization was introduced in 1956 by Swarc<sup>1</sup> for the anionic polymerization of styrene with an alkali metal/naphthalene initiator. He defined the anionic polymerization as a “living” polymerization, characterized by polymer chains that grow with monomer conversion. Anionic chain ends remain living in the sense that chain growth may be reinitiated by the addition of monomer, thus the term “living”.

In 1955, Tobolsky<sup>2</sup> identified the peculiar behavior of thiuram disulfides in free radical polymerization. Following these works, in 1982, Ostu<sup>3</sup> described the polymerization of MMA in the presence of phenylazotriphenylmethane and benzyl dithiocarbamate. He

demonstrated that these molecules so called iniferters could act simultaneously as initiator, chain transfer agent, and terminator in a polymerization reaction. These works provided for the first time a model for a controlled radical polymerization.

Since the 80's and Otsu's works, various methods began to emerge for controlled radical polymerization such as nitroxide mediated polymerization (NMP) in 1985 by Solomon and Rizzardo<sup>4</sup> and in 1993 by Georges<sup>5-6</sup>, metal-mediated radical polymerization (MMRP) in 1995 by Matyjaszewski<sup>7</sup> and Sawamoto<sup>8</sup> and reversible addition-fragmentation chain transfer polymerization (RAFT) in 1998 by Moad and Rizzardo<sup>9</sup>.

All of these methods are based on a reversible and dynamic equilibrium between active radical species and dormant covalent species (*Figure 1.1*). As the equilibrium is in favor of the formation of dormant chains, the proportion of chain irreversibly terminated is thus reduced.

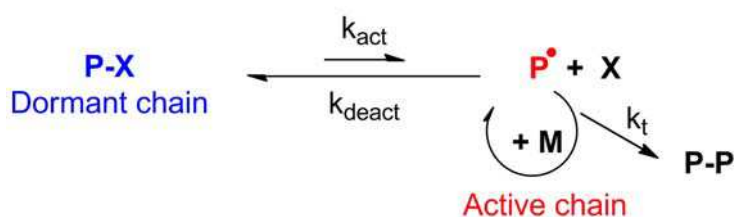


*Figure 1.1. Dynamic activation/deactivation equilibrium in controlled radical polymerization.*

Avoiding completely termination and irreversible chain transfer reactions is not possible under these methods. The term “living” is thus not adapted and the term “controlled” is more suitable. In 1995, Matyjaszewski<sup>10</sup> defined the controlled polymerization as “*a synthetic method for preparing polymers with predetermined molecular weights ( $DP = \Delta[M]/[I]_0$ ), low polydispersity and controlled functionality, and also block polymers. Transfer and termination are allowed in a controlled polymerization if their contribution is sufficiently reduced by the proper choice of the reaction conditions such that polymer structure is not affected.*” The main differences between CRP and LP are illustrated in *Figure 1.2*.

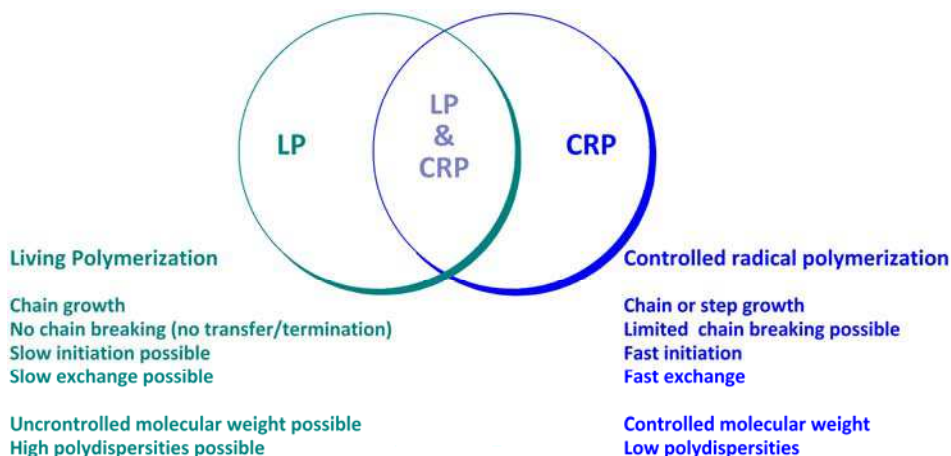


Figure 1.2. Comparison between LP and CRP, adapted from Matyjaszewski<sup>10</sup>.

As claimed by Matyjaszewski<sup>10</sup>, controlled radical polymerizations have to fill the following requirements.

- **Constant propagating radical concentration**

When determined by the activation-deactivation equilibrium, the propagating radical concentration is constant during the polymerization. In consequence, a linear dependence of  $\ln([M]_0/[M]_t)$  on time is expected (Equation 1.1).

$$\ln\left(\frac{1}{1-x}\right) = \ln\left(\frac{[M]_0}{[M]_t}\right) = k_p \times [P^\bullet] \times t \quad \text{Equation 1.1}$$

$x$ : monomer conversion

$k_p$ : propagation rate coefficient ( $L \cdot mol^{-1} \cdot s^{-1}$ )

$t$ : time (s)

$[P^\bullet]$ : propagating radical concentration ( $mol \cdot L^{-1}$ )

- **Linear dependence of  $DP_n$  on conversion**

The degree of polymerization ( $DP_n$ ) is determined by the ratio of the concentration of reacted monomer to the concentration of polymer chains, the latter corresponding to the introduced initiator concentration (Equation 1.2).

$$DP_n = \text{conversion} \times \frac{[M]_0}{[I]_0} \quad \text{Equation 1.2}$$

$[M]_0$ : initial monomer concentration ( $mol \cdot L^{-1}$ )

$[I]_0$ : initial initiator concentration ( $mol \cdot L^{-1}$ )

Due to fast initiation with respect to propagation and due to the negligible fraction of chains irreversibly terminated (bimolecular termination and chain transfer reactions), the number average molar mass ( $M_n$ ) increase linearly with the conversion (Equation 1.3).

$$M_n = DP_n \times M_{mono} + M_{ext} \quad \text{Equation 1.3}$$

$M_n$ : number average molar mass (g/mol)

$DP_n$ : number average degree of polymerization

$M_{mono}$ : monomer molar mass (g/mol)

$M_{ext}$ : chain end molar mass (g/mol)

- **Low  $M_w/M_n$**

The molar mass dispersity ( $M_w/M_n$ ) is low in CRP if the initiation is fast and if the different growing species exchange rapidly via dynamic equilibrium. In this case,  $M_w/M_n$  follows the Poisson distribution (Equation 1.4).

$$M_w/M_n = 1 + \frac{DP_n}{(1 + DP_n)^2} \xrightarrow{DP_n \rightarrow \infty} 1 + \frac{1}{DP_n} \quad \text{Equation 1.4}$$

$M_w/M_n$ : molar mass dispersity

$DP_n$ : number average degree of polymerization

- **Block copolymer**

The polymerization resumes after the addition of a new feed of monomer that can be the same as the first fed one or a different one hence leading to the formation of block copolymers.

As already reported, most CRP techniques are based on a reversible and dynamic equilibrium between active radical species and dormant species. However, depending of the mechanism used to achieve the activation/deactivation equilibrium, 2 classes of CRP have been distinguished: CRP based on reversible termination such as NMP or MMRP and CRP based on reversible transfer such as RAFT.

The aim of this literature review is not to describe all these CRP methods. Only the metal-mediated radical polymerization will be further developed as this technique will be temptatively employed to grow chains from latex particles.

## 1.1. Metal-mediated radical controlled polymerization

### 1.1.a. Historical development

In 1995, Matyjaszewski<sup>7</sup> and Sawamoto<sup>8</sup> discovered at the same time and independently a new method of controlled radical polymerization based on the principles of ATRA<sup>11</sup> in which the dormant-active equilibrium is catalyzed by a transition metal catalyst. The system developed by Matyjaszewski used copper catalyst and was called atom transfer radical polymerization (ATRP), whereas Sawamoto used a complex based on [Ru(II)] and called this method “transition metal-catalyzed living radical polymerization”. In this study, the term metal-mediated (radical) polymerization will be further used.

Metal-mediated polymerizations are based on the reversible reaction of a low oxidation-state metal complex,  $M_tX_n/L$  ( $M_tX_n$  represents the metal ion in oxidation state  $n$ , and  $L$  is a ligand), with an alkyl halide ( $R-X$ ). This reaction yields radicals and the corresponding high-oxidation-state metal complex,  $M_tX_{n+1}/L$  (Figure 1.3). The generated radicals propagate by the addition of monomer units and provide “well-defined” polymer. They are deactivated by the high-oxidation-state metal complex,  $M_tX_{n+1}/L$  into dormant chains.

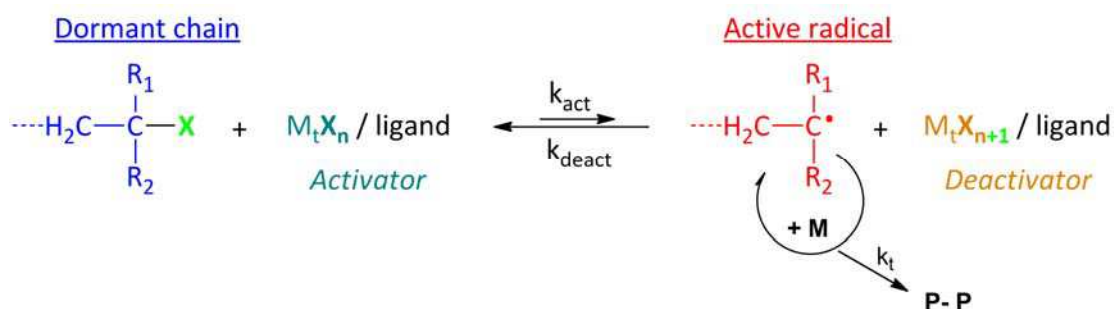


Figure 1.3. Metal-mediated polymerization mechanism.

Since its discovery, metal-mediated polymerization has been the subject of growing interest for the synthesis of polymers with well-defined molar mass and architecture. For instance, about 11 000 papers on ATRP have been published since 1995<sup>12</sup>. In his last review, Sawamoto<sup>13</sup> described the major discoveries and developments of metal-mediated polymerization, which are summarized as follows:



**Phase I (1995-2001)**

- Discovery of metal-catalyzed living radical polymerization
- Establishment of the dormant-active equilibrium concept
- Systematic development of metal catalysts and initiators
- Living radical polymerization of common conjugated monomers
- Precision synthesis for block, end-functionalized, (co)polymers

**Phase II (2001-2008)**

- Extension to iron-based catalysts (abundant and safer)
- Extremely active catalysts (reduction of catalyst concentration)
- Removal, recovery, and recycling of metal catalysts
- Living radical polymerizations of functionalized monomers
- Precision synthesis of (multi)functional polymers
- Bidirectional interaction with organic and organometallic chemistry particularly in catalyst development
- Extended applications in biology, biochemistry, medicine, and nanotechnology
- Combination with other controlled systems (polymerizations/reactions)

While the main target in phase I was based on more fundamental interests (improvement in control, clarification of the mechanism, block copolymerization, etc.), the demands for metal-mediated polymerization have been shifted to more applied interests requiring new development strategies (*Figure 1.4*).

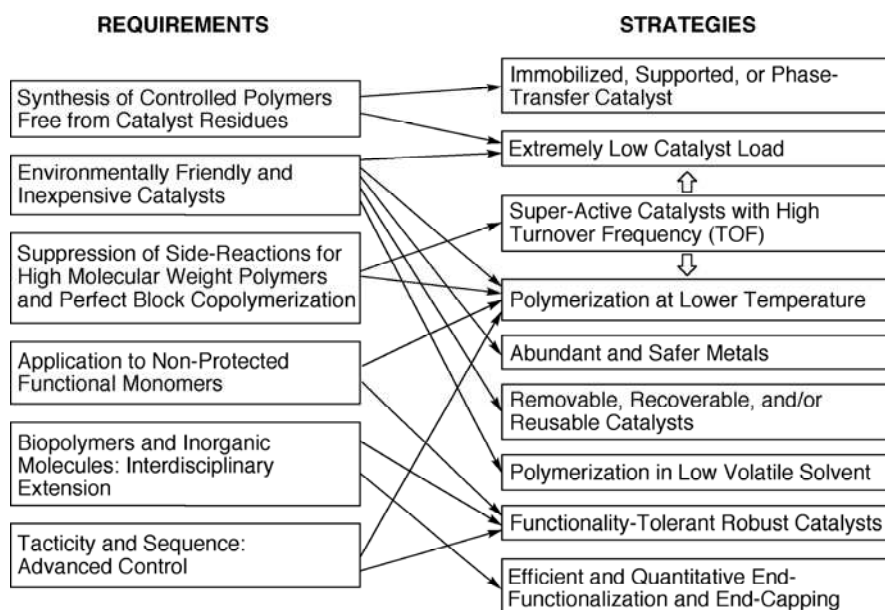


Figure 1.4. New requirements and strategies for metal-mediated polymerization. Reprinted with permission from Ref 13. Copyright 2009 American Chemical Society.

### 1.1.b. Components of the system

Metal-mediated radical polymerization (MMRP) is a multi-component system, which has been thoroughly investigated since it was developed. The main components are the initiator, the monomers and a metal complex, including an activator and a deactivator species. The choice of the solvent and the reaction temperature also significantly affected the polymerization.

#### 1.1.b.i. Initiator

In MMRP, fast and quantitative initiation is required to achieve well-defined polymers. Generally halogenated-components (R-X) are employed as initiators. To facilitate the radical generation, the R group must contain a conjugated or radical stabilizing group such as ester (haloester)<sup>14-15-16</sup>, ketone ( $\alpha$ -haloketone)<sup>17-18</sup>, phenyl (benzylic halides)<sup>19-20</sup>, nitrile ( $\alpha$ -halonitriles)<sup>20-21</sup> or arenesulfonyl group (sulfonyl halides)<sup>22-23</sup> (Figure 1.5). Alkyl halides (CCl<sub>4</sub> or CBr<sub>4</sub>) can also act as initiator but present poor initiation efficiencies. Moreover, multi functional initiations and chain transfer reactions often took place in presence of those initiators.

The stabilization order in the initiators is  $CN > C(O)R > C(O)OR > Ph > Cl$  and increasing the functional group number may increase the activity of the alkyl halide. Tertiary alkyl halides are better initiators than secondary alkyl halides themselves better initiators than primary alkyl halides<sup>24-25-26</sup>.

	X = Cl, Br, I	X = Cl, Br, I	X = Cl, Br	X = Br, I	X = Cl, Br	X = Cl, Br
<b>Radical Stabilizing group</b>	Phenyl	Ester	Nitrile	Ester	Pheny/Ester	Ester
<b>Monomer model</b>	Styrene	Acrylate	Acrylonitrile	Methacrylate	Styrene/Acrylate	Methacrylate
<b>Carbon radical</b>	Secondary	Secondary	Secondary	Tertiary	Secondary	Tertiary

Figure 1.5. Examples for common ATRP initiators. Adapted from Sawamoto et al.<sup>13</sup>

Bromine and chlorine are the most frequently used halogen atoms. The bond strength order in the alkyl halides is  $R-Cl > R-Br > R-I$  indicating that alkyl chlorides are the less efficient initiators and alkyl iodides the most efficient ones. The selection of the halogen depends on the metal complex and particularly on the halogen affinity of the metal so called halophilicity, parameter that follows the Hard and Soft Acid Base (HSAB) theory<sup>27</sup>. For instance, “soft” Ru is more compatible with “soft” Br than Cl and “hard” Cl with “hard” Fe.

The choice of the halogen also depends on the monomer. For example, Cl is more suitable for methacrylates and Br is more adapted for acrylates and styrenes.

### 1.1.b.ii. Monomer

Metal-mediated polymerization is based on the reversible activation on the carbon-halide bond derived from polymer chain end. Thus, the carbon-halogen bond dissociation energy of the dormant terminal groups depends on the conjugation effect. The more the monomer presents conjugating group, the higher the resulting radical is stable.

Among the monomers, methyl methacrylate<sup>15-28</sup>, acrylate<sup>14-29-30-31-32</sup> and styrene<sup>7-14-33</sup> are the most used in metal-mediated polymerization.

Metal-mediated radical polymerization of acrylonitrile<sup>34-35-36-37-38</sup>, acrylamide<sup>39-40-41</sup>, vinyl pyridine<sup>42</sup> and sodium (meth)acrylate<sup>43-44</sup> have also been reported.

It is important to remind that each monomer leads to a unique atom transfer equilibrium constant for active and dormant polymer species. Therefore, optimal conditions for polymerization which include concentration and type of complex, temperature, solvent need to be adapted for each monomer.

### 1.1.b.iii. Metal

In metal-mediated polymerization, the metal complex contributes to the activation and deactivation processes. Metal complex with a low oxidation state first activates the carbon-halogen bond of the initiator or of the corresponding dormant chain to generate an active radical species. In this activation step, the metal complex is oxidized to a one-electron higher oxidation state. After propagation of the radical formed with monomer units, the oxidized metal complex gives back the halogen to the latter and returns to his original low oxidation state. This catalytic cycle consists of a “one-electron” transfer, distinguished from other oxidation/reduction catalysis via two-electron transfer. Therefore, the metal center needs to present at least two states of valence with one electron difference. Moreover, it requires a moderate halophilicity to accept and release a halogen atom. It is on the basis of these requirements that transition metals have been employed for metal-mediated polymerization (*Figure 1.6*).

## Transition Metals

Scandium 21 Sc 44.955912(6)	Titanium 22 Ti 47.867(1)	Vanadium 23 V 50.9415(1)	Chromium 24 Cr 51.9961(6)	Manganese 25 Mn 54.938045(6)	Iron 26 Fe 55.845(2)	Cobalt 27 Co 58.933195(6)	Nickel 28 Ni 58.6934(4)	Copper 29 Cu 63.546(3)	Zinc 30 Zn 65.38(2)
Yttrium 39 Y 88.90585(2)	Zirconium 40 Zr 91.224(2)	Niobium 41 Nb 92.90638(2)	Molybdenum 42 Mo 95.96(2)	Technetium 43 Tc [98]	Ruthenium 44 Ru 101.07(2)	Rhodium 45 Rh 102.90550(2)	Palladium 46 Pd 106.42(1)	Silver 47 Ag 107.8682(2)	Cadmium 48 Cd 112.411(8)
Lanthanides 57-71 *	Hafnium 72 Hf 178.49(2)	Tantalum 73 Ta 180.94788(2)	Tungsten 74 W 183.84(1)	Rhenium 75 Re 186.207(1)	Osmium 76 Os 190.23(3)	Iridium 77 Ir 192.217(3)	Platinum 78 Pt 195.084(8)	Gold 79 Au 196.966569(4)	Mercury 80 Hg 200.59(2)

Transition metal  
 Transition metal commonly used in MMP  
 Transition metal reported in some examples in MMP  
 Transition metal less suitable for MMP

Figure 1.6. Transition metals used in MMP.

Among the transition metals, copper, iron and ruthenium have been the most used for metal-mediated polymerization. Metal-mediated polymerizations have been also achieved in presence of chromium, nickel, zinc, molybdenum, manganese, rhenium and osmium. The list and details of each system have been described in reviews<sup>13-42</sup>.

Some complexes with cobalt<sup>45</sup>, rhodium<sup>46</sup> and palladium<sup>47</sup> have been reported for metal-mediated polymerization but catalytic cycle of those complexes involves an oxidative addition. Therefore, these complexes might be less suitable for metal-mediated radical polymerization via one electron transfer.

### 1.1.b.iv. Ligand

The main role of the ligand in metal-mediated polymerization is to solubilize the transition-metal salt in the reaction medium and to adjust the redox potential of the metal for appropriate reactivity<sup>48</sup>.

For copper mediated polymerization, nitrogen-based ligands are most frequently used<sup>49-50-51-52</sup>. The activity of copper complexed with N-based ligands decreases with the number of coordinating site (N4 > N3 > N2 > N1). Namely, the activities of copper complexed with multidentate ligands are higher than those complexed with monodentate ones and the

activities of bridged or cyclic systems are higher than that of their linear analogues. Examples of some N-based ligands are displayed in Figure 1.7.

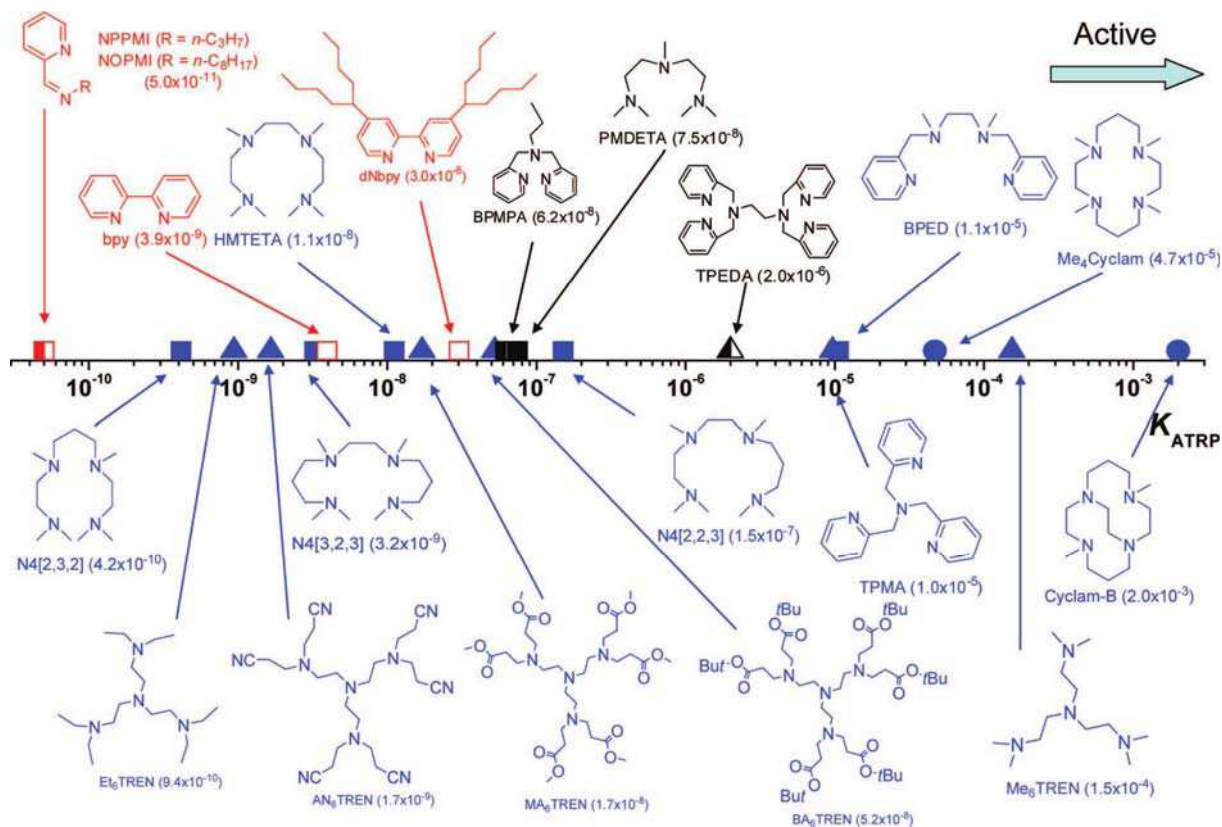


Figure 1.7. ATRP activation rate constants for various common bi-, tri- and tetradentate N-based ligands in presence of Cu(I) (where X = Br or Cl) in MeCN at 22°C. Reprinted with permission from Ref 51. Copyright 2008 American Chemical Society.

Phosphorus-based ligands have been successfully used to complex rhenium<sup>53</sup>, ruthenium<sup>54</sup>, iron<sup>55</sup>, rhodium<sup>56</sup>, nickel<sup>57</sup> and palladium<sup>47</sup> but not for copper.

### 1.1.c. Metal-mediated polymerization developments

During the development of ATRP, it was noticed that unavoidable terminations between macro-radicals led to a built-up of deactivating species shifting the equilibrium towards the dormant state and further lowers the active radical concentration. This is known as the persistent radical effect (PRE)<sup>58</sup>. This increase in deactivator concentration slows down the polymerization kinetics to such an extent that sometimes no polymerization is observed. Another drawback of traditional metal-mediated polymerization is the relatively large

amount of catalyst used, typically of the order of 0.1-1 mol % relative to monomer for ATRP. Thus, the final product contains a significant amount of metal complex.

Therefore, intensive researches have been carried out in the last decade to overcome these problems in particular the high catalyst concentration. In this purpose different development strategies have emerged<sup>59</sup>.

One of these strategies consists in removing the complex residue from the final product. Different post-purification techniques<sup>59-60</sup> have been developed including washing, extraction, precipitation and filtration through silica gel particularly at the laboratory scale. However, these methods use a large amount of solvents and complete separation of the catalyst is not achieved particularly in presence of functional polymers that interact with the metal complex.

Metal-mediated polymerizations have been performed in presence of supported catalysts so as to remove and recycle it easily. Silica or crosslinked polystyrene substrates have been usually employed as substrates. More recently, Shen et al.<sup>61</sup> reported the metal-mediated polymerization of MMA with a triamine ligand chemically attached to the surface of magnetic particles ( $\text{Fe}_3\text{O}_4$ ) providing an easy way to remove the catalyst with a magnet.

However, the most developed strategy to overcome the problem of the catalyst amount is the development of highly active catalysts and highly efficient processes with the help of numerous studies<sup>62-63-64</sup> and particularly the determination of the activation rate constant,  $k_{\text{act}}$  and deactivation rate constant,  $k_{\text{deact}}$  in the activation/deactivation equilibrium.

#### *1.1.c.i. Reverse/Simultaneous Reverse and Normal Initiation and activators generated by electron transfer ATRP*

With the development of new copper catalysts to polymerize less reactive monomers and/or to employ smaller amounts of complex, the systems became more oxygen sensitive and thus led to irreversible oxidation<sup>65-66-67-68</sup> and loss of the ATRP activator.

To overcome such oxidation problem, “reverse” ATRP (Figure 1.8) has first been developed by Matyjaszewski and co-workers<sup>69-70</sup>. This new process permitted to start an ATRP reaction with oxidatively stable, Cu(II) complexes; Cu(II) being reduced *in situ* to the activator Cu(I).

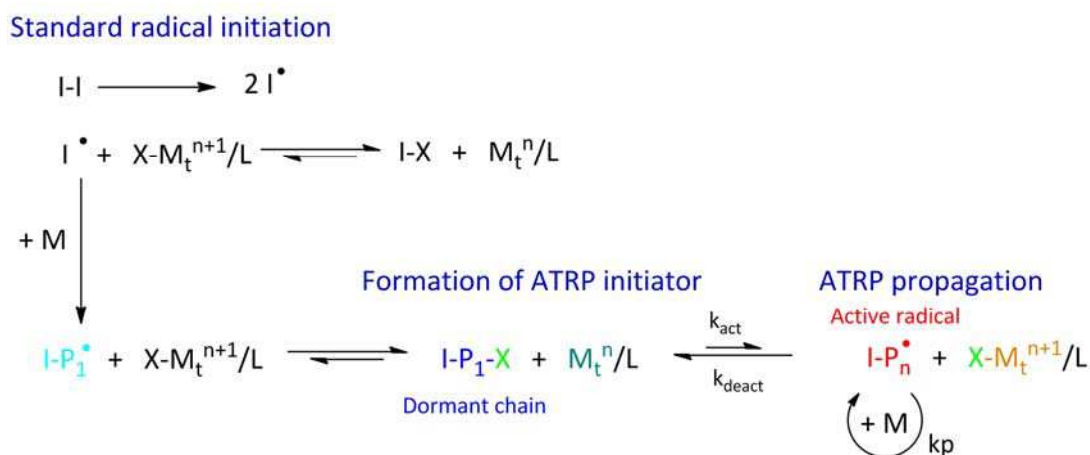


Figure 1.8. Reverse ATRP mechanism. Adapted from Matyjaszewski<sup>71</sup>.

However, this procedure requires a catalyst concentration comparable to the concentration of initiator and cannot be independently lowered. Moreover, pure block copolymers cannot be formed with this technique.

Simultaneous reverse and normal initiation (SR&NI) was developed to overcome the problem of the reverse ATRP by using dual initiating system comprising both standard free radical initiators (e.g. Azobisisobutyronitrile, AIBN) and ATRP initiators (Figure 1.9). In SR&NI, a low concentration of an active catalyst complex is generated by decomposition of a standard free radical initiator, such as AIBN, in a standard reverse ATRP procedure, while the majority of the polymer chains are initiated from an added alkyl (pseudo)halide via a normal ATRP process.



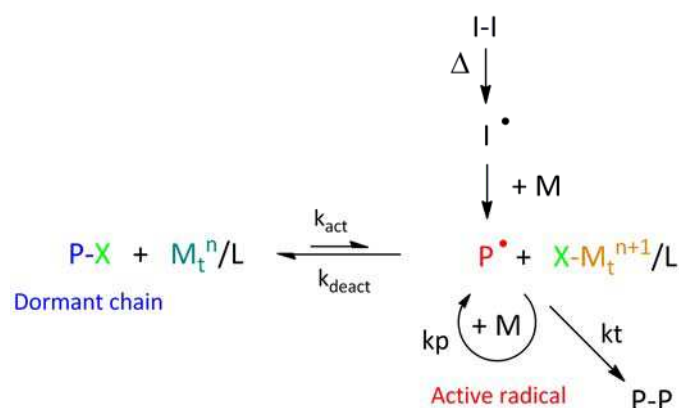


Figure 1.9. Simultaneous reverse and normal initiation ATRP (SR&NI ATRP) mechanism. Adapted from Matyjaszewski<sup>71</sup>.

SR&NI was initially developed for bulk polymerization using macroinitiators to prepare block copolymers<sup>72</sup>. However SR&NI was quickly adapted to miniemulsion systems where the use of an oxidatively stable catalyst precursor simplifies procedure<sup>73-74</sup> and allows the preparation of block, star, graft copolymers in heterogeneous media.

The main drawback of SR&NI is the formation of a small fraction of polymer chains initiated by the added free radical initiator. Rapidly, SR&NI evolved into activators generated by electron transfer (AGET)<sup>75</sup> from the deactivator using various reducing agents instead of a conventional free radical initiator (Figure 1.10).

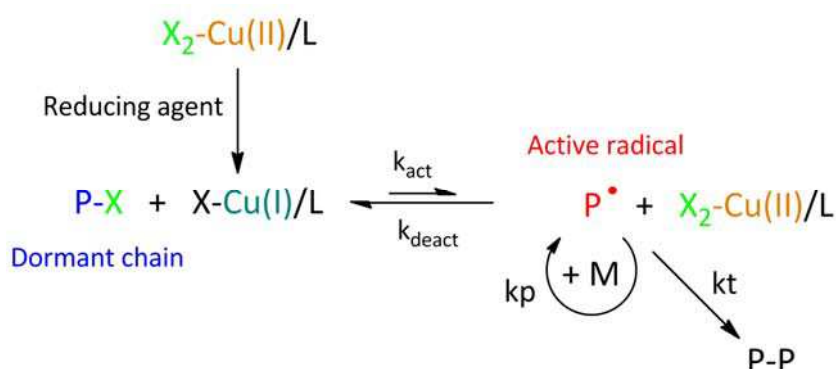


Figure 1.10. Activators generated by electron transfer ATRP (AGET ATRP) mechanism. Adapted from Matyjaszewski<sup>71</sup>.

In AGET ATRP, the reducing agents are unable to initiate new chains (in contrast to organic radicals). Thus no homopolymer is produced during block copolymerization under this procedure. The principle of AGET was demonstrated using tin(II) 2-ethylhexanoate<sup>76</sup>, ascorbic acid, glucose<sup>77-78</sup> or triethylamine<sup>79</sup> as the reducing agents. In 1998, Matyjaszewski

and co-workers report that copper(II) trifluoromethanesulfonate, Cu(OTf) complexes in the presence of Cu(0) appeared to be an excellent catalytic species for styrene and methyl methacrylate polymerization especially with the methylated triamine ligand. Retrospectively, this work provides an example of AGET ATRP with the use of zero valent copper as reducing agent<sup>80</sup>.

### 1.1.c.ii. Activators (re)generated by electron transfer ATRP and initiators for continuous activator regeneration

A major step toward reducing the amount of catalyst to ppm concentration was the development of initiation techniques called activators (re)generated by electron transfer (A(R)GET) and initiators for continuous activators regeneration (ICAR)<sup>81-82</sup>. The evolutions of the component ratio for the different systems are shown in *Table 1.1*.

*Table 1.1. Typical molar ratios of monomer (M), ATRP initiator (R-X), Cu(I)X, Cu(II)X<sub>2</sub>, ligand, and reducing agent or thermal radical initiator used in ATRP based methods. Adapted from Matyjaszewski<sup>83</sup>.*

Method	M/R-X/Cu(I)X/Cu(II)X <sub>2</sub>	Ligand	Reducing agent	Thermal radical initiator
ATRP	200 / 1 / 1 / -	1	-	-
Reverse ATRP	200 / - / - / 1	1	-	0.5
SR&NI ATRP	200 / 1 / - / 0.2	0.2	-	0.1
AGET ATRP	200 / 1 / - / 0.2	0.2	0.18	-
ICAR ATRP	200 / 1 / - / <0.01	0.01	-	<0.1
A(R)GET ATRP	200 / 1 / - / <0.01	0.1	<0.1	-

Both A(R)GET ATRP and ICAR ATRP techniques are based on the generation *in situ* of the activator species from Cu(II) via the use of reducing agents or thermal initiators respectively (*Figure 1.11*).

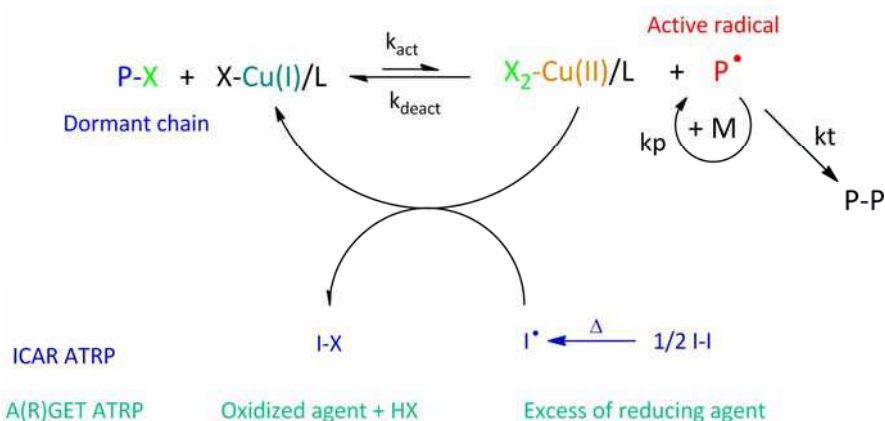


Figure 1.11. Activators (re)generated by electron transfer ATRP (A(R)GET ATRP) and initiators for continuous activators regeneration ATRP (ICAR ATRP) mechanisms. Adapted from Matyjaszewski<sup>84</sup>.

ICAR ATRP is distinguished from SR&NI procedures, as a larger excess of free radical reducing agent with respect to copper complex is employed in ICAR ATRP. The radicals are slowly generated during the reaction. With this technique, well controlled polystyrenes and poly(meth)acrylates ( $M_w/M_n < 1.2$ ) have been achieved with copper complex concentration between 5 - 50 ppm<sup>85</sup>.

The limitations of ICAR ATRP are in the synthesis of block copolymers, because the free radical initiator produces small amount of uncontrolled polymer chains. However, to compare with SR&NI, this amount is much lower since the required amount of thermal initiator is lower.

A(R)GET ATRP is a procedure that allows the use of ppm of catalyst in presence of appropriate reducing agent such as tin(II) 2-ethylhexanoate ( $\text{Sn}(\text{EH})_2$ )<sup>77</sup>, glucose<sup>77-86</sup> ascorbic acid<sup>87</sup>, phenol<sup>88</sup>, hydrazine and phenyl hydrazine<sup>81</sup>, excess inexpensive ligands<sup>89</sup>, nitrogen-containing monomers<sup>90</sup> or zero valent metal<sup>91</sup>. ARGET ATRP is an improvement of AGET ATRP. In the AGET process, the activators are generated by electron transfer, whereas in A(R)GET ATRP, the reducing agents constantly regenerate the ATRP activator, i.e. the Cu(I) species, from Cu(II) species irreversibly formed during termination processes.

The main advantages of A(R)GET ATRP are the possibility to perform the reaction without removing inhibitors or oxygen<sup>77</sup> and to prepare copolymers with higher molar masses while retaining chain end functionality due to the limited side reactions<sup>92</sup>.

For an effective A(R)GET ATRP, some requirements were specified<sup>77</sup>. The redox process should avoid the generation of initiating radicals and thus side reactions. A large excess of reducing agent has to be used. The concentration of the reducing agent has to take into account the amount of Cu(II) to be activated, the amount of air, radical traps (inhibitors), and the amount of terminated polymer chains generated in the polymerization.

Moreover, a sufficient amount of deactivator species is required in order to fix the rate of polymerization and control the reaction. In order to maintain the copper complex stability, it was demonstrated that the use of ligands strongly bound to the transition metal to create a highly active catalyst<sup>93</sup> was necessary.

More recently, Matyjaszewski and co-workers<sup>94-95</sup> proposed a new mechanism of ATRP mediated through electrochemical (re)generation of activators (eATRP). Instead of a reducing agent, the polymerization is initiated by applying a current potential. This procedure permitted to control the ratio of activator to deactivator which allowed to overcome drawbacks typically associated with conventional A(R)GET ATRP.

#### **1.1.d. Zero valent metal-mediated polymerization**

Since a few years, zero valent metal-mediated polymerization has gained in interest as it offers many attractive advantages which include ppm concentrations of deactivator, reduced polymerization costs, improved tolerance to oxygen, facile reaction setup, and simple reducing agent removal.

Two methods using zero valent metal have been reported so far and are still the subject of controversies. One approach developed by Matyjaszewski, consists in the use of zero valent metal as a reducing agent in an A(R)GET ATRP procedure. In the second approach developed by Percec, the zero valent metal act as an activator of the alkyl halide initiator via a single-electron transfer living radical polymerization (SET-LRP).

## 1.1.d.i. Single-electron transfer living radical polymerization

In 2006 Percec *et al.*<sup>96</sup> reported a highly efficient polymerization of methyl methacrylate in polar solvent, DMSO, in presence of sole Cu(0) and Me<sub>6</sub>TREN indicating a change in the reaction mechanism with respect to classical ATRP. This process was named single electron transfer-living radical polymerization (SET-LRP) and utilized elemental copper as an activating species in place of copper salts as in ATRP (Figure 1.12).

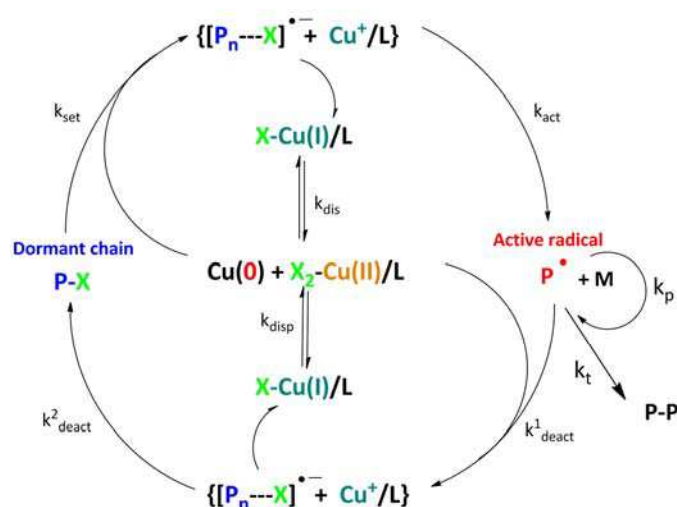


Figure 1.12. Single electron transfer-living radical polymerization (SET-LRP) mechanism. Adapted from Percec<sup>96</sup>.

SET-LRP is based on the ability of Cu(0) to abstract a halogen atom from an alkyl halide<sup>97-98-99</sup>. The formed Cu(I) disproportionates into Cu(II) that enables deactivation of the radicals and Cu(0) that promotes reactivation to propagating radicals.

Since its introduction, SET-LRP has gained in interest as SET-LRP possesses several advantages. Like in ARGET or ICAR ATRP, only a small amount of copper is present in solution. The use of elemental copper enables simple removal of the metal that forms particles in the reaction medium.

One typical characteristic of SET-LRP is the very high polymerization rate at room temperature. Moreover, high molar masses are achieved due to “perfect chain-end functionality”<sup>96</sup> as well as the syntheses of multiblock copolymers<sup>100</sup> or dendrimers<sup>101</sup>. Nevertheless, a report by Matyjaszewski indicates only 51% of chain end functionality under analogous reactions<sup>102</sup>.

SET-LRP was reported for the polymerization of acrylates<sup>96-103-104</sup>, methacrylates<sup>105-106</sup>, acrylamides<sup>107</sup>. It is also so far the only method able to control the radical polymerization of vinyl chloride<sup>96-108</sup>.

Generally, SET-LRP was carried out in presence of polar solvent, more suitable for the SET process, i.e. for the disproportionation of Cu(I), such as DMSO<sup>96</sup>, alcohols<sup>100</sup>, binary mixtures of water and other organic solvents<sup>96</sup> and pure water<sup>109-110-111</sup>. The Cu(I) constants disproportionation depending of various solvent are listed in *Table 1.2*.

*Table 1.2. Equilibrium constant for Cu(I) disproportionation ( $K_{disp}$ ) in various solvents. Adapted from Percec<sup>112</sup>.*

Solvent	$K_{disp}$
Acetone	0.03
DMF	$1.82 \times 10^4$
DMSO	1.5 - 4.4
EtOH	3.6
H <sub>2</sub> O	$0.89 \times 10^6$ - $5.80 \times 10^7$
MeCN	$6.3 \times 10^{-21}$
MeOH	4 - $6.3 \times 10^3$

Like in ATRP, the presence of a ligand is required to favor the disproportionation. Most of the studies performed the reaction in presence of PMDETA, TREN and essentially Me<sub>6</sub>TREN<sup>96</sup>.

#### 1.1.d.ii. SARA ATRP

As already reported, in 1997<sup>97</sup>, Cu(0) was first employed in ATRP to act as supplemental activator in the presence of ligand to form the major activator, Cu(I)/L. Then, Cu(0)<sup>80</sup> was employed as a reducing agent in A(R)GET ATRP to generate *in situ* the active species X-Cu(I)/L from X<sub>2</sub>-Cu(II)/L.

As Cu(0) behaves as a reducing agent and supplemental activator the process was called “supplemental activator and reducing agent” (SARA) ATRP<sup>113</sup>. The proposed mechanism for SARA ATRP is displayed in *Figure 1.13*.

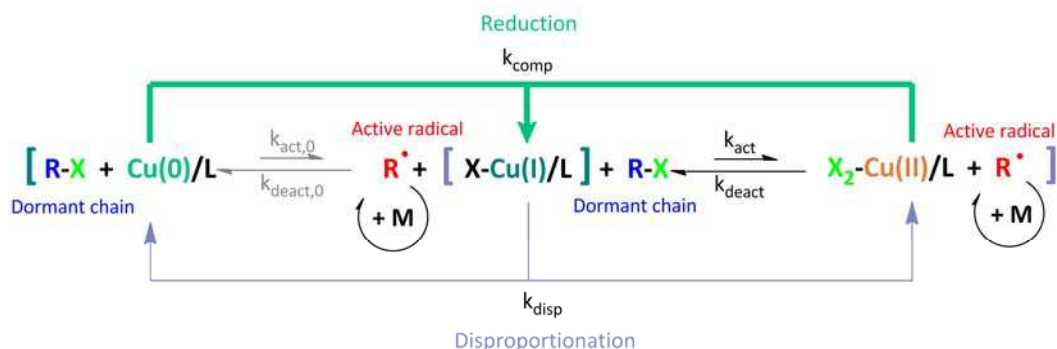


Figure 1.13. Supplemental activator and reducing agent ATRP (SARA ATRP) and initiators for continuous activators regeneration ATRP (ICAR ATRP) mechanisms. Adapted from Matyjaszewski<sup>114</sup>.

### 1.1.d.iii. Outer sphere vs inner sphere electron transfer

Since its introduction, SET-LRP has been the subject of controversy and was sometimes considered either as a form of ARGET ATRP<sup>114-115</sup> or as a similar procedure as ICAR ATRP<sup>116</sup>. The similarity between those polymerization techniques has led some researchers to specifically test their systems to identify which mechanism is operating<sup>117</sup>. SET-LRP mechanism involves an outer-sphere electron transfer (OSET) from the Cu(0) to the alkyl halide to form the Cu(I) species and a radical anions, in a similar way as that described by Bell and co-workers<sup>118</sup>.

Monteiro and co-workers<sup>103</sup> modeled the kinetics of the SET-LRP process and demonstrated the disproportionation reaction of the formed Cu(I)X into Cu(II) deactivator and nascent Cu(0) species. In another study, Percec<sup>119</sup> reported that the nature of the halide atom only have a little role on the decomposition of the radical-anions. This is because cleavage of the radical ion in the OSET process is an exothermic step, with only small energetic differences between the halides used.

The stronger argument in favour of OSET is the use of SET-LRP for controlled radical polymerization of vinyl chloride (VC)<sup>96</sup>. The polymerization of VC by CRP is quite challenging as bimolecular termination and chain transfer reactions to the monomer and polymer are not in favor of the establishment of sufficient deactivating species. In addition, VC dormant chain reactivation is not possible when conventional ATRP mediators are used, and deactivation of chains by halogen transfer becomes an irreversible chain ending event. Under SET-LRP conditions, reactivation of dormant chains was possible with copper(0) due

to more energetically favorable OSET activation. In addition, the concentration of deactivating copper(II) species was generated by disproportionation and therefore independent of chain transfer or termination. These two factors enabled the controlled polymerization of VC via SET-LRP with predictable molar masses.

Matyjaszewski claimed that the OSET process was not thermodynamically favorable which resulted in a low probability of radical anion formation. Moreover, ISET should be much faster than OSET<sup>91-102-120</sup>, i.e.  $\sim 10^{10}$  times faster according to Marcus analysis of electron transfer processes as energy barrier (26.8 kcal/mol) is not in favour of OSET compared to the energy barrier of ISET (13 kcal/mol) (Figure 1.14.)<sup>121</sup>.

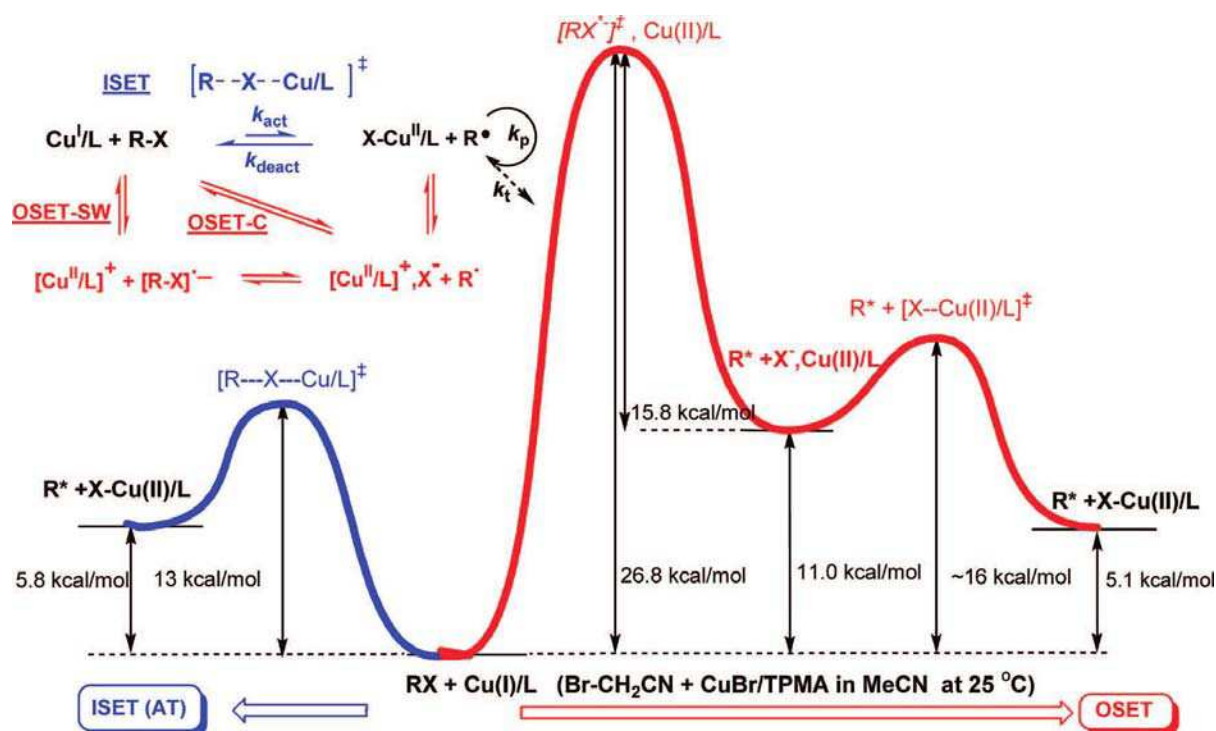


Figure 1.14. Comparison of the free energies during an ISET and OSET process for the reaction of bromoacetonitrile with Cu(I)/TPMA catalyst in acetonitrile at 20°C. Reprinted with permission from Ref 121. Copyright 2008 American Chemical Society.

Different kinetic and mechanistic studies concluded that alkyl halides preferentially react with the soluble Cu(I)/Me<sub>6</sub>TREN complex due to its very high ATRP activity<sup>122-123</sup> rather than with solid Cu(0) that has a relatively small surface area. Thus, the Cu(0) serves above all as a reducing agent and preferentially comproportionates into Cu(II) and Cu(I), formed as a “persistent radical” in the radical termination process.



It was also observed that the disproportionation/comproportionation ratio is a relatively low and for instance, only ~10% of CuBr/Me<sub>6</sub>TREN disproportionates in pure DMSO<sup>114</sup>. Since the comproportionation dominates, Cu(I) is always present in the system and is the predominant activator.

The mechanisms of SET-LRP and SARA ATRP are still under debate. However, as both of these techniques offer many attractive advantages, numerous papers using zero valent metal-mediated polymerization have been reported in the last years. Nevertheless, it was noticed that some of them used various additional names such as metal(0) mediated (controlled radical) polymerization, metal(0) catalyzed synthesis, transition metal-catalyzed living radical polymerization. Therefore, the term metal-mediated polymerization will be further used in this study and will refer to ATRP and SET based techniques.

#### *1.1.d.iv. Various metals used*

Among the transition metals used, copper is the most employed as copper catalysts are superior in metal-mediated polymerization in terms of versatility and cost in both SARA ATRP<sup>97-102-124</sup> and SET-LRP<sup>125</sup>.

For both processes, it appears that the surface area of the copper seems to be an important factor in the reaction. Copper powders with particles ranging from the micrometer<sup>96</sup> to nanometer (< 100 nm)<sup>126</sup> scale have been used for the polymerization of MA under SET-LRP conditions. It was found that using smaller copper particles increased the surface area available for activation and a larger polymerization rate was obtained. However, a slight decrease in chain end fidelity was also observed when using nanosized powder due to the substantially larger radical flux in the initial stages of the polymerization<sup>126</sup>.

The use of copper wire provided a more uniform surface area for activation than Cu(0) powder. It was found that the polymerization rate of SET-LRP was proportional to the copper surface area with a reaction order of 0.44<sup>127</sup>. The same conclusion was reported for ARGET ATRP and for ICAR ATRP<sup>128</sup>, i.e. a high surface area of Cu(0) leads to a higher rate of

generation and termination of radicals by supplemental activation. It was also shown that the rate of polymerization with copper wire could be enhanced by a pre-polymerization treatment to remove copper oxides from the surface<sup>129</sup>. Hydrazine<sup>61-130</sup> and various acids<sup>62-131</sup> have been used to enhance the polymerization rate in SET-LRP of methyl acrylate with good effect. Copper tubular reactor was also used for continuous SET-LRP but some broadening of the molar masses distributions was observed<sup>132</sup>.

Following the studies performed in presence of Cu(0), Fe(0), Zn(0) and Mg(0) were also used in ARGET ATRP<sup>133</sup>. It was concluded that the activity order of these metals was Zn(0) > Mg(0) > Fe(0) as Fe(0) is a weaker reducing agent than Zn(0) or Mg(0).

Despite the poor reactivity of the metal, Fe(0) mediated polymerization is growing in interest since Fe is environmentally friendly, cost-effective, biocompatible and abundant. Numerous papers report on the polymerization in presence of Fe(0) in powder<sup>30-96-129-134-135</sup>, wire<sup>133-136</sup> or tube<sup>137</sup>.

Samarium<sup>138</sup> and ytterbium<sup>139</sup> have been also employed in SET-LRP for the polymerization of acrylonitrile and methyl methacrylate respectively.

### **1.1.e. Metal-mediated polymerization in water solution**

#### *1.1.e.i. ATRP in water solution*

Water is the most ideal solvent for environmental, safety and economic interest. However, controlled radical polymerization performed in water is quite challenging as many problems occur during the polymerization.

In general, aqueous phase polymerizations are classified into homogeneous and heterogeneous systems. Details on heterogeneous systems have been the subject of many reviews<sup>140-141-142</sup> and will not be further discussed here.

The first successful reported aqueous ATRP was the polymerization of 2-hydroxyethyl acrylate (HEA) in presence of Cu(I)Br/bipyridine as catalyst and methyl 2-bromopropionate

or diethyl 2-methyl-2 bromomalonate as initiator<sup>143</sup>. Following this work, aqueous ATRP of neutral water soluble methacrylate, poly(ethylene oxide) methyl ether methacrylate (PEGMA)<sup>144</sup> was performed. It was shown that the reaction was faster in presence of water by comparison with the polymerization of the same monomer in bulk, which demonstrated that water affected the polymerization. Later studies on ATRP of PEGMA<sup>145</sup>, sodium 4-styrenesulfonate<sup>146-147</sup>, quaternized (alkylated) DMAEMA<sup>148-149</sup>, potassium 3-sulfopropyl methacrylate<sup>150</sup> and N-isopropylacrylamide<sup>151</sup> in protic media showed that addition of organic solvents (methanol or DMF) led to slower and better-controlled polymerizations. The same result was also found with the addition of a Cu(II)-X<sub>2</sub> complex.

Developing a successful aqueous ATRP needs some requirements, particularly concerning the choice of the catalyst due to the occurrence of several side reactions<sup>148</sup> displayed in *Figure 1.15*.

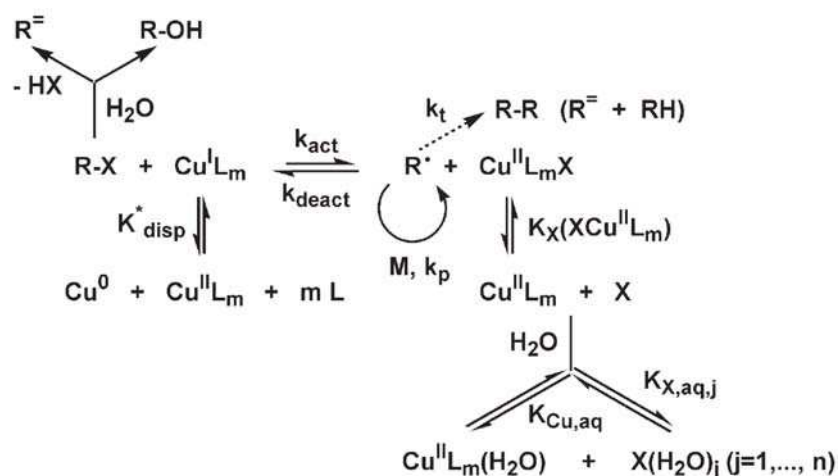


*Figure 1.15. Side reactions in copper mediated aqueous ATRP. Reprinted with permission from Ref 113. Copyright 2006 John Wiley and Sons.*

In polar solvents, the polymerization rates in ATRP are usually high even at ambient temperature, and the polymerizations are accelerated as the amount of water in the solvent is increased. Specific solvation of some polar monomers able to form hydrogen bonds with protic solvents leads to a small increase in  $k_p$ <sup>152-153</sup>. Moreover, copper-based ATRP deactivators (X<sub>2</sub>-Cu(II)/L) are relatively unstable in protic media and tend to dissociate, forming the complex Cu(II)/L<sup>148</sup>. Thus, the decrease of the deactivator concentration leads

not only to larger polymerization rate but also to an increase of the polydispersity of the polymers produced, according to the Equation 1.5.

$$M_w/M_n = 1 + \left( \frac{k_p [RX]_0}{k_{deact} [X_2 - Cu(II)/L]} \right) \times \left( \frac{2}{x} - 1 \right) \quad \text{Equation 1.5}$$

$M_w/M_n$ : molar mass dispersity

$k_p$ : propagation rate constant ( $L \cdot mol^{-1} \cdot s^{-1}$ )

$k_{deact}$ : deactivation rate constant ( $L \cdot mol^{-1} \cdot s^{-1}$ )

$[RX]$ : alkyl halide concentration

$[X_2 - Cu(II)/L]$ : copper based deactivator

Cu(I) species are generally unstable in water and tend to disproportionate. However, the stability of Cu(I) species could be improved with an appropriate ligand. In this purpose, many studies of the copper complex stability in presence of several ligands have been performed<sup>113-148-154-155</sup> (Figure 1.16). The results of these works showed that Cu(I)/bidy is more suitable for aqueous ATRP than Cu(I)/PMDETA.

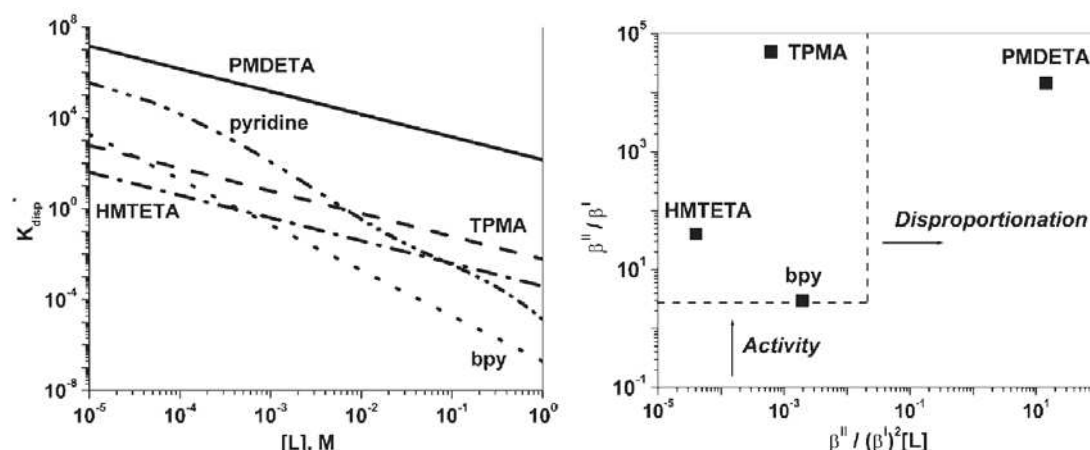


Figure 1.16. Disproportionation of Cu(I) in aqueous media in the presence of various ligands with N donor atoms as a function of free ligand concentration (left, reprinted with permission from Ref 113. Copyright 2006 John Wiley and Sons). Correlation between ATRP catalytic activity and disproportionation ability for several Cu(I) complexes ( $[L] = 0.01$  mM),  $\beta^I$  and  $\beta^{II}$  represents the stability constants of Cu(I) and Cu(II) complexes respectively (right, reprinted with permission from Ref 156. Copyright 2006 American Chemical Society).

According to the different works performed in water solution, it was concluded that the control of the aqueous ATRP could be improved by selecting ATRP catalysts that possess a high halogenophilicity (this value should depend upon the nature of the ligand and that of the metal). It is preferable to employ catalysts containing large initial amounts of deactivator and/or add extra halide salts to the system<sup>148-157-158</sup>.

SR&NI<sup>159</sup> and AGET ATRP<sup>160-161-162</sup> have been successfully performed in water solution. To provide good results in terms of both control and  $DP_n$ , the correct  $[Cu(II)]/[reducing\ agent]$  ratio and appropriate reducing agent nature are critical<sup>162</sup>. The ideal process should have a constant and high  $Cu(II)/Cu(I)$  ratio, which is difficult to achieve over the whole polymerization course by addition of a single reducing agent. In a recent work, Matyjaszewski and co-workers reported the AGET ATRP of poly(ethylene glycol) methacrylate (PEGMA) under continuous addition of ascorbic acid. Higher conversions were achieved by continuous addition of the reducing agent but a slight increase of the  $M_w/M_n$  value was observed due to irreversible termination reactions at high conversion or due to the presence of dimethacrylate impurities. The synthesis of amphiphilic star polymers with low molar mass dispersity ( $M_w/M_n$ ) and high molar mass by AGET ATRP using the “arm-first” method was successfully performed in highly diluted aqueous media<sup>163</sup> and lead to arborescent polyelectrolytes<sup>164</sup>.

#### 1.1.e.i. SET-LRP in water and in polar solvent

The solvent used in SET-LRP has a significant role as the disproportionation of the  $Cu(I)$  is a key step in the process. As previously shown, the disproportionation of  $Cu(I)$  strongly depends on the polarity of the solvent. Although some examples of SET-LRP in toluene<sup>100</sup> have been reported, most of the works performed the SET-LRP in polar solvent such as DMSO, alcohols and acetonitrile, MeCN<sup>125</sup>.

Most aqueous SET-LRP are performed in binary solvent mixtures at different content of water. In his last review article, Percec<sup>125</sup> listed the different binary mixtures employed (acetone/ $H_2O$ , DMF/ $H_2O$ , EtOH/ $H_2O$ , MeOH/ $H_2O$ ) and concluded that the addition of  $H_2O$  increased the polarity of the medium and enhanced the degree of disproportionation of  $X-Cu(I)$ , thus enhances the  $k_p^{app}$  and improves the molar mass predictability. Moreover, the binary mixtures of polar organic solvents and water seem to be useful for the polymerization of hydrophilic monomers such as N-isopropylacrylamide (NIPAM)<sup>107</sup>, poly(ethylene glycol) monomethyl ether methacrylate (poly(PEGMA)), 2-ethylhexyl acrylate (2-EHA)<sup>165-166-167</sup>.

Rosen *et al.*<sup>107</sup> investigated the solvent effect in the polymerization of NIPAM and N,N-dimethylacrylamide (DMAAm) in polar and dipolar aprotic solvents. The authors observed a “time dependence of disproportionation”, with increased disproportionation after greater reaction time. This time dependence is more significant in aqueous media, due to the insolubility of CuCl in H<sub>2</sub>O and thus, might be just the result of the limited solubility of X-Cu(I) crystals. This “time dependent disproportionation” is not expected for X-Cu(I) species generated in situ because they are produced directly in solution. As expected, very fast polymerizations were observed for both monomers with good control. However, in presence of binary mixtures of organic solvents and water the polymerization was significantly accelerated. To compensate the extremely fast activation and propagation, addition of external CuCl<sub>2</sub> was required. However, the authors concluded that the presence of solubilized CuCl<sub>2</sub>/L in the reaction mixture at the beginning of polymerization is only needed to mediate deactivation and to suppress side-reactions in the very early stages of polymerization. With sufficient extent of disproportionation and low levels of externally added CuCl<sub>2</sub>, the levels of deactivator are internally rather than externally controlled.

The SET-LRP in pure water was also performed for acrylamide and N,N-dimethyl-N-methacryloyloxyethyl-N-sulfobutyl ammonium at 25 °C in presence of 2-chloropropionamide as initiator with Cu(0) powder in the presence of Me<sub>6</sub>-TREN<sup>109</sup>. The SET-LRP of isobornyl methacrylate<sup>110</sup> was also reported using EBiB, PMDETA. However for both examples, it was observed that the polymerization was better controlled with addition of an organic solvent (DMSO) due to a too fast disproportionation of Cu(I) in water<sup>109</sup>. Interestingly, the rate of spontaneous polymerization was observed to increase up to 80 mol % of water content in DMSO after which it decreased. The decrease in the rate of polymerization above 80 mol % of water was attributed to the decreased compatibility between the aqueous phase and the hydrophobic monomeric phase<sup>110</sup>.

More recently, the SET-LRP of HEA<sup>111</sup> was successfully attempted in water using Cu(0), ethyl-2-bromoisobutyrate (EBiB) as initiator and Me<sub>6</sub>TREN, TREN or PMDETA as ligand. CuBr<sub>2</sub> was used in all experiments. The concentration of the initiator was fixed at 0.34 mol/L and a molar ratio 10/1/0.1/0.05-0.1 of HEA/EBiB/Ligand/CuBr<sub>2</sub> was selected. Generally, high

conversions (>90%) were achieved in a very short reaction time (~1h). Final molar mass values were comprised between 4 000 and 6 000 g/mol with a dispersity <1.32. Direct comparison of the kinetics of the polymerization performed in DMSO and in water, it was showed that the SET-LRP was faster in water in similar experimental conditions, due to the faster disproportionation rate. The effect of the chemical nature of the ligand was also investigated and a better control of the reaction was achieved with Me<sub>6</sub>TREN. No control at the beginning of the reaction was observed in presence of TREN. The use of PMDETA led to a faster polymerization than with Me<sub>6</sub>TREN and the polymerization was also not well controlled at the beginning. In this study, the synthesis of PEG-*b*-poly(HEA) using a PEG-Br as macroinitiator was reported and a good control over the molar masses and the  $M_w/M_n$  was observed.

## 1.2. Core-shell particle via surface-initiated polymerization

### **1.2.a. Introduction**

Emulsion polymerization allows the production of a wide range of polymers material such as adhesives, paints, binders, additives for paper, textiles and construction materials. This is due to the fact that emulsion polymerization process includes many advantages such as, the production of waterborne latexes with high molar mass polymers with high polymerization rate, the low viscosity of the reaction media and the production of polymeric materials with high specific surface area.

However, classical radical emulsion polymerization suffers from the same limitations as classical radical polymerization, i.e. non-control of the macromolecular architectures. Moreover, the types of particle morphologies produced under classical emulsion polymerization are limited.

Particle morphology strongly influences the latex properties and is thus important with regard to applications. Particularly, many applications such as painting and coating depend on latex surface properties. Therefore, there is a growing interest in the development of polymer surface modifications. In particular, modifications of latex particles have been the subject of many researches for the preparation of various morphologies, most frequently core-shell particles<sup>168</sup>.

Latex surface modification offers a rather easy way to introduce new functionality or to improve latex properties. One of these possible modifications is to bind covalently a polymer or a functional molecule using a surface initiated reaction.

Generally, polymer brushes could be prepared following two main strategies, the “grafting to” and the “grafting from” (*Figure 1.17*).

The “grafting to” strategy consists in attaching preformed polymer chains via either physisorption<sup>169</sup> or chemisorption<sup>170</sup> in which case the polymer is covalently bound to the surface. However, to produce thick and very dense polymer brushes with this strategy is



difficult due to steric repulsions between the polymer chains<sup>171-172</sup>. Furthermore, with increasing polymer molar mass, the reactive group on the substrate surface becomes less accessible for the polymer end-group.

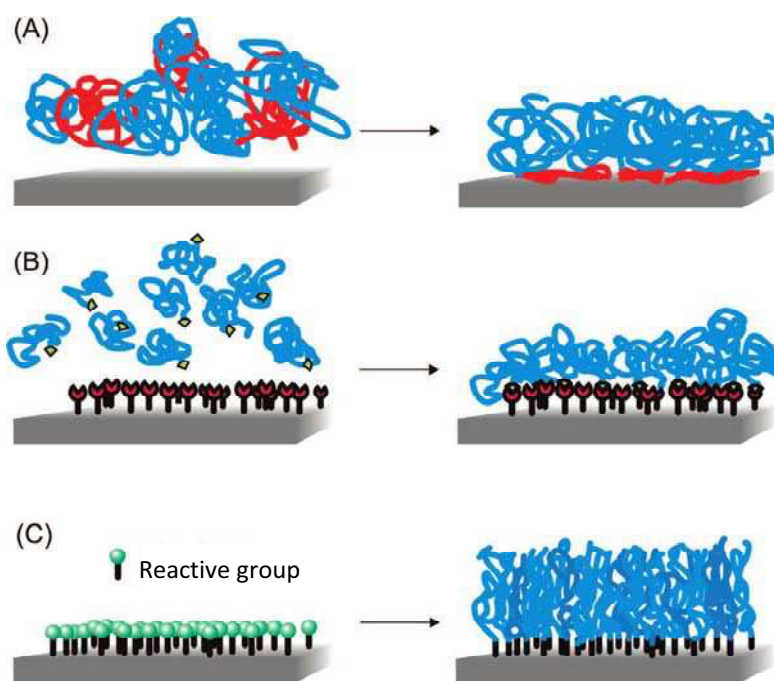


Figure 1.17. Synthetic strategies for the preparation of polymer brushes: (A) physisorption of diblock copolymers via preferential adsorption of the red blocks to the surface (grafting to approach); (B) chemisorption via reaction of appropriately end-functionalized polymers with complementary functional groups at the substrate surface ("grafting to" approach); (C) polymer brushes grown via surface-initiated polymerization techniques ("grafting from" approach). Reprinted with permission from Ref 173. Copyright 2009 American Chemical Society.

In the "grafting from" approach, polymer chains are grown from functionalized surface by surface-initiated polymerization<sup>172-174-175</sup> allowing high brush density. Over the past decade, many surface-initiated polymerization strategies have been applied to the synthesis of polymer brushes such as living ring-opening polymerization<sup>176</sup>, anionic polymerization<sup>177</sup>, living cationic polymerization<sup>178</sup>, ring-opening metathesis polymerization<sup>179</sup>, polymerization under UV<sup>180</sup>. However, most of the polymer brushes produced by the "grafting from" method are prepared via surface-initiated controlled radical polymerization<sup>173-181</sup>.

Strategies employed for grafting from polymer films or fibers or from inorganic surface are very similar to those used for polymer particles<sup>173</sup>. For this work, only the surface-initiated radical polymerization from latex particles will be further developed.

### 1.2.b. Core-shell particles synthesis by conventional free radical polymerization

In conventional radical polymerization, core-shell particles are traditionally prepared by seeded polymerizations, where the seed particles form the core and the second feed of monomer forms the shell. Thus, the morphology is thermodynamically controlled and depends on the polymer interfacial energy<sup>182</sup> (Figure 1.18). The core and the shell are not covalently linked but composed of different polymer chains.

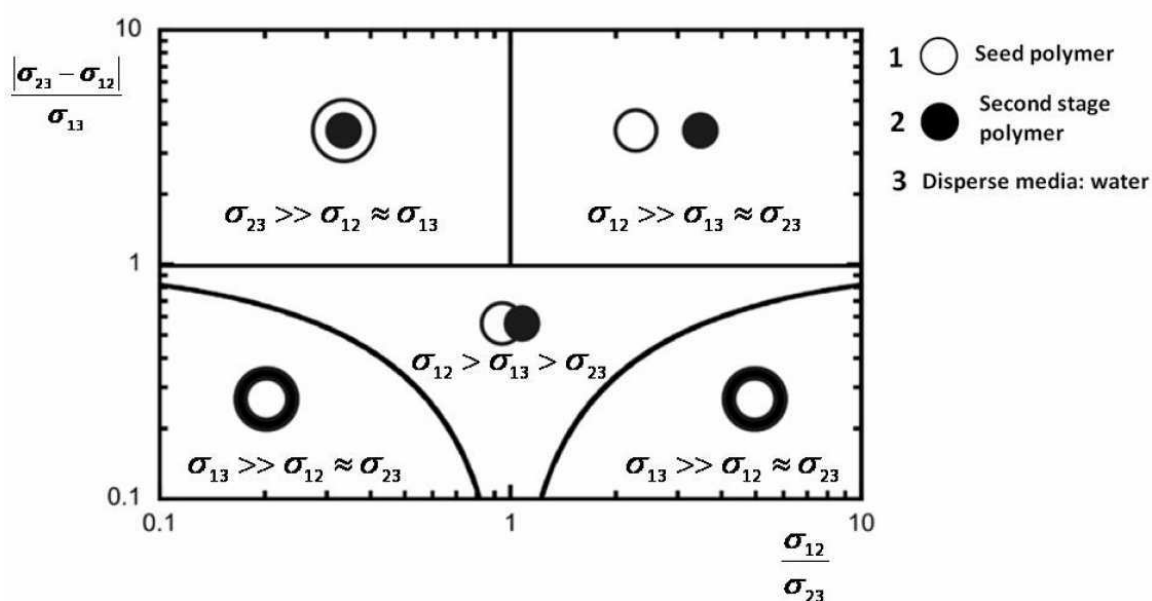


Figure 1.18. Graphical representation for the prediction of the thermodynamic morphology of composite particles. Adapted from Leiza and co-workers<sup>183</sup>.

Under this process, the formation of a hydrophilic shell at the surface of hydrophobic core is quite challenging as the hydrophilic monomer will preferentially polymerize in the water phase. Nevertheless, this type of core-shell particles, which contain a hydrophobic core and a hydrophilic shell, in particular a stimuli responsive shell, has become attractive for scientists since such systems may combine the properties characteristic of both the core and the shell.

Thermosensitive core-shell particles were first synthesized by Makino *et al.*<sup>184</sup>, Okubo and Ahmad<sup>185</sup>, and by Ballauff<sup>186</sup>. All these works reported the preparation of a shell of poly(N-isopropylacrylamide), poly(NIPAM) onto a poly(styrene) (PS) core. Pichot *et al.*<sup>187-188</sup> and Martinho *et al.*<sup>189</sup> used poly(methyl methacrylate) (poly(MMA)) substrate for the grafting of

poly(NIPAM). Recently, Xiao *et al.*<sup>190</sup> synthesized poly(acrylamide-co-styrene)-poly(acrylamide-acrylic acid) thermosensitive particles.

Generally, the synthesis of such core-shell particles is performed in two steps<sup>186</sup>. First, the core-seed latex, PS or poly(MMA), is prepared by conventional radical emulsion polymerization. Then, a small amount of the monomer NIPAM (5 wt%) is added, which creates a thin shell of poly(NIPAM) onto the core particles. After complete polymerization of the core, the poly(NIPAM) network shell is bounded to the core by a second seeded emulsion polymerization in presence of crosslinker (N,N-methylenebisacrylamide), which is carried out at  $T > LCST$  of the poly(NIPAM), i.e.  $>32^{\circ}C$ . Most probably, the poly(NIPAM) network is connected to the core particles by chain transfer in this step.

The morphology of those particles was directly investigated by cryo-TEM<sup>191</sup>. The cryo-TEM analysis showed inhomogeneities in the corona around the spherical PS core. It was concluded that during the two-step process chain transfer does not lead to complete attachment of the shell to the core and the strong swelling of the shell at room temperature may lead to a partial detachment of the chains<sup>191</sup>.

Conventional radical polymerization allows the preparation of core-shell particles and under appropriate conditions hydrophilic shell could be attached to the core particle. However, control of the grafting density, the polymer chain location and the shell thickness are quite challenging. Therefore, surface-initiated polymerization will be preferred to synthesize hydrophobic core-hydrophilic shell particles.

### **1.2.c. Surface-photoinitiated polymerization**

Photo-emulsion polymerization was employed by Ballauff *et al.*<sup>192</sup> to prepare well-defined PS-poly(NIPAM) core-shell particles. Via this “grafting-from” method, the polymer layers are formed by in situ polymerization initiated photo-initiator immobilized at the surface.

The procedure for surface-photoinitiated polymerization is performed in 3 steps. At first the core particles are prepared by conventional emulsion polymerisation. Then, after 1 hour

reaction in the first step when the styrene has not been fully converted, the particles are covered with a thin layer of a specific monomer: 2-[p-2-hydroxy-2-methylpropiophenone)]-ethylene glycol-methacrylate (HMEM) which acts as a photo-initiator. After the functionalization step, the latex is exposed to UV radiation to initiate the shell-monomer polymerization (Figure 1.19).

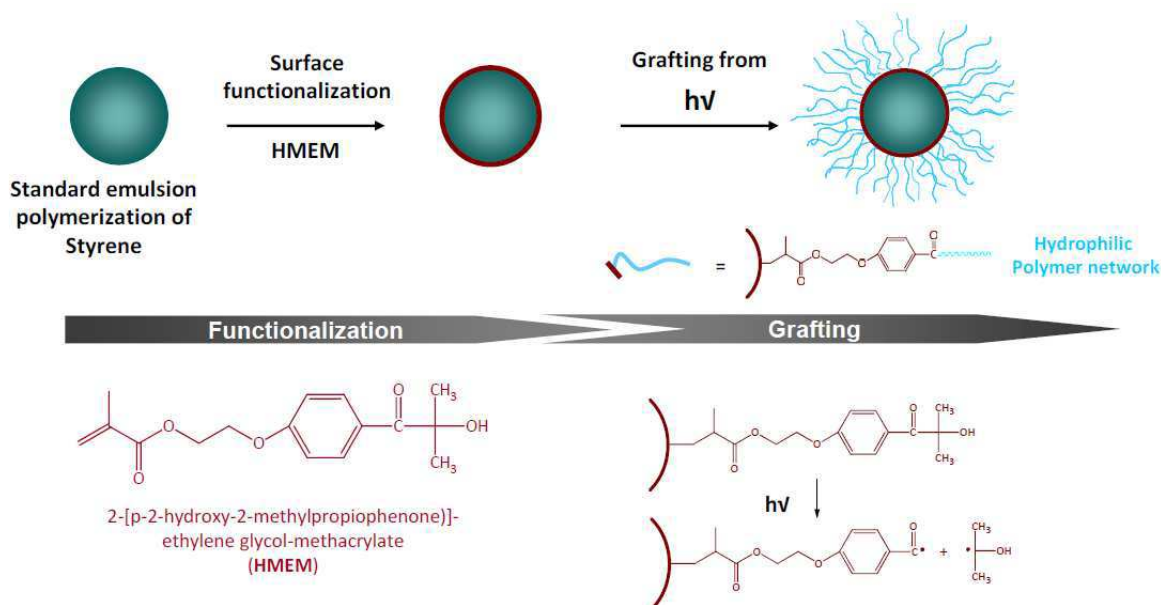


Figure 1.19. Schematic representation of core-shell particles preparation by photo-emulsion polymerization. Adapted from Ballauff<sup>192</sup>.

Different types of shell have been obtained using this procedure; core PS-shell poly((2-methylpropenyloxyethyl) trimethylammonium chloride)<sup>228</sup>, core PS-shell poly(ethylene glycol) methacrylate<sup>193</sup> and core PS-crosslinked shell poly(NIPAM)<sup>192</sup>.

Core-shell morphology was confirmed by cryo-TEM, dynamic light scattering (DLS) analyses and it was concluded that surface-photoinitiated polymerization leads to a more homogeneous cross-linked poly(NIPAM) shell than conventional emulsion polymerization.

#### 1.2.d. Surface-initiated metal-mediated polymerization

With the development of controlled radical polymerization (CRP), the “grafting from” method has been extensively employed for the controlled synthesis of core-shell particles<sup>173-181</sup>. Due to fast initiation and simultaneous growth of the chains, CRP allows grafting density and

brush thickness to be well-controlled. Moreover, CRP is tolerant to water and can thus be conducted in an aqueous medium and it is also compatible toward a wide range of monomers.

Controlled radical polymerizations such as reversible addition-fragmentation chain transfer (RAFT)<sup>194-195-196</sup>, nitroxide-mediated radical polymerization (NMP)<sup>197</sup> and photoiniferter mediated polymerization (IMP)<sup>198</sup> have been successfully employed for the synthesis of core-shell particles for the creation of a hydrophilic shell<sup>173-181</sup>. However, compared to other CRP methods, ATRP has been most extensively used to produce polymer brushes because ATRP is chemically versatile, compatible with a wide range of monomers and robust. Surface-initiated ATRP (SI-ATRP) has been performed in organic solution or in water<sup>173-199-200-201-202-203-204</sup> and particularly used on silica particles. However, only a few examples used polymer latexes<sup>181</sup> resulting from a radical emulsion polymerization as substrate for surface-initiated polymerization. This will be now further developed.

The use of aqueous functionalized latexes as support for surface-initiated ATRP (SI-ATRP) has been reported for the first time by Manuszak-Guerrini *et al.*<sup>205</sup> in 2000. The grafting strategy was to functionalize a crosslinked polystyrene latex with an inimer (i.e. a monomer bearing an alkyl halide group able to serve as an initiator in ATRP) at the particle surface and to activate it by a Cu(I) complex in the presence of a water-soluble monomer. Following this work, other teams used the same procedure to prepare core-shell particles by SI-ATRP<sup>206-207-208-209-210</sup> (Figure 1.20).

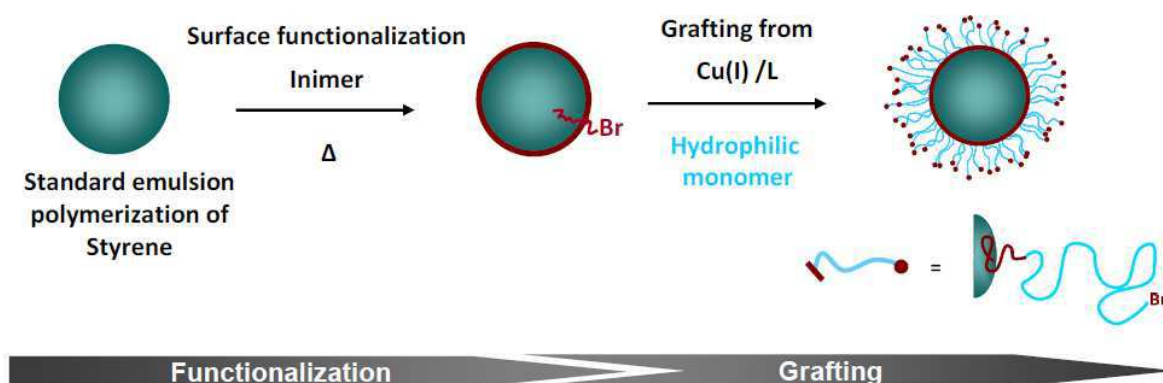


Figure 1.20. Schematic representation of core-shell particles preparation by SI-ATRP.

### 1.2.d.i. Latex functionalization

PS cores are usually used as substrate for SI-ATRP. Generally, PS latexes are prepared under conventional radical emulsion polymerization without surfactant. Under this process, latexes with low solids content (below 5 wt%) and large particles (above 500 nm) are usually achieved. To produce smaller particles (92 nm), Manuszak-Guerrini *et al.*<sup>205</sup> carried out the emulsion polymerization in presence of cationic and non ionic surfactants, which were further removed by dialysis.

Controlling the location of the initiating group at the extreme particle surface is the main parameter to provide efficient grafting reaction. Different strategies to functionalize latex particles have been reported to target a thin, uniform reactive layer at the surface and to avoid secondary nucleation.

The strategy consisting in introducing the reactive group via (co)polymerization of the inimer (*Figure 1.21*) was the most employed one. The case of polystyrene core particles and an acrylate functional monomer has been particularly investigated by Mittal *et al.*<sup>211-212</sup>. To favor the synthesis of functionalized particles and to avoid secondary nucleation, the introduction of the inimer along with a crosslinker had to be performed at 70% conversion of the monomers polymerization in the first stage emulsion polymerization. The way the functional monomer was introduced (shot or delayed addition; pure or mixed with styrene) also had an effect on the uniformity of the functionalized shell. However, in the presence of a crosslinker irregular morphologies could not be avoided.

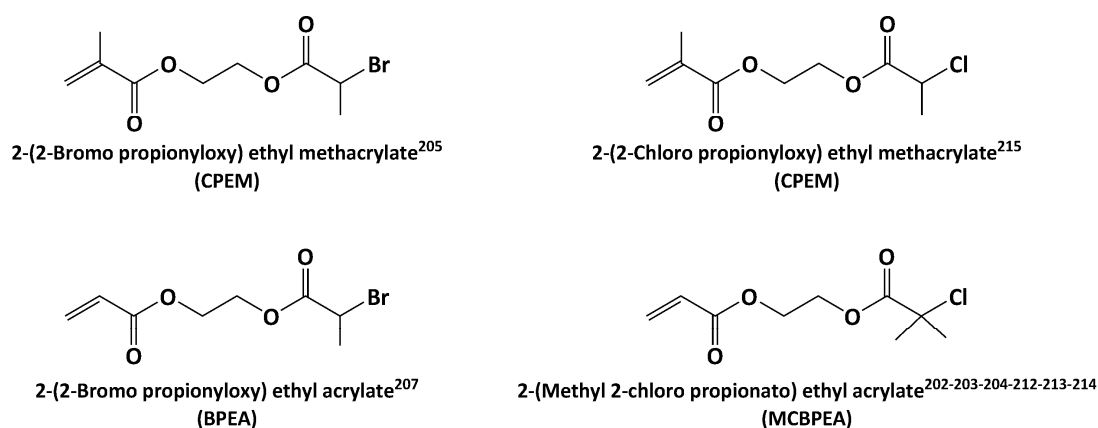


Figure 1.21. Monomers bearing an ATRP initiator group used in emulsion polymerization for the functionalization of latex particles.

A new type of functionalization was reported by Min *et al.*<sup>213</sup> using post modification of PS seed. In a first step, the crosslinked PS core was prepared under surfactant-free emulsion polymerization. Then, the particle surface was modified by chloromethylation in THF solution to functionalize particle surfaces with chlorine atom. In this work, the functionalization and the SI-ATRP were performed in organic solvent, THF and cyclohexane respectively.

In a recent study, Ishizu *et al.*<sup>214</sup> described an easier way to immobilize bromide group at the particle surface. In this case, functionalized crosslinked poly(MMA) particles were directly prepared by surfactant free-emulsion polymerization in presence of  $CBr_4$  as a chain transfer agent, providing a facile preparation of surface-immobilized ATRP initiators on colloidal polymers. The SI-ATRP was also performed in organic solvent in this work.

One example reported the functionalization of latex particles using an amphiphilic block copolymer prepared by ATRP as a stabilizer in emulsion polymerization<sup>215</sup>. In this case, the Br group at the end of the block copolymer is not covalently bound at the particle although strongly anchored.

Generally, very little information has been reported concerning the quantification or the location of the Br group using this two-step strategy probably due to the small amount of Br, which makes it difficult to detect. The good incorporation of the Br group was indirectly proven by performing the grafting reaction and controlling the location of the shell.

#### 1.2.d.ii. SI-ATRP in water solution

In all instances, the grafting reaction by ATRP was carried out with diluted latexes (low solids contents of ~5 wt%, except for the ref 215 in which the solids content was 16.6 wt%) and latexes were carefully cleaned by dialysis and/or by centrifugation to eliminate all traces of radical initiator (and to avoid the initiation of free chains in the aqueous phase when the ATRP was performed at high temperature<sup>205</sup>) and surfactant.

In the case of latexes synthesized with persulfate initiators, the negatively charged particle surface could affect the latex stability at the addition of ATRP cationic catalyst. The stabilization was maintained by the addition of nonionic surfactant just before the grafting reaction<sup>216</sup>.

SI-ATRP was usually performed at room temperature except for one example where the polymerization took place at 70°C or 80°C<sup>205</sup>.

X-Cu(I)<sup>205</sup>, mixture of X-Cu(I)/X<sub>2</sub>-Cu(II) or X-Cu(I)/Cu(0) powder<sup>206-207-208-211-216-217-218</sup> were used as catalysts for the SI-ATRP in presence of various multidentate amine ligands such as bipy, HMTETA and PMDETA. In some examples, supplemental free ATRP initiator was introduced in the latex serum<sup>207-208-216</sup> so as to enhance the control of surface initiated polymerizations. Brooks and co-workers reported the decrease of the molar mass and dispersity of the chains grafted by aqueous ATRP. However, in the case of block copolymerization, the addition of soluble initiator decreases the molar masses while dispersity of the chains<sup>207</sup> remains unaffected.

A wide range of hydrophilic monomers has been successfully grafted at the particle surface by SI-ATRP such as 2-hydroxyethyl acrylate (HEA)<sup>205</sup>, 2-(methacryloyloxy)ethyl trimethylammonium chloride (MAETACl)<sup>205</sup>, methoxyethylacrylamide (MEA)<sup>207</sup>, methoxypoly(ethylene glycol)-based *N*-substituted acrylamide macromonomers (MPEGNA<sub>m</sub>)<sup>218</sup> and a styrene derivative bearing a lactose residue (VBSAELA)<sup>219</sup>. Nevertheless *N,N*-dimethylacrylamide (DMAAm)<sup>206-216-217</sup> and NIPAM<sup>207-208-211</sup> have been particularly investigated.

No information concerning the kinetics of the SI-ATRP was reported but it appeared that complete conversion was generally never achieved even after a long polymerization time (24h<sup>205-208</sup>). It was attributed to the persistent radical effect and the accumulation of Cu(II) deactivator in the aqueous phase. Brooks and co-workers<sup>208</sup> observed that the final conversion was influenced by the monomer concentration. Monomer conversion increased with increasing monomer concentration when using HMTETA/CuCl catalyst. At high



monomer concentration, the latexes became very viscous, which probably affected the diffusion of monomer and copper complex.

Characterization of the grafted chains (molar masses, molar mass distribution, mass of chains per unit area of latex, etc.) have been particularly investigated by Brooks and co-workers<sup>206-207-208-211-216-220-221</sup>. It was concluded that parameters such as the concentration of monomer, of latex particles, of surface initiator, of deactivator [Cu(II)], and of free ATRP initiator has to be carefully adjusted to perform an efficient grafting.

At a constant grafted initiator concentration, the initial monomer concentration affects the final conversion, the grafting density and the  $M_n$  of the grafted chains and hence the shell thickness. Those three parameters increased with increasing monomer concentration. Under appropriate conditions, grafted chains with  $M_n$  above  $6 \times 10^5$  g/mol and grafting density of 0.8 chain per  $\text{nm}^2$  have been achieved. However, Brooks and co-workers<sup>208</sup> distinguished the global monomer concentration from the monomer concentration near the particle surface. Results obtained for the polymerization of NIPAM indicated lower grafting densities compared to those obtained with DMAAm under identical conditions. It was thus suggested that, monomer type also influenced the grafting reaction. The accessibility and diffusion of monomer near the interface depend on the chemical nature of the monomer and of the surface. Thus, a monomer with affinity for a particular surface could concentrate there and influence the early stages of the polymerization.

Increasing the concentration of the ATRP initiator increases the polymer grafting density. However, the nature of the surface could also affect the polymerization. In presence of a negatively charged latex (persulfate initiator), the positively charged catalyst is concentrated at the particle surface and affects the polymerization<sup>208</sup>. Chain transfer reactions to the complex can then occur as tertiary amines are known to be good radical chain transfer agents<sup>222</sup>.

The controlled character of the grafting reaction is influenced by the type of catalyst. Generally, a good control of the SI-ATRP was achieved. Low  $M_w/M_n$  were obtained, typically

in the 1.2–1.6 range in presence of PMDETA and HMTETA as ligands. The addition of supplemental deactivator, Cu(II) leads to a decrease of the  $M_w/M_n$  and  $M_n$  values at similar reaction time in accordance with ATRP mechanism. The addition of free ATRP initiator, either hydrophilic or hydrophobic, led to a decrease of  $M_n$ , but did not improve the control over the polymerization. In all instances, the presence of non-grafted polymer chains in the latex serum was noticed and was attributed to chain transfer reactions to the ligand. Recently, core-shell particles were prepared via a surface-initiated AGET ATRP procedure<sup>219</sup>. In this single work, Cu(II) complex was used in presence of ascorbic acid to initiate the polymerization.

The living character was evaluated by grafting block copolymers via a two-step SI-ATRP<sup>207-208</sup>. An increase of the molar mass and thickness of the hydrophilic layer was observed, proving an efficient re-initiation in the second step.

Different analyses were used to characterize the core-shell particles. The most current techniques are cryo-TEM, DLS, IR, NMR and elementary analysis if the shell contains a characteristic atom not present in the core. In the case of poly(NIPAM), variation of the particle size was monitored at different temperatures. Particles bearing a poly(NIPAM) shell exhibited a change in the chain conformation leading to a reduction of their hydrodynamic diameter upon an increase in temperature above the LCST. Efficient grafting reactions were proven as the variations of the diameter were completely reversible.

All the experimental conditions for the preparation of core-shell particles from latex particles via SI-ATRP in water medium are listed in *Table 1.3*.

Table 1.3. Overview of surface-initiated ATRP performed at room temperature in water medium from PS functionalized particles.

Ref	Inimer	Complex	Ligand	Shell
201 <sup>a)</sup>	BPEM	CuBr	bipy	poly(HEA) and poly(MAETACI)
202 <sup>b)</sup>	MCPEA	CuCl / CuCl <sub>2</sub> / Cu(0)	HMTETA	poly(DMAAm) and poly(NIPAM)
203 <sup>c)</sup>	MCPEA	CuCl / CuCl <sub>2</sub> / Cu(0)	HMTETA	poly(DMAAm), poly(NIPAM) and poly(MEA <sub>m</sub> ) poly(DMAAm)- <i>b</i> -poly(NIPAM), poly(DMAAm)- <i>b</i> -poly(MEA <sub>m</sub> ) poly(NIPAM)- <i>b</i> -poly(MEA <sub>m</sub> )
204 <sup>b)c)</sup>	MCPEA	CuCl / CuCl <sub>2</sub> / Cu(0)	HMTETA PMDETA	poly(NIPAM) poly(NIPAM)- <i>b</i> -poly(DMAAm)
205	BPEA	CuBr / CuBr <sub>2</sub> / Cu(0)	HMTETA	poly(NIPAM)
212 <sup>c)</sup>	MCPEA	CuCl / CuCl <sub>2</sub> / Cu(0)	HMTETA	poly(NIPAM)
213	MCPEA	CuCl / CuCl <sub>2</sub> / Cu(0)	HMTETA	poly(NIPAM)
214 <sup>b)</sup>	MCPEA	CuCl / CuCl <sub>2</sub> / Cu(0)	bipy	poly(MPEGNA <sub>m</sub> )
215	MCPEM	CuCl <sub>2</sub> / ascorbic acid	TPMA	poly(VBSAELA)

a) Reaction performed at 70-80°C

b) Addition of non ionic surfactant (Brij 35)

c) Addition of free ATRP initiator

### 1.2.d.iii. SI-SET-LRP

So far, no example of core-shell synthesis by SI-SET-LRP from latex particles and no example of SI-SET-LRP performed in pure water have been reported.

Huang and co-workers reported the preparation of amphiphilic block copolymer micelles by the “shell-first” method<sup>223-224</sup>. A double hydrophilic graft copolymers, poly(NIPAM)-*b*-[poly(HEA)-*g*-poly(2-vinylpyridine)] was prepared by metal-mediated polymerization in organic media. As the poly(NIPAM) is thermo-responsive, the copolymer exhibited “schizophrenic” micellization properties including thermo and pH-responsive behaviors in aqueous medium by a suitable combination of solution temperature and pH. The backbone was first prepared by SET-LRP of NIPAM and HEA at 25°C, using Cu(I)Br/tris(2-(dimethylamino)ethyl)amine as a complex in DMF/H<sub>2</sub>O mixture. Chloromethylation of the formed diblock copolymer poly(NIPAM)-*b*-poly(HEA) was performed with 2-chloropropionyl chloride to give a macroinitiator. Then the poly(NIPAM)-*b*-[poly(HEA)-*g*-poly(2-

vinylpyridine)] double hydrophilic graft copolymer was synthesized by ATRP using Cu(I)Br/dHbpy as a copper complex in DMF/H<sub>2</sub>O mixture. Regarding the experimental conditions, it is quite surprising that two different mechanisms were proposed, but the authors justified the SET-LRP process by the *in situ* generation of Cu(0) by the disproportionation of Cu(I).

Poly(NIPAM) was attached onto silicon<sup>225</sup> and cellulose<sup>226</sup> substrate by “grafting from” method in DMF and MeOH/H<sub>2</sub>O mixture respectively. Both examples used the term surface-initiated SET-LRP and performed the SET-LRP in presence of Cu(I)/L which disproportionate to generate Cu(0) *in situ*. Whatever the real mechanism, the grafting was proven in both cases. For the grafting of poly(NIPAM) onto silicon wafers, a good control of the surface initiated polymerization was observed but it was noticed that the addition of Cu(II)Br<sub>2</sub> and free initiator at the beginning of the polymerization was necessary for reversible radical generation and suppression of termination reactions. Poly(NIPAM) chains grafted from cellulose nanocrystals were less controlled ( $M_w/M_n > 2.1$ ) but the controlled character was improved in presence of Cu(II)Br<sub>2</sub>.

The use of Cu(0) alone for surface initiated polymerization was reported in one single example<sup>227</sup>. Poly(2-(dimethylamino) ethyl methacrylate) (poly(DMAEMA)), poly(2-(diethylamino)ethyl methacrylate) (poly(DEAEMA)), poly(2-(dimethylamino)ethyl acrylate) (poly(DMAEA)), poly(2-(tert-butylamino) ethyl methacrylate) (poly(TBAEMA)) were grafted onto silicon wafer substrate using different conditions (catalyst systems, solvents, and temperatures) These experiments are listed in *Table 1.4*.

Table 1.4. Reaction conditions for surface-initiated polymerization of DMAEMA, DEAEMA, DMAEA and TBAEMA brushes from silicon wafer substrates using ATRP [1–4] and SET-LRP [5–8] methods. Adapted from Ding and co-workers<sup>227</sup>.

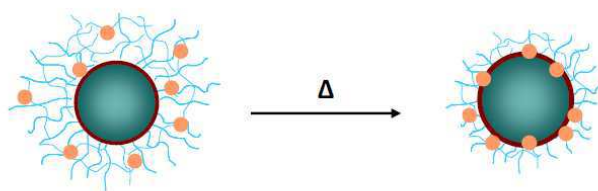
Ref	Monomer	Dry Polymer Thickness (nm)	Catalysts	Ligand	Solvent	T°C (°C)	Reaction time (h)
1	DMAEMA	29 ± 7.4	CuBr / CuBr <sub>2</sub>	bipy	IPA/H <sub>2</sub> O	40	48
2	DEAEMA	17 ± 2.2	CuCl / CuCl <sub>2</sub>	HMTETA	MeOH	60	72
3	DMAEA	34 ± 5.9	CuCl / CuCl <sub>2</sub>	Me6TREN	Bulk	90	72
4	TBAEMA	20 ± 0.7	CuCl / CuCl <sub>2</sub>	HMTETA	Bulk	90	72
5	DMAEMA	54 ± 5.8	Cu(0)	bipy	Bulk	40	10
6	DEAEMA	21 ± 1.9	Cu(0)	HMTETA	Bulk	40	4
7	PDMAEA	6 ± 0.6	Cu(0)	Me6TREN	DMSO	60	72
8	TBAEMA	17 ± 6.4	Cu(0)	HMTETA	DMSO	75	96

The authors compared surface-initiated ATRP and surface-initiated SET-LRP and demonstrated that the SET-LRP polymerizations proceeded faster and/or at relatively lower temperatures than the ATRP. The grafting was monitored by IR and XPS measurements but few information concerning the controlled character were reported.

### 1.2.e. Core-shell properties

“Smart” nanoparticles, i.e. core-shell particles bearing stimuli responsive shell (T or pH), may have several important advantages for applications based on adsorption–desorption processes.

For instance, Ballauff and co-workers immobilized metal nanoparticles (Ag, Au and Pd) inside the poly(NIPAM) shell prepared via surface-photoinitiated polymerization and used them as smart “nanoreactors”<sup>228-229</sup>. The catalytic activity of the nanoparticles was modulated by a thermodynamic transition. At low temperature, metallic nanoparticles embedded in such a network were fully accessible by the reactants. Above the transition, however, the shrinking of the network was followed by a concomitant slowing down of the diffusion of the reactants within the network. Thus the rate of reactions catalyzed by the nanoparticles was slowed down considerably. In this way, the network could act as a “nanoreactor” that can be opened or closed upon a change of temperature (*Figure 1.22*).



● **Metal nanoparticles**

Figure 1.22. Schematic representation of thermosensitive core-shell particles bearing metallic nanoparticles. Adapted from Ballauff and co-workers<sup>229</sup>.

Recently, PEG-based N-substituted acrylamide macromonomers grafted via SI-ATRP from the surface of polystyrene latexes showed good protection against nonspecific protein adsorption from blood plasma compared to the corresponding bare surfaces<sup>218</sup>. A similar result was obtained with polystyrene particles coated with lactose residues, which enhanced protection against adsorption of bovine serum albumin<sup>209</sup>.

More generally, core-shell particles with a hydrophilic shell are sterically stabilized and the corresponding latexes present a very good colloidal stability.

### 1.3. Conclusion

Since its discovery, metal-mediated polymerization (MMP) has been intensively studied as it is a versatile technique for the synthesis of value-added polymers for novel applications.

MMP has become more and more attractive for potential applications with the development of new systems presenting high efficiency at low catalyst concentration. The different parameters affecting the process have been the subject of numerous studies and are relatively well understood.

However, with the development of new methods, in particular ARGET ATRP and SET-LRP, some questions concerning the mechanism have emerged and are still under debate. The opposition between these two mechanisms leads to the emergence of numerous papers and various additional names which tend to be confusing. Whatever the real mechanism involved, the use of Cu(0) offers a rather easy way to proceed, allows the decrease the amount of catalyst and might have quite promising efficiency in water solution.

One potential application of CRP and particularly MMP is the preparation of core-shell particles by the “grafting from” process. Contrary to conventional radical polymerization, MMP allows the preparation of core-shell particles with a shell covalently bound to the core with high grafting density and good control of the shell thickness. Moreover, as the initiation takes place only at the particle surface, new morphologies can be achieved, in particularly core-shell particles with hydrophilic shell.

Particles grafted with hydrophilic polymer chains, particularly those with stimuli responsive properties, have been intensively investigated as they may have several important advantages for applications based on adsorption–desorption processes and the parameters affecting the most important outcomes (such as grafting density, chain length, and shell thickness) are now correctly understood.

However, the conditions of the synthesis (low solids contents, cleaned latexes, surfactant free latex) in those studies are not viable at the industrial scale. Moreover, most of these works were performed in normal ATRP conditions.

Therefore, the aim of this study was to find the best conditions for an efficient surface-initiated polymerization from latex particles. One of the main aim, is to develop functionalized particles as a platform to grow any kind of polymers. The functionalization procedure has to be compatible with industrial latex formulations, the initiating group has to be in minimum amount at the extreme particle surface and to be able to initiate a wide range of monomers. As the grafting reaction will be performed from “as-synthesized” latexes, the conditions with the surface-initiated polymerization have to be adjusted so as to avoid possible interactions of the remaining surfactant and initiator. Moreover, those conditions have to prevent latex destabilization, high viscosity and/or gel formations which may occur in the grafting of concentrated latex (high solids content). At last, for potential applications, the concentration of metal complex (metal salt/ligand) has to be the as low as possible.

Considering the previous literature survey and the goal we intend to reach, different parameters have to be adjusted, in particular the conditions for the grafting reaction as they are far from those generally used.

A catalyst system able to initiate efficiently the grafting reaction in water has to be the first target. Therefore, before any surface-initiated polymerization, Cu(0) mediated polymerization will be studied in water solution. This is the aim of the next chapter.



## 1.4. References

- <sup>1</sup> Szwarc, M. *Nature* **1956**, 176, 1168-1169
- <sup>2</sup> Ferington, T. E.; Tobolsky, A. V. *Journal of the American Chemical Society* **1955**, 77, 4510-4512
- <sup>3</sup> Otsu, T.; Yoshida, M. *Die Makromolekulare Chemie, Rapid Communications* **1982**, 3, 127-132
- <sup>4</sup> Solomon, D. H.; Rizzardo, E.; Cacioli, P. U.S. Patent 4,581,429, **1985**
- <sup>5</sup> Georges, M. K.; Veregin, R. P. N.; Kazmaier, P. M.; Hamer, G. K. *Macromolecules* **1993**, 26, 2987-2988
- <sup>6</sup> Georges, M. K.; Veregin, R. P. N.; Kazmaier, P. M.; Hamer, G. K. *Trends in Polymer Science* **1993**, 2, 66-72
- <sup>7</sup> Wang, J. S.; Matyjaszewski, K. *Journal of the American Chemical Society* **1995**, 117, 5614-5615
- <sup>8</sup> Kato, M.; Kamigaito, M.; Sawamoto, M.; Higashimura, T. *Macromolecules* **1995**, 28, 1721-1723
- <sup>9</sup> Chiefari, J.; Chong, Y. K.; Ercole, F.; Krstina, J.; Jeffery, J.; Le, T. P. T.; Mayadunne, R. T. A.; Meijs, G. F.; Moad, C. L.; Moad, G.; Rizzardo, E.; Thang, S. H. *Macromolecules* **1998**, 31, 5559-5562
- <sup>10</sup> Matyjaszewski, K. *Journal of Physical Organic Chemistry* **1995**, 8, 197-207
- <sup>11</sup> Curran, D. P. *Synthesis* **1988**, 489- 513
- <sup>12</sup> Matyjaszewski, K. *Macromolecules* **2012**, 45, 4015–4039
- <sup>13</sup> Ouchi, M. ; Terashima, T.; Sawamoto, M. *Chemical Reviews* **2009**, 109, 4963-5050
- <sup>14</sup> Wang, J. S.; Matyjaszewski, K. *Macromolecules* **1995**, 28, 7901-7910
- <sup>15</sup> Haddleton, D. M.; Jasieczek, C. B.; Hannon, M. J.; Shooter, A. J. *Macromolecules* **1997**, 30, 2190-2193
- <sup>16</sup> Moineau, G.; Minet, M.; Dubois, P.; Teyssie, P.; Senninger, T.; Jerome, R. *Macromolecules* **1999**, 32, 27-35
- <sup>17</sup> Uegaki, H.; Kamigaito, M.; Sawamoto, M. J. *Journal of Polymer Science Part A: Polymer Chemistry* **1999**, 37, 3003-3009

- 
- <sup>18</sup> Takahashi, H.; Ando, T.; Kamigaito, M.; Sawamoto, M. *Macromolecules* **1999**, *32*, 3820-3823
- <sup>19</sup> Matyjaszewski, K.; Wang, J. L.; Grimaud, T.; Shipp, D. A. *Macromolecules* **1998**, *31*, 1527-1534
- <sup>20</sup> Ando, T.; Kamigaito, M.; Sawamoto, M. *Tetrahedron* **1997**, *53*, 15445-15457
- <sup>21</sup> Matyjaszewski, K.; Jo, S. M.; Paik, H. J.; Gaynor, S. G. *Macromolecules* **1997**, *30*, 6398-6400
- <sup>22</sup> Percec, V.; Barboiu, B. *Macromolecules* **1995**, *28*, 7970-7972
- <sup>23</sup> Percec, V.; Kim, H. J.; Barboiu, B. *Macromolecules* **1997**, *30*, 8526-8528.
- <sup>24</sup> Goto, A.; Fukuda, T. *Macromolecular Rapid Communications* **1999**, *20*, 633-636
- <sup>25</sup> Matyjaszewski, K.; Goebelt, B.; Paik, H.-j.; Horwitz, C. P. *Macromolecules* **2001**, *34*, 430-440
- <sup>26</sup> Matyjaszewski, K.; Paik, H.-j.; Zhou, P.; Diamanti, S. J. *Macromolecules*, **2001**, *34*, 5125-5131
- <sup>27</sup> Ho, T.L. *Chemical Reviews* **1975**, *75*, 1-20
- <sup>28</sup> Grimaud, T.; Matyjaszewski, K. *Macromolecules* **1997**, *30*, 2216-2218
- <sup>29</sup> Davis, K. A.; Paik, H. J.; Matyjaszewski, K. *Macromolecules* **1999**, *32*, 1767-1776
- <sup>30</sup> Coca, S.; Jasieczek, C. B.; Beers, K. L.; Matyjaszewski, K. *Journal of Polymer Science Part A: Polymer Chemistry* **1998**, *36*, 1417-1424
- <sup>31</sup> Beers, K. L.; Matyjaszewski, K. *Journal of Macromolecular Science - Part A: Pure and Applied Chemistry* **2001**, *A38*, 731-739
- <sup>32</sup> Matyjaszewski, K.; Coca, S.; Jasieczek, C. B. *Macromolecular Chemistry and Physics* **1997**, *198*, 4011-4017
- <sup>33</sup> Wang, J. S.; Matyjaszewski, K. *Macromolecules* **1995**, *28*, 7572-7573
- <sup>34</sup> Matyjaszewski, K.; Jo, S. M.; Paik, H.-j.; Gaynor, S. G. *Macromolecules* **1997**, *30*, 6398-6400
- <sup>35</sup> Matyjaszewski, K.; Jo, S. M.; Paik, H.-j.; Shipp, D. A. *Macromolecules* **1999**, *32*, 6431-6438

- 
- <sup>36</sup> Hou, C.; Ji, C.; Qu, R.; Wang, C.; Sun, C.; Zhou, W.; Yu, M. *Journal of Applied Polymer Science* **2007**, 105, 1575–1580
- <sup>37</sup> Hou, C.; Guo, Z.; Liu, J.; Ying, L.; Geng, D. *Journal of Applied Polymer Science* **2007**, 104, 1382-1385
- <sup>38</sup> Hou, C.; Qu, R.; Sun, C.; Ji, C.; Wang, C.; Ying, L.; Jiang, N.; Xiu, F.; Chen, L. *Polymer* **2008**, 49, 3424–3427
- <sup>39</sup> Teodorescu, M.; Matyjaszewski, K. *Macromolecular Rapid Communications* **2000**, 21, 190-194
- <sup>40</sup> Huang, X.; Wirth, M. J. *Macromolecules* **1999**, 32, 1694-1696
- <sup>41</sup> Li, D.; Brittain, W. *Macromolecules* **1998**, 31, 3852-3855
- <sup>42</sup> Xia, J.; Zhang, X.; Matyjaszewski, K. *Macromolecules* **1999**, 32, 3531-3533
- <sup>43</sup> Ashford, E. J.; Naldi, V.; O'Dell, R.; Billingham, N. C.; Armes, S. P. *Chemical Communications* **1999**, 1285-1286
- <sup>44</sup> Wang, X. S.; Jackson, R. A.; Armes, S. P. *Macromolecules* **2000**, 33, 255-257
- <sup>45</sup> Matsubara, K.; Matsumoto, M. *Journal of Polymer Science Part A: Polymer Chemistry* **2006**, 44, 4222-4228
- <sup>46</sup> Kameda, N. *Polymer Journal* **2006**, 38, 516-522
- <sup>47</sup> Lecomte, P.; Drapier, I.; Dubois, P.; Teyssié, P.; Jérôme, R. *Macromolecules* **1997**, 30, 7631-7633
- <sup>48</sup> Xia, J.; Zhang, X.; Matyjaszewski, K. *ACS Symposium Series* **2000**, 760, 207-223
- <sup>49</sup> Pintauer, T.; Matyjaszewski, K. *Coordination Chemistry Reviews* **2005**, 249, 1155-1184
- <sup>50</sup> Tang, W.; Matyjaszewski, K. *Macromolecules* **2006**, 39, 4953–4959
- <sup>51</sup> Tang, W.; Kwak, Y.; Braunecker, W.; Tsarevsky, N. V.; Coote, M. L.; Matyjaszewski, K. *Journal of the American Chemical Society* **2008**, 130, 10702-10713
- <sup>52</sup> Kwak, Y.; Matyjaszewski, K. *Macromolecules* **2008**, 41, 6627-6635
- <sup>53</sup> Kotani, Y.; Kamigaito, M.; Sawamoto, M. *Macromolecules* **1999**, 32, 2420-2427

- 
- <sup>54</sup> Kato, M.; Kamigaito, M.; Sawamoto, M.; Higashimura, T. *Macromolecules* **1995**, *28*, 1721-1723
- <sup>55</sup> Matyjaszewski, K.; Wei, M.; Xia, J.; McDermott, N. E. *Macromolecules* **1997**, *30*, 8161-8164
- <sup>56</sup> Percec, V.; Barboiu, B.; Neumann, A.; Ronda, J. C.; Zhao, M. *Macromolecules* **1996**, *29*, 3665-3668
- <sup>57</sup> Uegaki, H.; Kotani, Y.; Kamigaito, M.; Sawamoto, M. *Macromolecules* **1997**, *30*, 2249-2253
- <sup>58</sup> Fischer, H. *Macromolecules* **1997**, *30*, 5666-5672
- <sup>59</sup> Tsarevsky, N. V.; Matyjaszewski, K. *Chemical Reviews* **2007**, *107*, 2270-2299
- <sup>60</sup> Shen, Y.; Tang, H.; Ding, S. *Progress in Polymer Science* **2004**, *29*, 1053-1078
- <sup>61</sup> Ding, S.; Radosz, M.; Shen, Y. *ACS Symposium Series* **2006**, *944*, 71-84
- <sup>62</sup> Braunecker, W. A.; Matyjaszewski, K. *Journal of Molecular Catalysis A: Chemical* **2006**, *254*, 155-164
- <sup>63</sup> Pintauer, T.; McKenzie, B.; Matyjaszewski, K. *ACS Symposium Series* **2003**, *854*, 130-147
- <sup>64</sup> Tsarevsky, N. V.; Tang, W.; Brooks, S. J.; Matyjaszewski, K. *ACS Symposium Series* **2006**, *944*, 56-70
- <sup>65</sup> Xia, J.; Gaynor, S. G.; Matyjaszewski, K. *Macromolecules* **1998**, *31*, 5958-5959
- <sup>66</sup> Tsarevsky, N. V.; Braunecker, W. A.; Tang, W.; Brooks, S. J.; Matyjaszewski, K.; Weisman, G. R.; Wong, E. H. *Journal of Molecular Catalysis A: Chemical* **2006**, *257*, 132-140
- <sup>67</sup> Gromada, J.; Spanswick, J.; Matyjaszewski, K. *Macromolecular Chemistry and Physics* **2004**, *205*, 551-566
- <sup>68</sup> Queffelec, J.; Gaynor, S. G.; Matyjaszewski, K. *Macromolecules* **2000**, *33*, 8629-8639
- <sup>69</sup> Xia, J.; Matyjaszewski, K. *Macromolecules* **1997**, *30*, 7692-7692
- <sup>70</sup> Xia, J.; Matyjaszewski, K. *Macromolecules* **1999**, *32*, 5199-202
- <sup>71</sup> Matyjaszewski, K. MATYJASZEWSKI POLYMER GROUP, <http://www.cmu.edu/maty/atrp-how/procedures-for-initiation-of-ATRP/index.html>
- <sup>72</sup> Gromada, J.; Matyjaszewski, K. *Macromolecules* **2001**, *34*, 7664-7671

- 
- <sup>73</sup> Matyjaszewski, K.; Gromada, J.; Li, M. *Patent Cooperation Treaty international patent application* (Carnegie Mellon University, USA) WO 03/031481, **2003**, 46
- <sup>74</sup> Min, K. E.; Li, M.; Matyjaszewski, K. *Journal of Polymer Science, Part A: Polymer Chemistry* **2005**, 43, 3616-3622
- <sup>75</sup> Jakubowski, W.; Matyjaszewski, K. *Macromolecules* **2005**, 38, 4139-4146
- <sup>76</sup> Ohno, K.; Goto, A.; Fukuda, T.; Xia, J.; Matyjaszewski, K. *Macromolecules* **1998**, 31, 2699-2701
- <sup>77</sup> Jakubowski, W.; Ke Min, K.; Matyjaszewski, K. *Macromolecules* **2006**, 39, 39-45
- <sup>78</sup> Goto, A.; Fukuda, T. *Macromolecular Rapid Communications* **1999**, 20, 633-636
- <sup>79</sup> Chambard, G.; Klumperman, B.; German, A. L. *Macromolecules* **2000**, 33, 4417-4421
- <sup>80</sup> Woodworth, B. E.; Metzner, Z.; Matyjaszewski, K. *Macromolecules* **1998**, 31, 7999-8004
- <sup>81</sup> Matyjaszewski, K.; Jakubowski, W.; Min, K.; Tang, W.; Huang, J. Y.; Braunecker, W. A.; Tsarevsky, N. V. *Proceedings of the National Academy of Sciences* **2006**, 103, 15309-15314
- <sup>82</sup> Pandey, J. D.; Saxena, O. C. *Journal of the American Chemical Society* **1969**, 397-399
- <sup>83</sup> Braunecker, W. A.; Matyjaszewski, K. *Progress in Polymer Sciences* **2007**, 32, 93-146
- <sup>84</sup> Matyjaszewski, K. *Macromolecules*, **2012**, 45, 4015-4039
- <sup>85</sup> Dong, H.; Tang, W.; Matyjaszewski, K. *Macromolecules* **2007**, 40, 2974-2977
- <sup>86</sup> Jakubowski, W.; Matyjaszewski, K. *Angewandte Chemie, International Edition* **2006**, 45, 4482-4486
- <sup>87</sup> Min, K.; Gao, H.; Matyjaszewski, K. *Macromolecules* **2007**, 40, 1789-1791
- <sup>88</sup> Gnanou, Y.; Hizal, G. *Journal of Polymer Science, Part A: Polymer Chemistry* **2004**, 42, 351-359
- <sup>89</sup> Kwak, Y.; Magenau, A. J. D.; Matyjaszewski, K. *Macromolecules* **2011**, 44, 811-819
- <sup>90</sup> Dong, H.; Matyjaszewski, K. *Macromolecules* **2008**, 41, 6868-6870
- <sup>91</sup> Zhang, Y. Z.; Wang, Y.; Matyjaszewski, K. *Macromolecules* **2011**, 44, 683-685
- <sup>92</sup> Pietrasik, J.; Dong, H.; Matyjaszewski, K. *Macromolecules* **2006**, 39, 6384-6390

- 
- <sup>93</sup> Tang, H.; Radosz, M.; Shen, Y. *Macromolecular Rapid Communications* **2006**, 27, 1127-1131
- <sup>94</sup> Magenau, A. J. D.; Strandwitz, N. C.; Gennaro, A.; Matyjaszewski, K. *Science* **2011**, 332, 81-84
- <sup>95</sup> Bortolamei, N.; Isse, A. A.; Magenau, A. J. D.; Gennaro, A.; Matyjaszewski, K. *Angewandte Chemie International Edition* **2011**, 50, 11391-11394
- <sup>96</sup> Percec, V.; Guliashvili, T.; Ladislaw, J. S.; Wistrand, A.; Stjerndahl, A.; Sienkowska, M. J.; Monteiro, M. J.; Sahoo, S. *Journal of the American Chemical Society* **2006**, 128, 14156-14165
- <sup>97</sup> Matyjaszewski, K.; Coca, S.; Gaynor, S. G.; Wei, M. L.; Woodworth 7348-7350
- <sup>98</sup> Percec, V.; Barboiu, B.; van der Sluis, M. *Macromolecules* **1998**, 31, 4053-4056
- <sup>99</sup> Otsu, T.; Yamaguchi, M.; Takemura, Y.; Kusuki, Y.; Aoki, S. *Journal of Polymer Science Part C Polymer Letters* **1967**, 5, 697-701
- <sup>100</sup> Lligadas, G.; Percec, V. *Journal of Polymer Science Part A: Polymer Chemistry* **2008**, 46, 2745-2754
- <sup>101</sup> Rosen, B. M.; Lligadas, G.; Hahn, C.; Percec, V. *Journal of Polymer Science Part A: Polymer Chemistry* **2009**, 47, 3940-3948
- <sup>102</sup> Matyjaszewski, K.; Tsarevsky, N. V.; Braunecker, W. A.; Dong, H.; Huang, J.; Jakubowski, W.; Kwak, Y.; Nicolay, R.; Tang, W.; Yoon, J. A. *Macromolecules* **2007**, 40, 7795-7806
- <sup>103</sup> Monteiro, M. J.; Guliashvili, T.; Percec, V. *Journal of Polymer Science, Part A: Polymer Chemistry* **2007**, 45, 1835-1847
- <sup>104</sup> Jiang, X.; Rosen, B. M.; Percec, V. *Journal of Polymer Science, Part A: Polymer Chemistry* **2010**, 48, 403-409
- <sup>105</sup> Fleischmann, S.; Percec, V. *Journal of Polymer Science, Part A: Polymer Chemistry* **2010**, 48, 2236-2242
- <sup>106</sup> Fleischmann, S.; Percec, V. *Journal of Polymer Science, Part A: Polymer Chemistry* **2010**, 48, 2243-2250
- <sup>107</sup> Nguyen, N. H.; Rosen, B. M.; Percec, V. *Journal of Polymer Science, Part A: Polymer Chemistry* **2010**, 48, 1752-1763

- <sup>108</sup> Hatano, T.; Rosen, B. M.; Percec, V. *Journal of Polymer Science, Part A: Polymer Chemistry* **2010**, *48*, 164-172
- <sup>109</sup> Ding, W.; LV, C.; Sun, Y.; Liu, X.; Yu, T.; Qu, G.; Luan, H. *Journal of Polymer Science Part A: Polymer Chemistry* **2009**, *49*, 432-440
- <sup>110</sup> Rajendrakumar, K.; Dhamodharan, D. *Journal of Polymer Science Part A: Polymer Chemistry* **2011**, *49*, 2165-2172
- <sup>111</sup> Nicol, E.; Derouineau, T.; Puaud, F.; Zaitsev, A. *Journal of Polymer Science Part A: Polymer Chemistry* **2012**, DOI: 10.1002/pola.26185
- <sup>112</sup> Nguyen, N. H.; Rosen, B. D.; Jiang, X.; Fleischmann, S.; Percec, V. *Journal of Polymer Science Part A: Polymer Chemistry* **2009**, *47*, 5577-5590
- <sup>113</sup> Tsarevsky, N. V.; Matyjaszewski, K. *Journal of Polymer Science Part A: Polymer Chemistry* **2006**, *44*, 5098-5112
- <sup>114</sup> Zhang, Y.; Wang, Y.; Peng, C. H.; Zhong, M.; Zhu, W.; Konkolewicz, D.; Matyjaszewski, K. *Macromolecules* **2012**, *45*, 78-86
- <sup>115</sup> Guliashvili, T.; Mendonca, P. V.; Serra, A. C.; Popov, A. V.; Coelho, J. F. J. *Chemistry - A European Journal* **2012**, *18*, 4607-4612
- <sup>116</sup> West, A. G.; Hornby, B.; Tom, J.; Ladmiraal, V.; Harrison, S.; Perrier, S. *Macromolecules* **2011**, *44*, 8034-8041
- <sup>117</sup> Liu, X. H.; Zhang, G. B.; Li, B. X.; Bai, Y. G.; Li, Y. S. *Journal of Polymer Science Part A: Polymer Chemistry* **2010**, *48*, 5439-5445
- <sup>118</sup> Bell, C. A.; Whittaker, M. R.; Gahan, L. R.; Monteiro, M. J. *Journal of Polymer Science Part A: Polymer Chemistry* **2007**, *46*, 146-154
- <sup>119</sup> Guliashvili, T.; Percec, V. *Journal of Polymer Science Part A: Polymer Chemistry* **2007**, *45*, 1607-1618
- <sup>120</sup> Isse, A. A.; Gennaro, A.; Lin, C. Y.; Hodgson, J. L.; Coote, M. L.; Guliashvili, T. *Journal of the American Chemical Society* **2011**, *133*, 6254-6264
- <sup>121</sup> Lin, C. Y.; Coote, M. L.; Gennaro, A.; Matyjaszewski, K. *Journal of the American Chemical Society* **2008**, *130*, 12762-12774
- <sup>122</sup> De Paoli, P.; Isse, A.; Bortolamei, N.; Gennaro, A. *Chemical Communications* **2011**, *47*, 3580-3582

- 
- <sup>123</sup> Bell, C. A.; Bernhardt, P. V.; Monteiro, M. J. *Journal of the American Chemical Society* **2011**, 133, 11944-11947
- <sup>124</sup> Hornby, B. D.; West, A. G.; Tom, J. C.; Waterson, C.; Harrison, S.; Perrier, S. *Macromolecular Rapid Communications* **2010**, 31, 1276-1280
- <sup>125</sup> Rosen, B. M.; Percec, V. *Chemical Reviews* **2009**, 5069-5119
- <sup>126</sup> Lligadas, G.; Rosen, B. M.; Bell, C. a.; Monteiro, M. J.; Percec, V. *Macromolecules* **2008**, 41, 8365-8371
- <sup>127</sup> Nguyen, N. H.; Rosen, B. M.; Lligadas, G.; Percec, V. *Macromolecules* **2009**, 42, 2379-2386
- <sup>128</sup> Zhong, M. J.; Matyjaszewski, K. *Macromolecules* **2011**, 44, 2668-2677
- <sup>129</sup> Levere, M. E.; Willoughby, I.; O'Donohue, S.; de Cuendias, A.; Grice, A. J.; Fidge, C.; Becer, C. R.; Haddleton, D. M. *Polymer Chemistry* **2010**, 1, 1086-1094
- <sup>130</sup> Nguyen, N. H.; Percec, V. *Journal of Polymer Science Part A: Polymer Chemistry* **2010**, 48, 5109-5119
- <sup>131</sup> Nguyen, N. H.; Percec, V. *Journal of Polymer Science Part A: Polymer Chemistry* **2011**, 49, 4241-4252
- <sup>132</sup> Chan, N.; Cunningham, M. F. Hutchinson, R. A. *Macromolecular Rapid Communications* **2011**, 32, 604-609
- <sup>133</sup> Zhang, Y. Z.; Wang, Y.; Matyjaszewski, K. *Macromolecules* **2011**, 44, 683-685
- <sup>134</sup> Zhou, L.; Zhang, Z.; Cheng, Z.; Zhou, N.; Zhu, J.; Zhang, W.; Zhu, X. *Macromolecular Chemistry and Physics* **2012**, 213, 439-446
- <sup>135</sup> Tom, J.; Hornby, B.; West, A.; Harrison, S.; Perrier, S. *Polymer Chemistry* **2010**, 1, 420-422
- <sup>136</sup> Wang, Y.; Zhang, Y. Z.; Parker, B.; Matyjaszewski, K. *Macromolecules* **2011**, 44, 4022-4025
- <sup>137</sup> Chen, H.; Zhang, M.; Yu, M.; Jiang, H. *Journal of Polymer Science Part A: Polymer Chemistry* **2011**, 49, 4721-4724
- <sup>138</sup> Chen, H.; Zong, G.; Chen, L.; Zhang, M.; Wang, C.; Qu, R. *Journal of Polymer Science Part A: Polymer Chemistry* **2011**, 49, 2924-2930
- <sup>139</sup> Liu, D., Ma, J., Chen, H., Yin, P., Ji, N.; Zong, G. *Journal of Polymer Science Part A: Polymer Chemistry* **2011**, 49, 5109-5115



- <sup>140</sup> Qiu, J.; Charleux, B.; Matyjaszewski, K. *Progress in Polymer Science* **2001**, 26, 2083-2134
- <sup>141</sup> Cunningham, M. F. *Progress in Polymer Science* **2008**, 33, 365-398
- <sup>142</sup> Zetterlund, P. B.; Kagawa, Y.; Okubo, M. *Chemical Reviews* **2008**, 108, 3747-3794
- <sup>143</sup> Coca, S.; Jasieczek, C. B.; Beers, K. L.; Matyjaszewski, K. *Journal of Polymer Science Part A: Polymer Chemistry* **1998**, 36, 1417-1424
- <sup>144</sup> Wang, X. S.; Lascelles, S. F.; Jackson, R. A.; Armes, S. P. *Chemical Communications* **1999**, 1817-1818
- <sup>145</sup> Perrier, S.; Haddleton, D. M. *Macromolecular Symposia* **2002**, 182, 261-272
- <sup>146</sup> Choi, C. K.; Kim, Y. B. *Polymere Bulletin* **2003**, 49, 433-439
- <sup>147</sup> Iddon, P. D.; Robinson, K. L.; Armes, S. P. *Polymer* **2004**, 45, 759-768
- <sup>148</sup> Tsarevsky, N. V.; Pintauer, T.; Matyjaszewski, K. *Macromolecules* **2004**, 37, 9768-9778
- <sup>149</sup> Li, Y.; Armes, S. P.; Jin, X.; Zhu, S. *Macromolecules* **2003**, 36, 8268-8275
- <sup>150</sup> Masci, G.; Bontempo, D.; Tiso, N.; Diociaiuti, M.; Mannina, L.; Capitani, D.; Crescenzi, V. *Macromolecules* **2004**, 37, 4464-4473
- <sup>151</sup> Masci, G.; Giacomelli, L.; Crescenzi, V. *Macromolecular Rapid Communications* **2004**, 25, 559-564
- <sup>152</sup> Gromov, V. F.; Khomikovskii, P. M. *Russian Chemical Reviews* **1979**, 48, 1040-1054
- <sup>153</sup> Beuermann, S.; Buback, M. *Progress in Polymer Science* **2002**, 27, 191-254
- <sup>154</sup> Navon, N.; Golub, G.; Cohen, H.; Paoletti, P.; Valtancoli, B.; Bencini, A.; Meyerstein, D. *Inorganic Chemistry* **1999**, 38, 3484-3488
- <sup>155</sup> The Chemical Society, London, Stability Constants of Metal-Ion Complexes; The Chemical Society: London, **1971** Supplement No. 1, Special Publication No. 25
- <sup>156</sup> Tsarevsky, N. V.; Matyjaszewski, K. *ACS Symposium Series* **2006**, 937, 79-94
- <sup>157</sup> Perrier, S.; Armes, S. P.; Wang, X. S.; Malet, F.; Haddleton, D. M. *Journal of Polymer Science Part A: Polymer Chemistry* **2001**, 39, 1696
- <sup>158</sup> Paneva, D.; Mespouille, L.; Manolova, N.; Degee, P.; Rashkov, I.; Dubois, P. *Macromolecular Rapid Communications* **2006**, 27, 1489-1494

- 
- <sup>159</sup> Li, M.; Min, K.; Matyjaszewski, K. *Macromolecules* **2004**, 37, 2106-2112
- <sup>160</sup> Min, K.; Gao, H.; Matyjaszewski, K. *Journal of the American Chemical Society* **2005**, 127, 3825-3830
- <sup>161</sup> Oh, J. K.; Min, K.; Matyjaszewski, K. *Macromolecules* **2006**, 39, 3161-3167
- <sup>162</sup> Oh, J. K.; Perineau, F.; Charleux, B.; Matyjaszewski, K. *Journal of Polymer Science Part A: Polymer Chemistry* **2009**, 47, 1771-1781
- <sup>163</sup> Li, W.; Matyjaszewski, K. *Journal of the American Chemical Society* **2009**, 131, 10378-10379
- <sup>164</sup> Gromadzki, D.; Tereshchenko, A.; Makuska, R. *Polymer* **2010**, 51, 5680-5687
- <sup>165</sup> Feng, C.; Shen, Z.; Gu, L.; Zhang, S.; Li, L.; Lu, G.; Huang, X. *Journal of Polymer Science Part A: Polymer Chemistry* **2008**, 46, 5638-5651
- <sup>166</sup> Masci, G.; Giacomelli, L.; Crescenzi, V. *Macromolecular Rapid Communications* **2004**, 25, 559-564
- <sup>167</sup> Feng, C.; Shen, Z.; Li, Y.; Gu, L.; Zhang, Y.; Lu, G.; Huang, X. *Journal of Polymer Science Part A: Polymer Chemistry* **2009**, 47, 1811-1824
- <sup>168</sup> Daniel, J. C. *Makromolekular Chemical Supplement* **1985**, 10, 359-390
- <sup>169</sup> Brandani, P.; Stroeve, P. *Macromolecules* **2003**, 36, 9502-9509
- <sup>170</sup> Minko, S.; Patil, S.; Datsyuk, V.; Simon, F.; Eichhorn, K. J.; Motorov, M.; Usov, D.; Tokarev, I.; Stamm, M. *Langmuir* **2002**, 18, 289-286
- <sup>171</sup> Balazs, A. C.; Singh, C.; Zhulina, E.; Chern, S. S.; Lyatskaya, Y.; Pickett, G. *Progress in Surface Science* **1997**, 55, 181-269
- <sup>172</sup> Rühle, J.; Knoll, W. *Journal of Macromolecular Science-polymer Reviews* **2002**, C42, 91-138
- <sup>173</sup> Barbey, R.; Lavanant, L.; Paripovic, D.; Schüwer, N.; Sugnaux, C.; Tugulu, S.; Klok, H. A. *Chemical Reviews* **2009**, 109, 5437-5527
- <sup>174</sup> Zhao, B.; Brittain, W. J. *Progress in Polymer Science* **2000**, 25, 677-710
- <sup>175</sup> Radhakrishnan, B.; Ranjan, R.; Brittain, W. J. *Soft Matter* **2006**, 2, 386-396
- <sup>176</sup> Jordan, R.; Ulman, A. *Journal of the American Chemical Society* **1998**, 120, 243-247

- <sup>177</sup> Ingall, M. D. K.; Honeyman, C. H.; Mercure, J. V.; Bianconi, P. A.; Kunz, R. R. *Journal of the American Chemical Society* **1999**, 121, 3607-3613
- <sup>178</sup> Zhao, B.; Brittain, W. J. *Macromolecules* **2000**, 33, 342-348
- <sup>179</sup> Kim, N. Y.; Jeon, N. L.; Choi, I. S.; Takami, S.; Harada, Y.; Finnie, K. R.; Girolami, G. S.; Nuzzo, R. G.; Whitesides, G. M.; Laibinis, P. E. *Macromolecules* **2000**, 33, 2793-2795
- <sup>180</sup> Guo, X.; Weiss, A.; Ballauff, M. *Macromolecules* **1999**, 32, 6043-6046
- <sup>181</sup> Charleux, B.; D'Agosto, F.; Delaittre, G. *Advances in Polymer Science* **2010**, 233, 125-183
- <sup>182</sup> Sundberg, D. C.; Durant, Y. J. *Polymer Reaction Engineering* **2003**, 11, 379-432
- <sup>183</sup> Herrera, V.; Pirri, R.; Asua, J. M.; Leiza, J. R., *Journal of Polymer Science Part A: Polymer Chemistry* **2007**, 45, 2484-2493
- <sup>184</sup> Makino, K.; Yamamoto, S.; Fujimoto, K.; Kawaguchi, H.; Oshima, H. *Journal of Colloid and Interface Science* **1994**, 166, 251-258
- <sup>185</sup> Okubo, M.; Ahmad, H. *Colloid and Polymer Science* **1996**, 274, 112-116
- <sup>186</sup> Dingenouts, N.; Norhausen, Ch.; Ballauff, M. *Macromolecules* **1998**, 31, 8912-8917
- <sup>187</sup> Castanheira, E. M. S.; Martinho, J. M. G.; Duracher, D.; Charreyre, M. T.; Elaissari, A.; Pichot, C. *Langmuir* **1999**, 15, 6712-6717
- <sup>188</sup> Santos, A. M.; Elaissari, A.; Martinho, J. M. G.; Pichot, C. *Polymer* **2005**, 46, 1181-1188
- <sup>189</sup> Prazeres, T. J. V.; Fedorov, A.; Martinho, J. M. G. *The Journal of Physical Chemistry* **2004**, 108, 9032-9041
- <sup>190</sup> Xiao, X. C.; Chu, L. Y.; Chen, W. M.; Wang, S.; Li, Y. *Advanced Functional Materials* **2003**, 13, 847-852
- <sup>191</sup> Crassous, J.; Drechsler, Y.; Talmon, Y.; Ballauff, M. *Langmuir* **2006**, 22, 2403-2406
- <sup>192</sup> Lu, Y.; Wittemann, A.; Drechsler, M.; Ballauff, M. *Macromolecular Rapid Communications* **2006**, 27, 1137-1141
- <sup>193</sup> Lu, Y.; Mei, Y.; Walker, R.; Ballauff, M.; Drechsler, M. *Polymer* **2006**, 47, 4985-4995
- <sup>194</sup> Hu, T. J.; You, Y. Z.; Pan, C. Y.; Wu, C. *The Journal of Physical Chemistry B* **2002**, 106, 6659-6662

- <sup>195</sup> D'Agosto, F.; Charreyre, M. T.; Pichot, C.; Gilbert, R. G.; *Journal of Polymer Science Part A: Polymer Chemistry* **2003**, 41, 1188-1195
- <sup>196</sup> Breed, D.R.; Thibault, R.; Xie, F.; Wang, Q.; Hawker, C.J.; Pine, D.J. *Langmuir* **2009**, 25, 4370-4376
- <sup>197</sup> Bian, K.; Cunningham, M.F. *Polymer* **2006**, 47, 5744-5753
- <sup>198</sup> Otsu, T.; Ogawa, T.; Yamamoto, T. *Macromolecules* **1986**, 19, 2087
- <sup>199</sup> Fristrup, C.J.; Jankova K.; Hvilsted S. *Soft Matter* **2009**, 5, 4623-4634
- <sup>200</sup> Edmondson, S.; Osborne, V.L.; Huck W. T. S. *Chemical Society Reviews* **2004**, 33, 14-22
- <sup>201</sup> Cayre, O.J.; Chagneux N.; Biggs, S. *Soft Matter* **2011**, 7, 2211-2234
- <sup>202</sup> Tsujii, Y.; Ohno, K.; Yamamoto, S.; Goto, A.; Fukuda, T. *Advances in Polymer Science* **2006**, 197, 1-45
- <sup>203</sup> Advincula, R. C.; Brittain, W. J.; Caster, K. C.; R uhe, J. (Eds.) *Polymer Brushes*, Wiley-VCH, Weinheim, Germany, **2004**
- <sup>204</sup> Ayres, N. *Polymer Chemistry* **2010**, 1, 769-777
- <sup>205</sup> Manuszak-Guerrini, M.; Charleux, B.; Vairon, J.P. *Macromolecular Rapid Communications* **2000**, 21, 669-674
- <sup>206</sup> Kizhakkedathu, J.N.; Brooks, D.E. *Macromolecules* **2003**, 36, 591-598
- <sup>207</sup> Kizhakkedathu, J.N.; Kumar K.R.; Goodman D.; Brooks D.E. *Polymer* **2004**, 45, 7471-7489
- <sup>208</sup> Kizhakkedathu, J.N. Norris-Jones R., Brooks D.E. *Macromolecules* **2004**, 37, 734-743
- <sup>209</sup> Zhang, M.; Liu L.; Wu C.; Fu G.; Zhao H.; He B. *Polymer* **2007**, 48, 1989-1997
- <sup>210</sup> Zhang, M.; Liu L.; Wu C.; Fu G.; Zhao H.; He B. *Journal of Colloid and Interface Science* **2006**, 301, 85-91
- <sup>211</sup> Mittal, V.; Matsko, N.B.; Butt e, A.; Morbidelli, M. *European Polymer Journal* **2007**, 43, 4868-4881
- <sup>212</sup> Mittal, V.; Matsko, N.B.; Butt e, A.; Morbidelli, M. *Polymer* **2007**, 48, 2806-2817
- <sup>213</sup> Min, K.; Hu, J.H. ; Wang, C.C.; Elaissari , A. *Journal of Polymer Science Part A: Polymer Chemistry* **2002**, 40, 892-900

- 
- <sup>214</sup> Liu, Y.Y.; Chen H.; Ishizu K. *Langmuir* **2011**, 27, 1168-1174
- <sup>215</sup> Muñoz-Bonilla, A.; Van Herk, A.M.; Heuts, J.P.A. *Polymer Chemistry* **2010**, 1, 624-627
- <sup>216</sup> Jayachandran, K. N.; Takacs-Cox, A.; Brooks, D. E.. *Macromolecules* **2002**, 35, 4247-4257
- <sup>217</sup> Kizhakkedathu, J. N.; Goodman, D.; Brooks, D. E. *ACS Symposium Series* **2003**, 854, 316-330
- <sup>218</sup> Kizhakkedathu, J. N.; Janzen, J.; Le, Y.; Kainthan, R. K.; Brooks, D. E. *Langmuir* **2009**, 25, 3794-3801
- <sup>219</sup> Taniguchi, T.; Kasuya, M.; Kunisada, Y.; Miyai, T.; Nagasawa, H.; Nakahira, T. *Colloids and Surfaces B: Biointerfaces* **2009**, 71, 194-199
- <sup>220</sup> Kizhakkedathu, J. N.; Goodman, D.; Brooks, D. E. *ACS Symposium Series* **2003**, 854, 316-330
- <sup>221</sup> Kizhakkedathu, J. N.; Janzen, J.; Le, Y.; Kainthan, R. K.; Brooks, D. E. *Langmuir* **2009**, 25, 3794-3801
- <sup>222</sup> Brandrup, J.; Immergut, E. H.; Eds. *Polymer Handbook*; John Wiley & Sons: New York, **1989**
- <sup>223</sup> Feng, C.; Li, Y.; Yang, D.; Li, Y.; Hu, J.; Zhai, S.; Lu, G.; Huang, X. *Journal of Polymer Science Part A: Polymer Chemistry* **2010**, 48, 15-23
- <sup>224</sup> Zhai, S.; Song, X.; Yang, D.; Chen, W.; Hu, J.; Lu, G.; Huang, X. *Journal of Polymer Science Part A: Polymer Chemistry* **2011**, 49, 4055-4064
- <sup>225</sup> Turan, E.; Caykara, T. *Journal of Polymer Science Part A: Polymer Chemistry* **2010**, 48, 5842-5847
- <sup>226</sup> Zoppe, J. O.; Habibi, Y.; Rojas, O. J.; Venditti, R. A.; Johansson, L.-S.; Efimenko, K.; Osterberg, M.; Laine, J. *Biomacromolecules* **2010**, 11, 2683-2691
- <sup>227</sup> Ding, S.; Floyd, J. A.; Walters, K. B. *Journal of Polymer Science Part A: Polymer Chemistry* **2009**, 47, 6552-6560
- <sup>228</sup> Lu, Y.; Mei, Y.; Drechsler, M.; Ballauff, M. *Angewandte Chemie International Edition* **2006**, 45, 813-816
- <sup>229</sup> Lu, Y.; Mei, Y.; Ballauff, M.; Drechsler, M. *The Journal of Physical Chemistry B* **2006**, 110, 3930-3937

## Chapter 2

# Copper-mediated polymerization in water

### Introduction

The use of Cu(0) in metal-mediated controlled radical polymerization has been particularly investigated as it offers a way to decrease the complex amount. Actually, despite the growing interest in Cu(0)-mediated polymerization observed in literature, only few examples<sup>1-2</sup> report the use of this technique in pure water. Those studies have been only very recently published and were not available when this work started.

As already reported in the previous chapter, performing copper-mediated polymerization in water is quite challenging as several side reactions may affect the good control of the polymerization<sup>3</sup>. Generally, a high activation rate constant ( $k_{act}$ ) is observed in water, which favors the generation of active radicals and thus increases termination processes<sup>3</sup>. Moreover partial dissociation of the halide ion from deactivator complex may occur in water solution providing a poor deactivation of the propagating radicals<sup>4</sup>. The choice of an appropriate ligand is all the most important in aqueous media since the performance of copper based complexes relies on the stability of the complexes. In water, some complexes Cu(II)/L and more particularly Cu(I)/L are unstable and suffer from disproportionation that affects their

activity<sup>4</sup>. At last, poor control of the polymerization may be caused by hydrolysis of the carbon-halogen bond, which decreases the chain-end functionality<sup>4</sup>.

In the particular case of aqueous A(R)GET ATRP, it was observed that an excess of halide salt favors the reformation of deactivator complex, which tends to dissociate in water<sup>4-5-6</sup>. However, this solution could not be employed in our system as an increase in the ionic force may destabilise the latex.

Therefore, before performing copper-mediated polymerization in presence of latex, some experiments have been carried out in water solution to better understand the polymerization behaviour.

To simplify the system, the reactions were performed in a homogeneous aqueous medium. Different types of hydrophilic monomers were tested with different catalyst systems. Three different initiators (*Figure 2.1*) were synthesized. The chemical structure of these initiators was chosen so as to be as close as possible to the BPEA chemical structure and to lead to water-soluble species.

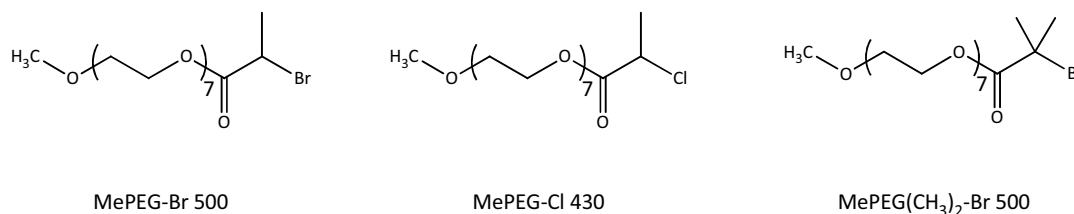


*Figure 2.1. Chemical structures of the initiators used for copper-mediated polymerization in aqueous medium.*

The aim of this study is to determine the best polymerization conditions in order to transpose them to the grafting reaction, i.e:

- A well defined initiation: as our initiation system is multi-component, the system composition has to be carefully chosen to avoid unwanted reactions such as non-controlled radical production and to control the kinetics of the initiation. Control experiments are required to check the possible reactions between the different components. The obtained

results will directly influence the choice of the composition for the grafting reaction but also the latex formulation.

- A high conversion: remaining monomer is not allowed for potential application. Complete or high monomer conversion has to be achieved and preferentially for a wide range of monomers.

- A controlled character: the controlled character of the copper-mediated radical polymerization is not the main target of this preliminary work. However, the tuning of the deactivator concentration and the absence of side reactions are of concern. Indeed, as the grafting polymerization on latexes will be performed at high solids content, termination via interparticle radical coupling will favour gel formation. By adjusting the deactivator concentration to reduce the propagating radical concentration, gel formation might be avoided. To direct the location of the chain polymer at the particle surface via covalent bonds, transfer reactions need also to be avoided. Transfer reactions could generate non grafted polymer and the accumulation of free polymer in the water could destabilize the latex by depletion effect.

This chapter will be devoted to the implementation of a model system in water. For this purpose, control experiments carried out in water will be presented in a first part. The influence of the different parameters studied will be reported in the second part.



## 2.1. Control experiments in water at room temperature

### 2.1.a. A true multicomponent system

Copper-mediated polymerization being based on a redox reaction, the presence of another redox couple, which might be able to initiate the polymerization, is prohibited. Therefore, control experiments were performed in water in presence of different component combinations (Table 2.1).

Three different hydrophilic monomers were selected (Figure 2.2): poly(ethylene glycol) methyl ether methacrylate (PEGMA 300,  $M_n = 300$  g/mol), 2-hydroxyethyl acrylate (HEA) and an acrylamide, *N*-acryloylmorpholine (NAM).

Table 2.1. Control experiments performed in water at room temperature.

Ref	Monomer		M/MePEG-Br/PMDETA/CuBr <sub>2</sub> /Cu(0) wire*	Conv. (NMR)	Time
CVSET	Nature	conc. (mol/L)	(molar equiv.)	(%)	(h)
22	PEGMA 300	0.12	13 / 1 / 0 / 0 / 0 cm	2	4
34	HEA	0.58	- / 0 / 0 / 0 / 7 cm	0	4
89	HEA	0.14	43 / 1 / 0 / 0 / 0 cm	0	7
90	HEA	0.16	88 / 0 / 1 / 0 / 0 cm	0	7
91	HEA	0.14	88 / 0 / 1 / 0 / 1.5 cm	0	7
93	HEA	0.13	43 / 1 / 0.5 / 0.2 / 0 cm	0	7
92	HEA	0.13	88 / 0 / 1 / 0.5 / 1.5 cm	0	7
37	NAM	0.23	- / 0 / 0 / 0 / 7 cm	0	4
49	NAM	0.30	37 / 1 / 0.5 / 0.1 / 0 cm	0	4
94	NAM	0.11	35 / 1 / 0 / 0 / 0 cm	0	7
95	NAM	0.11	64 / 0 / 1 / 0 / 0 cm	0	7
96	NAM	0.11	64 / 0 / 1 / 0 / 1.5 cm	0	7
97	NAM	0.11	64 / 0 / 1 / 0.5 / 1.5 cm	0	7

\*Copper wire:  $\phi = 1$  mm

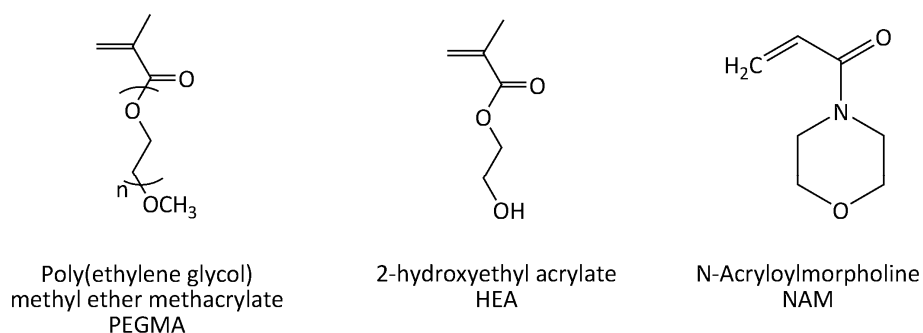


Figure 2.2. Chemical structures of the water soluble monomers used for copper-mediated polymerization in aqueous medium.

For all control experiments, no initiation was observed (the very low conversion obtained with PEGMA 300 could be neglected). No reaction thus takes place if all the components needed for an AGET ATRP initiation (ATRP initiator, Cu(0) and PMDETA/CuBr<sub>2</sub>) are not present.

### 2.1.b. Side-initiation in presence of the components present in the latexes

As the grafting reaction will be performed in the presence of raw latex, it was important to check that the remaining surfactant and initiator will not induce unwanted initiation. Control experiments were also performed in the presence of the surfactant or of the thermal initiator used in the emulsion polymerization.

These experiments were carried out in presence of NAM, Cu(0), PMDETA/CuBr<sub>2</sub> in the absence of halogenated initiator (Table 2.2).

Table 2.2. Control experiments performed in presence of Cu(0)\*, PMDETA, CuBr<sub>2</sub>, NAM, in water at room temperature with additional components, 3h reaction time.

Ref	NAM	NAM/PMDETA/CuBr <sub>2</sub>	Additional components		Conv. (NMR)
CVSET	conc. (mol/L)	(molar equiv.)	Nature	conc. (mol/L)	(%)
110	0.28	65 / 1 / 0.4	KPS	0.004	25
111	0.30	70 / 1 / 0.5	NaPS	0.004	15
113	0.50	115 / 1 / 0.4	SDS	0.002	0
114	0.30	70 / 1 / 0.4	Disponil FES77	2.5 mg/mL	0
115	0.30	76 / 1 / 0.5	ACPA	0.003	0

\* All experiments were performed in presence of 1.5 cm Cu(0) wire ( $\phi = 1$  mm)

No polymerization took place in presence of a water soluble azo-initiator (ACPA).

In the presence of potassium persulfate (KPS) or sodium persulfate (NaPS), 25% and 15% of NAM conversion were obtained, respectively. At this reaction temperature (25°C) thermal decomposition is not conceivable. The initiation observed for CVSET 110 and 111 is probably induced by the presence of PMDETA or/and CuBr<sub>2</sub> or/and Cu(0) but the true initiating system was not further investigated as all the components, PMDETA/CuBr<sub>2</sub> and Cu(0) are necessary for the copper-mediated polymerization.

0% conversion was obtained in presence of the anionic surfactants SDS and Disponil FES77 and thus, both of those surfactants could be used for the latex synthesis (*Figure 2.3*).

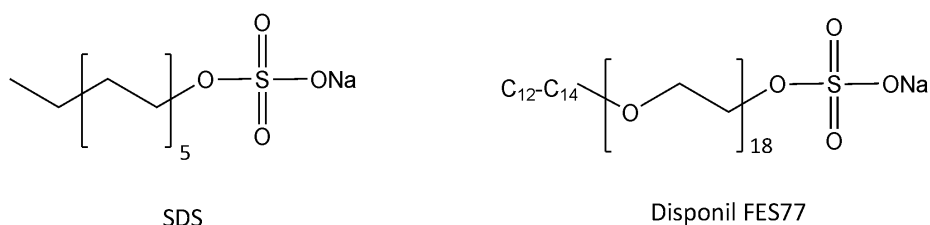


*Figure 2.3. Chemical structures of the surfactants used in the control experiments.*

## 2.2. Model system in water

### 2.2.a. Influence of the CuBr<sub>2</sub> concentration

In copper-mediated polymerization, the polymerization rate depends only on the  $[X\text{-Cu(I)/L}]/[X_2\text{-Cu(II)/L}]$  ratio<sup>7</sup>. Theoretically,  $[X_2\text{-Cu(II)/L}]$  could be decreased as long as an adequate concentration of CuBr<sub>2</sub> is maintained during the polymerization to achieve a well controlled polymerization<sup>8</sup>.

Different polymerizations were carried out to optimize the CuBr<sub>2</sub> initial concentration. These experiments are listed in Table 2.3 and the corresponding kinetics are shown in Figure 2.4.

Table 2.3. Copper-mediated polymerizations performed in presence of MePEG-Br 500 ( $8 \times 10^{-3}$  mol/L), Cu(0)\*, PMDETA, NAM, in water at room temperature. Variation of the CuBr<sub>2</sub> initial concentration.

Ref	CuBr <sub>2</sub>	NAM/MePEG-Br/PMDETA	Time	Conv. (NMR)	$M_{n,th}$ <sup>a)</sup>	$M_{n,exp}$ <sup>b)</sup>	$M_w/M_n$ <sup>b)</sup>
CVSET	(molar equiv.)	(molar equiv.)	(h)	(%)	(g/mol)	(g/mol)	
48	0	34 / 1 / 0.6	2	100	5 250	211 300	4.2
47	0.02	32 / 1 / 0.6	2	100	5 040	64 300	6.3
46	0.04	34 / 1 / 0.7	2	100	5 260	10 600	10.5
31	0.10	37 / 1 / 0.6	4	85	4 940	6 900	2.5
45	0.20	36 / 1 / 0.6	6	52	3 150	3 200	1.9
59	0.30	37 / 1 / 0.5	6	27	1 920	1 900	1.6
60	0.40	40 / 1 / 0.5	6	22	1 740	1 600	1.5
61	0.50	37 / 1 / 0.5	6	27	1 900	1 200	1.3
44	0.60	32 / 1 / 0.6	6	24	1 600	1 200	1.2

\* All experiments were performed in presence of 7 cm Cu(0) wire ( $\phi = 1$  mm)

<sup>a)</sup> Theoretical  $M_n$  calculated at final reaction conversion ( $M_{n,th} = M_I + ((m_{mono}/n_i) \times conv.)$ )

<sup>b)</sup> Number-average molar mass and  $M_w/M_n$  determined by SEC in DMF with a PMMA calibration

Before any comment concerning the kinetic of the copper-mediated polymerization or the molar mass evolution, it is important to remind that the samples have been analyzed without removing the copper complex. Thus, samples might evolve before characterizations are performed. It was particularly true for SEC measurements for which, after drying of the the sample under vacuum, it was sometimes observed that polymerizations already started or coupling reactions occurred during the sample preparation.

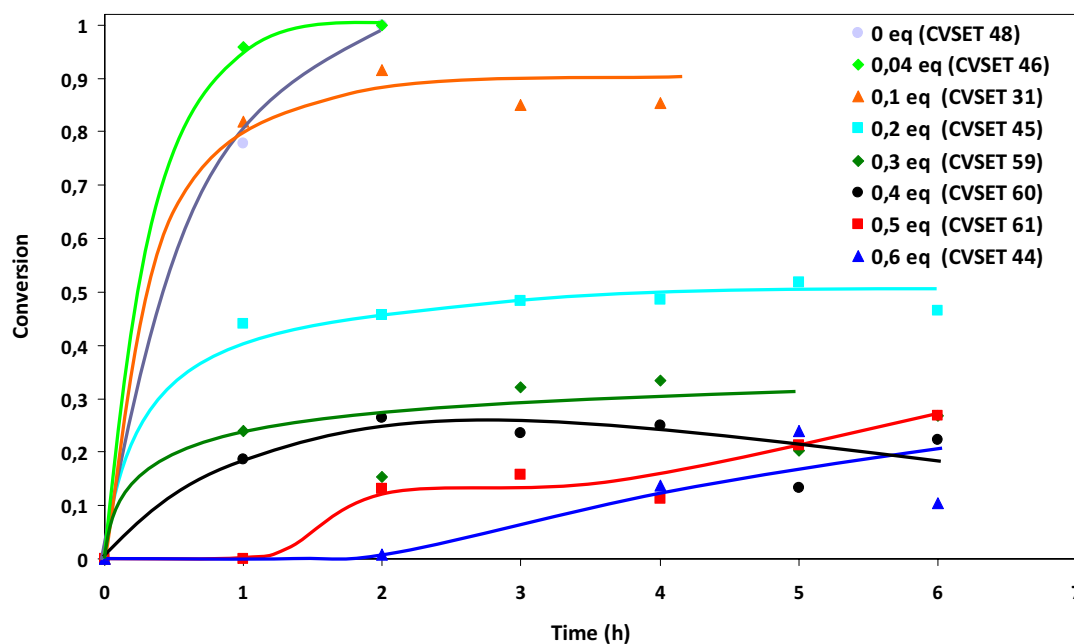


Figure 2.4. Copper-mediated polymerizations performed in presence of MePEG-Br 500 ( $8 \times 10^{-3}$  mol/L), Cu(0), PMDETA, NAM, in water at room temperature. Effect of the CuBr<sub>2</sub> concentration on the conversion of NAM. (The lines are simple guides for the eyes and have no physical meaning).

Based on Figure 2.4, it seems that the polymerization rate decreased when CuBr<sub>2</sub> concentration is increased. However, as the first sample was withdrawn at almost final conversion, it is difficult to determine the true polymerization rate.

Generally, the final conversions decreased when the initial concentration of CuBr<sub>2</sub> increased and final  $M_{n,exp}$  and  $M_w/M_n$  decreased.

Three different behaviors were observed (Figure 2.4):

- 0 to 0.1 molar equivalents of CuBr<sub>2</sub> with respect to MePEG-Br 500: complete or very high conversions (>75%) were achieved after ~1h together with high molar masses and broad mass molar distributions.

- 0.2 to 0.4 molar equivalents of CuBr<sub>2</sub> with respect to MePEG-Br 500: conversions increased to reach a plateau after 1h. The final conversions were low and the final  $M_{n,exp}$  were close to the targeted  $M_{n,theo}$  but the  $M_w/M_n$  remained still high for a controlled radical polymerization.

- 0.5 to 0.6 molar equivalents of  $\text{CuBr}_2$  with respect to MePEG-Br 500: a strong inhibition was observed up to 2h and conversion increased very slowly. The final  $M_{n,\text{exp}}$  were close to the targeted  $M_{n,\text{theo}}$  and the  $M_w/M_n$  values were low ( $<1.5$ ) as expected for a controlled radical polymerization.

Figure 2.5 displays the size exclusion chromatograms of the final polymer obtained at different  $\text{CuBr}_2$  molar equivalents. Generally, gaussian peaks were obtained, which were narrow for high  $\text{CuBr}_2$  concentrations and became broad for low  $\text{CuBr}_2$  concentrations. Complete consumption of the initiator was obtained at the end of the copper-mediated polymerization.

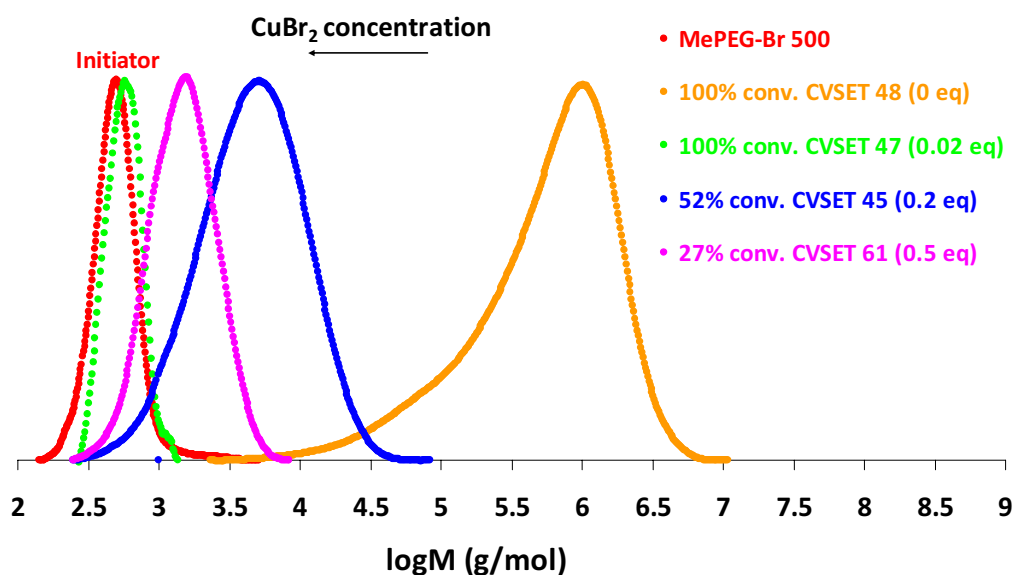


Figure 2.5. Size exclusion chromatograms of the final polymer for copper-mediated polymerizations performed in presence of MePEG-Br 500 ( $8 \times 10^{-3}$  mol/L), Cu(0), PMDETA, NAM, in water at room temperature at different  $\text{CuBr}_2$  molar equivalents.

A more accurate kinetics was followed over the case of the polymerization CVSET 61 (Figure 2.6) as the conversion slowly increased with the time and did not stop before 1h reaction time.

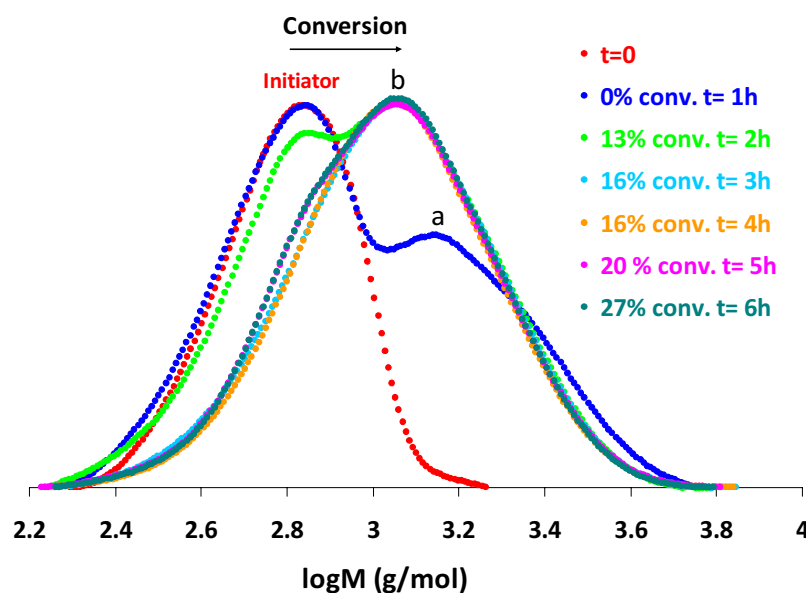


Figure 2.6. Evolution of the size exclusion chromatograms with monomer conversion for CVSET61 performed in presence of MePEG-Br 500 ( $8 \times 10^{-3}$  mol/L), Cu(0), NAM/PMDETA/CuBr<sub>2</sub> (37/0.6/0.5 molar equivalents with respect to initiator) in water at room temperature.

After 1h reaction time, 0% of conversion was achieved but a peak at  $M_n^a \approx 1\,300$  g/mol was observed. This result might be explained by bimolecular reactions between two initiator molecules during the first stage of the polymerization or during the sample preparation as the  $M_n^a$  is twice the molar mass of the initiator.

Matyjaszewski and co-workers<sup>9</sup> reported that, at low polymerization rate, Cu(II) species are able to abstract a hydrogen atom to generate a double bond and HBr from growing polymeric chain via a single electron oxidation process. This process essentially takes place at low monomer concentration and high Cu(II) concentration, i.e. in our conditions. However, no trace of the formation of new ethylenic protons has been detected by <sup>1</sup>H NMR.

After 6h of reaction 27% of conversion was obtained for CVSET 61 and the initiator was not completely consumed. Data indicate that polymer chains achieved the final molar mass ( $M_n^b \approx 1\,200$  g/mol) rapidly and stopped growing. Polymer chains were slowly initiated, grew rapidly and stopped growing. Short chains were constantly generated during the copper-mediated polymerization. Since the concentration of NAM and the  $M_n^b$  were low, it is difficult to determine the nature of the polymer and three possible structures could be proposed: MePEG-MePEG, MePEG-poly(NAM<sub>x</sub>) and MePEG-poly(NAM<sub>x</sub>)-MePEG, x remaining low.

To achieve high conversion, the required  $[\text{CuBr}_2]$  has to be low but no control of the polymerization could be obtained in this case. At the opposite, low molar masses and low  $M_w/M_n$  were obtained at high  $[\text{CuBr}_2]$  but the conversion was very low within 6h.

The best compromise between high conversion and controlled character was obtained with 0.1-0.2 molar equivalent of  $\text{CuBr}_2$  with respect to MePEG-Br 500.

### 2.2.b. Influence of the ligand

Ligands (L) are necessary to perform metal-mediated polymerization. The performance of copper based complexes relies on the stability of the  $\text{Cu(I)/L}$  and  $\text{Cu(II)/L}$  complexes. In water,  $\text{Cu(I)/L}$  complexes are generally unstable and may suffer from disproportionation that affects their activity. Therefore, it is all the most important, in aqueous media, to choose the appropriate ligand<sup>4-10</sup>.

#### 2.2.b.i. Nature of the ligand

Three N-based multidentate ligands commonly used in metal-mediated polymerization (Figure 2.7), 2,2'-bipyridine (bipy), tris[2-(dimethylamino)ethyl]amine ( $\text{Me}_6\text{TREN}$ ) and 1,1,4,7,7-pentamethyldiethylene triamine (PMDETA) were selected in this purpose. The experiments were listed in Table 2.4.

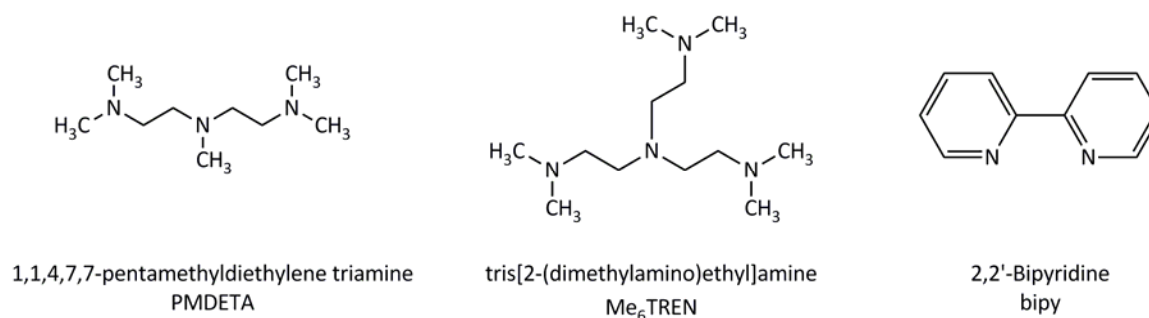


Figure 2.7. Chemical structures of the ligands used in this study.



Table 2.4. Copper-mediated polymerizations performed in presence of MePEG-Br 500, Cu(0)\*, NAM, CuBr<sub>2</sub> in water at room temperature in presence of different ligand.

Ref	Ligand		[MePEG-Br]	NAM/MePEG-Br/CuBr <sub>2</sub>	Time	Conv. (NMR)
CVSET	Nature	(molar equiv.)	conc. (10 <sup>-3</sup> mol/L)	(molar equiv.)	(h)	(%)
84	bipy	0.4	10	32 / 1 / 0.2	23	7
98	bipy	0.8	8	43 / 1 / 0.2	23	10
99	Me <sub>6</sub> TREN	0.2	8	42 / 1 / 0.2	23	15
100	Me <sub>6</sub> TREN	0.5	8	42 / 1 / 0.2	7	17
101	PMDETA	0.5	8	44 / 1 / 0.2	2	48

\* All experiments were performed in presence of 7 cm Cu(0) wire ( $\phi = 1$  mm)

Conversions obtained with bipy and Me<sub>6</sub>TREN were very low even at high molar equivalents with respect to MePEG-Br 500.

The best conversion was obtained with PMDETA. PMDETA is a common ligand that exhibits the advantage to be less expensive than Me<sub>6</sub>TREN and less toxic than bipy. For all these reasons, PMDETA was selected as a ligand for the rest of this study.

#### 2.2.b.ii. Influence of the PMDETA concentration

The performance of copper-based ATRP complex strongly depends on the stability constants of the Cu(II) and Cu(I) complexes with the chosen ligand. High stability constants are required in order to prevent catalyst deactivation through competitive coordination of monomer and/or polymer and to obtain high catalytic activity. PMDETA is well known for the high activity it confers to copper-based catalyst, but also for the poor stability in water of the later, due to very fast disproportionation of the Cu(I) complex<sup>11</sup>. Nevertheless, there is a possibility to overcome this problem by optimizing the [PMDETA]/[CuBr]<sup>12</sup> ratio, i.e. in our case by optimizing [PMDETA]/[CuBr<sub>2</sub>].

Copper-mediated polymerization were carried out in presence of MePEG-Br 500, NAM, Cu(0), CuBr<sub>2</sub>/PMDETA at different PMDETA concentrations (Table 2.5).

Table 2.5. Copper-mediated polymerizations performed in presence of MePEG-Br 500 (I), Cu(0)\*, NAM, CuBr<sub>2</sub> in water at room temperature at different PMDETA concentrations.

Ref	PMDETA	[MePEG-Br] conc. (10 <sup>-3</sup> mol/L)	NAM/I/CuBr <sub>2</sub> (molar equiv.)	Time (h)	Conv. (NMR) (%)	M <sub>n,th</sub> <sup>a)</sup> (g/mol)	M <sub>n,exp</sub> <sup>b)</sup> (g/mol)	M <sub>w</sub> /M <sub>n</sub> <sup>b)</sup>
CVSET 53	0	8	35 / 1 / 0.1	4	47	2 820	31 700	1.9
52	0.2	10	30 / 1 / 0.1	4	60	3 010	4 000	2.7
43	0.5	9	31 / 1 / 0.1	4	85	4 230	5 800	3.1
31	0.6	8	37 / 1 / 0.1	4	85	4 940	6 900	2.5
54	0.9	9	35 / 1 / 0.1	2	96	4 400	6 400	4.6

\* All experiments were performed in presence of 7 cm Cu(0) wire ( $\phi = 1$  mm)

<sup>a)</sup> Theoretical M<sub>n</sub> calculated at final reaction conversion ( $M_{n,th} = M_I + ((m_{mono}/n_I) \times conv.)$ )

<sup>b)</sup> Number-average molar mass and M<sub>w</sub>/M<sub>n</sub> determined by SEC in DMF with a PMMA calibration

47% of conversion and high final molar mass ( $M_n \approx 31\,700$  g/mol) were obtained in absence of PMDETA (CVSET 53). This result could be explained by the NAM chemical structure in which the presence of the morpholine group may help the complexation of Cu (Figure 2.2). NAM could then play the role of ligand.

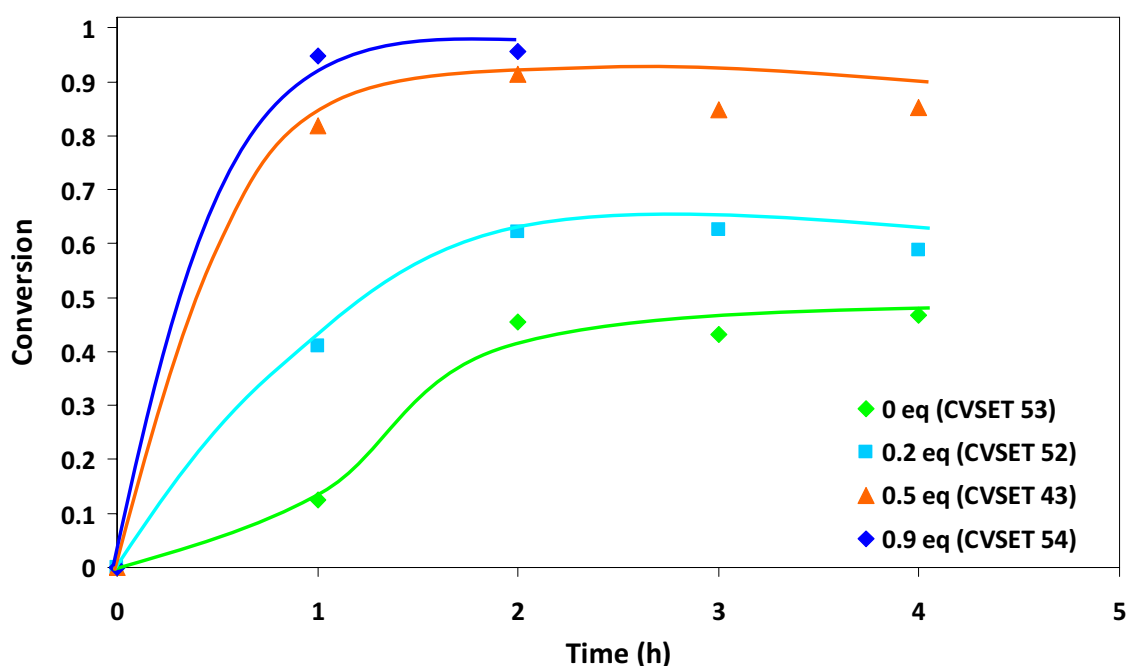


Figure 2.8. Copper-mediated polymerizations performed in presence of MePEG-Br 500 (I), Cu(0)\*, NAM, CuBr<sub>2</sub> in water at room temperature. Effect of the PMDETA concentration on the NAM conversion.

As shown in Figure 2.8, the conversion increased with increasing [PMDETA].

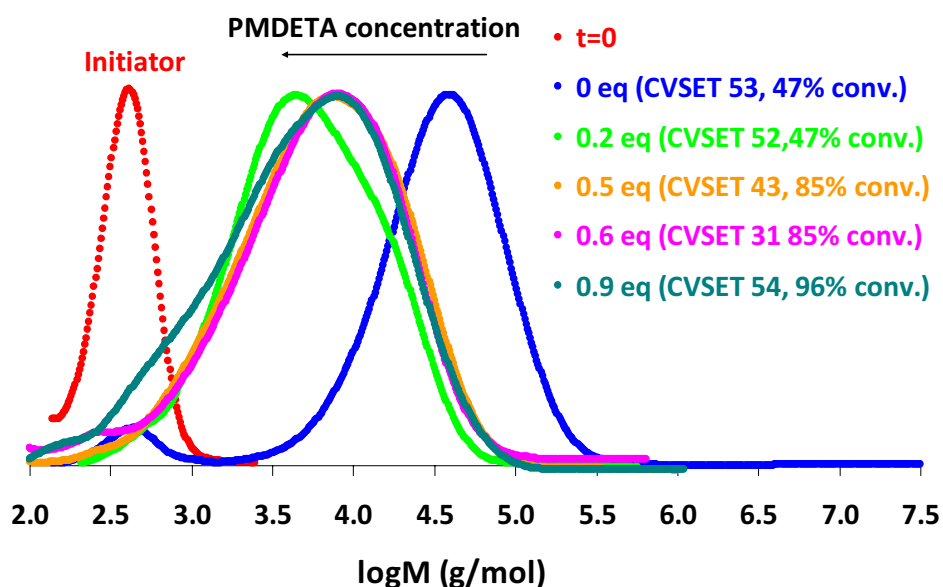


Figure 2.9. Size exclusion chromatograms of the final polymer for copper-mediated polymerization of NAM performed in presence of MePEG-Br 500 ( $8 \times 10^{-3}$  mol/L), Cu(0), PMDETA, in water at room temperature at different PMDETA molar equivalents.

The final molar masses, except for CVSET 53, were close to the targeted molar masses but  $M_w/M_n$  remained very high for a controlled polymerization. For CVSET 31 and 54, initiator still remained (Figure 2.9) due to possible bimolecular reactions or chain transfer reactions<sup>13-14-15-16</sup> induced by an excess of PMDETA.

Considering the conversion (85%) and the molar masses achieved, the value of 0.5 molar equivalent of PMDETA with respect to MePEG-Br 500. These conditions are selected for the rest of the study as they are a good compromise between PMDETA concentration and low molar masses.

### 2.2.c. Influence of the type of monomer

Different monomers were polymerized in presence of MePEG-Br 500, Cu(0), PMDETA/CuBr<sub>2</sub> (0.5/0.1 eq mol with respect to initiator). Reaction conditions are listed in Table 2.6.

As the initiator MePEG-Br is particularly suitable for acrylate monomers, high conversions (>98%) were achieved 2-hydroxyethyl acrylate (HEA) and poly(ethylene glycol) methyl ether acrylate (APEG 480). However, no control of the molar masses and broad molar mass

distributions were observed. Thus it could be concluded that the activation/deactivation process was not efficient to achieve a good control.

With sodium acrylate (NaA), only 31% of conversion was obtained, which was relatively low compared to the other acrylate monomers. The polymerization of sodium (meth)acrylate strongly depends on the pH and an optimal pH of 8-9 was found. Under their acidic form, those monomers could poison the complex by coordinating with the transition metal. Moreover, under acidic conditions, N-based ligand could be protonated<sup>17</sup>. As our polymerization took place at pH~7, part of the sodium acrylate might be under its acidic form and lead to low conversion.

Table 2.6. Copper-mediated polymerizations performed in presence of MePEG-Br 500 (I), Cu(0)\*, PMDETA (L), CuBr<sub>2</sub>, in water at room temperature with different monomers. 4h reaction time.

Ref	Monomer	M / I / L / CuBr <sub>2</sub>	[MePEG-Br]	Conv. (NMR)	$M_{n,th}$ <sup>a)</sup>	$M_{n,exp}$ <sup>b)</sup>	$M_w/M_n$ <sup>b)</sup>
CVSET	Nature	(molar equiv.)	conc. (10 <sup>-3</sup> mol/L)	(%)	(g/mol)	(g/mol)	
15	HEA	63 / 1 / 0.6 / 0.1	8	98	7 620	38 500	4.4
24	HEMA	31 / 1 / 0.5 / 0.1	9	59 <sup>c)</sup>	2 910	-	-
16	PEGMA 300	20 / 1 / 0.5 / 0.1	8	8	970	-	-
56	APEG 480	9 / 1 / 0.5 / 0.1	9	100	4 550	10 600	1.7
28	NaA	45 / 1 / 0.7 / 0.1	9	31	1 810	-	-
17	NaMA	42 / 1 / 0.6 / 0.1	8	16	1 220	-	-
31	NAM	37 / 1 / 0.6 / 0.1	8	85	4 940	6 900	2.5

\* All experiments were performed in presence of 7 cm Cu(0) wire ( $\phi = 1$  mm)

<sup>a)</sup> Theoretical  $M_n$  calculated at final reaction conversion ( $M_{n,th} = M_I + ((m_{mono}/n_I) \times conv.)$ )

<sup>b)</sup> Number-average molar mass and  $M_w/M_n$  determined by SEC in DMF with a PMMA calibration

<sup>c)</sup> Polymer precipitation after 2h

- Not determined due to poor polymer solubility

At the opposite, low conversions were obtained in presence of methacrylate monomers (PEGMA 300 and NaMA) which could be explained by the fact that the initiator is not suitable for methacrylate monomers. DMF SEC data were not reported due as poly(NaMA) and poly(NaA) samples were not very soluble in DMF.

The polymerization of NAM showed a high conversion (85%) and  $M_{n,exp}$  was close to the  $M_{n,theo}$  targeted.  $M_w/M_n$  remained still high (i.e. 2.5) for a controlled radical polymerization.

### 2.2.d. Influence of the type of initiator

As demonstrated in the previous paragraph, finding an initiating system adapted for all kinds of monomers is difficult. In particular, ATRP is influenced by the nature of the halogen atom. Bromine-based initiators are suitable for acrylates, while chlorine-based initiators are more adapted to methacrylates (based on the C-halogen bond energy).

Using a chlorine-based initiator is one possibility to improve control over methacrylate polymerization by shifting the equilibrium toward the dormant chains and hence avoiding a too high concentration of radicals that induces termination. Another possibility studied here, was the halogen exchange ( $I-X_a/Cu(II)X_b$ )<sup>18</sup>. The halogen exchange method from Br-based initiator to Cl-based end-groups allows the use of alkyl halides with low reactivity in the polymerization of monomers that forms a more reactive dormant species, such as a methacrylate. Taking advantage of the stronger alkyl-chlorine bond, the rate of initiation increases relative to propagation and leads to a better controlled polymerization of methacrylate monomers. These experiments are listed in *Table 2.7*.

*Table 2.7. (M)APEG copper-mediated polymerizations performed in presence of Cu(0)\*, PMDETA (L), CuX<sub>2</sub>, in water at room temperature, 4h reaction time. Influence of the nature of the halogen atom in both the initiator and the copper complex (I-X<sub>a</sub>/Cu(II)X<sub>b</sub>).*

Ref	Monomer	Initiating system	M / I / L / Cu <sup>2+</sup>	[I]	Conv. (NMR)
			(molar equiv.)	(10 <sup>-3</sup> mol/L)	(%)
16	PEGMA 300	MePEG-Br 500 / CuBr <sub>2</sub>	20 / 1 / 0.5 / 0.1	8	8
19	PEGMA 300	MePEG-Br 500 / CuCl <sub>2</sub>	13 / 1 / 0.5 / 0.1	9	10
55	PEGMA 300	MePEG-Cl 430 / CuCl <sub>2</sub>	15 / 1 / 0.6 / 0.1	8	91
56	APEG 480	MePEG-Br 500 / CuBr <sub>2</sub>	8.5 / 1 / 0.5 / 0.1	9	100
57	APEG 480	MePEG-Cl 430 / CuCl <sub>2</sub>	8.5 / 1 / 0.5 / 0.1	9	70

\* All experiments were performed in presence of 7 cm Cu(0) wire ( $\phi = 1$  mm)

In presence of the chlorine-based initiator the conversion of PEGMA (CVSET 55) was much higher than the conversion obtained in presence of the corresponding bromine-based initiator (CVSET 16). This clearly indicates that the Br-based initiator is not suitable for the polymerization of methacrylate and a better initiation is achieved with Cl-based initiator. However for CVSET 55, as shown in *Figure 2.10*, high molar mass was achieved and the initiator was slowly consumed with time indicating that MePEG-Cl did not provide a good control of the polymerization.

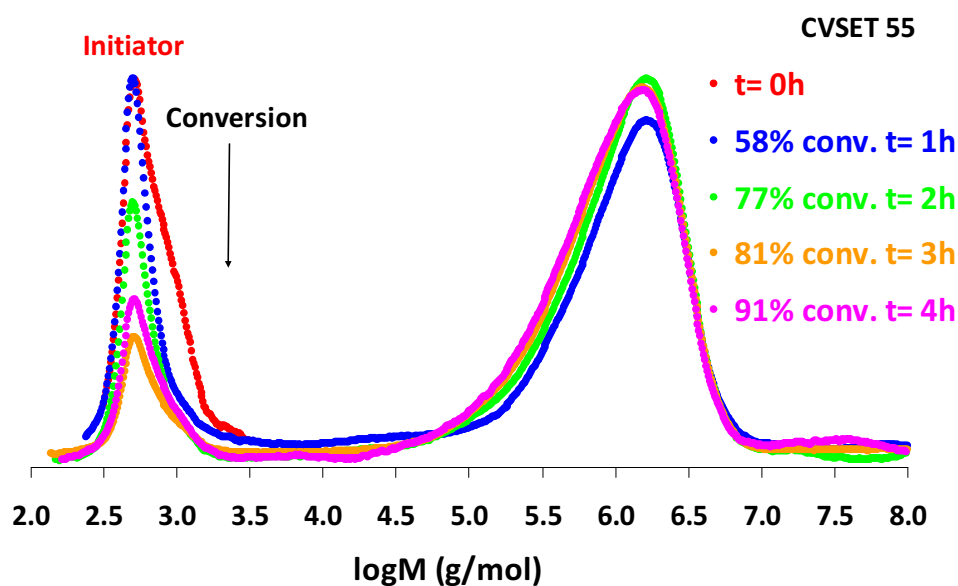


Figure 2.10. Copper-mediated polymerization performed of PEGMA in presence of Cu(0), PMDETA, in water at room temperature, 4h reaction time. Evolution of the size exclusion chromatograms with monomer conversion for CVSET 55 (MePEG-Cl/CuCl<sub>2</sub>).

No improvement in terms of conversion was observed in the PEGMA conversion when CuCl<sub>2</sub> (CVSET 19) was used instead of CuBr<sub>2</sub> (CVSET 16). However, only 0.1 equivalent molar with respect to the initiator was used for the halogen exchange and the amount of Cl may be too low to achieve a complete halogen exchange. This might explained this last result.

A slight decrease of the APEG conversion was observed in presence of MePEG-Cl initiator.

Evolution of the molar masses with monomer conversion was followed for CVSET 56 and 57 (Figure 2.11).

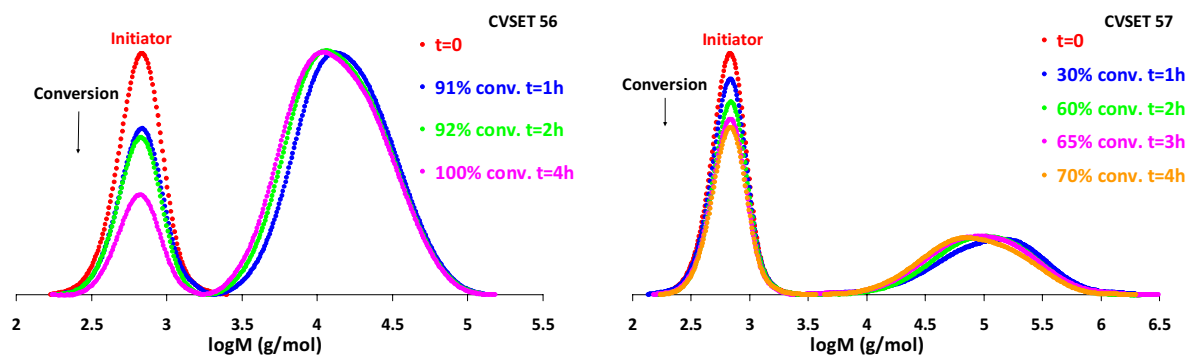


Figure 2.11. Copper-mediated polymerizations performed of APEG in presence of Cu(0), PMDETA, in water at room temperature, 4h reaction time. Evolution of the size exclusion chromatograms with monomer conversion for CVSET 56 (X-Br/CuBr<sub>2</sub>, left) and CVSET 57 (X-Cl/CuCl<sub>2</sub>, right).

For both reactions, polymer chains achieved the final molar mass rapidly and stopped growing. No evolution of the molar mass with conversion was observed. It was noticed that the initiator was slowly consumed with time in particular with the Cl-based initiator.

Following the results obtained with the MePEG-Cl initiator and PEGMA, the same study was performed with NAM (Table 2.8).

Table 2.8. Copper-mediated polymerizations of NAM performed in presence of MePEG- $X_a$  ( $I$ ,  $8 \times 10^{-3} M$ ), Cu(0)\*, PMDETA ( $L$ ), Cu $X$ , in water at room temperature. Influence of the nature of the halogen atom in both the initiator and the copper complex ( $I-X_a/Cu(II)X_b$ ).

Ref	Time	Initiating system	NAM / I / L / Cu <sup>2+</sup>	Conv. (NMR)	$M_{n,th}$ <sup>a)</sup>	$M_{n,exp}$ <sup>b)</sup>	$M_w/M_n$ <sup>b)</sup>
CVSET	h		(molar equiv.)	(%)	(g/mol)	(g/mol)	
31	4	MePEG-Br 500 / CuBr <sub>2</sub>	37 / 1 / 0.6 / 0.1	85	4 940	6 900	2.5
45	6	MePEG-Br 500 / CuBr <sub>2</sub>	36 / 1 / 0.6 / 0.2	46	2 850	3 200	1.9
60	6	MePEG-Br 500 / CuBr <sub>2</sub>	40 / 1 / 0.5 / 0.4	22	1 742	1 600	1.5
61	6	MePEG-Br 500 / CuBr <sub>2</sub>	37 / 1 / 0.5 / 0.5	27	1 910	1 300	1.3
78	4	MePEG-Br 500 / CuCl <sub>2</sub>	38 / 1 / 0.6 / 0.2	44	2 860	4 800	1.7
77	4	MePEG-Cl 430 / CuBr <sub>2</sub>	32 / 1 / 0.5 / 0.2	71	3 600	34 600	2.1
75	5	MePEG-Cl 430 / CuCl <sub>2</sub>	30 / 1 / 0.5 / 0.1	83	4 050	75 800	3.5
72	4	MePEG-Cl 430 / CuCl <sub>2</sub>	32 / 1 / 0.5 / 0.2	95	4 790	21 700	3.5
74	5	MePEG-Cl 430 / CuCl <sub>2</sub>	32 / 1 / 0.5 / 0.4	62	3 250	9 400	1.8
76	5	MePEG-Cl 430 / CuCl <sub>2</sub>	31 / 1 / 0.5 / 0.5	47	2 490	9 300	1.9
85	6	MePEG(CH <sub>3</sub> ) <sub>2</sub> -Br 500 / CuBr <sub>2</sub>	34 / 1 / 0.5 / 0.2	58	3 300	1 440	4.9

\* All experiments were performed in presence of 7 cm Cu(0) wire ( $\phi = 1$  mm)

<sup>a)</sup> Theoretical  $M_n$  calculated at final reaction conversion ( $M_{n,th} = M_I + ((m_{mono}/n_I) \times conv.)$ )

<sup>b)</sup> Number-average molar mass and  $M_w/M_n$  determined by SEC in DMF with a PMMA calibration

For fixed CuX<sub>2</sub> concentration, the final conversions were higher with the -Cl/CuCl<sub>2</sub> than with the -Br/CuBr<sub>2</sub> system. Kinetics in presence of MePEG-Cl and various [CuCl<sub>2</sub>] are displayed in Figure 2.12. The molar masses obtained with -Cl/CuCl<sub>2</sub> were not in line with the theoretical values and the molar mass distributions were broad.

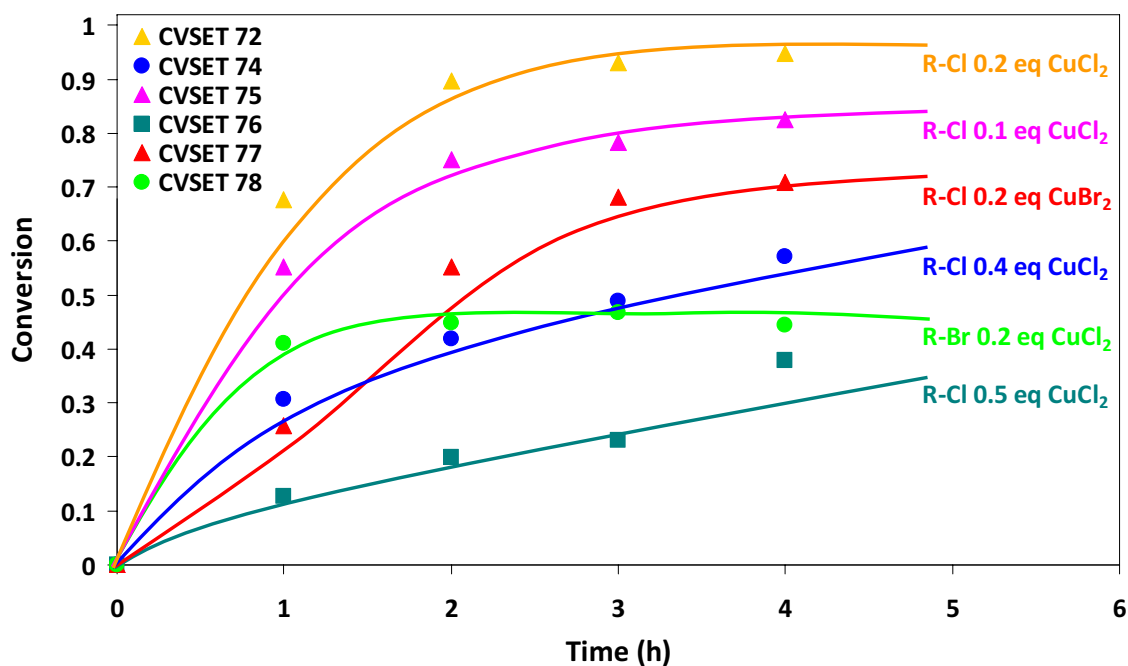


Figure 2.12. Copper-mediated polymerizations of NAM performed in presence of MePEG- $X_a$  ( $l$ ,  $8 \times 10^{-3} M$ ), Cu(0), PMDETA,  $CuX_2$  in water at room temperature. Influence of the  $CuCl_2$  concentration and of the nature of the halogen atom in both the initiator and the copper complex ( $l-X_a/Cu(II)X_b$ ) on the NAM conversion.

For CVSET 78 (MePEG-Br/CuCl<sub>2</sub>) the final results were close to those obtained for CVSET 45 (MePEG-Br/CuBr<sub>2</sub>) in terms of monomer conversions and final molar masses. But SEC data obtained for those polymers showed the presence of remaining initiator for CVSET 78 (Figure 2.13). In presence of CuCl<sub>2</sub>, the initiation was not quantitative and thus, Cl-based initiators are not suitable for the polymerization of NAM.

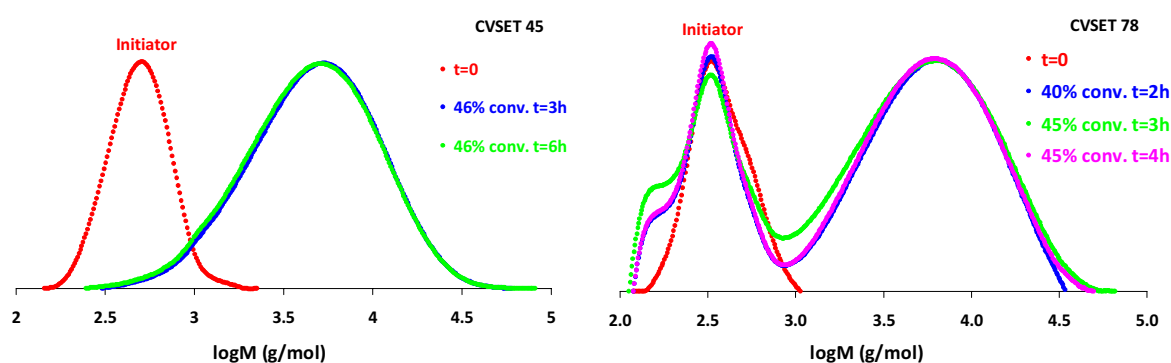


Figure 2.13. NAM copper-mediated polymerizations performed in presence of Cu(0), PMDETA, in water at room temperature. Evolution of the size exclusion chromatograms with monomer conversion for CVSET 45 (X-Br/CuBr<sub>2</sub>, left) and CVSET 78 (X-Br/CuCl<sub>2</sub>, right).

Lower conversion (71%) was achieved in presence of R-Cl/CuBr<sub>2</sub> (CVSET 77) compared to the conversion (95%) obtained in presence of R-Cl/CuCl<sub>2</sub> (CVSET 72). It seems that the system



R-Cl/CuBr<sub>2</sub> leads to a better activation/deactivation and thus, this system is more suitable for the NAM polymerization. However, for both polymerizations (CVSET 77 and 72) high molar masses were obtained, initiator still remained at the end of the polymerization and the molar masses did not evolve with the conversion (Figure 2.15).

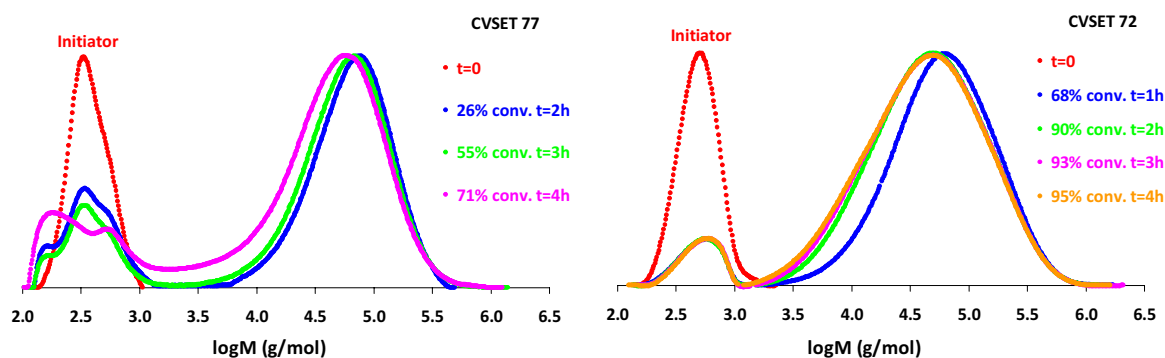


Figure 2.14. Copper-mediated polymerizations of NAM performed in presence of Cu(0), PMDETA, in water at room temperature. Evolution of the size exclusion chromatograms with monomer conversion for CVSET 77 (MePEG-Cl/CuBr<sub>2</sub>, left) and CVSET 72 (MePEG-Cl/CuCl<sub>2</sub>, right).

No significant improvement was observed in presence of MePEG(CH<sub>3</sub>)<sub>2</sub>-Br 500 initiator (CVSET 85, Table 2.8) while a more efficient initiation was expected in presence of a tertiary alkyl halides<sup>19-20-21</sup>. Moreover, the presence of remaining initiator was also observed (Figure 2.15). The final molar mass was close to the targeted molar mass but the  $M_w/M_n$  very high for a controlled character.

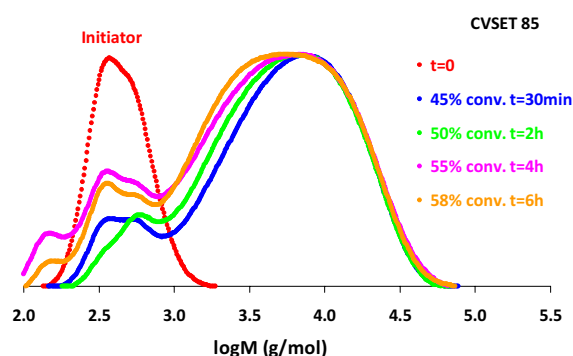


Figure 2.15. Copper-mediated polymerization of NAM performed in presence of Cu(0), MePEG(CH<sub>3</sub>)<sub>2</sub>-Br ( $8 \times 10^{-3}$  M) and PMDETA/CuBr<sub>2</sub> (0.5/0.2 molar equivalents with respect to initiator) in water at room temperature. Evolution of the size exclusion chromatograms with monomer conversion for CVSET 85.

This study concerning the initiator clearly indicates that the type of initiator and the initiating system influence the copper-mediated polymerization in water.

The initiating system MePEG-Br/CuBr<sub>2</sub> leads to 100% and 85% of conversion for APEG (CVSET 57) and NAM (CVSET 31) respectively as only 8% of conversion was achieved for PEGMA. This system is thus more suitable for acrylate and acrylamide monomers. For PEGMA, higher conversion was obtained in presence of MePEG-Cl/CuCl<sub>2</sub> (91%, CVSET55).

The study of the polymerization of NAM performed in presence of different initiating systems has shown that at same Cu(II) concentration, higher conversions were achieved with MePEG-Cl/CuCl<sub>2</sub> (95%, CVSET 72) than MePEG-Br/CuBr<sub>2</sub> (46%, CVSET 45), but final polymers presented higher molar masses and  $M_w/M_n$ .

The same conversions (~45%), molar masses (~3000 g/mol) and  $M_w/M_n$  (~1.9) were obtained in presence MePEG-Br/CuBr<sub>2</sub> (CVSET45) and MePEG-Br/CuCl<sub>2</sub> (CVSET 78). However, the presence of remaining initiator was observed for CVSET 78 which indicates that CuBr<sub>2</sub> is more suitable for the polymerization of acrylamide monomers. Therefore, bromine-based initiator and CuBr<sub>2</sub> were selected for our study as initiating system for the metal-mediated polymerization.

### 2.3. Conclusion

Performing copper-mediated polymerization in water solution was a way to get a better understanding of the system we planed to use for the surface grafting of our latexes. As such, although the control features of the different systems studied was checked, the main goal of this chapter was to identify condition that will allow a good initiation of the system. The results of the different studies allowed us to determine the best parameters for latex formulation and grafting reaction.

Control experiments demonstrated that initiation takes place only in the presence on all components required for an ATRP, i.e initiator, PMDETA/CuBr<sub>2</sub> and Cu(0). While unwanted reactions were not observed in presence of anionic surfactant such as SDS, the presence of thermal initiator, in particularly peroxides affected the initiation. Therefore, the use of an azo-type initiator (ACPA) will be more adapted for the latex synthesis.

From the results obtained in water solution, even though it presented a poor activity in presence of methacrylate monomers, the bromine-based initiator was selected. PMDETA and CuBr<sub>2</sub> at 0.5/0.1 molar equivalent with respect to the MePEG-Br was also selected as it was the best compromise in terms of conversion and concentration. Under these conditions (CVSET 31), 85% of conversion was obtained and the final polymer presented low molar mass (7 000 g/mol).

As the copper-mediated polymerizations performed in water solution were generally very fast, no information concerning the evolution of the molar masses has been determined. Under some cases, it was observed that the molar masses did not increase with the monomer conversion. On the other hand, the initiator was slowly consumed during the polymerization and most of the time, part of it still remained at the end of the polymerization. Polymer chains were constantly generated during the polymerization, grew rapidly and then terminated. The presence of a larger rate of termination reaction observed in water solution may indeed be strongly reduced if the reaction is situated on a latex surface due to difficulty for two radicals to “see” each other. These comments are of real interest for future transposition to the grafting of latex.

The system thus resembles to a conventional free radical process in which the control of the chain growth is not efficient. However, it relies on an initiation that only takes place from the alkyl halide species.

To transpose these results to latex surface grafting, it is first necessary to design a halogenated functionalized latex. This is the purpose of the following chapter.

## 2.4. Experimental part

### 2.4.a. Materials

All products were used as received and are reported in *Table 2.9*. Deionized water was employed in all the experiments.

*Table 2.9. List of the products*

	Products	MW g/mol	Purity	Supplier
ACPA	4,4'-Azobis(4-cyanopentanoic acid)	280.28	>98%	Aldrich
APEG	Poly(ethylene glycol) methyl ether acrylate	~ 480	-	Aldrich
bipy	2,2'-Bipyridine	156.18	> 99.9%	Aldrich
-	Bromoisobutyryl bromide	229.90	98%	Aldrich
-	2 Bromopromionyl bromide	215.87	97%	Aldrich
-	2-Chloropropionyl chloride	126.97	97%	Aldrich
Cu(0)	Copper wire ( $\varnothing = 1$ mm)	63.55	> 99.9%	Aldrich
CuBr <sub>2</sub>	Copper II bromide	223.35	> 99%	Aldrich
CuCl <sub>2</sub>	Copper II chloride	134.45	> 99.99%	Aldrich
CH <sub>2</sub> Cl <sub>2</sub>	Dichloromethane anhydrous	84.93	>99.8%	Aldrich
Disponil FES77	Sodium lauryl ether sulfate	-	-	Cognis
Et <sub>3</sub> N	Triethylamine	101.19	>99%	Aldrich
HEA	2-Hydroxyethyl acrylate	116.12	96%	Aldrich
HEMA	2-Hydroxyethyl methacrylate	130.14	97%	Aldrich
KPS	Potassium persulfate	270.32	> 99.99%	Aldrich
PEGMA	Poly(ethylene glycol) methyl ether methacrylate	~ 300	-	Aldrich
MePEG-OH 350	Poly(ethylene glycol) methyl ether	~300	-	Aldrich
Me <sub>6</sub> TREN	Tris[2-(dimethylamino)ethyl]amine	230.39	-	Aldrich
NaA	Sodium acrylate	94.04	97%	Aldrich
NAM	N-Acryloylmorpholine	141.17	97%	Aldrich
NaMA	Sodium methacrylate	108.07	99%	Aldrich
NaPS	Sodium persulfate	238.10	> 99%	Aldrich
PMDETA	1,1,4,7,7-Pentamethyldiethylene triamine	173.30	99%	Aldrich
SDS	Sodium dodecyl sulfate	288.38	> 99%	Aldrich

### 2.4.b. Synthesis of the initiators

The initiators were synthesized according to a protocol published previously<sup>22</sup> (Figure 2.16).

The amounts of the reactants used for the synthesis are summarized in Table 2.10.

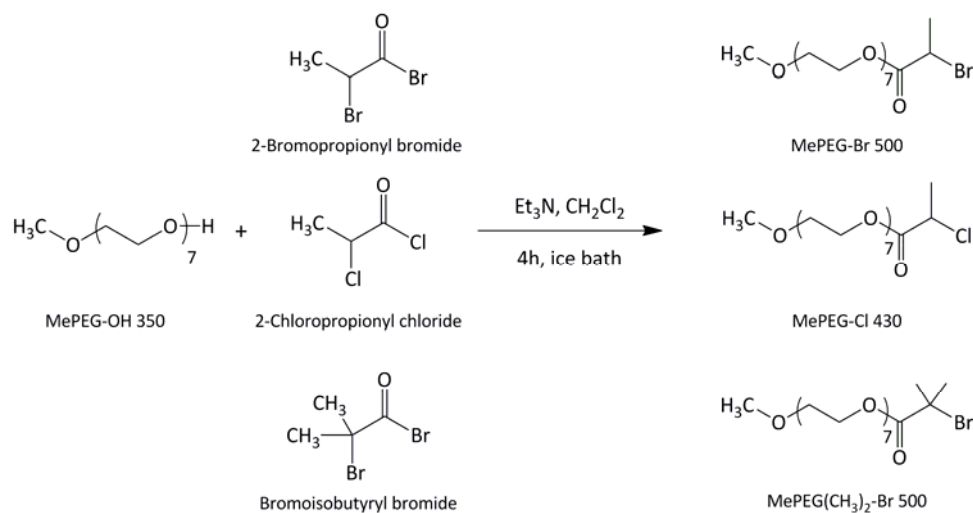


Figure 2.16. Water soluble initiators syntheses.

Table 2.10. Synthesis of the initiators: amounts of the reactants used.

Reactants	MePEG-Br 500		MePEG-Cl 450		MePEG(CH <sub>3</sub> ) <sub>2</sub> -Br 500	
	g	mol	g	mol	g	mol
2-Bromopropionyl bromide	71.24	0.33	-	-	-	-
2-Chloropropionyl chloride	-	-	49.86	0.39	-	-
Bromoisobutyryl bromide	-	-	-	-	37.93	0.17
MePEG-OH 350	105	0.30	165	0.3	52.5	0.15
Et <sub>3</sub> N	33.39	0.33	33.39	0.33	16.69	0.17
CH <sub>2</sub> Cl <sub>2</sub>	305	3.6	305	3.6	150	1.8

In a typical example (MePEG-Br 500) a solution of 2-bromopropionyl bromide (71.24 g, 0.33 mol) in 45 mL of CH<sub>2</sub>Cl<sub>2</sub>, was added dropwise to a stirred solution (cooled in an ice bath) of methoxypoly(ethylene glycol) 350 (105 g, 0.30 mol) and triethylamine (33.96 g, 0.33 mol) in 185 mL of CH<sub>2</sub>Cl<sub>2</sub>, during 3 hours under an atmosphere of argon. After complete addition, the reaction was further stirred at room temperature for 24 hours. The precipitate was removed by filtration and the organic phase was washed with water (3 × 50 mL). It was then dried over magnesium sulfate and CH<sub>2</sub>Cl<sub>2</sub> was evaporated under vacuum to give a yellowish liquid.

**MePEG-Br 500** : 300 MHz  $^1\text{H}$  NMR ( $\text{CDCl}_3$ ):  $\delta$  (ppm) = 4.37 (q, 1H, CH), 4.28 (m, 2H,  $\text{CH}_2\text{-O}$ ), 3.69 (m, 2H,  $\text{CH}_2\text{-O}$ ), 3.61 (s, 22H,  $\text{CH}_2\text{-O}$ ), 3.51 (m, 2H,  $\text{CH}_2\text{-O}$ ), 3.34 (s, 3H,  $\text{CH}_3$ ), 1.79 (d, 3H,  $\text{CH}_3$ )

**MePEG-Cl 430** : 300 MHz  $^1\text{H}$  NMR ( $\text{CDCl}_3$ ):  $\delta$  (ppm) = 4.35 (q, 1H, CH), 4.23 (m, 2H,  $\text{CH}_2\text{-O}$ ), 3.66 (m, 2H,  $\text{CH}_2\text{-O}$ ), 3.56 (s, 22H,  $\text{CH}_2\text{-O}$ ), 3.46 (m, 2H,  $\text{CH}_2\text{-O}$ ), 3.29 (s, 3H,  $\text{CH}_3$ ), 1.61 (d, 3H,  $\text{CH}_3$ )

**MePEG( $\text{CH}_3$ )<sub>2</sub>-Br** : 300 MHz  $^1\text{H}$  NMR ( $\text{CDCl}_3$ ):  $\delta$  (ppm) = 4.24 (m, 2H,  $\text{CH}_2\text{-O}$ ), 3.66 (m, 2H,  $\text{CH}_2\text{-O}$ ), 3.56 (s, 22H,  $\text{CH}_2\text{-O}$ ), 3.46 (m, 2H,  $\text{CH}_2\text{-O}$ ), 3.29 (s, 3H,  $\text{CH}_3$ ), 1.85 (s, 6H,  $\text{CH}_3$ )

#### 2.4.c. Copper-mediated polymerization in water

In a typical copper-mediated polymerization example CVSET31 (Table 2.6), 30 g  $\text{H}_2\text{O}$ , 0.12 g MePEG-Br, 1.3 g NAM, 0.027 g PMDETA, 0.25 mL  $\text{CuBr}_2$  solution at 0.1 M, 0.08 g trioxane (NMR reference) were mixed in a 50 mL round flask closed with a septum and deoxygenated with  $\text{N}_2$  for 30 min. 7 cm Copper wire was introduced under  $\text{N}_2$  through the septum. The reaction was stirred in a water bath at 25 °C. Samples were periodically withdrawn to monitor the monomer conversion by NMR. The final sample was dried under vacuum at room temperature, dissolved in DMF and filtered over a 0.20  $\mu\text{m}$  pore-size PTFE membrane before molar mass measurements by SEC.

## 2.5. References

<sup>1</sup> Rajendrakumar, K.; Dhamodharan, D. *Journal of Polymer Science Part A: Polymer Chemistry* **2011**, 49, 2165-2172

<sup>2</sup> Nicol, E.; Derouineau, T.; Puaud, F.; Zaitsev, A. *Journal of Polymer Science Part A: Polymer Chemistry* **2012**, DOI: 10.1002/pola.26185

<sup>3</sup> Braunecker, W. A.; Tsarevsky, N. V.; Gennaro, A.; Matyjaszewski, K. *Macromolecules* **2009**, 42, 6348-6360

<sup>4</sup> Tsarevsky, N. V.; Pintauer, T.; Matyjaszewski, K. *Macromolecules* **2004**, 37, 9768-9778

<sup>5</sup> Bortolamei, N.; Isse, A. A.; Magenau, A. J. D.; Gennaro, A.; Matyjaszewski, K. *Angewandte Chemie International Edition* **2011**, 50, 11391-11394

<sup>6</sup> Konkolewicz, D.; Magenau, A. J. D.; Averick, S. E.; Simakova, A.; He, H.; Matyjaszewski, K. *Macromolecules* **2012**, 45, 4461-4468

- 
- <sup>7</sup> Magenau, A. J. D.; Kwak, Y.; Matyjaszewski, K. *Macromolecules* **2010**, 43, 9682–9689
- <sup>8</sup> Hornby, B. D.; West, A. G.; Tom, J. C.; Waterson, C.; Harrison, S.; Perrier, S. *Macromolecular Rapid Communications* **2010**, 31, 1276–1280
- <sup>9</sup> Matyjaszewski, K.; Davis, K.; Patten, T. E.; Wei, M. *Tetrahedron* **1997**, 53, 15321-15329
- <sup>10</sup> Tsarevsky, N. V.; Matyjaszewski, K. *ACS Symposium Series* **2006**, 937, 79-94
- <sup>11</sup> Tsarevsky, N. V.; Braunecker, W. A.; Matyjaszewski, K. *Journal of Organometallic Chemistry* **2007**, 692, 3212-3222
- <sup>12</sup> Huang, J.; Pintauer, T.; Matyjaszewski, K. *Journal of Polymer Science Part A: Polymer Chemistry* **2004**, 42, 13, 3285–3292
- <sup>13</sup> Davis, K. A.; Paik, H.-j.; Matyjaszewski, K. *Macromolecules* **1999**, 32, 1767-1776
- <sup>14</sup> Xia, J.; Matyjaszewski, K. *Macromolecules* **1997**, 30, 7697-7700
- <sup>15</sup> Roos, S. G.; Muller, A. H. E. *Macromolecular Rapid Communications* **2000**, 21, 864-867
- <sup>16</sup> Bednarek, M.; Biedron, T.; Kubisa, P. *Macromolecular Chemistry and Physics* **2000**, 201, 58-66
- <sup>17</sup> Matyjaszewski, K.; Xia, J. *Chemical Review* **2011**, 101, 2921-2990
- <sup>18</sup> Peng, C.H., Kong, J., Seeliger, F., Matyjaszewski, K., *Macromolecules* **2011**, 44, 7546-7557
- <sup>19</sup> Goto, A.; Fukuda, T. *Macromolecular Rapid Communications* **1999**, 20, 633-636
- <sup>20</sup> Matyjaszewski, K.; Goebelt, B.; Paik, H.-j.; Horwitz, C. P. *Macromolecules* **2001**, 34, 430-440
- <sup>21</sup> Matyjaszewski, K.; Paik, H.-j.; Zhou, P.; Diamanti, S. J. *Macromolecules*, **2001**, 34, 5125-5131
- <sup>22</sup> Matyjaszewski, K.; Gaynor, S.K.; Kulfan, A.; Podwika, M. *Macromolecules* **1997**, 30, 5192-5194





# Chapter 3

## Latex Functionalization

### Introduction

Since this work is devoted to the use of raw latexes and could have potential industrial applications, the composition of such latexes has to be carefully studied to avoid any undesired interaction with the grafting step. The latex composition also has to be the closer as possible to industrial formulations. Polymer latexes based on *n*-butyl acrylate (*n*BA) and methyl methacrylate (MMA) were selected. The glass transition temperature ( $T_g$ ) of the poly(MMA-*co*-*n*BA) copolymer is easily adjustable over a wide range of temperatures by simply changing the composition without altering fundamentally the experimental protocol. A common anionic surfactant, SDS, was selected since it does not initiate by itself any kind of unwanted reaction (chapter 2). The use of peroxides as initiators is prohibited. As demonstrated in chapter 2, the remaining peroxides could interfere with the ATRP initiating system and thus impact the grafting step. An azo-type initiator, 4,4'-azobis(4-cyanopentanoic acid) (ACPA) was selected. The protocol used to synthesize the functionalized latexes was imposed by our industrial partner. A typical semi-continuous process was selected.

Controlling the location of the Br-containing group at the extreme surface of the particle is a key point to obtain an efficient initiation. As described in the literature review chapter, the synthesis of functionalized latexes has been particularly investigated by Morbidelli<sup>1</sup> et al. so

as to obtain the best conditions for a surface functionalization. To favour the synthesis of functionalized crosslinked particles and to avoid secondary nucleation, the introduction of the inimer had to be performed at 70% conversion of the monomers. Following this work, we decided to proceed with a similar protocol adapted to our system. The functional monomer 2-(2-bromopropionyloxy)ethyl acrylate, (BPEA, *Figure 3.1*) was used in a very low amount to introduce a thin layer of brominated groups able to initiate the polymerization from the surface. BPEA, was thus added at the end of the latex synthesis before complete conversion of the core monomers (~ 90%). During this step, MMA was used as a comonomer for two main reasons. MMA, as a rather polar monomer, might prevent the burial of the bromine atoms during the functionalization step. Moreover, fast chain propagation allows the good adsorption of the oligoradicals and thus prevents their precipitation and the generation of a second crop of particles.

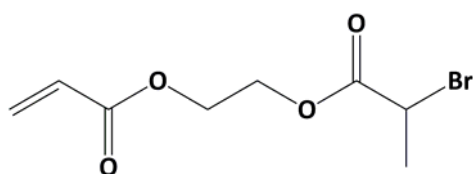


*Figure 3.1.* 2-(2-bromopropionyloxy)ethyl acrylate (BPEA) chemical structure.

This chapter will be devoted to the synthesis of Br-functionalized latex particles. In a first part the synthesis of functionalized crosslinked and non-crosslinked latexes will be presented. A second part will be devoted to the analysis of the particle surface by Time-of-Flight Secondary Ion Mass Spectrometry (ToF-SIMS) to show the presence of the bromide-base groups at the surface of the particles. A study concerning the halogen transfer ability will also be presented. The experimental procedure will be described in the last part of this chapter.

### 3.1. Functionalized latex synthesis

#### 3.1.a. Synthesis of poly(MMA-co-nBA) crosslinked functionalized latexes

Crosslinked latex particles were synthesized via free-radical emulsion copolymerization of MMA and nBA using ACPA as initiator at 70°C. A semi-continuous process was employed and particles were crosslinked with 1,4-butanediol diacrylate (*Figure 3.2*), a divinyllic monomer, in order to maintain their shape and integrity during the various analyses and purification steps.

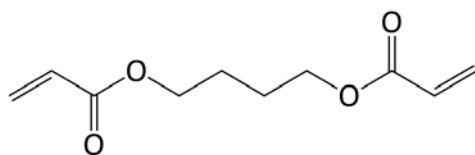


*Figure 3.2.* 1,4-Butanediol diacrylate (BDDA) chemical structure.

After conversion of 90% of the core monomers, a feed of BPEA, MMA and BDDA was employed to functionalize the latexes. The experimental conditions are reported in *Table 3.1*.

*Table 3.1.* Synthesis\* of poly(methyl methacrylate-co-n-butyl acrylate) (poly(MMA-co-nBA)) latex particles crosslinked with 1,4-butanediol diacrylate (BDDA) and functionalized at the surface by 2-(2-bromopropionyloxy)ethyl acrylate (BPEA).  $T = 70\text{ }^{\circ}\text{C}$ .

Latex number <sup>a)</sup>	Composition of the core nBA/MMA/BDDA (wt%)	Composition of the shell MMA/BPEA/BDDA (wt%)	Shell/core weight ratio (wt%)	BPEA conv. (%)	Overall BPEA content (mol/g <sub>Latex</sub> )	Final diameter D (DLS) (nm / dispersity)
2	30.7/66.7/2.6	-	-	-	0	125 / 0.03
31	30.7/66.7/2.6	95.0/1.8/3.2	5.1/94.9	95	$1.5 \times 10^{-6}$	110 / 0.02
28	30.7/66.7/2.6	88.5/8.8/2.7	6.0/94.0	98	$7.5 \times 10^{-6}$	114 / 0.02
44	30.7/66.7/2.6	81.3/1.7/2.0	5.9/94.0	98	$1.5 \times 10^{-5}$	128 / 0.04
15	30.7/66.7/2.6	65.0/32.5/2.5	7.5/92.5	95	$3.9 \times 10^{-5}$	110 / 0.03
26; 41; 42	30.7/66.7/2.6	48.6/49.0/2.4	9.7/90.3	97	$7.3 \times 10^{-5}$	116 / 0.02

\* The experimental procedure is described in the Experimental Part

<sup>a)</sup> Simplified references. Refer to the Experimental Part

Almost quantitative conversions of BPEA were obtained as assessed by gas chromatography. The final latexes exhibited high solids content and were stable. Based on the electron microscopy and dynamic light scattering (DLS) analyses of the final latexes (*Figure 3.3*), a

monomodal particle size distribution was observed, indicating the absence of secondary nucleation.

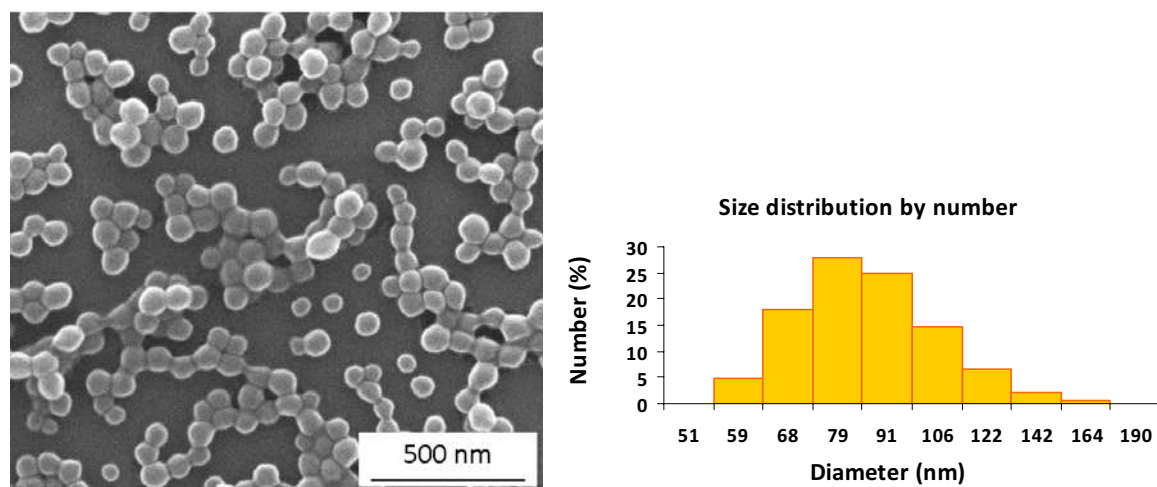


Figure 3.3. Scanning electron microscopy image and particle size distribution from DLS of the latex 41.

### 3.1.b. Kg scale transfer

After the successful synthesis of a monomodal latex, a test was performed at a larger scale. The synthesis was carried out following the same procedure in a 5L reactor. In this case, after 2 hours no polymerization was observed and the reaction was stopped for safety reasons.

The long inhibition time in the 5L reactor was attributed to a long nucleation step. The nucleation depends on the rate of formation of the radicals, a process that strongly depends on a lot of parameters (temperature, initiator, surfactant...). Controlling the nucleation step is a key point to control the polymerization rate and the particle size distribution. The addition of a seed at the start of the reaction is a way to control the nucleation. As our goal was to obtain well defined and isometric particles, the nucleation stage has to be the shortest possible. For this reason, the protocol was modified and a polystyrene (PS) seed (Vorprodukt T 33 wt%) was added in the formulation at 1.5 wt% of the core composition (Table 3.2).

Table 3.2. Synthesis\* of poly(methyl methacrylate-co-n-butyl acrylate) (poly(MMA-co-nBA)) latex particles crosslinked with 1,4-butanediol diacrylate (BDDA) in the presence of a PS seed at  $T = 80^{\circ}\text{C}$  and functionalized at the surface by 2-(2-bromopropionyloxy)ethyl acrylate (BPEA) at  $T = 70^{\circ}\text{C}$ .

Latex number <sup>a)</sup>	Composition of the core PS/nBA/MMA/BDDA (wt%)	Composition of the shell MMA/BPEA/BDDA (wt%)	Shell/core weight ratio (wt%)	Overall BPEA content (mol/g <sub>Latex</sub> )	Final diameter D (DLS) (nm / dispersity)
50	1.5 / 30.7 / 65.3 / 2.5	81.2 / 1.6 / 2.2	5.9 / 94.1	$1.5 \times 10^{-5}$	135 / 0.01
53	1.5 / 29.3 / 66.7 / 2.5	32.9 / 65.8 / 1.3	1.5 / 98.5	$1.5 \times 10^{-5}$	138 / 0.01
52	1.5 / 29.5 / 66.5 / 2.5	49.0 / 48.6 / 2.4	8.7 / 91.3	$7.1 \times 10^{-5}$	130 / 0.03

\* The experimental procedure is described in the Experimental Part

<sup>a)</sup> Simplified references. Refer to the Experimental Part

High BPEA conversions were obtained with the PS seeds and latexes exhibited narrow particle size distribution (Figure 3.4). They were stable at 40% solids contents. Except a slight increase of the particle size, the presence of the seeds did not affect the latex synthesis in terms of stability, monomer conversion and particle size distribution.

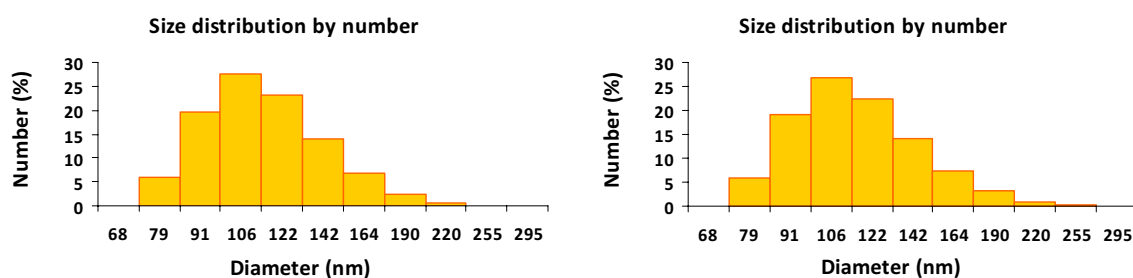


Figure 3.4. Particle size distribution from DLS of the latex 50 (shell/core weight ration 5.9/94.1) (left) and 53 (shell/core weight ration 1.9/98.5) (right).

### 3.1.c. Synthesis of poly(MMA-co-nBA) non-crosslinked functionalized latex particles

Crosslinked particles have the advantage to maintain their shape integrity for analytical purpose but for potential applications in film formation, crosslinked particles are not adapted. Therefore, we have also synthesized a series of non-crosslinked poly(MMA-co-nBA) latexes using the same protocol as before, in a 5L reactor in the presence of a PS seed latex. The experimental conditions are reported in Table 3.3.

Table 3.3. Synthesis\* of non-crosslinked poly(methyl methacrylate-co-n-butyl acrylate) (poly(MMA-co-nBA)) latex particles in presence of a PS seed at  $T = 80^{\circ}\text{C}$ , functionalized at the surface by 2-(2-bromopropionyloxy)ethyl acrylate (BPEA).

Latex number <sup>a)</sup>	Composition of the core PS/nBA/MMA (wt%)	Composition of the shell MMA/BPEA (wt%)	Shell/core weight ratio (wt%)	BPEA conv. (%)	Overall BPEA content (mol/g <sub>Latex</sub> )	Final diameter D (DLS) (nm / dispersity)
51	1.5 / 33.3 / 65.2	83.1 / 16.9	5.8 / 94.2	>99	$1.5 \times 10^{-5}$	135 / 0.01
8	1.5 / 33.3 / 65.2	51.0 / 49.0	9.7 / 90.3	-	$7.1 \times 10^{-5}$	138 / 0.01

\* The experimental procedure is described in the Experimental Part

<sup>a)</sup> Simplified references. Refer to the Experimental Part

Regarding BPEA conversion and particle diameter, the final latex characteristics were very similar to those of the crosslinked latexes synthesized with PS seeds. The particle size distribution obtained by DLS was narrow. A population of small particles was observed by SEM for the latex 8 but in a tolerable amount (Figure 3.5).

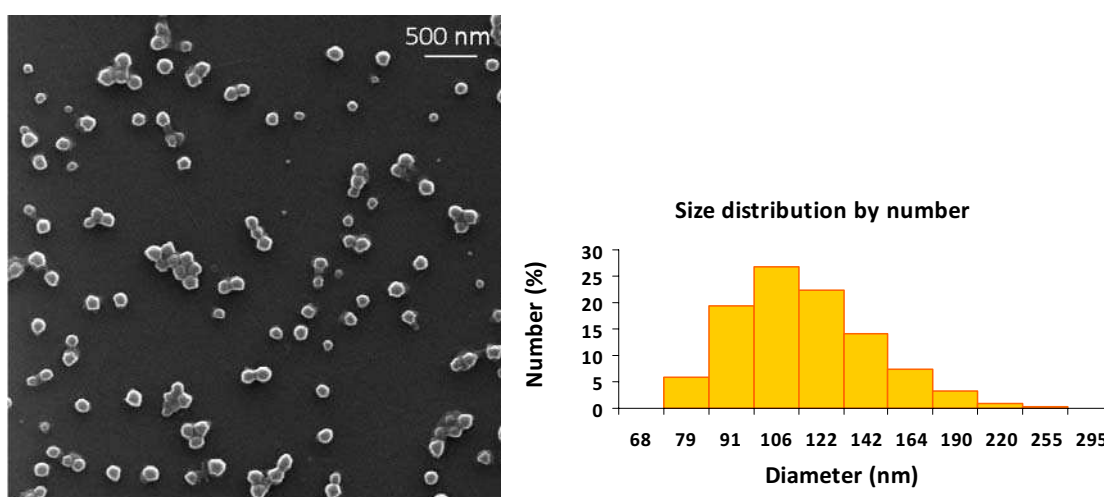


Figure 3.5. Scanning electron microscopy image and particle size distribution from DLS of the non-crosslinked latex 8.

### 3.2. Particle surface analysis by ToF-SIMS

The structure of the inimer and the use of MMA, a rather polar monomer, were conditions selected to prevent the burial of the bromine atom during the functionalization step. Nevertheless, it was important to check the location of the Br functions due to the very low amount of BPEA used during the functionalization step and to the presence of remaining core monomers, particularly the accumulation of *n*BA caused by the composition drift.

ToF-SIMS analysis was thus selected to detect the Br-functional group at the surface of our latexes as already done in a few papers<sup>2,3,4</sup>. This surface analysis technique is based on the *m/z* detection of secondary ions emitted (positively charged and negatively charged as obtained in two separate data acquisitions) following the bombardment of solids using primary ions in the keV range. If a limited number of primary ions are used for this purpose (static conditions), the information depth is limited to a few atomic layers. Moreover, this technique allows the detection of very low amounts (detection limit of ppm to ppb), which is appropriate considering the quantity of BPEA involved in the surface modification of our latexes.

The latexes were first carefully dialyzed to remove all non-converted monomers and water-soluble oligomers and the dried powder was then pressed onto an indium foil at room temperature. The glass transition temperature of the particle being 52°C for crosslinked latex and 50°C for the non-crosslinked latex (as determined by DSC, i.e., above room temperature) a good shape stability and the absence of film formation by chain interdiffusion is expected. This is an important point when targeting the surface analysis exclusively.

*Figure 3.6* displays ToF-SIMS spectra in the positive and negative modes in selected *m/z* ranges. It illustrates the main observations at the surface of latexes before and after the surface modification with the BPEA inimer.



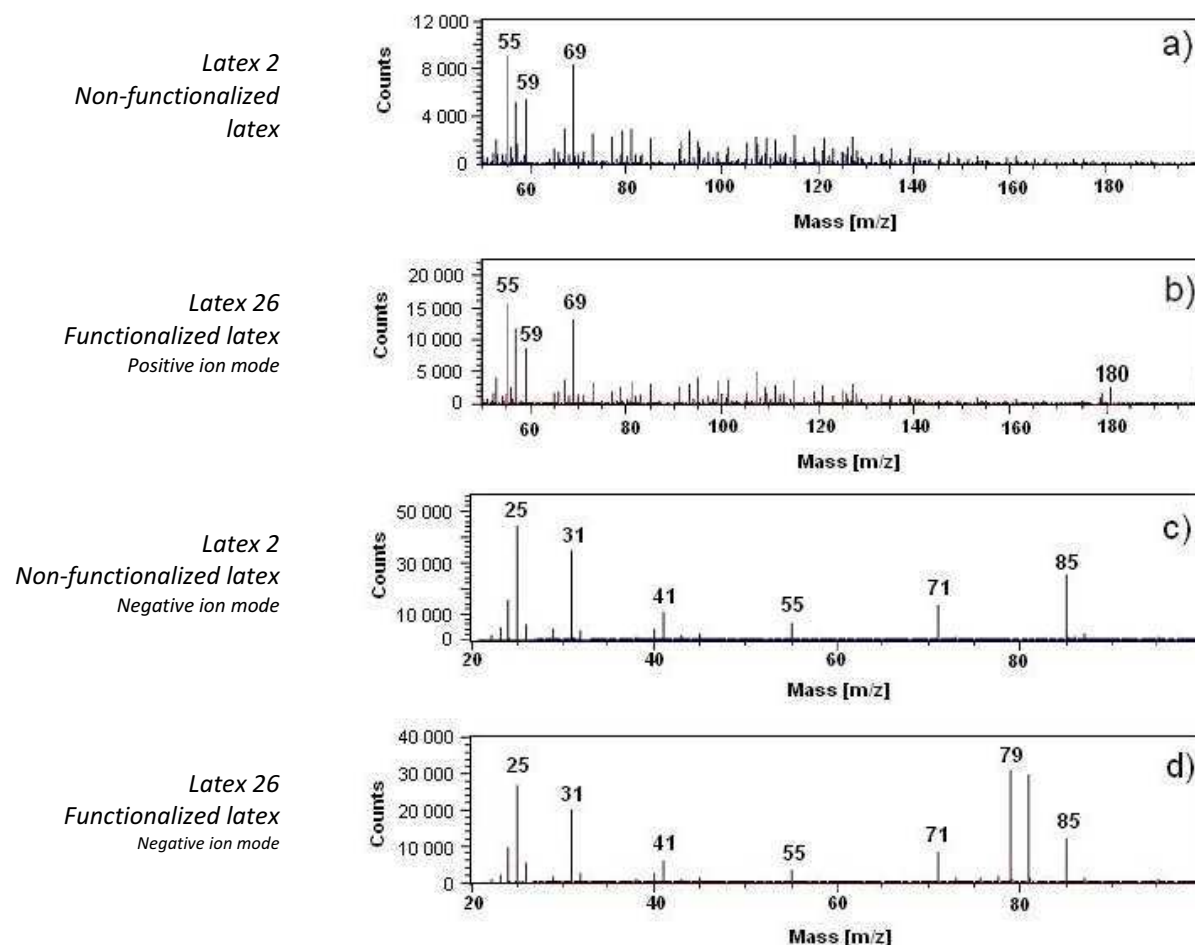


Figure 3.6. Positive ion mode ToF-SIMS spectrum ( $m/z = 50-200$ ) for (a) latex 2, (b) latex 26. Negative ion mode ToF-SIMS spectrum ( $m/z = 20-100$ ) for (c) latex 2, (d) latex 26.

The spectra obtained for the latex 2 (non-functionalized) in the positive mode (Figure 3.6.a) and in the negative mode (Figure 3.6.c) present peaks characteristic for poly(MMA)<sup>2</sup> (as well as other peaks detected in the non illustrated  $m/z$  ranges). This confirms that the analyzed latexes had the expected chemical structure (see also Table 3.4) without significant contamination (see e.g. Br and Cl ubiquitous contamination in Table 3.4).

After surface functionalization with the BPEA inimer, ToF-SIMS spectra of latex 26 in both the positive mode (Figure 3.6.b) and the negative mode (Figure 3.6.d) indicate that the main signatures of the latexes are still detected, which is consistent with the intended limited extent in surface modification. In addition, peaks characteristic for bromopropionyloxy-group were detected. The most obvious signature was Br, which was detected in the negative mode with both isotopes in the expected isotopic ratio (50/50) at  $m/z = 78.913$  and  $m/z = 80.911$  (corresponding to <sup>79</sup>Br<sup>-</sup>,  $m/z = 78.918$  and to <sup>81</sup>Br<sup>-</sup>,  $m/z = 80.916$ ). However, it

was important to confirm that the high relative intensity for  $^{79}\text{Br}^-$  was a direct signature for bromopropionyloxy-group and not a signature for Br contamination noticed by the very slight amount detected for the unmodified latex 2 (see in *Table 3.4*). The detection of peaks in the positive mode at  $m/z = 178.981$  corresponding to  $\text{C}_5\text{H}_8\text{O}_2^{79}\text{Br}^+$ ,  $m/z = 178.971$  and a peak at  $m/z = 180.972$  (corresponding to  $\text{C}_5\text{H}_8\text{O}_2^{81}\text{Br}^+$ ,  $m/z = 180.969$ ) brought this confirmation. The relative intensity for  $179^+$  for the latex 2 is not due to the presence of BPEA. The peak  $179^+$  is detected at  $m/z = 179.122$  (corresponding to  $\text{C}_8\text{H}_3\text{O}_5^+$ ) instead of  $m/z = 178.971$ , excluding any relation to the bromopropionyloxy-group.

ToF-SIMS is not a quantitative analysis since this method depends on matrix effect. The absolute quantification of the bromide concentration at the particle surface is therefore not possible. Nevertheless, comparing the normalized peak intensities offers a way to compare the different samples at different BPEA concentrations (*Table 3.4*).

*Table 3.4. ToF-SIMS normalized intensity (in %) for various characteristic peaks\*.*

Entry	Overall BPEA <sup>a)</sup> content  (mol/g <sub>poly</sub> )	Characteristic signatures for core latex		Characteristic signatures for bromopropionyloxy-group	
		$^{59+}$	$^{85-}$	$^{79-}$	$^{179+}$
		$\text{CH}_3\text{O}-\text{C}\equiv\text{O}^+$		$^{79}\text{Br}^-$	
2	0	$13.7 \pm 2.2$	$21.9 \pm 2.6$	$0.9 \pm 0.2$	$1.2 \pm 0.3$
31	$3.75 \times 10^{-6}$	$16.5 \pm 1.0$	$27.3 \pm 1.8$	$3.7 \pm 0$	$1.4 \pm 0.2$
28	$1.87 \times 10^{-5}$	$16.7 \pm 0.7$	$17.2 \pm 7.2$	$5.4 \pm 2.2$	$2.0 \pm 0.2$
50	$3.75 \times 10^{-5}$	$17.8 \pm 1.6$	$16.6 \pm 2.7$	$9.8 \pm 3.7$	$2.9 \pm 0.1$
51	$3.75 \times 10^{-5}$	$16.9 \pm 1.6$	$15.7 \pm 0.9$	$15.1 \pm 0.5$	$3.4 \pm 0.3$
53	$3.75 \times 10^{-5}$	$17.3 \pm 1.7$	$16.2 \pm 1.9$	$5.1 \pm 0.2$	$1.8 \pm 0.3$
15	$9.75 \times 10^{-5}$	$16.0 \pm 0.4$	$18.8 \pm 3.1$	$39.9 \pm 3.6$	$7.4 \pm 0.7$
26	$1.83 \times 10^{-4}$	$13.4 \pm 3.6$	$15.5 \pm 2.5$	$39.8 \pm 4.7$	$6.6 \pm 1.1$

\*Peaks at :  $m/z = 59^+$  corresponding to  $\text{C}_2\text{H}_3\text{O}_2^+$  and  $m/z = 85^-$  corresponding to  $\text{C}_4\text{H}_5\text{O}_2^-$ , characteristic of the core latex;  $m/z = 79^-$  corresponding to  $^{79}\text{Br}^-$  and  $m/z = 179^+$  corresponding to  $\text{C}_5\text{H}_8\text{O}_2^{79}\text{Br}^+$ , characteristic of bromopropionyloxy-group

<sup>a)</sup>  $\text{BPEA} = \text{mol}_{\text{BPEA}}/\text{mol}_{\text{poly}}(\text{MMA-co-nBA})$

As expected, when the BPEA concentration used for surface modification increased, characteristic signatures for the bromopropionyloxy-group varied accordingly in normalized intensity. But for the latexes 15 ( $9.75 \times 10^{-5}$  mol/g<sub>poly</sub> BPEA) and 26 ( $1.83 \times 10^{-4}$  mol/g<sub>poly</sub> BPEA), the similar values obtained could be explained by the very limited information depth of the ToF-SIMS technique. BPEA might be more incorporated in latex 26 than in latex 15 but the amount in the sample depth probed by ToF-SIMS was similar. A maximum covering of the particle surface seems to be reached at  $9.75 \times 10^{-5}$  mol/g<sub>poly</sub> BPEA.

The crosslinked latex (50) and the non-crosslinked latex (51) were functionalized using the same BPEA concentration ( $3.75 \times 10^{-5}$  mol/g<sub>poly</sub>). Similar ToF-SIMS data were obtained for these two latexes. The functionalization step does not seem to depend, in this case, on the core structure although different swelling properties are expected.

Reducing the amount of BPEA is a criterion for potential applications. Latex 53 was synthesized with a concentrated functional shell in order to increase the local BPEA concentration without increasing the overall BPEA amount (*Table 3.2*). Both latexes 50 and 53 were synthesized at  $1.5 \times 10^{-5}$  mol/g<sub>latex</sub> BPEA but the composition MMA/BPEA/BDDA of the functionalized shell was respectively 81.2/1.6/2.2 and 32.9/65.8/1.3. Regarding the ToF-SIMS data, the bromopropionyloxy-group amount detected at the surface of the particle for the latex 53 was close to the BPEA amount detected for the latex 50. The amount of the MMA/BPEA monomer mixture used during the functionalization of the latex 53 was decreased and was probably not sufficient to reach a total surface coverage.

### 3.3. Halogen transfer ability

Prior to any polymerization from the surface, and in order to assess the accessibility of the surface anchored Br toward a halogen exchange reaction with water-soluble species, the latex was further subjected to a reaction with Cu(0) and CuCl<sub>2</sub>/PMDETA. The switch from Br signature to Cl one should show that activation of the alkyl bromide group of BPEA is possible and would further confirm the appropriate location of bromopropionyloxy-group.

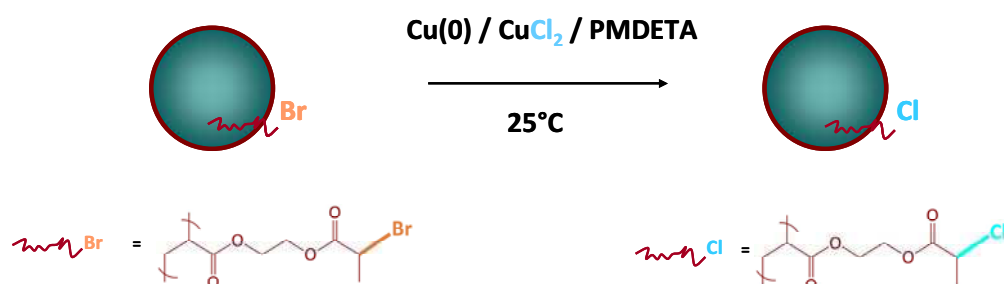


Figure 3.7. General principle of halogen transfer reaction.

The halogen transfer reactions performed with latexes are summarized in Table 3.5 and described in the experimental part. The functionalized latex (26 and 42) with the highest BPEA concentration ( $7.3 \times 10^{-5} \text{ mol/g}_{\text{latex}}$ ) was chosen and a control reaction with the non-functionalized latex (2) was also performed.

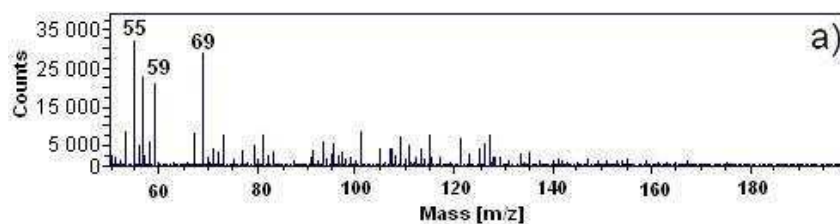
Table 3.5. Halogen transfer reactions performed at 25°C in presence of Cu(0\*) and PMDETA/CuCl<sub>2</sub>.

Entry	Functionalized latex	BPEA <sup>a)</sup> (mol/g <sub>latex</sub> )	BPEA/PMDETA/CuCl <sub>2</sub> (molar equivalent)
2 G2	2	0	0 / 1 / 0.5
26 G6	26	$7.4 \times 10^{-5}$	1 / 0.5 / 0.1
42 G23	42	$1.4 \times 10^{-5}$	1 / 0.5 / 1

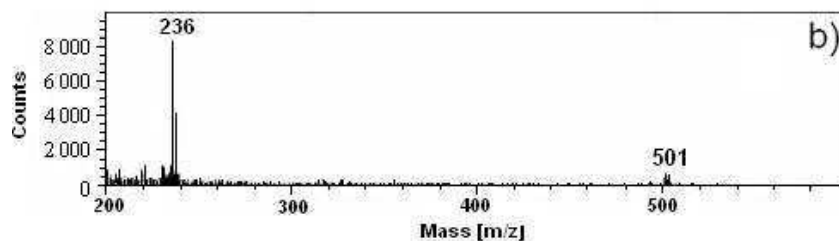
\* All experiments were performed in presence of 1 cm Cu(0) wire ( $\phi = 1\text{mm}$ )

<sup>a)</sup> BPEA =  $\text{mol}_{\text{BPEA}} / m_{\text{Total latex}}$

Latex 2 G2  
Non-functionalized latex  
BPEA/PMDETA/CuCl<sub>2</sub>/Cu(0)  
0/1/0.5/1 cm



Latex 26 G6  
Functionalized latex  
BPEA/PMDETA/CuCl<sub>2</sub>/Cu(0)  
1/0.5/0.1/1 cm



Latex 42 G23  
Functionalized latex  
BPEA/PMDETA/CuCl<sub>2</sub>/Cu(0)  
1/0.5/1/1 cm

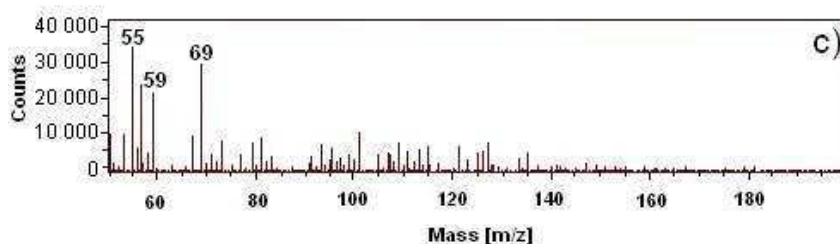
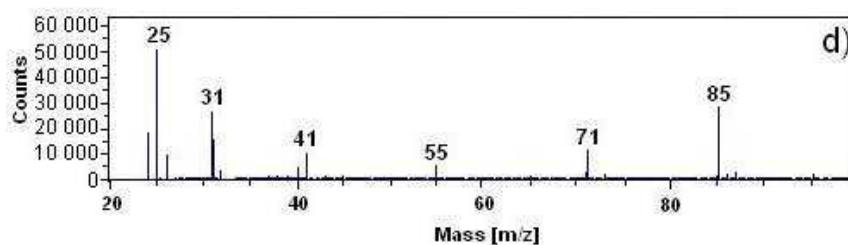
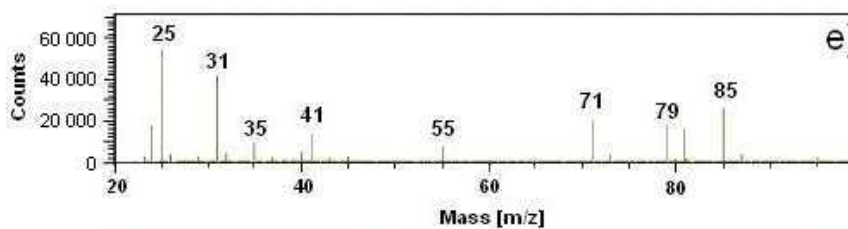


Figure 3.8. Positive ion mode ToF-SIMS spectrum ( $m/z = 60-200$ ) for (a) latex 2 G2, (b) latex 26 G26 ( $m/z = 200-500$ ), (c) latex 42 G23.

Latex 2 G2  
Non-functionalized latex  
BPEA/PMDETA/CuCl<sub>2</sub>/Cu(0)  
0/1/0.5/1 cm



Latex 26 G6  
Functionalized latex  
BPEA/PMDETA/CuCl<sub>2</sub>/Cu(0)  
1/0.5/0.1/1 cm



Latex 42 G23  
Functionalized latex  
BPEA/PMDETA/CuCl<sub>2</sub>/Cu(0)  
1/0.5/1/1 cm

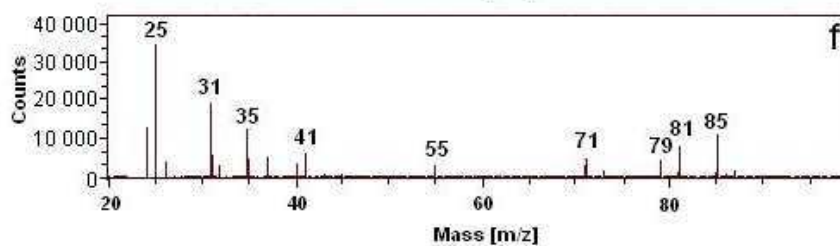
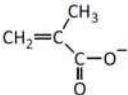
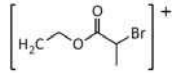


Figure 3.9. Negative ion mode ToF-SIMS spectrum ( $m/z = 20-100$ ) for (d) latex 2 G2, (e) latex 26 G6, (f) latex 42 G23.

Figure 3.8.a) and Figure 3.9.d) displays the ToF-SIMS spectra in the positive and negative mode respectively for the latex 2 G2. As expected, no characteristic signature for the presence of Cl<sup>-</sup> was observed and the ToF-SIMS data of latex 2 G2 are very similar to those of latex 2 (Table 3.6). No reaction or absorption of chloride atom at the particle surface is observed if reaction with Cu(0)/CuCl<sub>2</sub>/PMDETA is performed in the presence of a non functionalized latex.

Table 3.6. ToF-SIMS normalized intensity (in %) for various characteristic peaks\*.

Entry	Characteristic signatures for core latex		Characteristic signatures for bromopropionyloxy-group		Characteristic signature for Cl
	$ ^{59+}$	$ ^{85-}$	$ ^{79-}$	$ ^{179+}$	$ ^{35-}$
	$\text{CH}_3\text{O}-\text{C}\equiv\text{O}^+$		$^{79}\text{Br}^-$		$^{35}\text{Cl}^-$
2	13.7 ± 2.2	21.9 ± 2.6	0.9 ± 0.2	1.2 ± 0.3	0.5 ± 0.5
2 G2	17.9 ± 0.1	16.8 ± 6.7	1.8 ± 1.8	1.3 ± 0.3	0.4 ± 0.1
26 G6	14.3 ± 0.6	18.9 ± 1.6	14.1 ± 0.7	2.4 ± 0.2	8.9 ± 1.6
42 G23	11.0 ± 8.6	12.4 ± 2.0	9.1 ± 1.3	1.7 ± 1.5	21.6 ± 4.8

\*Peaks at :  $m/z = 59^+$  corresponding to  $\text{C}_2\text{H}_3\text{O}_2^+$  and  $m/z = 85^-$  corresponding to  $\text{C}_4\text{H}_5\text{O}_2^-$ , characteristic of the core latex;  $m/z = 79^-$  corresponding to  $^{79}\text{Br}^-$  and  $m/z = 179^+$  corresponding to  $\text{C}_5\text{H}_8\text{O}_2^{79}\text{Br}^+$ , characteristic of bromopropionyloxy-group,  $m/z = 35^-$  corresponding to  $^{35}\text{Cl}^-$ , characteristic of the ion exchange reaction between Br and Cl but contribution from Cl ubiquitous contamination cannot be excluded.

Figure 3.9.e) and f) were obtained after reacting a functionalized latex with CuCl<sub>2</sub>/PMDETA in the presence of Cu(0). The characteristic signatures for bromopropionyloxy-group ( $^{79}\text{Br}^-$  but as well as  $\text{C}_5\text{H}_8\text{O}_2^{79}\text{Br}^+$ ) are still detected but with a significantly lower normalized intensity (Table 3.6). Cl was detected in the negative mode with both isotopes (and in the expected isotopic ratio): a peak at  $m/z = 34.970$  (corresponding to  $^{35}\text{Cl}^-$ ,  $m/z = 34.969$ ) and a peak at  $m/z = 36.967$  (corresponding to  $^{37}\text{Cl}^-$ ,  $m/z = 36.966$ ) in a higher level than the ubiquitous contamination. This confirmed an exchange reaction, most likely based on the radical process that is required for initiation and controlled propagation (based on the activation/deactivation equilibrium of ATRP).

It was expected that peaks similar to  $179^+/181^+$ , thus possibly  $\text{C}_5\text{H}_8\text{O}_2^{35}\text{Cl}^+$  and  $\text{C}_5\text{H}_8\text{O}_2^{37}\text{Cl}^+$  could be detected but they were not identified even for the latex 42 G23 obtained with 1 molar equivalent of Cl<sup>-</sup> with respect to BPEA. The absence of a peak at  $m/z = 135$

( $C_5H_8O_2^{35}Cl^+$ ) did not invalidate the halogen transfer but could be attributed to an absence of fragmentation, during the ToF-SIMS analysis.

Two characteristic peaks were also observed in the positive mode only for the functionalized latex 26 G6 (*Figure 3.8.b*) and 42 G23 (data not illustrated). A peak at  $m/z = 236.099$  was attributed to the presence of PMDETA/Cu complex and a peak at  $m/z = 501.237$  to the presence of PMDETA/SDS/Cu complex.

### 3.4. Conclusion

In this chapter the functionalization of polymer particles with an inimer bearing an ATRP initiator functional group (BPEA) was studied.

A successful protocol was found to synthesize functionalized latexes by emulsion polymerization in a semi-continuous process. Some improvements on the initial protocol, such as the addition of a PS seed latex, were performed in order to scale up the functionalization of the particle without modification of the final latex characteristics. The obtained latexes were all stable at 40 % of solids content and exhibited a narrow particle size distribution.

Although a high BPEA conversion was obtained and no secondary nucleation was observed by classical analytical tools, a more accurate control of the location of the bromide group was the main point of this study. The presence of the bromide atom at the particle surface was assessed by ToF-SIMS analysis and was indeed detected for all functionalized latexes. A molecular fragment of the bromopropionyloxy-group bearing the bromine atom was also observed, attesting the presence of BPEA covalently bound at the particle surface. Bromopropionyloxy-group was detected at low concentration ( $3.75 \times 10^{-6}$  mol/g<sub>poly</sub>) and its characteristic signature increased with the increase of BPEA concentration to a maximum of  $9.75 \times 10^{-5}$  mol/g<sub>poly</sub>.

A halogen atom exchange reaction performed with the functionalized latex in the presence of Cu(0) and PMDETA/CuCl<sub>2</sub> demonstrated the possible activation of the surface alkyl bromide group of BPEA by water soluble active species. The characteristic signal of bromine was replaced by the characteristic signal of chlorine that confirmed a halogen transfer reaction that is required for an ATRP mechanism.

After the successful introduction of BPEA and the assessment of the good accessibility of the alkyl bromide group, functionalized latexes were further used as substrates for the surface-initiated polymerization of hydrophilic monomers. This study will be developed in the next chapter.



### 3.5. Experimental part

#### 3.5.a. Materials

All products were used as received and are listed in *Table 3.7*. Deionized water was employed in all experiments.

*Table 3.7. List of the products*

	Products	Mw g/mol	Purity	Supplier
ACPA	4,4'-Azobis(4-cyanopentanoic acid)	280.28	>98%	Aldrich
BDDA	1,4-Butanediol diacrylate	198.22	-	BASF
Cu(0)	Copper wire ( $\phi = 1\text{mm}$ )	63.55	> 99.9%	Aldrich
CuBr <sub>2</sub>	Copper II bromide	223.35	> 99%	Aldrich
CuCl <sub>2</sub>	Copper II chloride	134.45	> 99.99%	Aldrich
Disponil SDS	Sodium dodecyl sulfate	288.38	15 wt% aq solution	Cognis
MMA	Methyl methacrylate	100.12	-	BASF
NaHCO <sub>3</sub>	Sodium hydrogen carbonate	84.01	0.07 M aq solution	BASF
NAM	<i>N</i> -Acryloylmorpholine	141.17	97%	Aldrich
NaOH	Sodium hydroxide solution	40.00	0.25 M aq solution	BASF
<i>n</i> BA	<i>n</i> -Butyl acrylate	128.17	-	BASF
PMDETA	1,1,4,7,7-Pentamethyldiethylene triamine	173.30	99%	Aldrich
PS seed (29 nm)	Vorprodukt T6772	-	33 wt%	BASF

#### 3.5.b. BPEA synthesis

The inimer 2-(2-bromopropionyloxy)ethyl acrylate (BPEA) was synthesized by reaction of 2-hydroxyethyl acrylate (Sigma Aldrich, 96%) and 2-bromopropionyl bromide (Sigma Aldrich, 97%), according to a protocol published previously<sup>5</sup>. A solution of 2-bromopropionyl bromide (79.33 g, 0.38 mol) in 50 mL of CH<sub>2</sub>Cl<sub>2</sub>, was added dropwise to a stirred solution (cooled in an ice bath) of 2-hydroxyethyl acrylate (40.64 g, 0.35 mol) and triethylamine (38.96 g, 0.38 mol) in 220 mL of CH<sub>2</sub>Cl<sub>2</sub>, during 3 hours under an atmosphere of argon. After complete addition, the reaction was further stirred at room temperature for 24 hours. The precipitate was removed by filtration and the organic phase was washed with water (3 × 50 mL). It was then dried over magnesium sulfate, filtered and CH<sub>2</sub>Cl<sub>2</sub> was evaporated under vacuum. The obtained yellow oil was distilled under vacuum in the presence of 0.5 wt% of

hydroquinone to give a colorless liquid. 300 MHz  $^1\text{H}$  NMR ( $\text{CDCl}_3$ ):  $\delta$  (ppm) = 6.44 (d, 1H,  $\text{CH}_2=$ ), 6.13 (dd, 1H,  $=\text{CH}$ ), 5.87 (d, 1H,  $\text{CH}_2=$ ), 4.41 (m, 5H,  $\text{H}_2\text{C-O}$  and  $\text{CH-Br}$ ), 1.83 (d, 3H,  $\text{CH}_3$ ).

### 3.5.c. Synthesis of poly(MMA-co-nBA) crosslinked latex

In a typical example (latex 26 in Table 3.1), a monomer in water emulsion was first prepared using 260 g of deionized water, 26.5 g of SDS solution, 5.6 g of sodium hydrogen carbonate solution, 88 g of nBA, 190 g of MMA, and 7.3 g of BDDA. An aqueous solution of ACPA initiator (6.28 g of the solution prepared with 48 g of deionized water, 3.0 g of ACPA and 11.7 g of NaOH aqueous solution 0.25M) was introduced into a 2-liter reactor preloaded with 138 g of deionized water, equipped with a thermocouple, a cooling condenser and a paddle stirrer, and heated at 70 °C. After 15 minutes, the monomer-in-water emulsion was gradually added to the reactor for a total time of 180 minutes while 56.5 g of the residual initiator solution was fed during 215 minutes. After complete addition of the monomer emulsion (achieving 92% conversion), a mixture containing 15 g of the BPEA inimer, 15 g of MMA and 0.7 g of BDDA was added during 30 minutes and the reaction medium was stirred at 70 °C for 60 more minutes and then cooled to room temperature. The final latex had a solids content of 40 wt% (obtained by gravimetric analysis). The particle diameter was determined using DLS. The conversion of BPEA was determined by gas chromatography.

### 3.5.d. Synthesis of poly(MMA-co-nBA) crosslinked latex with PS seed

In a typical example (latex 50 in Table 3.2), a monomer in water emulsion was first prepared using 929.4 g of deionized water, 125.0 g of SDS solution, 26.0 g of sodium hydrogen carbonate solution, 416.1 g of nBA, 884.1 g of MMA and 34.2 g of BDDA. An aqueous solution of ACPA initiator (29.5 g of the solution prepared with 259.1 g of deionized water, 14.1 g of ACPA and 21.8 g of NaOH aqueous solution 0.25M) was introduced into a 5-liter reactor preloaded with 843.4 g of deionized water and 61.5 g of Vorprodukt T, equipped with a thermocouple, a cooling condenser and a paddle stirrer, and heated at 80 °C. After 15 minutes, the monomer-in-water emulsion was gradually added to the reactor for a total time of 180 minutes while 265.5 g of the residual initiator solution was fed during 215 minutes. After complete addition of the monomer emulsion (achieving 92% conversion), the

temperature was decreased at 70°C and a mixture containing 14.2 g of the BPEA inimer, 69.6 g of MMA and 1.9 g of BDDA was added during 30 minutes and the reaction medium was stirred at 70 °C for 60 more minutes and then cooled to room temperature. The final latex had a solids content of 40 wt% (obtained by gravimetric analysis). The particle diameter was determined using DLS. The conversion of BPEA was determined by gas chromatography.

### **3.5.e. Synthesis of poly(MMA-co-nBA) non crosslinked latex with PS seed**

In a typical example (latex 51 in *Table 3.3*), a monomer in water emulsion was first prepared using 930.8 g of deionized water, 125.0 g of SDS solution, 26.0 g of sodium hydrogen carbonate solution, 452.1 g of nBA, 884.1 g of MMA. An aqueous solution of ACPA initiator (29.5 g of the solution prepared with 259.1 g of deionized water, 14.1 g of ACPA and 21.8 g of NaOH aqueous solution 0.25M) was introduced into a 5-liter reactor preloaded with 842.0 g of deionized water and 61.5 g of Vorprodukt T, equipped with a thermocouple, a cooling condenser and a paddle stirrer, and heated at 80 °C. After 15 minutes, the monomer-in-water emulsion was gradually added to the reactor for a total time of 180 minutes while 265.5 g of the residual initiator solution was fed during 215 minutes. After complete addition of the monomer emulsion (achieving 92% conversion), the temperature was decreased at 70°C and a mixture containing 14.2 g of the BPEA inimer, 69.6 g of MMA was added during 30 minutes and the reaction medium was stirred at 70 °C for 60 more minutes and then cooled to room temperature. The final latex had a solids content of 40 wt% (obtained by gravimetric analysis). The particle diameter was determined using DLS. The conversion of BPEA was determined by gas chromatography.

### **3.5.f. Halogen transfer mediated by Cu(0)/CuCl<sub>2</sub>/PMDETA**

For the example 26 G6 (*Table 3.6*), 5 g of latex 26 were carefully deoxygenated with a nitrogen flow for 30 minutes. A deoxygenated mixture of 0.03 g (0.5 eq mol with respect to BPEA) of PMDETA, and 0.36 g (0.1 eq mol with respect to BPEA) of a CuCl<sub>2</sub> aqueous solution at 0.1 M were slowly added under stirring. The reaction medium was heated at 25°C and a 1 cm length piece of copper wire was introduced. The reaction was stirred for 6h. The copper wire was removed and the latex was dialyzed against water for 2 weeks (the water medium was changed 4 times per day) using a Spectra/Por® dialysis membrane (cut-off at 12 000-14 000 Da), dried at room temperature, grinded to a powder for ToF SIMS analysis.

For the examples 42 G23 and 2 G2 (*Table 3.6*), 5 g of latex and 15 g of deionized water were carefully deoxygenated with a nitrogen flow for 30 minutes. A deoxygenated mixture of 0.03 g (0.5 eq mol with respect to BPEA) of PMDETA, and 3.6 g (1 eq mol with respect to BPEA) of a CuCl<sub>2</sub> aqueous solution at 0.1 M and 5g of water were slowly added under stirring. The reaction medium was heated at 25°C and a 1 cm length piece of a copper wire was introduced. The reaction was stirred for 6h. The copper wire was removed and the latex was dialyzed against water for 2 weeks (the water medium was changed 4 times per day) using a Spectra/Por® dialysis membrane (cut-off at 12 000-14 000 Da), dried at room temperature, grinded to a powder for ToF SIMS analysis.

### 3.5.g. Latex references

The latexes synthesized in this chapter are listed in *Table 3.8*. The principal characteristics are reported and the latex references were simplified in the main text.

*Table 3.8. Functionalized latexes synthesized in this study.*

Latex number	New entry	Latex <sup>a)</sup>	Overall BPEA <sup>b)</sup> content (mol/g <sub>Latex</sub> )
GK90-2	2	Cross-linked poly(MMA-co-nBA)	0
GK2808-31	31	Cross-linked poly(MMA-co-nBA)	$1.5 \times 10^{-6}$
GK2808-28	28	Cross-linked poly(MMA-co-nBA)	$7.5 \times 10^{-6}$
GK2808-44	44	Cross-linked poly(MMA-co-nBA)	$1.5 \times 10^{-5}$
GK2808-50	50	Cross-linked poly(MMA-co-nBA), PS seed	$1.5 \times 10^{-5}$
GK2808-53	53	Cross-linked poly(MMA-co-nBA), PS seed	$1.5 \times 10^{-5}$
GK28008-51	51	Non cross-linked poly(MMA-co-nBA), PS seed	$1.5 \times 10^{-5}$
GK2808-15	15	Cross-linked poly(MMA-co-nBA)	$3.9 \times 10^{-5}$
GK2808-26; 41; 42	26; 41; 42	Cross-linked poly(MMA-co-nBA)	$7.3 \times 10^{-5}$
GK2808-52	52	Cross-linked poly(MMA-co-nBA), PS seed	$7.1 \times 10^{-5}$
GK98-8	8	Non cross-linked poly(MMA-co-nBA)	$7.1 \times 10^{-5}$

<sup>a)</sup> 40 % solids content

<sup>b)</sup>  $BPEA = \text{mol}_{BPEA} / m_{\text{Total latex}}$

### 3.6. References

- 
- <sup>1</sup> Mittal, V.; Matsko, N.B.; Butté, A.; Morbidelli, M. *Polymer* **2007**, 48, 2806-2817
  - <sup>2</sup> Davies, M.C., Lynn, R.A.P.; Davis, S.S.; Hearn, J.; Vickerman, J.C.; Paul, A.J. *J. Colloid Interface Sci.* **1993**, 161, 83-90
  - <sup>3</sup> Davies, M.C.; Lynn, R.A.P.; Hearn, J.; Vickerman, J.C.; Paul, A.J.; Watts J.F. *Langmuir* **1996**, 12, 3866-3875
  - <sup>4</sup> Ihalainen, P.; Backfolk, K.; Sirvio, P.; Peltonen, J. *Colloids and Surfaces, A* **2010**, 354, 320-330
  - <sup>5</sup> Matyjaszewski, K.; Gaynor, S.K.; Kulfan, A.; Podwika, M. *Macromolecules* **1997**, 30, 5192-5194

## Chapter 4

# Surface-initiated Polymerization

### Introduction

Core-shell particles prepared by conventional radical emulsion polymerization are usually obtained under a thermodynamic control. Generally, after the polymerization of the core, a second monomer feed is added to form the shell. In this case, the core and the shell are not covalently linked and the resulting core-shell morphology depends only on the polymer interfacial energy<sup>1</sup>. In particular, obtaining particles with a hydrophilic hairy layer according to this procedure is not possible. The hydrophilic monomer will preferentially polymerize in the water phase. Surface-initiated polymerization is one way to synthesize a hairy shell covalently bound to the core, and to avoid free polymer in the water phase.

A conventional batch procedure was chosen for the surface-initiated polymerization and the reactions were carried out at room temperature. Except dilutions, latexes were used “as synthesized”, i.e. without purification such as dialysis and/or centrifugation. A latex destabilization was observed during the first grafting reactions (not reported) when pure hydrophilic monomer was introduced and despite the precautions taken. To overcome this difficulty, aqueous solutions of the hydrophilic monomers were further employed.

The reagent concentrations were directly adapted from the model experiments performed in water solution (chapter 2) and for a typical grafting reaction PMDETA/CuBr<sub>2</sub> was used in a 0.5/0.1 molar ratio with respect to BPEA. Cu(0) wire was used as a reducing agent.

For a better understanding of the study, the latexes used in this chapter are listed in *Table 4.1*. The main characteristics are reported and the latex references were simplified.

*Table 4.1. Functionalized latexes used in this study.*

Latex number	New entry	Latex <sup>a)</sup>	Shell/core weight ratio (wt%)	Overall BPEA <sup>b)</sup> content (mol/g <sub>Latex</sub> )	Final diameter D (DLS) (nm / dispersity)
GK90-2	<b>2</b>	Crosslinked poly(MMA-co-nBA)	-	0	125 / 0.03
GK2808-31	<b>31</b>	Crosslinked poly(MMA-co-nBA)	5.1 / 94.9	$1.5 \times 10^{-6}$	110 / 0.02
GK2808-50	<b>50</b>	Crosslinked poly(MMA-co-nBA), PS seed	5.9 / 94.1	$1.5 \times 10^{-5}$	135 / 0.01
GK2808-15	<b>15</b>	Crosslinked poly(MMA-co-nBA)	7.5 / 92.5	$3.9 \times 10^{-5}$	110 / 0.03
GK2808-26; 41; 42	<b>26; 41; 42</b>	Crosslinked poly(MMA-co-nBA)	9.7 / 90.3	$7.3 \times 10^{-5}$	115 / 0.02
GK98-8	<b>8</b>	Non-crosslinked poly(MMA-co-nBA)	9.7 / 90.3	$7.1 \times 10^{-5}$	140 / 0.01

<sup>a)</sup> 40 % solids content

<sup>b)</sup>  $BPEA = mol_{BPEA} / m_{Total\ latex}$

This chapter will be developed into two main studies. Surface-initiated polymerization of NAM will be presented in the first part. The success of the grafting reaction will be evaluated via different analyses. The surface-initiated polymerization of different hydrophilic monomers will be illustrated in the second part and the use of several metals other than Cu(0) for metal-mediated surface-initiated polymerization will be reported in the last part of the chapter.

## 4.1. Control experiments

Control experiments were performed in presence of a non-functionalized latex (2) and a functionalized latex (42) at  $7.3 \times 10^{-5}$  mol/g<sub>latex</sub> BPEA and are listed in *Table 4.2*.

*Table 4.2. Control experiments performed at room temperature, in presence of the latexes 2 and 42.*

Entry	BPEA <sup>a)</sup>	NAM	NAM/BPEA/PMDETA/CuBr <sub>2</sub> /Cu(0) <sup>b)</sup>	Time	Conv. (NMR)	Final solids content <sup>c)</sup>
	(mol/g <sub>latex</sub> )	(g/g <sub>polymer</sub> )	(molar equiv.)	(h)	(%)	(wt%)
2 G1	0	0.13	10 / 0 / 1 / 0.5 / 1.5 cm	5	0	37
42 G14	$4.6 \times 10^{-5}$	0.25	5.5 / 1 / 0 / 0 / 0 cm	6	0	32
42 G15	$4.6 \times 10^{-5}$	0.25	5.5 / 1 / 0 / 0 / 1 cm	6	0	31
42 G17	$4.6 \times 10^{-5}$	0.25	5.5 / 1 / 0.5 / 0.1 / 0 cm	6	0	31
42 G18	$4.6 \times 10^{-5}$	0.25	5.5 / 1 / 0.5 / 0 / 1 cm	6	0	31

<sup>a)</sup>  $BPEA = mol_{BPEA} / m_{Total\ latex}$

<sup>b)</sup> Cu(0) wire ( $\varnothing = 1mm$ )

<sup>c)</sup> Obtained by gravimetry. Identical to initial solids content as NAM is non volatil

As expected no polymerization was observed in presence of functionalized latex and only a part of the initiating system (42 G14; 42 G15; 42 G17 and 42 G18).

No polymerization was obtained with a non-functionalized latex (2 G1) in presence of PMDETA/CuBr<sub>2</sub> and Cu(0).

Control experiments in presence of latex corroborated the results obtained in water. There was no side initiation from residual ACPA, SDS or from components of the catalytic system.

So, surface-initiated polymerization could be now attempted as it was proven that no side reaction may occur in presence of remaining surfactant and initiator.



## 4.2. Surface-initiated polymerization of NAM in presence of Cu(0)

Following the results obtained in copper-mediated polymerization performed in water solution, NAM was selected as a hydrophilic monomer. NAM is a neutral monomer soluble in many organic solvents. It carries an amide group that can easily be detected by FT-IR since not present in the monomers of composing the core.

### 4.2.a. Surface-initiated polymerizations at different BPEA concentrations

#### 4.2.a.i. Core-shell latex synthesis

Surface-initiated polymerizations were performed in presence of latexes synthesized at different BPEA concentrations. These experiments are listed in Table 4.3 and the experimental protocol is described in the experimental part.

Table 4.3. Surface-initiated polymerizations of NAM performed at 25 °C in presence of PMDETA/CuBr<sub>2</sub> and Cu(0)\* from crosslinked poly(MMA-co-nBA) latex particles functionalized at the surface by BPEA, at different Br concentrations.

Entry	BPEA <sup>a)</sup> (mol/g <sub>Latex</sub> )	NAM <sup>b)</sup> (g/g <sub>poly</sub> )	NAM/BPEA/PMDETA/CuBr <sub>2</sub> (molar equiv.)	Time (h)	Conv. (NMR) (%)	D (DLS) after grafting (nm / dispersity)	Final solids content <sup>c)</sup> (wt%)
31 G2	1.4 × 10 <sup>-6</sup>	0.05	97.5 / 1 / 0.6 / 0.10	8	30	120 / 0.08	38
31 G1	1.1 × 10 <sup>-6</sup>	0.22	441.5 / 1 / 0.8 / 0.15	1		Formation of a gel	
50 G1	1.1 × 10 <sup>-5</sup>	0.05	9.5 / 1 / 0.5 / 0.1	1		Formation of a gel	
50 G2	7.3 × 10 <sup>-6</sup>	0.10	21.6 / 1 / 0.5 / 0.1	6	50	170 / 0.20	20
15 G6	2.1 × 10 <sup>-5</sup>	0.05	4.1 / 1 / 0.5 / 0.1	7	100	105 / 0.03	24
15 G2	2.0 × 10 <sup>-5</sup>	0.26	20.5 / 1 / 0.5 / 0.1	7	93	210 / 0.30	30
15 G4	1.9 × 10 <sup>-5</sup>	0.42	33.3 / 1 / 0.5 / 0.1	7	71	270 / 0.30	31
26 G3	6.1 × 10 <sup>-5</sup>	0.13	5.0 / 1 / 0.6 / 0.1	6	96	140 / 0.04	38
41 G4	4.9 × 10 <sup>-5</sup>	0.23	8.9 / 1 / 0.5 / 0.1	4	86	120 / 0.06	33
42 G1	4.6 × 10 <sup>-5</sup>	0.25	9.7 / 1 / 0.5 / 0.1	6	85	120 / 0.01	31
26d G1	1.1 × 10 <sup>-5</sup>	0.40	13.3 / 1 / 0.5 / 0.1	6	88	260 / 0.20	8.6

\* All experiments were performed in presence of 3.5 cm Cu(0) (ϕ= 1mm)

<sup>a)</sup> BPEA = mol<sub>BPEA</sub>/m<sub>Total latex at t=0</sub>

<sup>b)</sup> [NAM] = m<sub>NAM</sub>/m<sub>core particles</sub>

<sup>c)</sup> Obtained by gravimetry. Identical to initial solids content as NAM is non volatil

The first observation is that NAM is polymerized and conversion from 31% (31 G2) to complete conversion (15 G6) were obtained. According to the control experiments, it could reasonably be concluded that the polymerization of NAM was initiated by the surface

bromide groups. Moreover the experiment 26d G1 was performed in presence of the dialyzed latex 26. The results are very similar to those obtained in presence of raw latex (26, 41, 42) confirming again that ACPA and SDS do not interfere with the grafting process.

Eventually, 41 G4 and 42 G1 were performed in the same conditions from latexes 41 and 42 synthesized following the same procedure. Very similar results were obtained indicating a good reproducibility of the surface-initiated polymerization under those conditions.

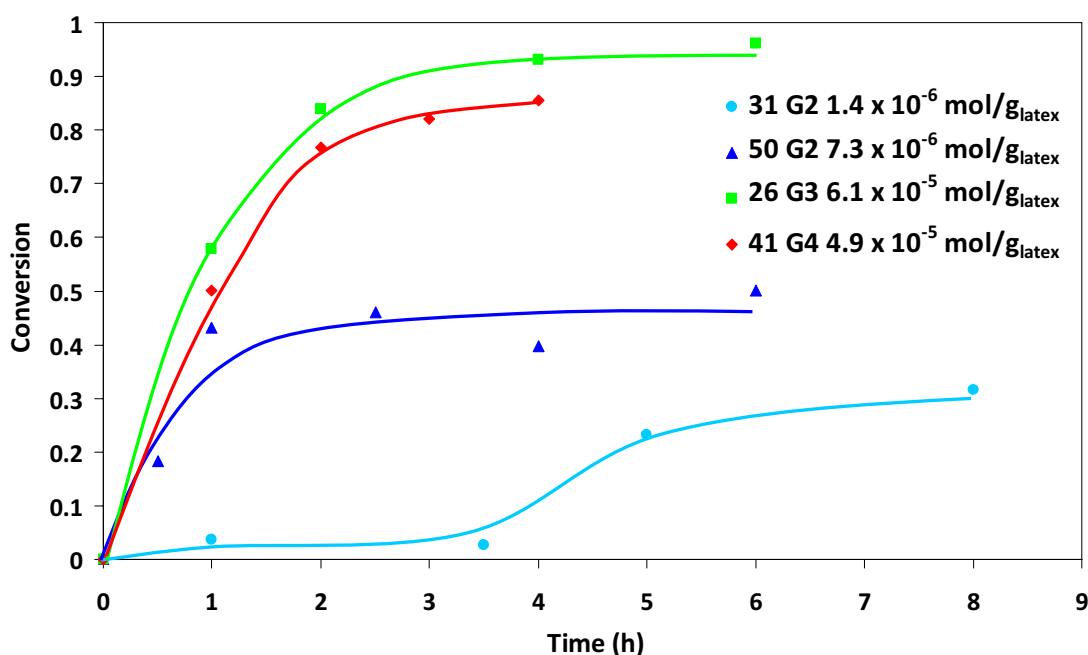


Figure 4.1. Conversion of NAM measured by <sup>1</sup>H NMR analyses vs time for the surface-initiated polymerizations performed at 25 °C in presence of PMDETA/CuBr<sub>2</sub> and Cu(0)\* from crosslinked poly(MMA-co-nBA) latex particles at different BPEA concentrations.

Figure 4.1 displays the polymerization kinetics. In general, polymerizations reached a plateau after 2-3h reaction time. For 31 G2 an inhibition time of 3h was observed. A plateau was also reached after 2h reaction time.

Low conversions were obtained with latexes 31 (31%) and 50 (50%) corresponding to a low amount of bromopropionyloxy-groups, i.e.  $1.4 \times 10^{-6}$  and  $7.3 \times 10^{-6}$  mol/g<sub>latex</sub> respectively. Higher conversions from 71% (15 G4) to 100% (15 G6) were achieved for the latexes with higher bromopropionyloxy-group concentration ( $>1.9 \times 10^{-5}$  mol/g<sub>latex</sub>), meaning that a minimum Br-group is necessary to provide an efficient surface-initiated polymerization.

Comparing 15 G2 and 41 G4 in *Table 4.3*, no significant differences were obtained in term of final conversions (93%, 86% respectively) although the amount of bromopropionyloxy-group available is doubled from 15 G2 to 41 G4 (*Table 4.3*). However, as suggested by ToF-SIMS results (chapter 3, *Table 3.4*) the concentration of bromide group at the particle surface was not different for those two latexes, which could be then considered as a similar substrates.

Latex 15 was used as a substrate for surface-initiated polymerization at different NAM concentrations. 15 G6, 15 G2 and 15 G4 were carried out in presence of PMDETA/CuBr<sub>2</sub> (0.5/0.1 molar equivalent with respect to BPEA) and respectively at 0.05, 0.26 and 0.42  $\frac{g_{NAM}}{g_{poly(MMA-co-nBA)}}$ . Surprisingly, the final conversions decreased when the NAM concentration was increased. One possible explanation, is a competitive copper ions complexation between NAM and PMDETA<sup>2</sup> (chapter 2, *Table 2.5*) decreasing thus the concentration of the active species Cu(I)/PMDETA.

The final latex diameters increased with increasing NAM conversion. Generally, they were in a range of 120 to 140 nm with a low dispersity value. In some examples, much higher final diameters were achieved with however high dispersity indicating aggregation. For 31 G1 and 50 G1 gels were formed after only 1h reaction time. At high substrate concentration, short interparticle distance may favor interparticle cross-linking via radical termination. Gel formation was avoided with a higher dilution (51 G2).

#### 4.2.a.ii. Stability test and viscosity analysis

A hairy layer at the particle surfaces provides steric repulsions and improves the colloidal stability. Sterically stabilized latexes are particularly insensitive to electrolytes and are resistant to freeze-thaw cycles.

To prove the efficient grafting of the hydrophilic shell and the resulting improved stability of latexes, tests were performed in presence of a high concentration of CaCl<sub>2</sub> or after 3 freeze-thaw cycles (*Table 4.4*).

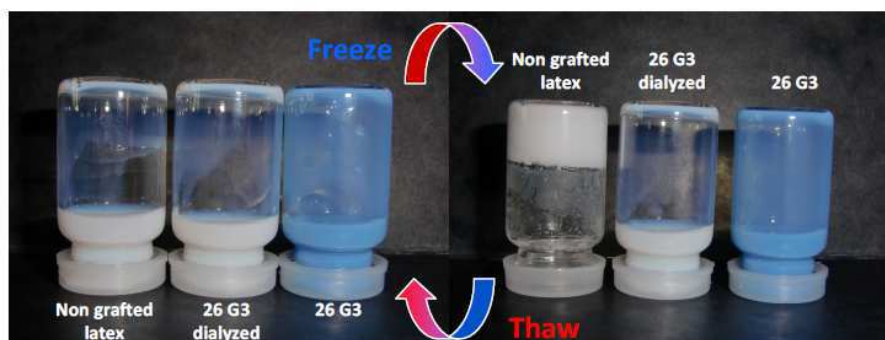


Figure 4.2. Stability tests to freeze-thaw cycles for 26 and 26 G3 latexes grafted with poly(NAM).

Table 4.4. Stability tests to freeze-thaw cycles and  $\text{CaCl}_2$  high concentration and latex viscosity measurements for latexes grafted with poly(NAM).

Entry	Solids content <sup>a)</sup>	Poly(NAM) <sup>b)</sup>	D (DLS) before freezing	D (DLS) after 3 freeze-thaw cycles	Critical $\text{CaCl}_2$ aggregation conc.	Latex viscosity
	(wt%)	(g/g <sub>poly</sub> )	(nm / dispersity)	(nm / dispersity)	(M)	(10 <sup>-3</sup> Pa.s)
Non grafted latex (26)	40	-	100 / 0.03	785 / 0.8	$\leq 4.5 \times 10^{-3}$	0.9
Non grafted Latex (26) + Poly(NAM)	20	-	100 / 0.10	1 500 / 0.5	$\leq 4.5 \times 10^{-3}$	-
31 G2	38	0.15	120 / 0.08	6 000 / 0.5	$\leq 4.5 \times 10^{-3}$	2.4
50 G2	20	0.05	170 / 0.20	3 000 / 1	$\leq 4.5 \times 10^{-3}$	-
15 G6	24	0.05	105 / 0.03	110 / 0.06	> 2.25	1.6
15 G2	30	0.24	210 / 0.30	190 / 0.25	> 2.25	22.1
15 G4	31	0.29	270 / 0.30	235 / 0.30	> 2.25	287.7
26 G3	38	0.29	140 / 0.04	145 / 0.05	> 2.25	2.6
41 G4	33	0.19	120 / 0.06	120 / 0.03	> 2.25	-
42 G1	31	0.21	145 / 0.05	150 / 0.08	> 2.25	-
26d G1	8.6	0.25	260 / 0.2	230 / 0.24	> 2.25	2.7

<sup>a)</sup> Obtained by gravimetry. Identical to initial solids content as NAM is non volatil

<sup>b)</sup>  $m_{\text{NAM}} (\text{g/g}_{\text{poly}}) \times \text{conversion}$

Non grafted latexes either pure or in presence of free poly(NAM) were destabilized after freeze-thaw tests and in presence of low a  $\text{CaCl}_2$  concentration ( $\leq 4.5 \times 10^{-3}$  M).

Poly(NAM) grafted latexes obtained with high NAM conversions (15G6, 15 G2, 15G4, 26 G3, 41 G4 and 42 G1) remained stable after 3 freeze-thaw cycles (low variations of the particle diameter and dispersity) and under high ionic strength ( $\text{CaCl}_2$  aqueous solution >2.25 M). Latex 26 G3 was dialyzed and also tested. 26 G3 and 26 G3 dialyzed latexes

remained stable after 3 freeze-thaw cycles whereas latex 26 (non grafted latex) was destabilized (*Figure 4.2*).

For 31 G2 and 50 G2, the poor stability did not invalidate the grafting. These results could be imputed to the particle morphology. Considering the low bromopropionyloxy-group concentration at the particle surfaces, only a few polymer chains were most probably grafted and the particles were not completely covered by the shell. Instead of hairy layer particles, at low bromide group concentration, surface-initiated polymerization has probably generated “patched” particles and their stabilization is not high enough to survive the stability tests.

In general, the latexes formed by grafting poly(NAM) chains were stable and exhibited a high viscosity. They became more viscous when the poly(NAM)/core ratio increased (series 15, *Table 4.5*). Except for 15 G2 and 15 G4, the final viscosity values were below 3 mPa.s for a solids contents above 25 wt%.

As shown in *Figure 4.3*, the presence of poly(NAM) at the particle surface allowed the good dispersion of the grafted latex in  $\text{CH}_2\text{Cl}_2$  whereas a phase separation was observed between the organic phase and the non grafted latex. As the core of the grafted latex was crosslinked and due to the propensity of poly(NAM) to be soluble in water but also in a range of organic solvents, core-shell particles stabilized the  $\text{H}_2\text{O}/\text{CH}_2\text{Cl}_2$  interface. Thus a Pickering emulsion was probably formed.

A better redispersion in water was also noticed for the grafted latex powder 26 G3 (180 nm, PDI = 0.1) than for the non grafted latex (multipopulation, PDI = 0.5). Initial particle diameters were 145 nm (PDI = 0.05) and 115 nm (PDI = 0.02) respectively.

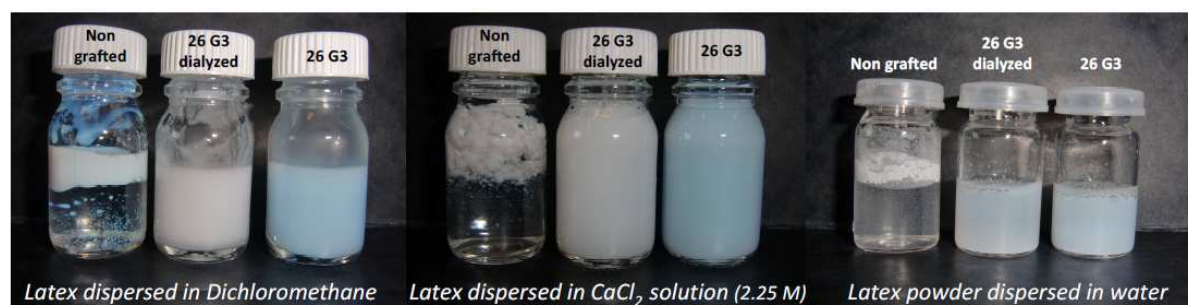


Figure 4.3. Grafted latex stability dispersed in different solutions.

#### 4.2.a.iii. FT-IR analysis

Even though all the stability tests showed the evidence of grafting, FT-IR analyses were performed to further confirm that the poly(NAM) was covalently bound to the core. Latexes were dialyzed against water using a Spectra/Por® dialysis membrane (cut-off at 12 000-14 000 Da) to remove the water phase content (i.e. including non grafted species) before the analysis.

On the FT-IR spectra of the poly(NAM) (Figure 4.4), a band at  $1640\text{ cm}^{-1}$ , corresponding to the amide group (amide I stretching vibration) was observed. This band, not detected for the non grafted latex, was also observed after thorough cleaning of the grafted latexes, confirming the efficient incorporation of poly(NAM) in the latex by covalent bonding.

To determine quantitatively the poly(NAM) content, a calibration curve was first planned by mixing non grafted latex and poly(NAM) at different ratios. The non grafted latex exhibits a specific ester band at  $1725\text{ cm}^{-1}$  (ester stretching vibration). This band being present in all latexes and corresponding to the same amount of C = O groups (core of all latexes), it was used as an internal reference. The intensity ratio of the amide band and the ester band was plotted against  $g_{\text{NAM}}/g_{\text{core}}$ . However, the resulting plot was not linear and the analyses were not reproducible particularly for the low ratios of poly(NAM). The quantitative determination of the grafted poly(NAM) was thus not sufficiently accurate to use this technique.

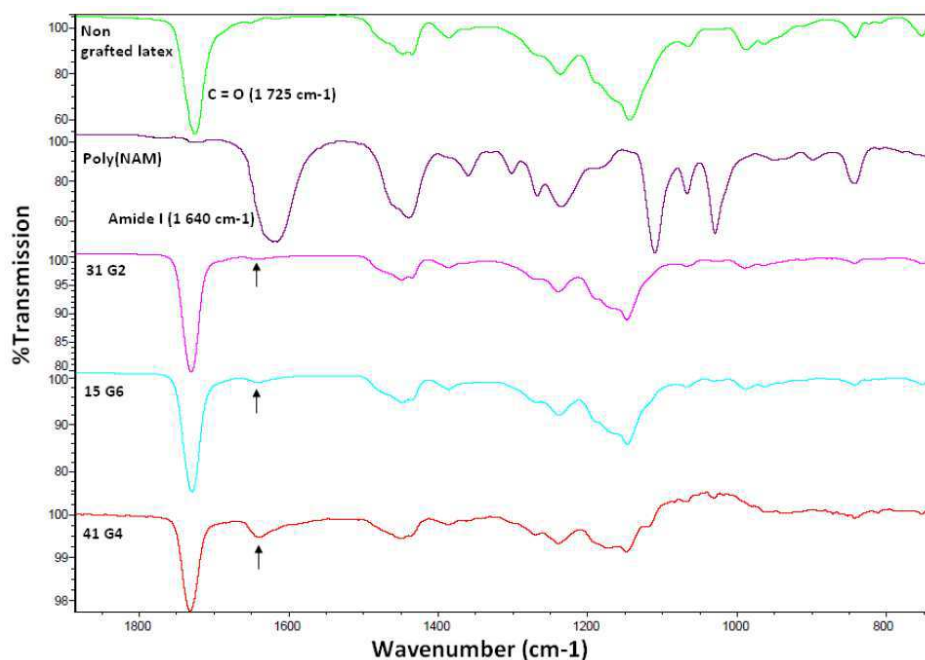


Figure 4.4. FT-IR analyses of dialyzed grafted latexes.

#### 4.2.a.iv. ToF-SIMS analysis

Dialyzed grafted latexes were also analyzed by ToF-SIMS to confirm the location of the poly(NAM). Despite the hydrophilic nature of the polymer, it was important to check whether the poly(NAM) was at the extreme particle surface and whether this surface was completely or only partially modified.

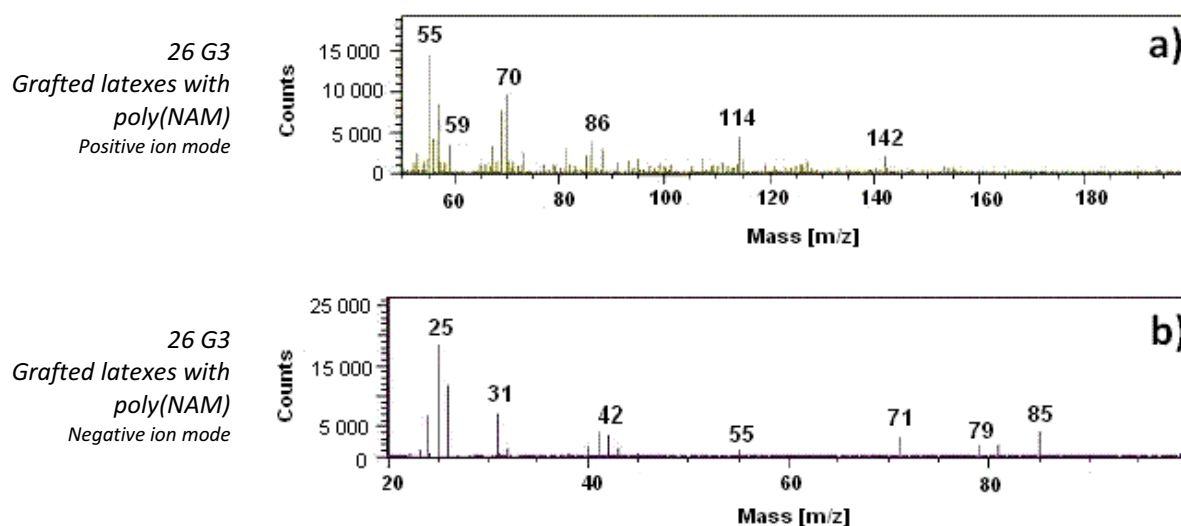


Figure 4.5. (a) Positive ion mode ( $m/z = 50-200$ ) and (b) negative ion mode ( $m/z = 20-100$ ) ToF-SIMS spectra for the latex 26 G3.

Few N-based signatures detected for non-functionalized latex (2) and for non-grafted latexes (31, 15 and 26) were due to the use of ACPA as an initiator, which contains a -CN group.

Figure 4.5 corresponds to the spectra obtained for the latex 26 G3 in negative and positive modes. Additional N-based signatures were observed and assigned to characteristic peaks of poly(NAM) such as those at  $m/z = 26.004$  (corresponding to  $\text{CN}^-$ ,  $m/z = 26.003$ ),  $m/z = 42.007$  (corresponding to  $\text{CNO}^-$ ,  $m/z = 41.998$ ),  $m/z = 70.038$  (corresponding to  $\text{C}_3\text{H}_4\text{NO}^+$ ,  $m/z = 70.028$ ),  $m/z = 86.064$  (corresponding to  $\text{C}_4\text{H}_8\text{NO}^+$ ,  $m/z = 86.060$ ),  $m/z = 114.069$  (corresponding to  $\text{C}_5\text{H}_8\text{NO}_2^+$ ,  $m/z = 114.055$ ) and at  $m/z = 142.095$  (corresponding to  $\text{C}_7\text{H}_{12}\text{NO}_2^+$ ,  $m/z = 142.087$ ).

The presence of new N-based signatures was confirmed by the normalized intensity values reported in Table 4.5.

Table 4.5. ToF-SIMS normalized intensity (in %) for various characteristic peaks\*.

Entry	Characteristic signatures for core latex		Characteristic signatures for bromopropionyloxy-group		Characteristic signatures for poly(NAM)		
	$I^{59+}$	$I^{85-}$	$I^{79-}$	$I^{179+}$	$I^{26-}$	$I^{42-}$	$I^{142+}$
			$^{79}\text{Br}^-$		$\text{CN}^-$	$\text{CNO}^-$	$\text{C}_7\text{H}_{12}\text{NO}_2^+$ 
2	13.7 ± 2.2	21.9 ± 2.6	0.9 ± 0.2	1.2 ± 0.3	5.8 ± 0.2	0.4 ± 0.1	1.6 ± 0.2
31	16.5 ± 1.0	27.3 ± 1.8	3.7 ± 0.0	1.4 ± 0.2	7.4 ± 0.6	0.5 ± 0.1	1.8 ± 0.2
31 G2	16.8 ± 1.2	15.6 ± 5.0	1.4 ± 0.4	1.5 ± 0.0	15.8 ± 0.1	2.7 ± 0.5	3.7 ± 0.1
15	16.0 ± 0.4	18.8 ± 3.1	39.9 ± 3.6	7.4 ± 0.7	4.4 ± 0.2	0.3 ± 0.0	2.0 ± 0.0
15 G2	5.5 ± 1.1	4.8 ± 4.7	5.4 ± 2.6	1.1 ± 0.2	19.1 ± 6.9	5.8 ± 3.9	9.1 ± 1.4
26	13.4 ± 3.6	15.5 ± 2.5	39.8 ± 4.7	6.6 ± 1.1	5.7 ± 1.3	0.3 ± 0.1	1.5 ± 0.2
26 G3	7.0 ± 0.5	9.1 ± 1.3	4.7 ± 0.2	1.1 ± 0.1	23.7 ± 2.6	7.5 ± 1.1	8.1 ± 0.8

\*Peaks at :  $m/z = 59^+$  corresponding to  $\text{C}_2\text{H}_3\text{O}_2^+$  and  $m/z = 85^-$  corresponding to  $\text{C}_4\text{H}_5\text{O}_2^-$ , characteristic of the core latex;  $m/z = 79^-$  corresponding to  $^{79}\text{Br}^-$  and  $m/z = 179^+$  corresponding to  $\text{C}_5\text{H}_8\text{O}_2^{79}\text{Br}^+$ , characteristic of bromopropionyloxy-group;  $m/z = 26^-$  corresponding for a major part to  $\text{CN}^-$  but contribution from  $\text{C}_2\text{H}_2^-$  cannot be excluded,  $m/z = 42^-$  corresponding to  $\text{CNO}^-$  and  $m/z = 142^+$  corresponding to  $\text{C}_7\text{O}_2\text{H}_{12}\text{N}^+$ .

<sup>a)</sup> A possible ion structure for  $\text{C}_7\text{O}_2\text{H}_{12}\text{N}^+$  resulting from the poly(NAM) fragmentation

The normalized intensity values for core latex specific peaks significantly decreased, which illustrated a significant grafting of poly(NAM) at the surface for 15 G2 and 26 G3 latexes. For



31 G2 the characteristic signature of the poly(MMA-co-nBA) remained still high, but an increase in the intensities of the characteristic N-based signatures indicated the grafting of poly(NAM). The hydrophilic shell grafted at particle surfaces with low bromine concentration, was probably not dense enough to cover completely the particle surface.

Br was still detected but the specific peaks for bromopropionyloxy-moiety (i.e.  $C_5H_8O_2^{79}Br^+$  and  $C_5H_8O_2^{81}Br^+$ ) not anymore. The normalized intensity for  $179^+$  was back to the value previously observed (and not corresponding to  $C_5H_8O_2^{79}Br^+$ ) for the latex 2. This result is consistent with polymerization mechanism in which chains are extended from bromopropionyloxy-group while maintaining a dormant Br end-group. If  $C_5H_8O_2^{79}Br^+$  was as expected not detected anymore, peak combining poly(NAM) and Br end-group was however not detected.

The latexes were dialyzed before the ToF-SIMS measurements. However, as already reported in chapter 3.3, a few amount of SDS remained in the latex and was detected at  $m/z = 265^-$ . Moreover, characteristic peaks of copper complex were detected. The peak at  $m/z = 236^+$  and the peak at  $m/z = 501^+$  were respectively attributed to the complex PMDETA/Cu and PMDETA/Cu/SDS.

Table 4.6. ToF-SIMS normalized intensity (in %) for various characteristic peaks\*.

Entry	Characteristic signatures for SDS $ ^{265-}$	Characteristic signatures for copper complexes $ ^{236+}$	Characteristic signatures for copper complexes $ ^{501+}$	Characteristic signatures for $CuBr_2$ $ ^{221-}$
				$CuBr_2$
2	0.6 ± 0.1	0.3 ± 0.1	0 ± 0	0.1 ± 0
31	0.9 ± 0.1	0.3 ± 0.1	0 ± 0	-
31 G2	0.2 ± 0.1	1.3 ± 0.1	0.1 ± 0	0.1 ± 0
15	0.3 ± 0.1	0.3 ± 0	0 ± 0	-
15 G2	0.6 ± 0.5	0.9 ± 0.7	0.5 ± 0.2	0.1 ± 0
26	0.5 ± 0.2	0.2 ± 0	0 ± 0	-
26 G3	1.0 ± 0.2	1.2 0.2	0.5 ± 0	0.1 ± 0

\*Peaks at :  $m/z = 265^-$  corresponding to  $C_{12}H_{25}O_4S^-$ , characteristic of SDS;  $m/z = 236^+$  corresponding to  $C_9H_{23}N_3Cu^+$  and  $m/z = 501^+$  corresponding to  $C_{23}H_{32}N_3O_4Cu^+$ , characteristic of copper complexes;  $m/z = 221^-$  corresponding  $CuBr_2$ .

The intensities of CuBr<sub>2</sub> characteristic peak were identical for the different samples and rather low, indicating that the dialyses were efficient for all the samples.

For the grafted latexes, the intensities of copper complexes increased with respect to those obtained for non grafted latexes. These results confirmed again that the copper complexes were most likely trapped in the poly(NAM) shell.

#### 4.2.a.v. Electrospray charge-detection mass spectroscopy

Recently, electrospray charge-detection mass spectrometry (ECD-MS) has been successfully used by the LASIM and LCPP teams to determine molar masses and molar mass distributions of polymer particles<sup>3</sup>. By this method, the particles are directly ionized without alteration of their structure. The charge and velocity of the charged particles are first measured under static conditions. Then under voltage gradient, the charged particles are accelerated. The  $m/z$  ratio is determined from velocity measurements and acceleration voltage. The mass of each individual ion is then calculated from the knowledge of  $m/z$  ratio and the charge  $z$ . The general principle of the technique is displayed in *Figure 4.6*.

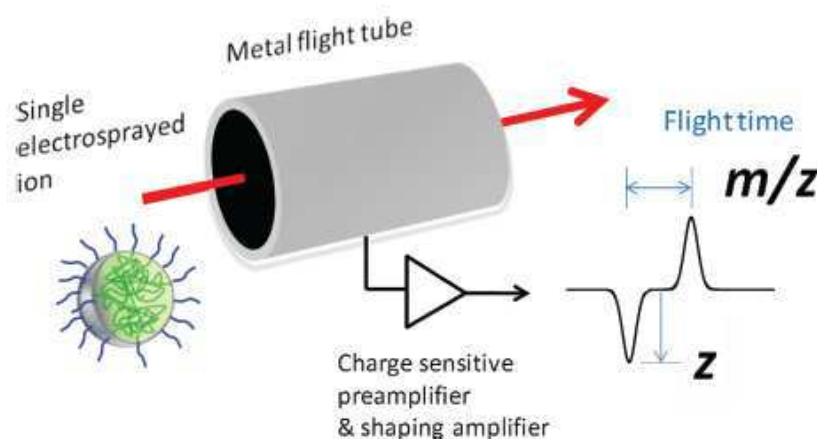


*Figure 4.6. Principle of charged detection mass spectrometry applied to weighing electro sprayed latex particles. Reprinted with permission from ref 3. Copyright 2012 American Chemical Society.*

The CD-ESI analyses were performed for 42 (functionalized latex) and 42 G1 (poly(NAM) grafted latex. Both latexes were cleaned by dialysis before measurements.

*Figure 4.7* displays the amplitude of the image-charge signal, which is proportional to  $z$  and the time-of-flight for the two samples.

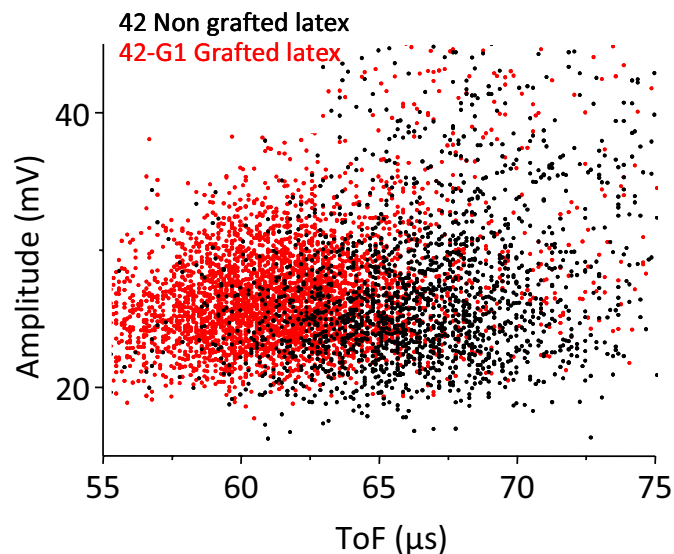


Figure 4.7. Amplitude (mV) vs ToF ( $\mu\text{s}$ ) for the non grafted latex 42 and for the grafted poly(NAM) latex 42 G1.

Both latexes have been successfully charged. However, it appeared that more ions have been detected for the grafted poly(NAM) latex 42 G1. In this case, the ion population is denser and centered at higher amplitude. The time of flight was also shorter.

It seems thus that in the presence of a poly(NAM) shell, the particles are better ionized. Mass-charge diagrams and charge spectra histogram (Figure 4.8) confirmed that the grafted latex is 30% more charged than non grafted latex at a same mass ( $M \approx 580$  MDa). All these results confirm again that the poly(NAM) was grafted at the surface of the particle.

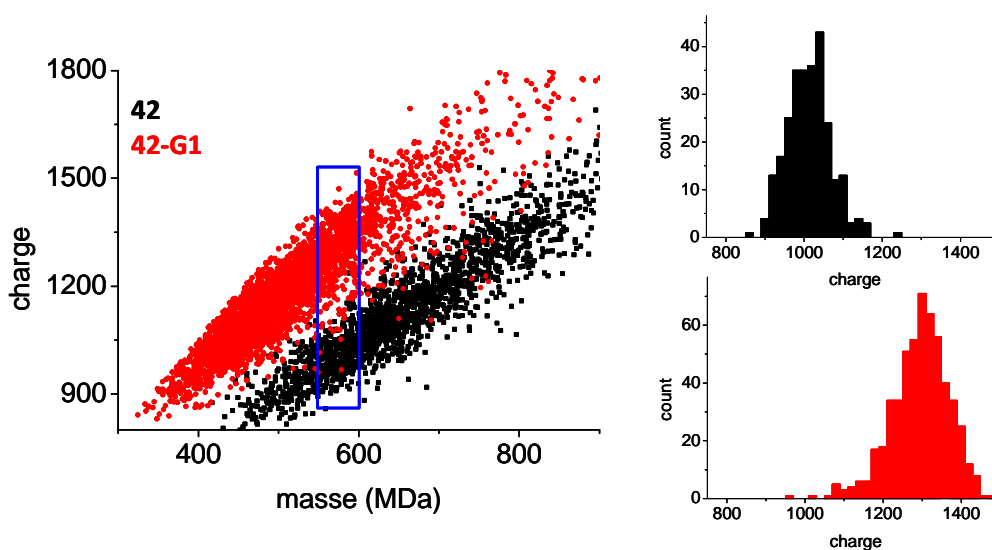


Figure 4.8. Mass-charge diagram (left) and charge spectra histograms (right) for the non grafted latex 42 and for the grafted poly(NAM) latex 42 G1.

Since the non-grafted latex are poorly charged, only part of the population has been detected, i.e. the more charged and larger particles. Therefore, the determination of the molar mass of the non-grafted latex is not possible by this method. The molar mass average ( $\sim 600$  MDa) is certainly over estimated.

For the grafted latex, a molar mass average of  $\sim 450$  MDa have been determined. This value is in adequation with the calculated molar masses 540 MDa and 340 MDa from the particle diameter obtained by DLS (hydrated particles) and TEM (dry particles) respectively assuming a density of 1.15 for the polymer.

#### 4.2.a.vi. Serum analysis

Grafted latexes were cleaned by centrifugation to determine the water soluble content. As grafted latexes were very stable, a complete separation of the serum and latex particles was difficult to achieve. A very small amount of grafted particles was still present in the serum (confirmed by DLS). Nevertheless, the serum was dried and analyzed by  $^1\text{H}$  NMR spectroscopy.

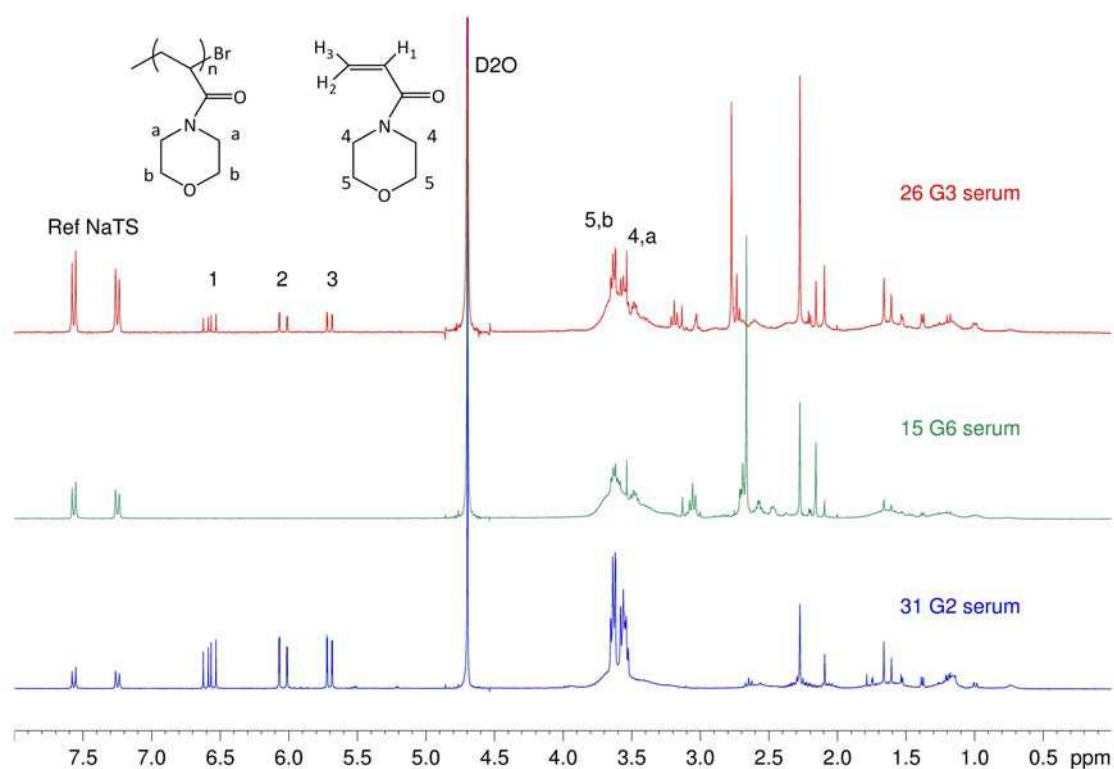


Figure 4.9.  $^1\text{H}$  NMR spectra of the dried serum residues obtained by centrifugation of grafted latexes in  $\text{D}_2\text{O}$ .

Figure 4.9 displays  $^1\text{H}$  NMR spectra of grafted latex dried serum. The presence of poly(NAM) in a small amount was detected but since a few amount of latex particles still remained in the serum, part of the signal might be attributed to grafted poly(NAM). This did not allow the quantification of the non-grafted poly(NAM), which appeared to be anyway rather small.

Latexes 42 and 42 G1 were further analyzed by analytical ultracentrifugation (AUC). By this technique, latex particles are fractionated under ultracentrifugation according to their size, density and are detected with absorbance optics. In general, AUC is used to determine particle size distribution<sup>4</sup>. It is also possible to detect the presence of water soluble content by measuring the turbidity variations of the water phase media. With this method, oligomers were not detected in the latex 42 G1 confirming again the low amount of non-grafted polymer chains.

#### 4.2.b. Surface-initiated polymerization with different cores

Crosslinked particles are convenient for analysis purposes as their integrity is maintained. But, for potential applications, these latexes are not adapted, particularly for film formation. Therefore a non-crosslinked latex (8) was used as a substrate for surface-initiated polymerization (Table 4.7).

Table 4.7. Surface-initiated polymerizations of NAM performed at 25 °C in presence of PMDETA/CuBr<sub>2</sub> and Cu(0)\* from crosslinked and non-crosslinked poly(MMA-co-nBA) aqueous latex particles functionalized at the surface by BPEA ( $4.6 \times 10^{-5}$  mol/g<sub>Latex</sub>)\*\*.

Entry	NAM (g/g <sub>poly</sub> ) <sup>a)</sup>	NAM (molar equiv.)	Time (h)	Conv. (NMR) (%)	D <sup>b)</sup> (DLS) after grafting (nm / dispersity)	Final solids Content <sup>c)</sup> (wt%)	Critical CaCl <sub>2</sub> aggregation conc. (M)
42 G1 Crosslinked	0.25	9.7	6	85	120 / 0.01	31	> 2.25
8 G1 Non-crosslinked	0.25	9.6	6	94	230 / 0.30	31	> 2.25

\* All experiments were performed in presence of 3.5 cm Cu(0) ( $\phi = 1\text{mm}$ ) and PMDETA/CuBr<sub>2</sub> at 0.5/ 0.1 molar equivalent with respect to BPEA

\*\* BPEA =  $\text{mol}_{\text{BPEA}} / m_{\text{Total latex at } t=0}$

<sup>a)</sup> [NAM] =  $m_{\text{NAM}} / m_{\text{core particles}}$

<sup>b)</sup> Initial particle diameters: 115 nm (0.02) for latex 42 and 140 nm (0.01) for latex 8

<sup>c)</sup> Obtained by gravimetry. Identical to initial solids content as NAM is non volatil

For both grafting experiments, the conversion of NAM reached a plateau at high conversion values after 2h reaction time (Figure 4.10). It was noticed that in presence of non-crosslinked latex, the final conversion was higher.

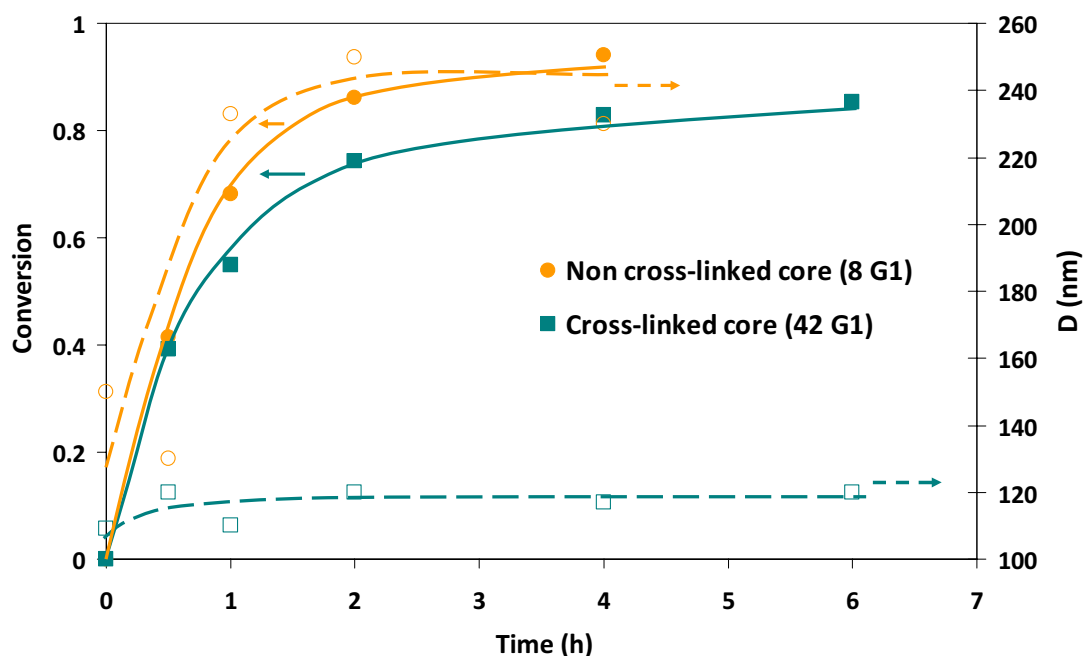


Figure 4.10. Particle size (DLS) and conversion of NAM measured by  $^1\text{H}$  NMR analysis vs time for the Cu(0) surface-initiated polymerizations from crosslinked and non-crosslinked latex.

The main difference between those two substrates was the final particle size. The particle diameter for latex 8 G1 was 230 nm with high dispersity (0.3), whereas it was only 120 (with narrow particle size distribution) for the crosslinked latex. This difference in particle size may then be attributed to aggregation. Stability test results obtained for the non-crosslinked latex 8 G1 and crosslinked latex 42 G1 were nevertheless very similar.

Latex 8 G1 was dialyzed against water to remove the hydrosoluble content. The polymer was fully soluble in  $\text{CDCl}_3$  and was analyzed by  $^1\text{H}$  NMR in  $\text{CDCl}_3$  to confirm the presence of poly(NAM).

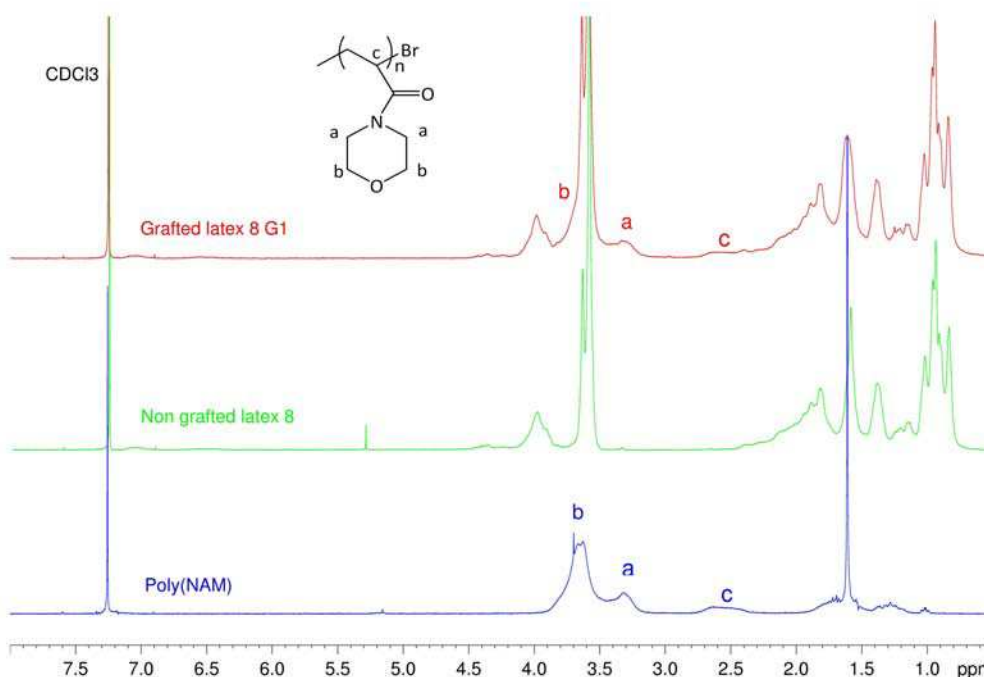


Figure 4.11.  $^1\text{H}$  NMR spectra of non-crosslinked latexes in  $\text{D}_2\text{O}$  obtained after dialysis. Latex 8 corresponding to a non grafted latex and latex 8 G1 to a poly(NAM) grafted latex.

Based on the  $^1\text{H}$  NMR spectra (Figure 4.11) of 8 and 8 G1 dialyzed latexes, the broad peak at 3.2 ppm corresponding to  $\text{CH}_2\text{-N}$  of the morpholine ring corroborated the grafting of poly(NAM) chains.

#### 4.2.c. Surface-initiated polymerization at different copper complex concentrations

The effect of the copper complex concentration ( $\text{PMDETA}/\text{CuBr}_2$ ) was studied for the grafting reaction from latexes 41 and 8. The concentration of  $\text{PMDETA}/\text{CuBr}_2$  was decreased but the molar ratio  $\text{PMDETA}/\text{CuBr}_2$  was maintained at 0.5 with the same amount of  $\text{Cu}(0)$ . The experiments performed at various copper complex concentrations are listed in Table 4.8.

Table 4.8. Surface-initiated polymerizations of NAM performed at 25 °C in presence of PMDETA/CuBr<sub>2</sub> and Cu(0)\* from crosslinked and non-crosslinked poly(MMA-co-nBA) aqueous latex particles functionalized at the surface with the help BPEA in presence of various copper complex concentrations.

Entry	BPEA <sup>a)</sup>	NAM <sup>b)</sup>	NAM/BPEA/PMDETA/CuBr <sub>2</sub>	Time	Conv.(NMR)	D (DLS) after grafting	Final solids content <sup>c)</sup>
	(mol/g <sub>Latex</sub> )	(g/g <sub>poly</sub> )	(molar equiv.)	(h)	(%)	(nm / dispersity)	(wt%)
41 G4	4.9 x 10 <sup>-5</sup>	0.23	8.9 / 1 / 0.5 / 0.1	4	86	120 / 0.06	33
41 G1	4.6 x 10 <sup>-5</sup>	0.26	9.9 / 1 / 0.25 / 0.05	5	89	130 / 0.05	31
41 G2	4.9 x 10 <sup>-5</sup>	0.25	9.7 / 1 / 0.1 / 0.025	2		Formation of a gel	
8 G1	4.6 x 10 <sup>-5</sup>	0.25	9.6 / 1 / 0.5 / 0.1	6	94	230 / 0.30	31
8 G3	4.7 x 10 <sup>-5</sup>	0.25	9.5 / 1 / 0.25 / 0.05	1		Formation of a gel	

\* All experiments were performed in presence of 3.5 cm Cu(0) ( $\phi = 1\text{mm}$ )

<sup>a)</sup> BPEA =  $\text{mol}_{\text{BPEA}} / m_{\text{Total latex at } t=0}$

<sup>b)</sup> [NAM] =  $m_{\text{NAM}} / m_{\text{core particles}}$

<sup>c)</sup> Obtained by gravimetry. Identical to initial solids content as NAM is non volatil

For the latex 41, stable suspensions were obtained in presence of 0.5/0.1 and 0.25/0.05 molar equivalents of PMDETA/CuBr<sub>2</sub> with respect to BPEA. A gel was formed at 0.1/0.025 molar ratio of PMDETA and CuBr<sub>2</sub> (41 G2). It could be concluded that a minimum complex concentration is necessary to avoid gel formation. Based on the kinetic curves of Figure 4.12, by increasing the copper complex concentration, the polymerization rate decreased. Again, a minimum amount of deactivator (CuBr<sub>2</sub>) is required to decrease the concentration of propagating radicals and so the probability of interparticle coupling.

For the non-crosslinked particles, a gel was formed at 0.25/0.05 molar ratio of PMDETA and CuBr<sub>2</sub>. The initial diameter of the non-crosslinked particles was higher than that of the crosslinked particles, 140 nm and 115 nm respectively. Since non-crosslinked particles diameter could increase due to the swelling process, interparticle coupling reactions were also favored as the interparticle distance decreased.



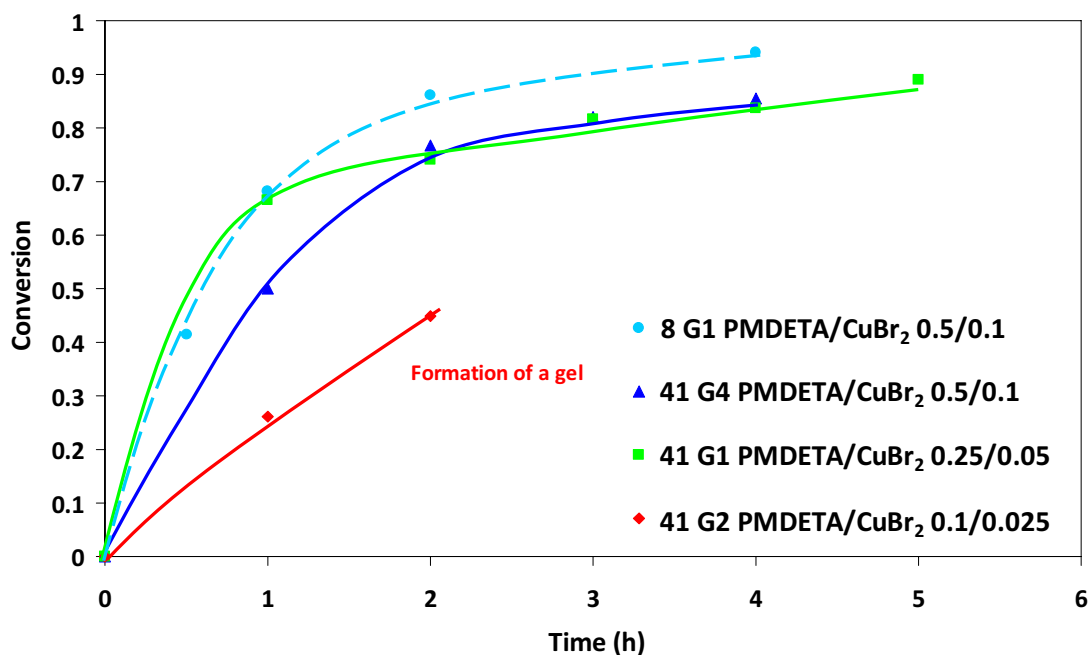


Figure 4.12. Conversion of NAM measured by  $^1\text{H}$  NMR analyses vs time for the Cu(0) surface-initiated polymerizations from crosslinked and non-crosslinked latex at various copper complex concentrations.

#### 4.2.d. Two-step grafting reaction

In ATRP, the chain ends of the grafted polymer chains should normally be capped with an active halogen atom. ToF-SIMS of the grafted latex has demonstrated the presence of Br-group at the particle surface that may be able to reinitiate a second polymerization step.

In this purpose, surface-initiated polymerization was performed using latex grafted with poly(NAM). Sodium 4-styrene sulfonate (NaSS) was chosen as a second hydrophilic monomer. Two kinds of protocol were tested. As grafted latexes already contained copper complex, one test was carried out without additional PMDETA/CuBr<sub>2</sub>. For the other test, a molar ratio of PMDETA/CuBr<sub>2</sub> (0.5/0.1) was added with respect to BPEA. These experiments are listed in Table 4.9.

Table 4.9. Surface-initiated polymerizations of NaSS performed at 25 °C in presence of PMDETA/CuBr<sub>2</sub> and Cu(0)\* from crosslinked poly(MMA-co-nBA) latex particles grafted with poly(NAM) shell (41 G4 and 41 G20\*\*).

Entry	BPEA <sup>a)</sup>	NaSS <sup>b)</sup>	NaSS/BPEA/PMDETA/CuBr <sub>2</sub>	Time	Conv.(NMR)	D (DLS) after grafting	Final solids content <sup>c)</sup>
	(mol/g <sub>Latex</sub> )	(g/g <sub>poly</sub> )	(molar equiv.)	(h)	(%)	(nm / dispersity)	(wt%)
41 G4 R2	2.4 x 10 <sup>-5</sup>	0.3	3.4 / 1 / 0.5 / 0.1	6	100	210 / 0.1	17
41 G4 R3	2.5 x 10 <sup>-5</sup>	0.3	3.5 / 1 / 0 / 0	6	34	145 / 0.03	18
41 G20 R2	2.2 x 10 <sup>-5</sup>	0.2	3.5 / 1 / 0.5 / 0.1	6	81	195 / 0.04	15
41 G20 R3	2.2 x 10 <sup>-5</sup>	0.2	3.5 / 1 / 0 / 0	6	0	120 / 0.04	15

\* All experiments were performed in presence of 1 cm Cu(0) (ϕ= 1mm)

\*\* 41 G4 and 41 G20 were synthesized following the same conditions and exhibited the same characteristics

<sup>a)</sup> BPEA = mol<sub>BPEA</sub>/m<sub>Total latex at t=0</sub> calculated with the BPEA concentration of the non-grafted latex

<sup>b)</sup> [NaSS] = m<sub>NaSS</sub>/m<sub>Latex particles grafted with poly(NAM)</sub>

<sup>c)</sup> Obtained by gravimetry. Identical to initial solids content as all hydrophilic monomers are non volatil

The final conversions were influenced by the presence of additional copper complex (Figure 4.13). In presence of added PMDETA/CuBr<sub>2</sub>, high conversions were achieved. At the opposite, low or no polymerization was observed in absence of additional copper complex.

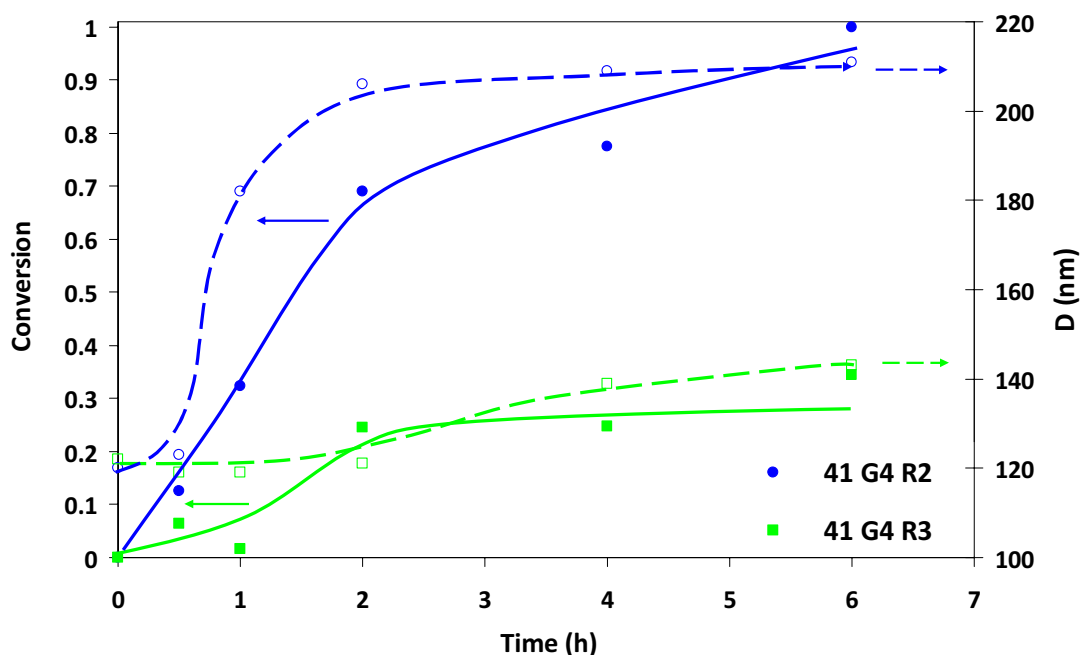


Figure 4.13. Particle size evolution and conversion of NaSS measured by <sup>1</sup>H NMR analyses vs time for the surface-initiated polymerizations from crosslinked poly(MMA-co-nBA) latex particles grafted with poly(NAM) shell in presence or not of copper complex.

We have shown earlier in this chapter that the influence of NAM concentration on the polymerization kinetics was explained by a possible competitive copper ion complexation

between NAM or poly(NAM) and PMDETA, reducing the amount of the active species Cu(I)/PMDETA. It could thus be concluded that, during the grafting reaction, part of the complex is trapped in the poly(NAM) shell, reducing the amount of copper complex in the water phase directly in contact with Cu(0). Consequently, without additional PMDETA/CuBr<sub>2</sub> the polymerization rate was low as the complex was segregated within the poly(NAM) shell.

For 41 G4 R2 and 41 G20 R2, 100% and 81% of conversion were achieved respectively. The particle diameters increased with conversion from 140 nm to ~200 nm. A high dispersity value (0.1) due to possible aggregation for 41 G4 R2 was noticed. But both final latexes were stable.

Electron microscopy observations of the dried latexes were performed by TEM and SEM (Figure 4.14).

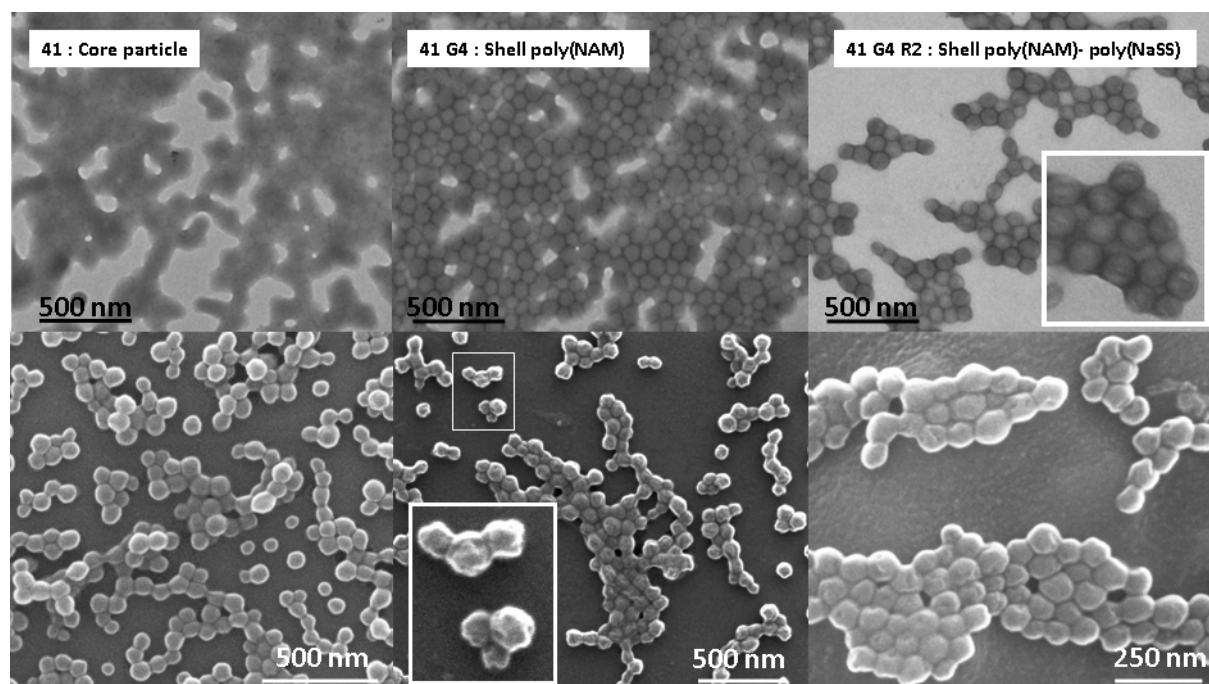
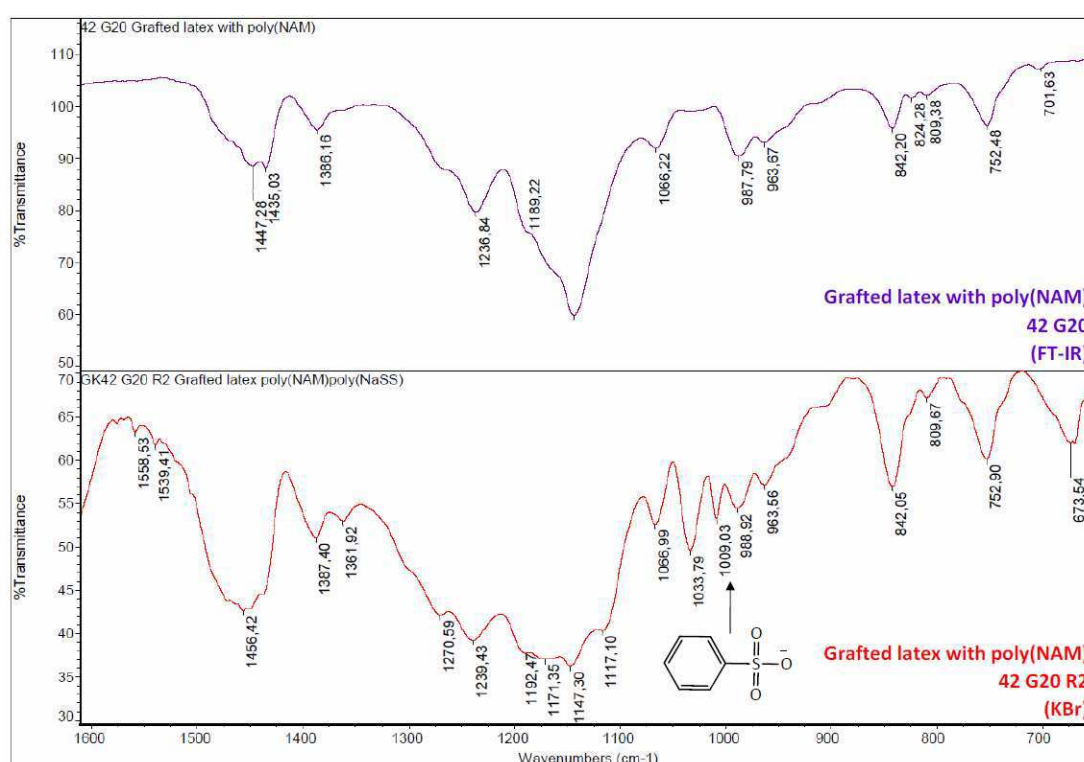


Figure 4.14. Transmission electron microscopy (top) and scanning electron microscopy image (bottom) of 41, 41 G4 and 41 G4 R2 (from left to right).

The core particles (41) observed by SEM were spherical and their surface was smooth. Poly(MMA) depolymerizes under electron beam and no observation of the core was possible by TEM. But after the formation of the poly(NAM) shell, the particle integrity was maintained during the analysis. The observation of the core-shell particle surface by SEM

displayed a modification, as they appeared significantly rougher. After the polymerization of NaSS the particle surface was smoother again. By TEM observations, no variation of the morphology was however noticed.

To confirm the incorporation of poly(NaSS), the dialyzed latex 41 G20 R2 was analysed by FT-IR. As displays in *Figure 4.15*, FT-IR spectrum for latex 42 G20 R2 exhibited new peaks and more particularly, a band centered at  $1\ 009\ \text{cm}^{-1}$  resulting from the vibrations of the phenyl ring was observed, attesting the presence of poly(NaSS).



*Figure 4.15.* FT-IR spectra of the dialyzed latex grafted with poly(NAM) (top) and of the latex grafted with poly(NAM)-poly(NaSS) (KBr pellet).

The increase of the particle size indicated a growth of the shell. But it was difficult to conclude on the real initiation sites, either the functionalized poly(NAM) chains or the non-converted Br-group at the surface. For this purpose, ToF-SIMS analyses were performed so as to locate the poly(NaSS). As the ToF-SIMS is an analysis of extreme surface, it is possible to draw conclusion on the extreme surface composition. If a second poly(NaSS) shell is polymerized from poly(NAM), the main signature detected will be poly(NaSS). If the

poly(NaSS) polymerized from the core surface (i.e from non reacted Br-group), both poly(NaSS) and poly(NAM) will be detected.

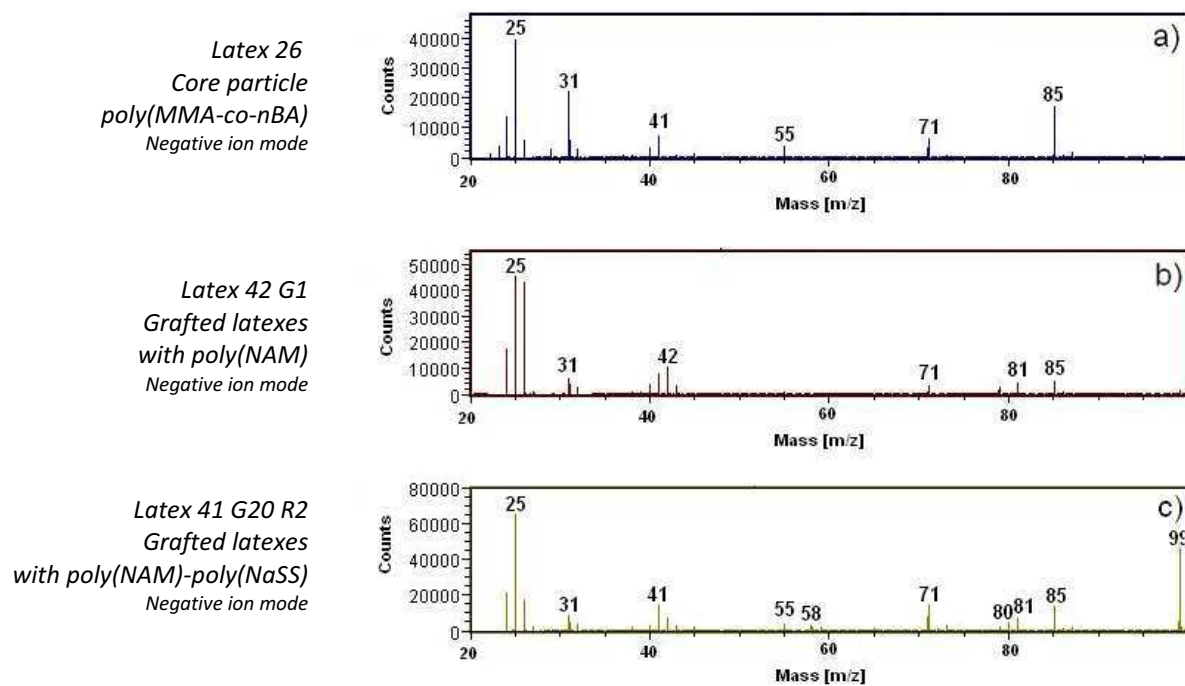


Figure 4.16. Negative ion mode ToF-SIMS spectra ( $m/z = 50-200$ ) for (d) latex 26, (e) latex 42 G1 grafted with poly(NAM), (f) latex 41 G20 R2 grafted with poly(NAM)-poly(NaSS).

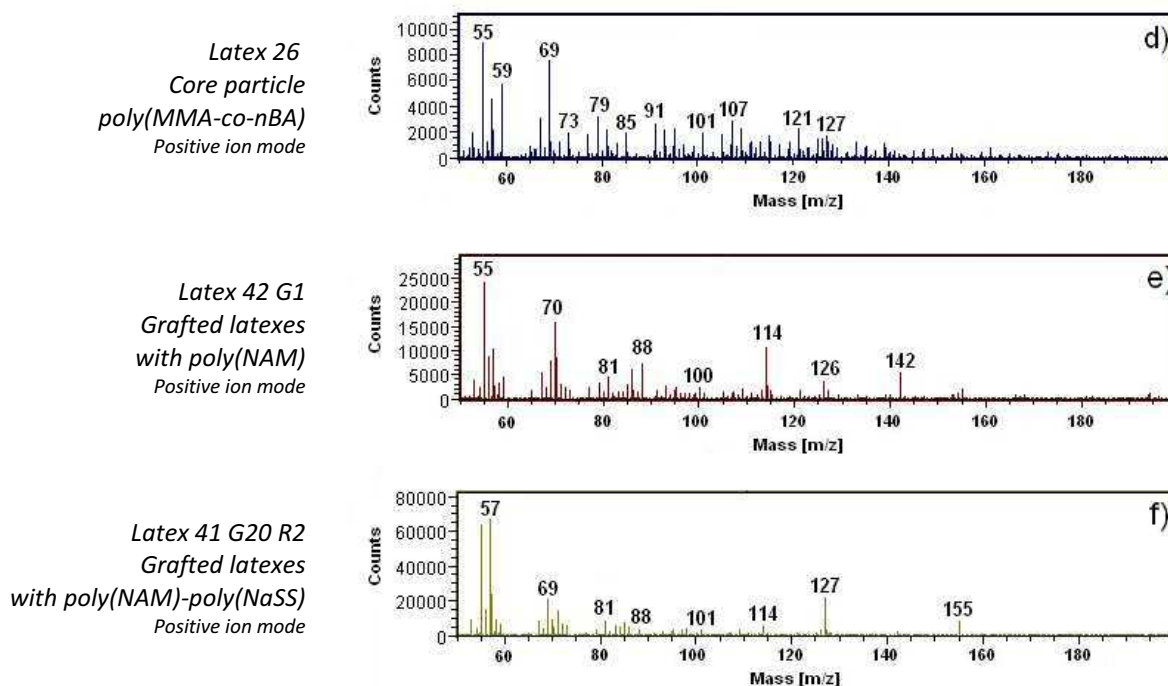


Figure 4.17. Positive ion mode ToF-SIMS spectra ( $m/z = 50-200$ ) for (d) latex 26 core particle, (e) latex 42 G1 grafted with poly(NAM), (f) latex 41 G20 grafted with poly(NAM)-poly(NaSS).

The ToF-SIMS spectra in negative and positive modes are different after the different reaction steps attesting a surface modification (Figure 4.16 and Figure 4.17).

For the latex grafted with poly(NAM) and poly(NaSS), the normalized intensity of the characteristic signature for the core and the poly(NAM) decreased (Table 4.10) but surprisingly no characteristic signature for the poly(NaSS) appeared. A characteristic peak at  $m/z = 79.9$  (corresponding to  $\text{SO}_3^-$ ) was still detected in negative mode but the peak intensity was very low and ubiquitous contamination could not be excluded. Generally, ToF-SIMS spectra of benzene ring exhibit characteristic peaks at  $m/z = 77$  (corresponding to  $\text{C}_6\text{H}_5^+$ ),  $m/z = 91$  (corresponding to  $\text{C}_7\text{H}_7^+$ ),  $m/z = 103$  (corresponding to  $\text{C}_8\text{H}_7^+$ ),  $m/z = 105$  (corresponding to  $\text{C}_8\text{H}_9^+$ ) and  $m/z = 115$  (corresponding to  $\text{C}_9\text{H}_7^+$ )<sup>5</sup>. Those peaks were not observed in the positive ion mode spectrum.

Table 4.10. ToF-SIMS normalized intensity (in %) for various characteristic peaks\*.

Entry	Characteristic signatures for core latex $ ^{59+}$	Characteristic signatures for bromopropionyloxy-group $ ^{79-}$	Characteristic signatures for bromopropionyloxy-group $ ^{179+}$	Characteristic signatures for poly(NAM) $ ^{142+}$
	$\text{CH}_3\text{O}-\text{C}\equiv\text{O}^+$	$^{79}\text{Br}^-$	$\left[ \text{H}_2\text{C}-\text{O}-\text{C}(=\text{O})-\text{CH}_2-\text{Br} \right]^+$	$\text{C}_7\text{H}_{12}\text{NO}_2^+$ $\left[ \text{O} \begin{array}{c} \diagup \quad \diagdown \\ \text{N} \\ \diagdown \quad \diagup \end{array} \text{C}(=\text{O})-\text{CH}_2 \right]^+_{a)}$
Latex 26 Core	$13.7 \pm 2.2$	$0.9 \pm 0.2$	$1.2 \pm 0.3$	$1.6 \pm 0.2$
Latex 42 G1 Shell Poly(NAM)	$6.8 \pm 1.1$	$5.9 \pm 0.6$	$1.3 \pm 0.2$	$11.5 \pm 0.2$
Latex 41 G20 R2 Shell Poly(NAM) Poly(NaSS)	$4.1 \pm 0.5$	$3.4 \pm 0.6$	$0.6 \pm 0.0$	$3.3 \pm 0.1$

\*Peaks at :  $m/z = 59^+$  corresponding to  $\text{C}_2\text{H}_3\text{O}_2^+$  and  $m/z = 85^-$  corresponding to  $\text{C}_4\text{H}_5\text{O}_2^-$ , characteristic of the core latex;  $m/z = 79^-$  corresponding to  $^{79}\text{Br}^-$  and  $m/z = 179^+$  corresponding to  $\text{C}_5\text{H}_8\text{O}_2^{79}\text{Br}^+$ , characteristic of bromopropionyloxy-group;  $m/z = 26^-$  corresponding for a major part to  $\text{CN}^-$  but contribution from  $\text{C}_2\text{H}_2^-$  cannot be excluded,  $m/z = 42^-$  corresponding to  $\text{CNO}^-$  and  $m/z = 142^+$  corresponding to  $\text{C}_7\text{O}_2\text{H}_{12}\text{N}^+$ .

<sup>a)</sup> A possible ion structure for  $\text{C}_7\text{O}_2\text{H}_{12}\text{N}^+$  resulting from the poly(NAM) fragmentation

In conclusion, NaSS was polymerized by surface-initiated polymerization from grafted poly(NAM) particles, based on FT-IR analyses. But the ToF-SIMS data suggested a burial of the poly(NaSS) chains either during the drying, or during the polymerization.

### 4.3. Surface-initiated polymerization of different hydrophilic monomers in presence of Cu(0)

The surface-initiated polymerization of NAM was successful and the different analyses of the grafted latexes have demonstrated that the shell was covalently bound at the core surface. Following this study, the surface-initiated polymerization method was extended to other hydrophilic monomers display in Figure 4.18 and in Table 4.11.

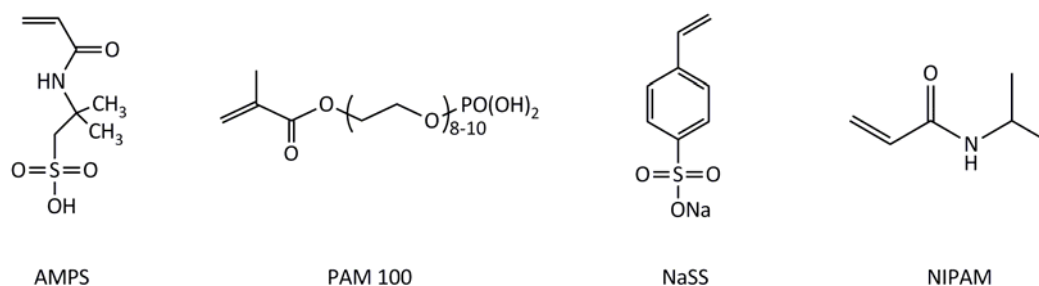


Figure 4.18. Chemical structure of AMPS, Sipomer PAM 100, NaSS and NIPAM.

Table 4.11. Surface-initiated polymerizations of different hydrophilic monomers performed at 25 °C in presence of PMDETA/CuBr<sub>2</sub> and Cu(0)\* from crosslinked and non-crosslinked poly(MMA-co-nBA) latex particles functionalized at the surface with the help of BPEA.

Entry	BPEA <sup>a)</sup> (mol/g <sub>Latex</sub> )	Monomer Nature	(g/g <sub>poly</sub> ) <sup>b)</sup>	(molar equiv.)	Time (h)	Conv. (NMR) (%)	D (DLS) after grafting (nm/dispersity)	Final solids content <sup>c)</sup> (wt%)	Critical CaCl <sub>2</sub> aggregation conc. (M)
31 G3	1.4 x 10 <sup>-6</sup>	HEA	0.05	135.8	8	20	110 / 0.03	40	≤ 4.5 x 10 <sup>-3</sup>
15 G5	2.1 x 10 <sup>-5</sup>	HEA	0.07	7.2	7	100	125 / 0.02	25	≤ 1
42 G12	4.2 x 10 <sup>-5</sup>	HEA	0.07	2.5	6	92	135 / 0.02	25	> 2.25
8 G7	4.7 x 10 <sup>-5</sup>	HEA	0.13	5.9	6	96	190 / 0.03	30	> 2.25
31 G11	1.2 x 10 <sup>-6</sup>	AMPS	0.07	92.8	1	Formation of a gel			
15 G3	2.2 x 10 <sup>-5</sup>	AMPS	0.06	3.3	7	38	105 / 0.01	25	≤ 1
42 G20	3.1 x 10 <sup>-5</sup>	PAM100	0.05	0.7	4	100	125 / 0.04	17	< 4.5 x 10 <sup>-3</sup>
8 G8	4.6 x 10 <sup>-5</sup>	PAM100	0.05	0.7	6	100	145 / 0.03	25	< 4.5 x 10 <sup>-3</sup>
31 G8	1.4 x 10 <sup>-6</sup>	APEG	0.05	34.7	8	64	120 / 0.06	38	≤ 4.5 x 10 <sup>-3</sup>
15 G7	2.1 x 10 <sup>-5</sup>	PEGMA	0.05	2.0	1	100	115 / 0.05	26	≤ 0.18
15 G8	2.1 x 10 <sup>-5</sup>	NaSS	0.05	2.8	4	100	135 / 0.03	22	≤ 1
41 G19	4.5 x 10 <sup>-5</sup>	NIPAM	0.12	4.6	6	100	165 / 0.07	28	≤ 0.09

\* All experiments were performed in presence of 3.5 cm Cu(0) (ϕ= 1mm) and PMDETA/CuBr<sub>2</sub> at 0.5/ 0.1 molar equivalents with respect to BPEA

<sup>a)</sup> BPEA = mol<sub>BPEA</sub>/m<sub>Total latex at t=0</sub>

<sup>b)</sup> [NAM] = m<sub>NAM</sub>/m<sub>core particles</sub>

<sup>c)</sup> Obtained by gravimetry. Identical to initial solids content as all those hydrophilic monomers are non volatil



The polymerizations were carried out in presence of Cu(0), PMDETA/CuBr<sub>2</sub> (0.5/0.1 molar equivalent with respect to BPEA). Different latexes were used as substrate in *Table 4.11*.

In general, all hydrophilic monomers polymerized. It was however noticed that in presence of a low Br-group concentration, the conversion was low. High conversions were achieved in presence of latexes 15, 41, 42 and 8, corresponding to a high Br-group concentration. The same results were obtained with NAM.

The stability to high CaCl<sub>2</sub> concentration was not as good as the one described for latexes grafted with poly(NAM). For instance, critical CaCl<sub>2</sub> aggregation concentration for latex 15 G6 in presence of 0.05 g<sub>NAM</sub>/g<sub>poly</sub> was higher than 2.5M.

For latex 31 G3, the poor stability could be explained by an incomplete coverage of the particle surface by the shell. The same result was obtained for latex 31 G2 (0.15 g<sub>NAM</sub>/g<sub>poly</sub>).

For the latexes at high Br-group concentration, the amount of hydrophilic monomer was probably too low particularly for APEG, PEGMA and PAM 100. The targeted DP<sub>n</sub> was low and the resulting shell thickness was probably too thin to lead to good steric stabilization.

This study concerning the hydrophilic monomers was not the subject of many investigations. However, it is a preliminary work to generalize the grafting protocol to other hydrophilic monomers than NAM and it should be further explored.

#### 4.4. Surface-initiated polymerization of NAM in presence of different metals

Among the transition metals used in metal-mediated polymerization, copper was the most studied one due to its high catalytic activity.

As already reported in the literature review, for the development of MMP, Cu(0)-mediated polymerization has gained in interest as it allows the reduction of copper complex concentration, facilitates reaction setup and metal removal. However, the inherent problems of copper could not be completely eradicated. Therefore, there is a growing interest in using other zero valent metals such as Fe(0), Zn(0) instead of Cu(0).

##### 4.4.a. Surface-initiated polymerization

Following the results obtained in presence of Cu(0), surface-initiated polymerizations were also tested in presence of different metals.

These experiments are listed in Table 4.12. Latex particles bearing the highest bromopropionyloxy-group concentration were used as substrate (latexes 41 and 42). All the experiments were performed in presence of  $7 \times 10^{-2}$  mol/L<sub>aqueous</sub> Br-group, PMDETA/CuBr<sub>2</sub> (0.5/0.1 molar equivalents with respect to the BPEA).

Table 4.12. Surface-initiated polymerizations of NAM performed at 25 °C in presence of PMDETA/CuBr<sub>2</sub> and zero valent metal\* from crosslinked poly(MMA-co-nBA) latex particles functionalized at the surface by BPEA, 6h reaction time.

Entry	Metal	Conv	D <sup>a)</sup> (DLS) after grafting	Final solids content of the grafted latex	Critical CaCl <sub>2</sub> aggregation conc.
		(%)	(nm / dispersity)	(wt%)	(M)
42 G1	Cu wire, $\phi=1$ mm, 3.5 cm	85	120 / 0.01	31	> 2.25
42 G2	Al foil, 2 cm <sup>2</sup>	94	125 / 0.02	30	> 2.25
41 G5 <sup>b)</sup>	Al foil, 2 cm <sup>2</sup>	98	140 / 0.11	33	> 2.25
41 G6	Fe wire, $\phi=1$ mm, 3.5 cm	13	140 / 0.14	30	$\leq 0.45 \times 10^{-3}$
41 G7	Zn disk, 1.5 cm x 1 mm	90	120 / 0.01	32	> 2.25
41 G13	Al <sub>2</sub> O <sub>3</sub> Powder, 0.09 g	24	110 / 0.01	30	$\leq 0.45 \times 10^{-3}$

\* BPEA concentration:  $7 \times 10^{-2}$  mol/L<sub>aqueous</sub>, PMDETA/CuBr<sub>2</sub> 0.5/0.1 molar equivalents with respect to BPEA

<sup>a)</sup> Initial diameter:  $D = 115$  nm, PDI = 0.02

<sup>b)</sup> 1 / 0.25 / 0.05 molar equivalents BPEA/PMDETA/CuBr<sub>2</sub>

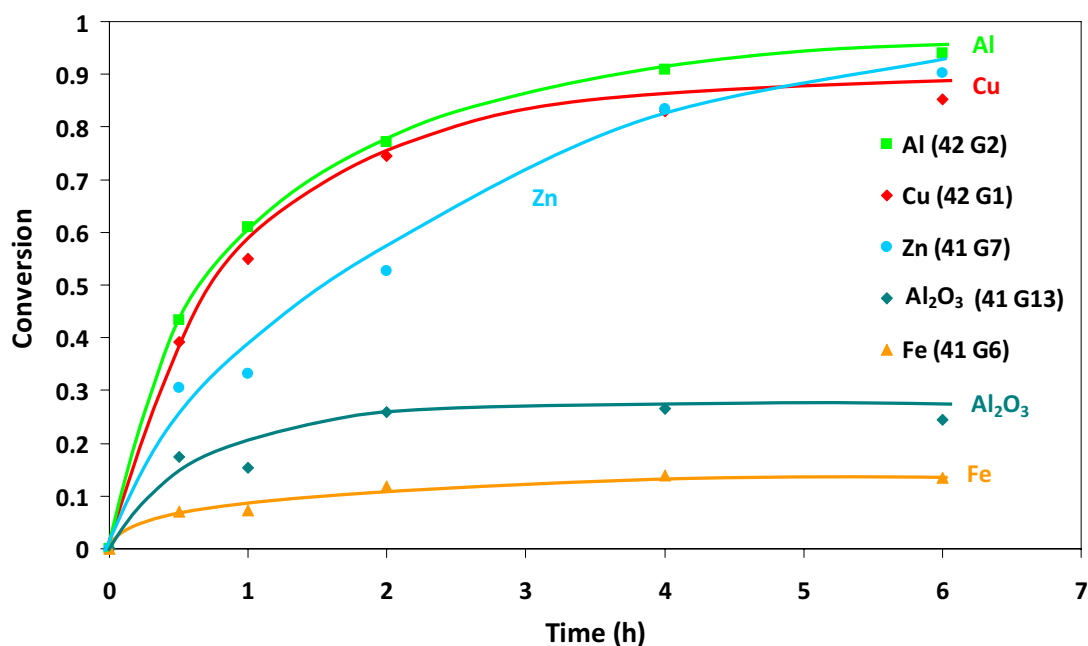


Figure 4.19. NAM conversion vs time for surface-initiated polymerizations performed at 25 °C in presence PMDETA/CuBr<sub>2</sub> at 0.5/0.1 molar equivalents with respect to BPEA ( $7 \times 10^{-2}$  mol/Laqueous) from functionalized latex 41 and 42 in presence of several metals.

High conversions were obtained by surface-initiated polymerization in presence of Zn(0), and Cu(0). The increase of the particle size and the good stability in highly concentrated CaCl<sub>2</sub> solutions indicated that the grafting was successful. In presence of latex and of the three metals tested, the conversion increased during all the reaction (>85%, within 6h, Figure 4.19).

Low polymerization rate and low conversions were obtained with Fe (13%) and might be explained by the poor reactivity of the Fe(0) in comparison with Zn(0) and Cu(0) as already reported by Matyjaszewski and co-workers<sup>6</sup>.

Among the different metals used in this study, Al(0) was the only one not belonging to the transition metals group. However, the redox potential difference of Al<sup>3+</sup>/Al(0) (-1.66V) and Cu<sup>2+</sup>/Cu(0) (+0.34V) is suitable for the redox reaction. Therefore, Al(0) was used for surface-initiated polymerization as the polymerization mechanism involves the reduction of CuBr<sub>2</sub>.

All the results obtained for the polymerization in presence of Al(0) indicate an efficient grafting reaction, i.e. high conversion (>85%), an increase of the particle diameter and good

a stability in highly concentrated  $\text{CaCl}_2$  solutions. The low conversion obtained in presence of  $\text{Al}_2\text{O}_3$  (24%) clearly indicates that  $\text{Al(0)}$  is mainly responsible for the reaction and not the surface oxide.

ToF-SIMS analyses were performed for the latexes 42 G1 (Cu) and 42 G2 (Al). As illustrated in Table 4.13, N-based signatures were detected for all these grafted latexes.

Table 4.13. ToF-SIMS normalized intensity (in %) for various characteristic peaks\*.

Entry	Characteristic signatures for core latex		Characteristic signatures for bromopropionyloxy-group		Characteristic signatures for poly(NAM)		
	$I^{59+}$	$I^{85-}$	$I^{79-}$	$I^{179+}$	$I^{26-}$	$I^{42-}$	$I^{142+}$
	$\text{CH}_3\text{O}-\text{C}\equiv\text{O}^+$		$^{79}\text{Br}^-$		$\text{CN}^-$	$\text{CNO}^-$	$\text{C}_7\text{H}_{12}\text{NO}_2^+$ 
2	$13.7 \pm 2.2$	$21.9 \pm 2.6$	$0.9 \pm 0.2$	$1.2 \pm 0.3$	$5.8 \pm 0.2$	$0.4 \pm 0.1$	$1.6 \pm 0.2$
26	$13.4 \pm 3.6$	$15.5 \pm 2.5$	$39.8 \pm 4.7$	$6.6 \pm 1.1$	$5.7 \pm 1.3$	$0.3 \pm 0.1$	$1.5 \pm 0.2$
42 G1 (Cu)	$6.8 \pm 1.1$	$5.6 \pm 0.5$	$5.9 \pm 0.6$	$1.3 \pm 0.1$	$29.9 \pm 5.5$	$8.2 \pm 1.6$	$11.5 \pm 0.7$
42G2 (Al)	$4.4 \pm 0.6$	$9.3 \pm 0.2$	$4.1 \pm 0.3$	$0.9 \pm 0.1$	$25.6 \pm 1.5$	$11.5 \pm 0.1$	$7.1 \pm 0.6$

\*Peaks at :  $m/z = 59^+$  corresponding to  $\text{C}_2\text{H}_3\text{O}_2^+$  and  $m/z = 85^-$  corresponding to  $\text{C}_4\text{H}_5\text{O}_2^-$ , characteristic of the core latex;  $m/z = 79^-$  corresponding to  $^{79}\text{Br}^-$  and  $m/z = 179^+$  corresponding to  $\text{C}_5\text{H}_8\text{O}_2^{79}\text{Br}^+$ , characteristic of bromopropionyloxy-group;  $m/z = 26^-$  corresponding for a major part to  $\text{CN}^-$  but contribution from  $\text{C}_2\text{H}_2^-$  cannot be excluded,  $m/z = 42^-$  corresponding to  $\text{CNO}^-$  and  $m/z = 142^+$  corresponding to  $\text{C}_7\text{O}_2\text{H}_{12}\text{N}^+$ .

<sup>a)</sup> A possible ion structure for  $\text{C}_7\text{O}_2\text{H}_{12}\text{N}^+$  resulting of the poly(NAM) fragmentation

For the latex 42 G1 (Cu) and the latex 42 G2 (Al), the normalized intensity values for core latex and bromopropionyloxy-group specific peaks decreased, which indicates a rather high grafting density of poly(NAM).

In this study, surface-initiated polymerizations were successfully performed in presence of different zero valent metals. Regarding the different results,  $\text{Zn(0)}$  is more suitable to replace  $\text{Cu(0)}$  than  $\text{Fe(0)}$ . More interestingly, an efficient grafting reaction was obtained in presence of  $\text{Al(0)}$ .

#### 4.4.b. Removal of the copper salt

The studies of metal-mediated polymerization performed in water indicated that the presence of  $\text{CuBr}_2$  was also necessary to achieve a better initiation. For the surface-initiated polymerization,  $\text{CuBr}_2$  was required to prevent gel formation. Therefore, reducing the amount of copper complex during the polymerization was not possible.

Recently, Bicak and co-workers<sup>7</sup> have proposed a simple method for the removal of copper from ATRP mixtures, based on chemical reduction of the  $\text{Cu(II)}$  by zinc powder.

Following this work, the same experiments were performed in our latexes. The grafted latex 42 G1 was slowly stirred in presence of  $\text{Zn(O)}$  or  $\text{Al(O)}$  during 6h at room temperature. As displayed in *Figure 4.20*, the blue coloration was faded for the latexes 42 G1 Al and 42 G1 Zn after the reaction. Moreover, the metal pieces (Al and Zn) were covered with a thin layer of  $\text{Cu(O)}$ . A slight re-coloration was noticed after the metal removal indicating the oxidation of  $\text{Cu(I)}$  generated by the redox reaction.

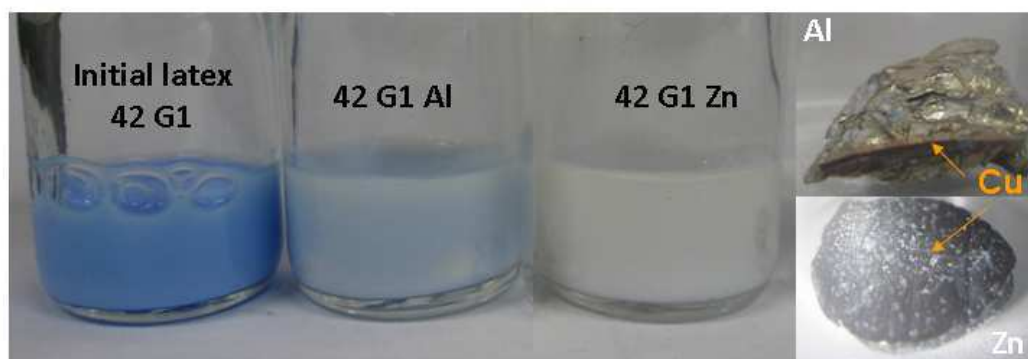


*Figure 4.20. Latexes coloration after the copper removal experiments.*

The amount of Cu in dry latexes was determined by elemental analyses (*Table 4.14*).

*Table 4.14. Amount of Cu (wt% of the solids content) for the latex 42 G1 after grafting reaction and after copper removal experiments in the presence of Zn (42 G1 Zn) and Al (42 G1 Al).*

Latex	Amount of Cu (wt% of the solids content)
42 G1	0.120
42 G1 Al	0.018
42 G1 Zn	0.017

For the initial grafted latex 42 G1, 0.12 wt% of Cu was determined; value relatively close to 0.10 wt% expected based on the amount of the  $\text{CuBr}_2$  initially introduced.

After copper removal experiments, the amount of Cu was drastically decreased from 0.12 wt% to 0.018-0.017 wt%.

Despite the fact that Cu was still remained after the copper removal experiments, this technique allowed to decrease the amount of Cu in the final product and to remove the blue color.

## 4.5. Conclusion

The aim of the study was to find the best surface-initiated polymerization procedure to graft a hydrophilic shell at the surface of raw latex particles. Different analyses were performed to prove that the hydrophilic shell was initiated from the surface bromide groups but none of them allowed quantification of the amount of grafted chains. Moreover, the grafted chains were not isolated and the living or controlled character was not studied.

Generally, the grafting reaction was efficient in terms of conversion and final colloidal stability improvement. The experimental conditions of an efficient grafting were determined and three main parameters were adjusted.

For an efficient polymerization, a minimum BPEA concentration is required at the particle surface. In our case, this minimum was obtained with the latex functionalized with a concentration at  $3.9 \times 10^{-5}$  mol/g<sub>latex</sub> of BPEA. Surface-initiated polymerizations from latexes with low bromopropionyloxy-group concentration were also achieved but low conversion and poor colloidal stability were obtained. These latexes are not adapted for the synthesis of particles bearing a hydrophilic shell but could be used for different applications for which the complete surface coverage is not necessary, i.e. for the grafting reaction of functional molecules.

The rate of the surface-initiated polymerization depended on the complex concentration (PMDETA/CuBr<sub>2</sub>). A gel formation was observed at low copper complex concentration and probably resulted from interparticle coupling due to a high concentration of propagating radicals. In contrast, by increasing the CuBr<sub>2</sub> the concentration of propagating radical decreased and thus gel formation was avoided.

The solids content of the latex also influenced the formation of gel. Particularly the hydrophilic monomer/particle ratio has to be carefully adjusted. At high solids contents, the interparticle distance is too small. The probability of interparticle cross-linking via radical termination will increase for long hydrophilic chains. For the same reason, the hydrophilic monomer/Br ratio has to be controlled to avoid high viscosity and gel formation.

The study of the influence of all these parameters allowed a better understanding of the behaviour of our surface-initiated polymerization system and a good prediction of the final latex characteristic that may be achieved. As a result, *Figure 4.21* can be put forward to schematically illustrate the influence of monomer, initiator and latex concentrations on the final latex properties at constant complex molar ratio 1/0.5/0.1 BPEA/PMDETA/CuBr<sub>2</sub>. The different experimental parameters are represented depending of the targeted application.

For hydrophobic-core particles bearing a hydrophilic-shell, high Br concentration at the particle surface is necessary. In this case, high solids content and dense shell could be obtained. At the opposite, for specific applications requiring only a few amount of functional monomer, surface-initiated polymerizations have to be performed at low solids content and low BPEA surface concentration.

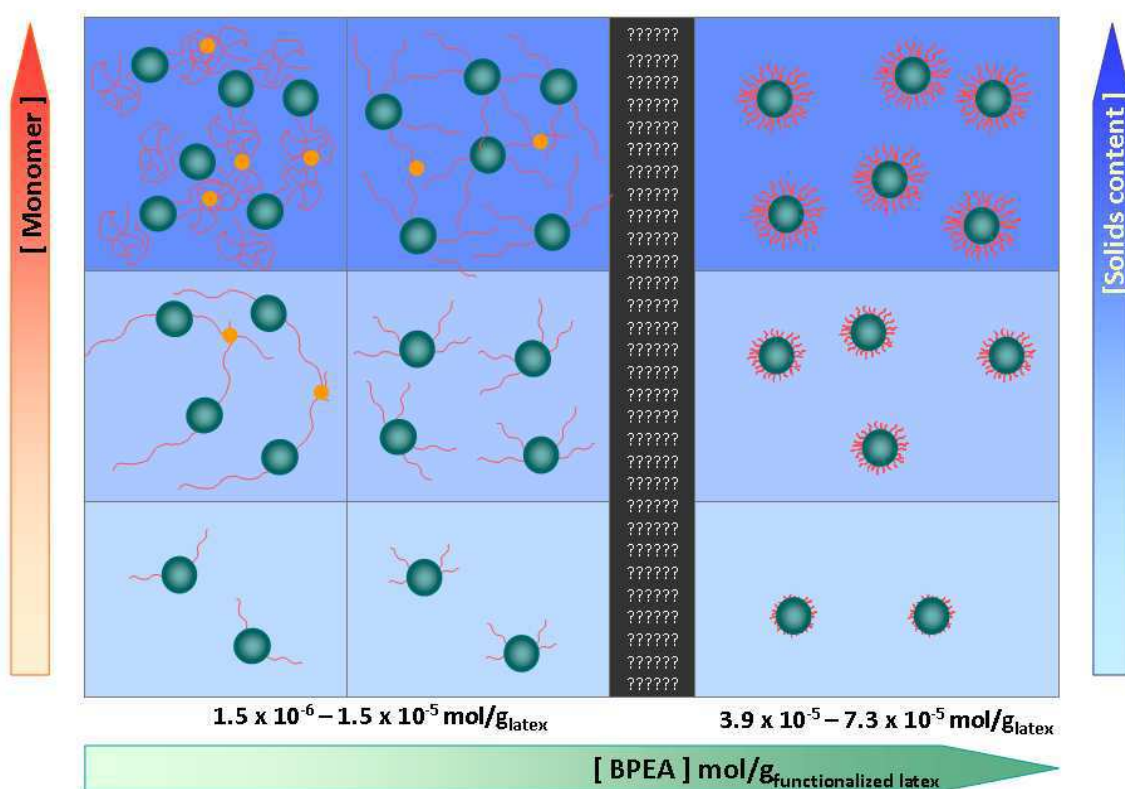


*Figure 4.21. Schematic representation of the surface-initiated polymerization. Influence of monomer, BPEA and latex concentrations on the gel formation. The influence of the complex concentration ratio is not reported.*



Copper-mediated surface-initiated was also successfully achieved for the polymerization of different hydrophilic monomers, such as HEA, AMPS, PAM 100, NaSS and NIPAM. This is a preliminary work to generalize the grafting protocol to other hydrophilic monomers than NAM and should be further investigated.

Cu(0) has also been replaced by Zn(0), Fe(0) and Al(0) for the grafting reactions. Except for Fe(0), the surface-initiated polymerizations obtained with Zn(0) and Al(0) were very similar to those obtained in presence of Cu(0). Those results are quite promising for potential applications as it is possible by this way to reduce/replace the copper.

## 4.6. Experimental part

### 4.6.a. Materials

All products were used as received and are listed in *Table 4.15*. Deionized water was employed in all the experiments.

*Table 4.15. List of the products*

	Products	Mw g/mol	Purity	Supplier
Al(0)	Aluminium foil	26.98	-	-
Al <sub>2</sub> O <sub>3</sub>	Aluminium oxide neutral, Brockmann I	101.96	99%	Acros
AMPS	2-Acrylamido-2-methylpropane sulfonic acid	207.25	-	BASF
APEG	Poly(ethylene glycol) methyl ether acrylate	~ 480	-	Aldrich
Cu(0)	Copper wire ( $\varnothing = 1$ mm)	63.55	> 99.9%	Aldrich
CuBr <sub>2</sub>	Copper II bromide	223.35	> 99%	Aldrich
Fe(0)	Iron wire ( $\varnothing = 1$ mm)	55.85	> 99.99%	Aldrich
HEA	2-Hydroxyethyl acrylate	116.12	96%	Aldrich
PEGMA	Poly(ethylene glycol) methyl ether methacrylate	~ 300	-	Aldrich
NAM	N-Acryloylmorpholine	141.17	97%	Aldrich
NaSS	Sodium 4-vinylbenzenesulfonate	206.19	> 90%	Aldrich
NaTS	Sodium p-toluenesulfonate	194.18	95%	Aldrich
NIPAM	N-Isopropylacrylamide	113.16	97%	Aldrich
PAM 100	Phosphate esters of poly(ethylene glycol) monomethacrylate	~ 390	-	Rhodia
PMDETA	1,1,4,7,7-Pentamethyldiethylene triamine	173.30	99%	Aldrich
Zn(0)	Zinc	65.38	> 99.9%	Riedel-de Haën

### 4.6.b. Metal-mediated surface-initiated polymerization

For a typical example, 42 G1 (*Table 4.3*), 25 g of latex 42, 7 g of deionized water and 0.1 g of sodium p-toluenesulfonate diluted in 1 mL water were mixed and carefully deoxygenated with a nitrogen flow for 30 minutes. A deoxygenated mixture containing 2.5 g NAM, 0.16 g PMDETA, 2 mL of CuBr<sub>2</sub> aqueous solution at 0.1 M and 2 g water was slowly added under stirring. The reaction medium was heated at 25°C and a piece of a copper wire was introduced (3.5 cm/ $\varnothing = 1$  mm). Samples were periodically withdrawn to monitor the conversion by <sup>1</sup>H NMR after dilution in D<sub>2</sub>O. The copper wire was removed at the end of reaction and the latex was dialyzed against water for 2 weeks (the water medium was

changed 4 times per day) using a Spectra/Por® dialysis membrane (cut-off at 12 000-14 000 Da), dried at room temperature, grinded to a powder for further analysis.

#### **4.6.c. Surface-initiated polymerization from grafted poly(NAM) particles**

For a typical example, 42 G4 R2 (Table 4.9), 5 g of latex 42 G4, 5 g of deionized water were mixed and carefully deoxygenated with a nitrogen flow for 30 minutes. A deoxygenated mixture containing 0.2 g NaSS, 0.026 g PMDETA, 0.5 mL of CuBr<sub>2</sub> aqueous solution at 0.1 M and 2 g water was slowly added under stirring. The reaction medium was heated at 25°C and a piece of a copper wire was introduced (1 cm/∅ = 1 mm). Samples were periodically withdrawn to monitor the conversion by <sup>1</sup>H NMR after dilution in D<sub>2</sub>O.

#### **4.6.d. Stability tests**

For ionic strength stability tests of raw and dialyzed grafted latexes, a drop of latex dispersion was added to 5 mL solutions of CaCl<sub>2</sub> with concentrations of 4.5 mM, 9.0 mM, 22.5 mM, 45 mM, 91 mM, 0.18 M, 0.47 M, 1 M, and 2.25 M. The colloidal stability of the dispersion was assessed by a simple visual test.

For freeze-thaw stability tests, a 2 mL dispersion of grafted particles was frozen for 2 h and then thawed. This cycle was repeated three times. The colloidal stability of the dispersion was assessed by DLS measurements.

#### **4.6.e. Electrospray charge-detection mass spectroscopy**

The charge detection-mass spectrometer analyses were performed of a custom-built instrument with an ESI source and vacuum interface that generate the ion beam directly towards the charge detector. ESI solutions are prepared diluting the dialyzed latex to a concentration of around  $1 \cdot 10^{14}$  NPs/L in water/methanol (50/50 v/v). The charge detection device (CDD) is used in a single pass mode, was built after Keaton and Stradling pattern. The signal induced on the tube is picked up by a JFET transistor and is amplified by low-noise, charge-sensitive preamplifier and then shaped and differentiated by a home-built amplifier. The signal is recorded with a waveform digitizer card that records the entire waveform for each ion passing through the detector tube at a sampling rate of 10 MHz. The pulses have time duration of ~60 μs and sampling rates are large enough to preserve the shape of the

signal. The data are transferred to a desk-top computer where they are analyzed to compute the charge and mass of each ion. The present signal processing and data transfer rates allow the acquisition of up to 2500 events per second. A user program calculates the time between the maxima of positive and negative pulses, the amplitudes of the two pulses and the ratio between their absolute values.

#### 4.7. References

- 
- <sup>1</sup> Sundberg, D. C.; Durant, Y. J. *Polymer Reaction Engineering* **2003**, 11, 379-432
  - <sup>2</sup> Tang, W.; Kwak, Y.; Braunecker, W.; Tsarevsky, N. V.; Coote, M. L.; Matyjaszewski, K. *Journal of the American Chemical Society* **2008**, 130, 10702-10713
  - <sup>3</sup> Doussineau, T.; Bao, C. Y.; Antoine, R.; Dugourd, P.; Zhang, W.; D'Agosto, F.; Charleux, B. *ACS Macro Letters* **2012**, 1, 414-417
  - <sup>4</sup> Wohlleben, W.; Lechner, M. D. *Colloid and Polymer Science* **2008**, 286, 149-157
  - <sup>5</sup> Delcorte, A.; Segda, B. G.; Bertrand, P. *Surface Science* **1997**, 381, 18- 32
  - <sup>6</sup> Zhang, Y.; Wang, Y.; Matyjaszewski, K. *Macromolecules* **2010**, 44 , 683- 685
  - <sup>7</sup> Canturk, F.; Karagoz, B.; Bicak, N. *Journal of Polymer Science: Part A: Polymer Chemistry* **2011**, 49, 3536–3542



## **Conclusion**

The aim of this work was to add a polymer shell at the surface of polymer particles prepared via radical emulsion polymerization by post-synthesis modification, using a “grafting from” approach based on aqueous metal-mediated radical polymerization.

The literature review concerning the recent progresses in the area of metal-mediated controlled radical polymerization (MMCRP) has shown that this method has been intensively studied as it is a versatile technique for the synthesis of value-added polymers with novel applications. Since its discovery, great efforts have been done to develop highly efficient systems with low amounts of metal complex. Recently, the use of Cu(0) has been particularly investigated since it offers a rather easy way to proceed and it allows the decrease the complex concentration.

However, only few examples have reported metal-mediated polymerization in water solution. Therefore, before any grafting reaction, a part of this study was devoted to metal-mediated polymerization in aqueous solution, using a soluble initiator based on a halogenated PEG, as a model reaction for grafting.

## Metal-mediated polymerization in water

Copper-mediated polymerization was first performed in water. The goal of this study was not to control the polymerization of hydrophilic monomers but rather to get a better understanding of the system we planned to use for the surface grafting of our latexes.

Copper-mediated polymerizations of hydrophilic monomers were performed at room temperature using a water soluble initiator (MePEG-X), Cu(0) wire and PMDETA/CuX<sub>2</sub>. The influence of different parameters such as, the concentration of the components, nature of the initiating system and nature of the monomer were studied.

Generally, the different polymerizations performed in water solution were very fast. The conversions increased during the first hour to reach a plateau. Final conversions were directly influenced by PMDETA and CuBr<sub>2</sub> concentration. High conversions were obtained in presence of a low concentration of CuBr<sub>2</sub> with high PMDETA concentration.

A dependence between final molar masses and the initiating system has been observed. Low CuBr<sub>2</sub> concentration led to high molar masses. Generally, the use of MePEG-Cl/CuX<sub>2</sub> or MePEG-Br/CuCl<sub>2</sub> generated polymer chains with high molar masses. Moreover, initiator still remained at the end of the polymerization, indicating a slow and partial initiation.

Due to a fast polymerization, it was not possible to determine in an accurate way the molar mass evolution. In some examples, it was observed that the molar masses did not increase with the monomer conversion. Polymer chains were constantly generated during the polymerization, grew rapidly and then terminated under probably an irreversible mechanism. However, the transposition to latex surface initiated polymerization may be interesting since in that case, radicals will be segregated at the particle surface. The probability for two growing macroradicals to “see” each other will diminish and thus the rate of termination reactions may be minimized.

Based on the different results (final conversion and final molar mass), a model system has been defined in which Cu(0) and MePEG-Br/PMDETA/CuBr<sub>2</sub> were used in 1/0.5/0.1 molar ratio as it was the best compromise in terms of conversion and concentration.

Besides, control experiments performed with a part of the initiating system demonstrated that initiation took place only in the presence of all the components required for an ATRP, i.e initiator, PMDETA/CuBr<sub>2</sub> and Cu(0). Moreover, this initiation only took place on the alkyl halogen species which is a key point to achieve an efficient “grafting from” reaction.

Therefore, despite the fact that the control of the copper-mediated was not fully achieved, metal-mediated polymerization was a suitable technique to perform the “grafting from” reaction.

As observed in this study, to control a MMRP in water is quite challenging. Thus, even if this work is not complete, it provides a preliminary work in this field of growing interest. Namely, the recent progresses in this area have been published very recently (2009-2012).

### Latex functionalization

To provide an efficient grafting reaction, controlling the location of the initiating group at the extreme particle surface is the main parameter. Different strategies to functionalize latex particles have been already reported to target a thin and uniform reactive layer at the surface, and to avoid secondary nucleation (see Chapter 1).

In this study, the strategy to functionalize latex particles consisted in introducing the reactive group via copolymerization of the inimer, the BPEA. A successful protocol was found to design functionalized latexes by emulsion polymerization in a semi-continuous process. To achieve high BPEA conversion at the particle surface and to avoid secondary nucleation, BPEA mixed with MMA was introduced before complete conversion of the core monomer, typically at 90% of conversion.



Under these conditions, high conversion of BPEA was achieved and no secondary nucleation was observed.

Despite the structure of BPEA and the use of MMA to prevent the burial of the Br atom during the functionalization step, different characterization tools were employed to check the location of the bromide group.

The presence of the bromine atom at the particle surface was assessed by ToF-SIMS analysis and was indeed detected for all functionalized latexes. A molecular fragment of the bromopropionyloxy-group was also observed, attesting the presence of BPEA covalently bound at the particle surface.

To complete the study, a halogen transfer reaction was performed from functionalized latexes to assess the accessibility and the activation of the surface bromide group. This reaction was carried out with the functionalized latex in the presence of Cu(0) and PMDETA/CuCl<sub>2</sub>. A switch from Br signature to Cl one was indeed observed by ToF-SIMS. It confirmed that the bromine atom at the particle surface allowed the exchange reaction that is required for surface-initiating polymerization.

### Surface-initiated polymerization

Surface-initiated polymerization of NAM was carried out from raw latexes, applying directly the experimental conditions defined from metal-mediated polymerizations performed in water solution.

Generally, the grafting reaction was efficient in terms of conversion and final colloidal stability improvement. The proof of the grafting of poly(NAM) was confirmed by FT-IR, ToF-SIMS and stability tests. From this study, the criteria for efficient surface-initiation have been determined.

A minimum concentration of bromide group was required at the particle surface. At low bromopropionyloxy-group concentration, low conversion and poor colloidal stability were obtained indicating a poor grafting density and/or a low shell thickness. Thus, latexes functionalized with a low amount of bromine atoms were not adapted for the synthesis of particles bearing a hydrophilic shell. However they could be used for different applications where the complete particle surface coverage is not necessary such as the “grafting onto” of specific molecules or macromolecules.

The complex concentration (PMDETA/CuBr<sub>2</sub>) strongly influenced the polymerization rate. Moreover, at low complex concentration, gel formation was observed probably caused by interparticle coupling due to a high concentration of propagating radicals. Therefore, a minimum amount of CuBr<sub>2</sub> was necessary to decrease the concentration of propagating radical and thus avoid interparticle coupling reaction. However, a simple procedure was successfully applied to remove the copper complex in the final latex using zero valent metal pieces. This technique, based on chemical reduction of the Cu(II) by Zn(0) or Al(0), allowed the reduction of copper complex concentration, so as the reduction of the blue color.

The solids content of the latex also influenced the formation of gel. Particularly the hydrophilic monomer/particle ratio has to be carefully adjusted. At high solids contents, the interparticle distance was too small, increasing thus the probability of interparticle cross-linking via radical termination. For the same reason, the hydrophilic monomer/Br ratio has to be controlled to avoid high viscosity and gel formation.

As the aim of our project was to grow any kind of polymers from a single type of functionalized particles, the surface-initiated polymerization was extended to other hydrophilic monomers such as HEA, AMPS, PAM 100, NaSS and NIPAM. These studies were a preliminary work to generalize the grafting protocol.

In a complementary study, Cu(0) was also successfully replaced by Zn(0) and Al(0) for the grafting of poly(NAM). Taking advantage of the high redox potential difference of Zn<sup>2+</sup>/Zn(0)

(-0.76V) or  $\text{Al}^{3+}/\text{Al}(0)$  (-1.66V) and  $\text{Cu}^{2+}/\text{Cu}(0)$  (+0.34V),  $\text{Zn}(0)$  and  $\text{Al}(0)$  were used as reducing agents to generate  $\text{Cu}(I)$  from  $\text{CuBr}_2$  in agreement with A(R)GET ATRP mechanism.

In this study, conditions in which grafting could be performed at room temperature, using high particle concentration in the presence of surfactant and initiator remaining from the emulsion polymerization step were identified. It was the first time such grafting conditions have been applied with success from “real latexes”.

The overall work presented in this manuscript has been the subject of one publication (*Macromolecules* **2012**, 45, 2972-2980) and one patent (submitted in Feb. 2012).

# Annexes

## Characterization techniques

### Characterization techniques

#### **A.1. <sup>1</sup>H NMR spectroscopy**

<sup>1</sup>H NMR spectroscopy for kinetic analysis (i.e., conversion of the monomer in the aqueous polymerization) was performed in 5 mm diameter tubes in D<sub>2</sub>O solution at 25 °C using a Bruker Avance 300 (300 MHz) spectrometer. The chemical shift scale was calibrated on the basis of the solvent peak ( $\delta = 4.79$  ppm) and sodium p-toluenesulfonate was used as an internal reference (aromatic H peaks).

Monomer conversion was calculated following the *Equation A.1*.

$$x = \frac{I_{M0} - I_{Mt}}{I_{M0}} \quad \begin{array}{l} I_{M0} : \text{Peak integral of the vinylic proton of the monomer at } t_0 \\ I_{Mt} : \text{Peak integral of the vinylic proton of the monomer at } t \end{array}$$

*Equation A.1. Equation for monomer conversion calculation.*

For the sample analyzed in presence of H<sub>2</sub>O, a broad and intense peak characteristic of H<sub>2</sub>O was observed at 4,79 ppm but latter did not influence the vinylic peaks shift.

### **A.2. Size exclusion chromatography (SEC)**

The SEC analyses were performed in DMF at 70 °C with 0.01 mol.L<sup>-1</sup> of LiBr, at a flow rate of 1 mL/min. All polymers were analyzed at a concentration of 2.5 - 5 mg/mL after filtration through a 0.20 µm pore-size PTFE membrane. Separation was performed with a guard column and three PSS GRAM columns (7µm, 300x7.5mm). The average molar masses (number-average molar mass  $M_n$  and weight-average molar mass  $M_w$ ) and the dispersity index ( $PDI = M_w/M_n$ ) were derived from the RI signal by a calibration curve based on poly(MMA) standards. The calibration was constructed with narrow molar mass standards from 580 g/mol to 3 053 000 g/mol. A third-degree polynomial regression was applied. WinGPC Unity software was used for data collection and calculation.

Before measurement, samples were dried under vacuum at room temperature. It was noticed that sometime polymerizations or coupling reactions started under these conditions (already occurring for the sample  $t=0$ , monitored by NMR).

### **A.3. Dynamic light scattering (DLS)**

The intensity-average diameters of the latex particles and the dispersity factor were measured by dynamic light scattering (DLS) at a temperature of 25°C using a Zetasizer Nano Series (Nano ZS) from Malvern Instrument using the Zetasizer 6.2 software. The instrument was calibrated with a standard polystyrene latex in water exhibiting a particle size of  $220 \pm 6$  nm. Before measurements, the latex samples were diluted with deionized and filtered water.

### **A.4. Gas chromatography (GC)**

Gas chromatography (GC) of the polymer dispersions was used to determine the residual amount of BPEA inimer. It was performed with a HP6890N equipment from Agilent Technologies with a 30 m column (DB 5, 5% polydiphenylsiloxane / 95% polydimethylsiloxane) and a temperature ramp of 8°C/min from 120 °C to 280 °C. The injection temperature was 280°C.

#### **A.5. Differential scanning calorimetry (DSC)**

Differential scanning calorimetry (DSC) was measured in a Q2000 by TA Instruments. The instrument was calibrated with adamantane, water and indium. For determination of the glass transition temperature, 8-9 mg were placed in an aluminum pan. The sample was rapidly cooled from 150 °C to – 110°C and afterwards scanned with a heating rate of 2 K/min. Glass transition was determined at the half step height (according to ISO 11357-2)

#### **A.6. Transmission electron microscopy (TEM)**

For transmission electron microscopy (TEM), samples were dropped on a carbon-coated copper grid and dried under air. The TEM images were examined at an accelerating voltage of 120 kV with a Philips CM120 transmission electron microscope (Centre Technologique des Microstructures (CTμ), University Claude Bernard Lyon 1, Villeurbanne)

#### **7.7. Scanning electron microscopy (SEM)**

Scanning electron microscopy (SEM) images were examined on a FEI QUANTA 250 FEG scanning electron microscope, at an acceleration voltage of 15 kV (Centre Technologique des Microstructures (CTμ), University Claude Bernard Lyon 1, Villeurbanne). A drop of the particle suspension was placed on a formvar film on a 200 mesh copper grid, dried and covered by a thin layer of Gold/Palladium (Sputtering Au/Pd with Baltec MED020 – 5.9 nm).

#### **A.8. Time-of-Flight Secondary Ion Mass Spectrometry (ToF-SIMS)**

Time-of-Flight Secondary Ion Mass Spectrometry (ToF-SIMS) measurements were carried out at the Laboratoire des Sciences Analytiques, University Claude Bernard Lyon 1 (Villeurbanne) using a Physical Electronics TRIFT III ToF-SIMS instrument operated with a pulsed 22 keV Au<sup>+</sup> ion gun (ion current of 2 nA) rastered over a 300 μm×300 μm area. An electron gun was operated in pulsed mode at low electron energy for charge compensation. Ion dose was kept below the static conditions limit. Data were analyzed using the WinCadence™ software. Mass calibration was performed on hydrocarbon secondary ions. Before the analysis, the latexes were dialyzed in water for 2 weeks using a Spectra/Por® dialysis membrane (cut-off at 12 000-14 000 Da), dried at room temperature, grinded to a powder and this powder was pressed onto an indium foil. Data were normalized to the total intensity minus H<sup>+/-</sup> intensity

(because of its critical dependence on slight variations in the experimental settings) and minus the intensity of peaks related to ubiquitous contamination or to the sample preparation (i.e.  $\text{Na}^+$  and  $\text{In}^+$  in the positive mode and  $\text{F}^-$  in the negative mode). Standard deviations were calculated from measurements performed on three different areas.

#### **A.9. Fourier transform infra-red (FT-IR)**

Fourier transform infra-red (FT-IR) analyses were performed on a Nicolet iS10 spectrometer with an ATR diamond crystal and a DTGS KBr detector. The data were measured with a resolution of  $4\text{ cm}^{-1}$  from  $525\text{ cm}^{-1}$  to  $4000\text{ cm}^{-1}$ . A background spectrum was collected and subtracted from the sample spectrum. The latexes were dialyzed against water for 2 weeks using a Spectra/Por® dialysis membrane (cut-off at 12 000-14 000 Da), dried at room temperature, grinded to powder and then dissolved in dichloromethane. A drop of the dispersion was deposited onto the diamond crystal, dried and then analyzed.

#### **A.10. Viscosity measurement**

Viscosity measurements were performed at  $25^\circ\text{C}$  using a parallel-plate (25 mm in diameter) geometry fixture on a TA Instruments AR2000ex rheometer. The shear rate was fixed at  $50\text{ s}^{-1}$  and the gap between the upper plate and the Peltier plate was set at a distance of  $1000\text{ }\mu\text{m}$ .

#### **A.11. Stability tests**

The ionic strength and freeze-thaw stability of the grafted latexes was tested (raw latexes or dialyzed latexes). A drop of latex dispersion was added to 5 mL solutions of  $\text{CaCl}_2$  with concentrations of 4.5 mM, 9.0 mM, 22.5 mM, 45 mM, 91 mM, 0.18 M, 0.47 M, 1 M, and 2.25 M. The colloidal stability of the dispersion was assessed by a simple visual test. A 2 mL dispersion of grafted particles was frozen for 2 h and then thawed. This cycle was repeated three times. The colloidal stability of the dispersion was assessed by DLS measurements.

**A.12. Electrospray charge-detection mass spectroscopy (ECD-MS)**

The charge detection-mass spectrometer analyses were performed of a custom-built instrument with an ESI source and vacuum interface that generate the ion beam directly towards the charge detector. ESI solutions are prepared diluting the dialyzed latex to a concentration of around  $1 \cdot 10^{14}$  NPs/L in water/methanol (50/50 v/v). The charge detection device (CDD) is used in a single pass mode, and was built after Keaton and Stradling pattern. The signal induced on the tube is picked up by a JFET transistor and is amplified by low-noise, charge-sensitive preamplifier and then shaped and differentiated by a home-built amplifier. The signal is recorded with a waveform digitizer card that records the entire waveform for each ion passing through the detector tube at a sampling rate of 10 MHz. The pulses have time duration of  $\sim 60 \mu\text{s}$  and sampling rates are large enough to preserve the shape of the signal. The data are transferred to a desk-top computer where they are analyzed to compute the charge and mass of each ion. The present signal processing and data transfer rates allow the acquisition of up to 2500 events per second. A user program calculates the time between the maxima of positive and negative pulses, the amplitudes of the two pulses and the ratio between their absolute values.





## Efficient Copper-Mediated Surface-Initiated Polymerization from Raw Polymer Latex in Water

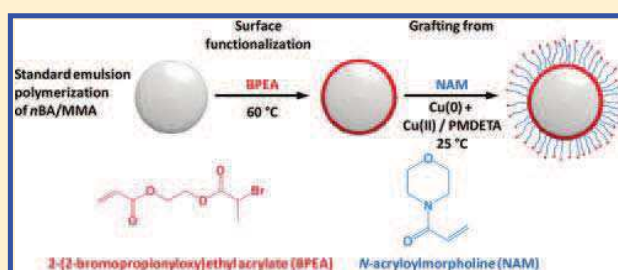
Virginie Chabrol,<sup>†</sup> Didier Léonard,<sup>§</sup> Matthias Zorn,<sup>‡</sup> Bernd Reck,<sup>‡</sup> Franck D'Agosto,<sup>†</sup> and Bernadette Charleux<sup>\*,†</sup>

<sup>†</sup>Université de Lyon, Univ Lyon 1, CPE Lyon, CNRS, UMR 5265, C2P2 (Chemistry, Catalysis, Polymers & Processes), Bât. 308F, 43 Bd du 11 Novembre 1918, F-69616 Villeurbanne, France

<sup>‡</sup>BASF SE, Carl-Bosch-Str.38, 67056 Ludwigshafen, Germany

<sup>§</sup>Université de Lyon, F 69622, Lyon, France. Institut des Sciences Analytiques, UMR 5280, Laboratoire des Sciences Analytiques, Bât. J. Raulin, Université Claude Bernard-Lyon 1, F-69622 Villeurbanne, France

**ABSTRACT:** The copper-mediated radical polymerization of *N*-acryloylmorpholine initiated from the surface of latex particles in water was studied to form hydrophobic core/hydrophilic shell particles. The latexes were synthesized via classical radical emulsion polymerization and were functionalized at their surface by a comonomer bearing a Br-functional group (the so-called inimer). The latter was introduced to initiate the grafting reaction, in the presence of the Cu(0)/CuBr<sub>2</sub>/PMDETA (1,1,4,7,7-pentamethyldiethylenetriamine) catalytic system. Conditions in which the grafting step could be performed at room temperature, using high particle concentration in the presence of surfactant and initiator remaining from the emulsion polymerization were identified. The success of the functionalization and grafting steps was evaluated by TOF-SIMS (time-of-flight secondary ion mass spectrometry), by FTIR, and by the final properties of the so-formed core-shell particles. It is the first time such grafting conditions have been applied with success from “real latexes”.



### INTRODUCTION

Core-shell particles with a hydrophobic polymer core and a hydrophilic polymer shell have been the subject of many studies<sup>1–3</sup> as they can find a wide range of applications in fields such as coatings, paints, adhesives, impact modifiers, support for biological molecules, etc. Various strategies to incorporate a hydrophilic polymer shell have been employed with the use for instance of an amphiphilic block copolymer as a stabilizer in emulsion polymerization or via emulsion copolymerization of the hydrophobic monomers with a water-soluble (macro)-monomer. There has also been a growing interest in the “grafting from” method<sup>1,3–6</sup> with the development of controlled/living radical polymerization (CRP) techniques.<sup>7</sup> The general principle of the “grafting from” strategy consists in introducing initiating groups at the particle surface and in activating them to grow polymer chains via CRP. Because of fast initiation and simultaneous growth of the chains, CRP allows grafting density and brush thickness to be well-controlled.<sup>1,3–6</sup> Among the various CRP methods, atom transfer radical polymerization (ATRP) has been particularly used on different colloidal substrates, in organic solution, or in water.<sup>8,9,1,3–6</sup> The latter mainly include silica particles, whereas only a few examples are related to the use of polymer latexes,<sup>2</sup> resulting from a free-radical emulsion polymerization recipe. The use of functionalized latexes as support for aqueous surface-initiated ATRP (SI-ATRP) has been reported for the first time by Manuszak-Guerrini et al.<sup>10</sup> in 2000. The grafting

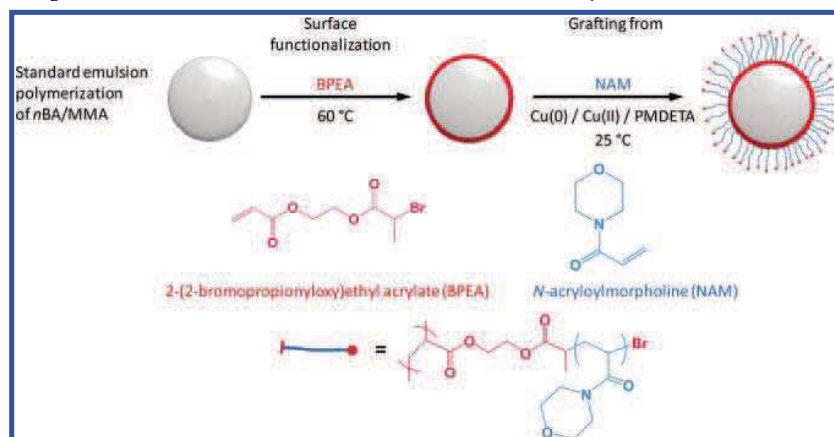
strategy was to functionalize a cross-linked polystyrene latex with an inimer (i.e., a monomer bearing an alkyl halide group able to serve as an initiator in ATRP) at the particle surface and to activate it by a Cu(I) complex in the presence of a water-soluble monomer. Following this seminal work, other teams have used the same strategy to prepare core-shell particles by SI-ATRP.<sup>11–15</sup> Mittal et al.<sup>16,17</sup> studied the functionalization process by the inimer so as to find the best conditions for the SI-ATRP of *N*-isopropylacrylamide. To favor the synthesis of functionalized particles and to avoid secondary nucleation, the introduction of the inimer along with a cross-linker had to be performed at 70% conversion of the monomers in the first stage emulsion polymerization. Another method to functionalize a latex by surface halide groups was chloromethylation of polystyrene particles as described by Min et al.<sup>18</sup> More recently, Liu et al.<sup>19</sup> proposed an easier way to immobilize bromide group at the surface of cross-linked poly(methyl methacrylate) (polyMMA) particles using CBr<sub>4</sub> as a chain transfer agent in the emulsion polymerization step. A different approach for SI-ATRP from latex particles was performed without covalently incorporating the initiator at the particle surface.<sup>20</sup> The authors took advantage of the Br functional group at the hydrophilic end of an amphiphilic block copolymer previously prepared via

**Received:** February 1, 2012

**Revised:** March 8, 2012

**Published:** March 22, 2012

Scheme 1. General Principle of the Cu-Mediated Surface-Initiated Radical Polymerization Used in This Work



ATRP and used as a stabilizer in the emulsion polymerization process. It was further reacted as the initiating site for the ATRP of a water-soluble monomer, hence leading to the formation of a second hydrophilic shell. In all instances, the grafting reaction by ATRP was carried out with diluted latexes (low solids contents of  $\sim 5$  wt %; except in ref 20 in which the solids content was 16.6 wt %) that were carefully cleaned by dialysis and/or by centrifugation to eliminate all traces of low molar mass initiator and surfactant.

In this context, the aim of this work was to incorporate a hydrophilic polymer shell at the surface of submicrometric polymer particles from emulsion polymerization by postsynthesis modification, using a “grafting from” approach based on aqueous CRP. The use of a single type of functionalized particles as a platform to grow any kind of hydrophilic polymers with tailor-made characteristics (see Scheme 1) would allow to target different applications from the same starting latex recipe. It also offers the opportunity to incorporate a polymer shell that cannot be introduced in another way (via the amphiphilic block copolymer strategy for instance) without impacting the features of the grafted particles.

To reach this goal, we considered the following key points: (i) the choice of the CRP method and the possibility to functionalize the latex particles with an inimer suitable for the selected technique; (ii) the ability to perform the grafting reaction from “as-synthesized” concentrated latexes, without elimination of the surfactant and of the remaining initiator. To fulfill both criteria, ATRP was selected as it uses a variety of alkyl halide initiators that can be easily turned into inimers. The latter can be polymerized via classical radical emulsion polymerization without interference with the initiating and propagating radicals. Finally, the method can be performed at room temperature, hence preventing unwanted initiation by the remaining radical initiator. All those criteria impede the use of other CRP methods such as nitroxide-mediated polymerization (performed at elevated temperature) and reversible addition–fragmentation chain transfer (in which the reactive group of the functional monomer will react during the functionalization step). However, a drawback of ATRP is the need for large quantities of catalyst (in particular copper(I) halide), which contaminate the final product and are difficult to remove. The reduction of the amount of copper has been achieved through the use of techniques such as activators (re)generated by electron transfer (A(R)GET).<sup>21</sup> Since a few years, the use of copper metal has been particularly investigated because Cu(0)

is easier to handle than Cu(I) or Cu(II) salts. As a reducing agent for Cu(II) in A(R)GET ATRP<sup>22</sup> or as an activator in single electron transfer living radical polymerization (SET-LRP),<sup>23</sup> the role of Cu(0) in the mechanism of copper-mediated polymerization is not fully understood and still under debate<sup>24</sup> but will not be the focus of this work. In all cases, however, it offers a rather easy way to proceed and allows to decrease the amount of catalyst. The couple Cu(0)/Cu(II) was thus employed as a catalyst for our grafting reactions from latex particles in aqueous media at room temperature. The use of AGET ATRP with Cu(II) and ascorbic acid as a reducing agent has been reported in a single article.<sup>25</sup> However, the grafting of polymer chains from latex particles has never been performed with Cu(0) in concentrated latex, in the presence of surfactant and residual initiator (“real” latex). With the aim of studying the efficiency of the reaction, the aqueous SI-ATRP of *N*-acryloylmorpholine (NAM), used as a model of neutral water-soluble monomer, was considered and the effect of the concentrations of both the inimer and the Cu(0)/CuBr<sub>2</sub> catalyst (with 1,1,4,7,7-pentamethyldiethylenetriamine, PMDETA, as a ligand) was evaluated.

## EXPERIMENTAL PART

**Materials.** Sodium dodecyl sulfate (DISPONIL SDS, 15 wt % aqueous solution) was purchased from Cognis. Sodium hydrogen carbonate (NaHCO<sub>3</sub>, 0.07 M aqueous solution), NaOH solution (0.25 M aqueous solution), *n*-butyl acrylate (*n*BA), methyl methacrylate (MMA), and 1,4-butanediol diacrylate (BDDA) were obtained from BASF. 4,4'-Azobis(4-cyanopentanoic acid) (ACPA, >98%), *N*-acryloylmorpholine (NAM, 97%), 1,1,4,7,7-pentamethyldiethylenetriamine (PMDETA, 99%), CuBr<sub>2</sub> (>99%), CuCl<sub>2</sub> (99.999%) and copper wire (>99.9%; diameter = 1 mm) were used as received from Sigma-Aldrich. Deionized water was employed in all the experiments. The inimer 2-(2-bromopropionyloxy)ethyl acrylate (BPEA) was synthesized by an esterification reaction between 2-hydroxyethyl acrylate (Sigma-Aldrich, 96%) and 2-bromopropionyl bromide (Sigma-Aldrich, 97%), according to a protocol published previously,<sup>26</sup> and briefly described here. A solution of 2-bromopropionyl bromide (79.33 g, 0.38 mol) in 50 mL of CH<sub>2</sub>Cl<sub>2</sub> was added dropwise to a stirred solution (cooled in an ice bath) of 2-hydroxyethyl acrylate (40.64 g, 0.35 mol) and triethylamine (38.96 g, 0.38 mol) in 220 mL of CH<sub>2</sub>Cl<sub>2</sub>, during 3 h under an atmosphere of argon. After complete addition, the reaction was further stirred at room temperature for 24 h. The precipitate was removed by filtration, and the organic phase was washed with water (3 × 50 mL). It was then dried over magnesium sulfate, and CH<sub>2</sub>Cl<sub>2</sub> was evaporated under vacuum. The obtained yellow oil was distilled under vacuum in the presence of 0.5 wt % of

**Table 1.** Synthesis<sup>a</sup> of Poly(*n*-butyl acrylate-*co*-methyl methacrylate) (Poly(*n*BA-*co*-MMA)) Latex Particles Cross-Linked with 1,4-Butanediol Diacrylate (BDDA) and Functionalized at the Surface with 2-(2-Bromopropionyloxy)ethyl Acrylate (BPEA) (*T* = 70 °C)

latex no.	composition of the core <i>n</i> BA/MMA/BDDA (wt %)	composition of the shell MMA/BPEA/BDDA (wt %)	shell/core weight ratio (wt %)	BPEA conv (%)	overall BPEA content (mol/g <sub>Latex</sub> )	final diameter <i>D</i> from DLS (nm)
L0	30.7/66.7/2.6				0	112
L1	30.7/66.7/2.6	95.0/1.8/3.2	5.1/94.9	95	1.5 × 10 <sup>-6</sup>	110
L2	30.7/66.7/2.6	65.0/32.5/2.5	7.5/92.5	95	3.9 × 10 <sup>-5</sup>	110
L3	30.7/66.7/2.6	48.6/49.0/2.4	9.7/90.3	97	7.3 × 10 <sup>-5</sup>	116

<sup>a</sup>The experimental procedure is described in the Experimental Part.

hydroquinone to give a colorless liquid. 300 MHz <sup>1</sup>H NMR (CDCl<sub>3</sub>): δ (ppm) = 6.44 (d, 1H, CH<sub>2</sub>=), 6.13 (dd, 1H, =CH), 5.87 (d, 1H, CH<sub>2</sub>=), 4.41 (m, 5H, H<sub>2</sub>C–O and CH–Br), 1.83 (d, 3H, CH<sub>3</sub>).

**Characterization Techniques.** NMR. <sup>1</sup>H NMR spectroscopy for kinetic analysis (i.e., conversion of the monomer NAM in the surface-initiated aqueous polymerization) was performed in 5 mm diameter tubes in D<sub>2</sub>O solution at 25 °C using a Bruker Avance 300 (300 MHz) spectrometer. The chemical shift scale was calibrated on the basis of the solvent peak (δ = 4.79 ppm), and sodium *p*-toluenesulfonate was used as an internal reference (aromatic H peaks).

**DLS.** The intensity-average diameters of the latex particles and the dispersity factor were measured by dynamic light scattering (DLS) at a temperature of 25 °C using a Zetasizer Nano Series (Nano ZS) from Malvern Instrument using the Zetasizer 6.2 software. The instrument was calibrated with a standard polystyrene latex in water exhibiting a particle size of 220 ± 6 nm. Before measurements, the latex samples were diluted with deionized water.

**Gas Chromatography.** Gas chromatography (GC) of the polymer dispersions was used to determine the residual amount of BPEA inimer. It was performed with HP6890N equipment from Agilent Technologies with a 30 m column (DB 5, 5% polydiphenylsiloxane/95% polydimethylsiloxane) and a temperature ramp of 8 °C/min from 120 to 280 °C. The injection temperature was 280 °C.

**SEM.** Scanning electron microscopy (SEM) images were examined on a FEI QUANTA 250 FEG scanning electron microscope, at an acceleration voltage of 15 kV (Centre Technologique des Microstructures (CTμ), Claude Bernard University, Lyon, France). A drop of the particle suspension was placed on a Formvar film on a 200 mesh copper grid, dried, and covered by a thin layer of gold/palladium (sputtering Au/Pd with Baltec MED020-5.9 nm).

**DSC.** Differential scanning calorimetry was measured in a Q2000 by TA Instruments. The instrument is calibrated with adamantane, water, and indium. For determination of the glass transition temperature, 8–9 mg was placed in an aluminum pan. The sample was rapidly cooled from 150 to –110 °C and afterward scanned with a heating rate of 2 K/min. Glass transition was determined at the half step height (according to ISO 11357-2).

**FTIR.** Fourier transform infrared analyses were performed on a Nicolet iS10 spectrometer with an ATR diamond crystal and a DTGS KBr detector. The data were measured with a resolution of 4 cm<sup>-1</sup> from 525 to 4000 cm<sup>-1</sup>. A background spectrum was collected and subtracted from the spectrum. The latex were dialyzed against water for 2 weeks using a Spectra/Por dialysis membrane (cutoff at 12 000–14 000 Da), dried at room temperature, grinded to powder, and then dissolved in dichloromethane. A drop of the dispersion was deposited onto the diamond crystal, dried, and then analyzed.

**ToF SIMS.** Time-of-flight secondary ion mass spectrometry (ToF-SIMS) measurements were carried out using a Physical Electronics TRIFT III ToF-SIMS instrument operated with a pulsed 22 keV Au<sup>+</sup> ion gun (ion current of 2 nA) rastered over a 300 μm × 300 μm area. An electron gun was operated in pulsed mode at low electron energy for charge compensation. Ion dose was kept below the static conditions limit. Data were analyzed using the WinCadence software. Mass calibration was performed on hydrocarbon secondary ions. Before the analysis, the latexes were dialyzed in water for 2 weeks using a Spectra/Por dialysis membrane (cutoff at 12 000–14 000 Da), dried

at room temperature, and grinded to a powder, and this powder was pressed onto an indium foil. Data were normalized to the total intensity minus H<sup>+/–</sup> intensity (because of its critical dependence on slight variations in the experimental settings)<sup>27</sup> and minus the intensity of peaks related to ubiquitous contamination or to the sample preparation (i.e., Na<sup>+</sup> and In<sup>+</sup> in the positive mode and F<sup>–</sup> in the negative mode). Standard deviations were calculated from measurements performed on three different areas.

**Viscosity Measurements.** Viscosity measurements were performed at 25 °C using a parallel-plate (25 mm in diameter) geometry fixture on a TA Instruments AR2000ex rheometer. The shear rate was fixed at 50 s<sup>-1</sup>, and the gap between the upper plate and the Peltier plate was set at a distance of 1000 μm.

**Stability Tests.** The ionic strength and freeze–thaw stability of the grafted latexes were tested (raw latexes or dialyzed latexes). A drop of latex dispersion was added to 5 mL solutions of CaCl<sub>2</sub> with concentrations of 4.5 mM, 9.0 mM, 22.5 mM, 45 mM, 91 mM, 0.18 M, 0.47 M, 1 M, and 2.25 M. The colloidal stability of the dispersion was assessed by a simple visual test. A 2 mL dispersion of grafted particles was frozen for 2 h and then thawed. This cycle was repeated three times. The colloidal stability of the dispersion was assessed by DLS measurements.

**Synthesis of Poly(MMA-*co*-*n*BA) Cross-Linked Functionalized Latex Particles.** In a first step, functionalized, cross-linked latex particles were synthesized via free-radical emulsion polymerization in an automated reactor at the BASF Laboratories for Advanced Materials and Systems Research. Particles were cross-linked with 1,4-butanediol diacrylate, a divinyl monomer, in order to maintain their shape and integrity for analytical purposes. In a typical example (latex L3 in Table 1), a monomer in water emulsion was first prepared using 260 g of deionized water, 26.5 g of SDS solution, 5.6 g of sodium hydrogen carbonate solution, 88 g of *n*BA, 190 g of MMA, and 7.3 g of BDDA. An aqueous solution of ACPA initiator (6.28 g of the solution prepared with 48 g of deionized water, 3.0 g of ACPA, and 11.7 g of NaOH aqueous solution 0.25 M) was introduced into a 2 L reactor preloaded with 138 g of deionized water, equipped with a thermocouple, a cooling condenser, and a paddle stirrer, and heated at 70 °C. After 15 min, the monomer-in-water emulsion was gradually added to the reactor for a total time of 180 min while 56.5 g of the residual initiator solution was fed during 215 min. After complete addition of the monomer emulsion (achieving 92% conversion), a mixture containing 15 g of the BPEA inimer, 15 g of MMA, and 0.7 g of BDDA was added during 30 min, and the reaction medium was stirred at 70 °C for an additional 60 min and then cooled to room temperature. The final latex had a solids content of 40 wt % (obtained by gravimetric analysis). The particle diameter was determined using DLS. The conversion of BPEA was determined by gas chromatography. All data are summarized in Table 1.

**Copper-Mediated Surface-Initiated Polymerization of NAM.** The latexes (raw or slightly diluted in water) with a low amount of sodium *p*-toluenesulfonate (4 mg/g<sub>Latex</sub>) were deoxygenated with a nitrogen flow for 30 min. A deoxygenated mixture of NAM, PMDETA, 0.1 M CuBr<sub>2</sub> aqueous solution, and additional water was slowly added under stirring. The reaction medium was heated at 25 °C, and a piece of a copper wire was introduced (0.14 cm/g<sub>Latex</sub> i.e., 12.6 cm<sup>2</sup>/g<sub>Latex</sub>). Samples were periodically withdrawn to monitor the

**Table 2. Surface-Initiated Polymerization of *N*-Acryloylmorpholine (NAM) Performed at 25 °C from Cross-Linked Poly(*n*-butyl acrylate-*co*-methyl methacrylate) Aqueous Latex Particles Functionalized at the Surface with 2-(2-Bromopropionyloxy)ethyl Acrylate (BPEA)**

entry	functionalized latex	overall BPEA content (mol/g <sub>Latex</sub> )	NAM (g/g <sub>polymer</sub> )	NAM/BPEA/PMDETA/CuBr <sub>2</sub> (molar equiv)	time (h)	conv (%)	<i>D</i> from DLS after grafting (nm) /dispersity	final solids content of the grafted latex <sup>a</sup> (wt %)	final viscosity <sup>b</sup> (10 <sup>-3</sup> Pa s)	color <sup>c</sup>
L1G1	L1	1.4 × 10 <sup>-6</sup>	0.05	97.5/1/0.6/0.10	8	30	120/0.08	38	2.4	*
L1G2	L1	1.1 × 10 <sup>-6</sup>	0.22	441.5/1/0.8/0.15	1		formation of a gel			*
L2G1	L2	2.1 × 10 <sup>-5</sup>	0.05	4.1/1/0.5/0.10	7	100	105/0.03	24	1.6	***
L2G2	L2	2.6 × 10 <sup>-5</sup>	0.26	20.5/1/0.5/0.10	2	40	171/0.09	37	33.3	*****
L2G3	L2	2.0 × 10 <sup>-5</sup>	0.26	20.5/1/0.5/0.10	7	93	210/0.3	30	22.1	***
L2G4	L2	1.9 × 10 <sup>-5</sup>	0.42	33.3/1/0.5/0.10	7	71	270/0.3	31	287.7	***
L3G0	L3	6.6 × 10 <sup>-5</sup>	0	0/1/0.5/0.10 <sup>d</sup>	6					
L3G1	L3	6.1 × 10 <sup>-5</sup>	0.125	5.0/1/0.6/0.09	6	96	140/0.04	38	2.6	*****
L3G2	L3	4.9 × 10 <sup>-5</sup>	0.23	8.9/1/0.5/0.10	4	86	119/0.06	33	1.6	****
L3G3 <sup>e</sup>	L3	5.5 × 10 <sup>-5</sup>	0.25	10.9/1/0.5/0.10	8	79	140/0.03	41	1.7	*****
L3G4	L3	4.7 × 10 <sup>-5</sup>	0.25	9.9/1/0.2/0.05	5	89	130/0.05	31	5.9	***
L3G5	L3	4.8 × 10 <sup>-5</sup>	0.25	9.7/1/0.1/0.025	2		formation of a gel			**
L3G6 <sup>f</sup>	L3	1.1 × 10 <sup>-5</sup>	0.40	13.3/1/0.5/0.10	6	88	260/0.2	8.6	2.7	**
Control Experiments										
L0G1	L0	0	0.13	9.8/0/1/0.5/(Cu(0) wire: 1.5 cm)	5	0				
L3G7	L3	3.4 × 10 <sup>-5</sup>	0.15	6.3/1/0/0/(Cu(0) wire: 0 cm)	5	0				
L3G8	L3	3.4 × 10 <sup>-5</sup>	0.15	6.1/1/0/0/(Cu(0) wire: 1 cm)	5	0				
L3G9 <sup>g</sup>	L3	3.4 × 10 <sup>-5</sup>	0.15	6.0/1/0.7/0/(Cu(0) wire: 1 cm)	5	9				
L3G10 <sup>g</sup>	L3	3.4 × 10 <sup>-5</sup>	0.15	6.3/1/0.7/0.15/(Cu(0) wire: 0 cm)	5	11				

<sup>a</sup>Obtained by thermogravimetric analysis—includes the nonreacted NAM, which is nonvolatile. <sup>b</sup>At 20 wt % solids (except latex L3G6 measured at 8 wt %). <sup>c</sup>Color qualitative scale: \* (light blue) to \*\*\*\*\* (dark blue). <sup>d</sup>CuCl<sub>2</sub> instead of CuBr<sub>2</sub>. <sup>e</sup>Two successive feeds of NAM (feed 1: 81% conversion in 2 h; feed 2: 67% conversion in 8 h – overall conversion = 79%). <sup>f</sup>The latex L3 was dialyzed before the grafting reaction, to remove the initiator and surfactant. <sup>g</sup>Latex destabilization.

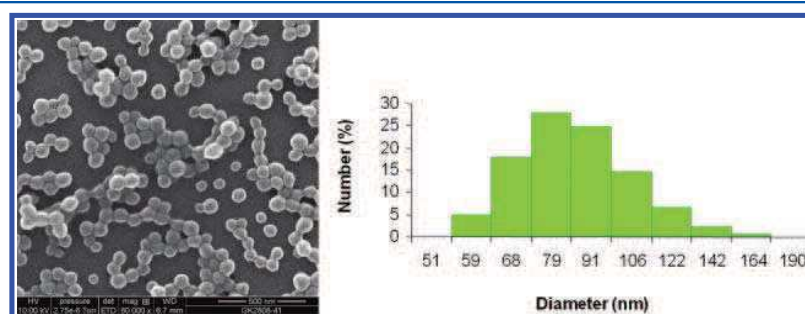


**Figure 1.** Scanning electron microscopy image and particle size distribution from DLS of the final latex L3.

conversion by <sup>1</sup>H NMR after dilution in D<sub>2</sub>O. All reaction details and exact quantities are reported in Table 2.

## RESULTS AND DISCUSSION

**Surface Functionalization of Latex Particles with the BPEA Inimer.** The latex particles were based on methyl methacrylate and *n*-butyl acrylate and were slightly cross-linked with 1,4-butanediol diacrylate to maintain their integrity during the analyses. The experimental conditions are reported in Table 1. The surface functionalization of such latex particles has been already reported in the literature.<sup>16,17</sup> The functional monomer BPEA was used in a very low amount to introduce a thin layer of brominated groups able to initiate the polymerization from the surface. The main requirements that had to be fulfilled are the absence of secondary nucleation and a high conversion of BPEA with a preferential location at the particle surface. BPEA was thus added at the end of the latex synthesis before complete conversion of the core monomers (~90%). During this step, MMA was used as a comonomer, to ensure an

efficient anchoring of the adsorbed oligoradicals by fast chain propagation and to avoid their precipitation and the generation of a second crop of particles. The final conversion of BPEA was high as assessed by gas chromatography (see Table 1). On the basis of the scanning electron microscopy and DLS analyses of the final latexes (Figure 1), a monomodal particle size distribution was observed, indicating the absence of secondary nucleation.

Because of the very low amount of BPEA used and due to the remaining core monomers present during the functionalization step, it was important to check the location of the inimer. Burial of the inimer may actually occur during the polymerization, even though the use of additional MMA should lead to a rather polar polymer that remains preferentially at the particle surface. ToF-SIMS has already been used to detect functional groups at the surface of synthetic latex particles<sup>28–30</sup> and was selected for the present analytical purpose. This surface analysis technique is based on the *m/z* detection of secondary ions (positively charged and negatively charged as obtained in two

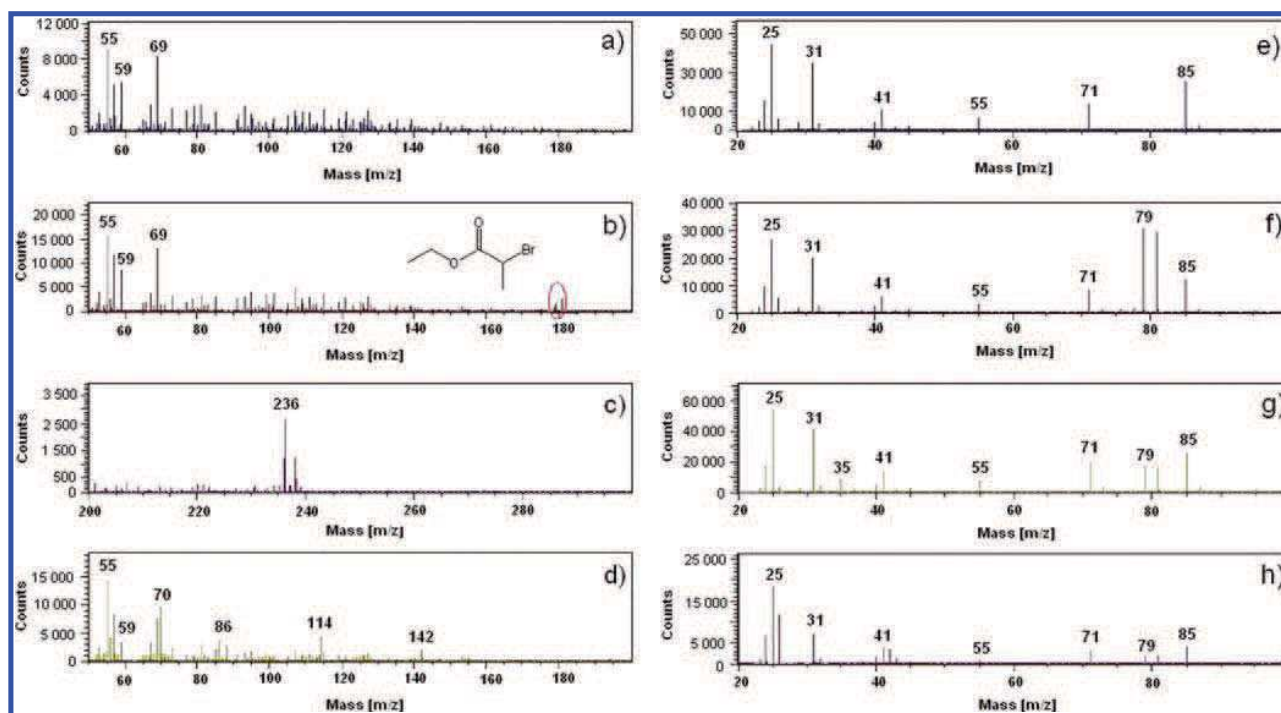


Figure 2. Positive ion mode ToF-SIMS spectrum ( $m/z = 50\text{--}200$ ) for (a) latex L0, (b) latex L3, (c) latex L3G0 ( $m/z = 200\text{--}300$ ), and (d) latex L3G1. Negative ion mode ToF-SIMS spectrum ( $m/z = 20\text{--}100$ ) for (e) latex L0, (f) latex L3, (g) latex L3G0, and (h) latex L3G1.

Table 3. ToF-SIMS Normalized Intensity (in %) for Various Characteristic Peaks<sup>a</sup> for Latexes L0, L1, L2, L3, L3G0, L3G1, and L3G3 (see Table 2)

entry	characteristic signatures for core latex		characteristic signatures for BPEA		characteristic signature for Cl	characteristic signatures for polyNAM		
	$I^{59+}$	$I^{85-}$	$I^{79-}$	$I^{179+}$		$I^{35-}$	$I^{26-}$	$I^{42-}$
L0	$13.7 \pm 2.2$	$21.9 \pm 2.6$	$0.9 \pm 0.2$	$1.2 \pm 0.3$	$0.5 \pm 0.5$	$5.8 \pm 0.2$	$0.4 \pm 0.1$	$1.6 \pm 0.2$
L1	$16.5 \pm 1.0$	$27.3 \pm 1.8$	$3.7 \pm 0$	$1.4 \pm 0.2$	$0.6 \pm 0.2$	$7.4 \pm 0.6$	$0.5 \pm 0.1$	$1.8 \pm 0.2$
L2	$16.0 \pm 0.4$	$18.8 \pm 3.1$	$39.9 \pm 3.6$	$7.4 \pm 0.7$	$0.2 \pm 0$	$4.4 \pm 0.2$	$0.3 \pm 0$	$2.0 \pm 0$
L3	$13.4 \pm 3.6$	$15.5 \pm 2.5$	$39.8 \pm 4.7$	$6.6 \pm 1.1$	$0.2 \pm 0$	$5.7 \pm 1.3$	$0.3 \pm 0.1$	$1.5 \pm 0.2$
L3G0	$14.3 \pm 0.6$	$18.9 \pm 1.6$	$14.1 \pm 0.7$	$2.4 \pm 0.2$	$8.9 \pm 1.6$	$3.7 \pm 0.5$	$0.4 \pm 0$	$1.6 \pm 0.1$
L3G1	$7.0 \pm 0.5$	$9.1 \pm 1.3$	$4.7 \pm 0.2$	$1.1 \pm 0.1$	$0.7 \pm 0.1$	$23.7 \pm 2.6$	$7.5 \pm 1.1$	$8.1 \pm 0.8$
L3G3 <sup>b</sup>	$5.4 \pm 0.1$	$7.2 \pm 0.5$	$2.4 \pm 0.1$	$0.9 \pm 0$	$7.0 \pm 3.4$	$29.1 \pm 0.4$	$10.5 \pm 0$	$8.4 \pm 0.1$

<sup>a</sup>Peaks at:  $m/z = 59^+$  corresponding to  $C_2H_3O_2^+$  and  $m/z = 85^-$  corresponding to  $C_4H_3O_2^-$ , characteristic of the core latex;  $m/z = 79^-$  corresponding to  $^{79}Br^-$  and  $m/z = 179^+$  corresponding to  $C_5H_8O_2^{79}Br^+$ , characteristic of BPEA;  $m/z = 35^-$  corresponding to  $^{35}Cl^-$ , characteristic of the ion exchange reaction between Br and Cl but contribution from Cl ubiquitous contamination cannot be excluded (it is especially the case for L3G3);  $m/z = 26^-$  corresponding for a major part to  $CN^-$  but contribution from  $C_2H_2^-$  cannot be excluded,  $m/z = 42^-$  corresponding to  $CNO^-$  and  $m/z = 142^+$  corresponding to  $C_7O_2H_{12}N^+$ . <sup>b</sup>Measurements performed only on two areas and therefore poorly accurate.

separate data acquisitions) emitted following the bombardment of solids using primary ions in the keV range. If a limited number of primary ions are used for this purpose (static conditions), the information depth is limited to a few atomic layers. Moreover, this technique allows the detection of very low amounts<sup>31</sup> (detection limit of ppm to ppb), which is appropriate considering the quantity of BPEA involved for surface modification of the latexes. The latexes were first carefully dialyzed to remove all nonconverted monomers and water-soluble oligomers, and the dried powder was then pressed onto an indium foil at room temperature. The particles being cross-linked and their glass transition temperature being 52 °C (as determined by DSC, i.e., above room temperature) a good shape stability and the absence of film formation by chain interdiffusion is expected. This is an important point when targeting the surface analysis exclusively.

Figure 2 displays ToF-SIMS spectra in the positive and negative modes in selected  $m/z$  ranges. It illustrates the main observations at the surface of latexes before and after the various steps of the surface modification (modification with BPEA inimer, test for ion-exchange, surface-initiated polymerization of NAM). Table 3 provides normalized intensity values (in %) for secondary ion peaks specific to the latexes and to the various surface modifications. Figures 2a and 2e correspond to the spectra obtained on the latex L0 (nonfunctionalized) in the positive mode ( $m/z = 50\text{--}200$ ) and in the negative mode ( $m/z = 20\text{--}100$ ), respectively. ToF-SIMS spectra display peaks characteristic for polyMMA<sup>28</sup> (as well as other peaks detected in the nonillustrated  $m/z$  ranges), i.e., in the displayed  $m/z$  range, a peak at  $m/z = 59.014$  (corresponding to  $C_2H_3O_2^+$ ,  $m/z = 59.013$ ) and those at  $m/z = 31.016$  (corresponding to  $CH_3O^-$ ,  $m/z = 31.018$ ),  $m/z = 55.018$  (corresponding to

$C_3H_3O^-$ ,  $m/z = 55.018$ ), and  $m/z = 85.029$  (corresponding to  $C_4H_5O_2^-$ ,  $m/z = 85.029$ ). This confirmed that latexes had the expected chemical structure (see also Table 3) without significant contamination (see e.g. Br and Cl ubiquitous contamination in Table 3).

After surface functionalization with BPEA inimer, both ToF-SIMS spectra of latex L3 in the positive mode (Figure 2b) and in the negative mode (Figure 2f) indicate that the main signatures of the latexes are still detected, which is consistent with the intended limited extent in surface modification. In addition, peaks characteristic for BPEA were detected. The most obvious signature was Br, which was detected in the negative mode with both isotopes (and in the expected isotopic ratio): a peak at  $m/z = 78.913$  (corresponding to  $^{79}Br^-$ ,  $m/z = 78.918$ ) and a peak at  $m/z = 80.911$  (corresponding to  $^{81}Br^-$ ,  $m/z = 80.916$ ). However, Br being ubiquitous contamination (see in Table 3 the very slight amount detected for the unmodified latex L0), it was important to confirm that the high relative intensity for  $^{79}Br^-$  was a direct signature for BPEA. The detection of peaks in the positive mode at  $m/z = 178.981$  corresponding to  $C_5H_8O_2^{79}Br^+$ ,  $m/z = 178.971$ —see BPEA chemical structure in Scheme 1) and a peak at  $m/z = 180.972$  (corresponding to  $C_5H_8O_2^{81}Br^+$ ,  $m/z = 180.969$ ) brought this confirmation.

Table 3 (entries L0–L2) indicates that when modifying the BPEA concentration used for surface modification (see entries L0–L2 in Table 1), characteristic signatures for BPEA varied accordingly in normalized intensity. ToF-SIMS data are known to be highly dependent on severe matrix effects, which hinder any absolute quantification from these data. However, when comparing similar samples only varying as a function of the BPEA content, matrix effects can be considered as close enough to allow a semiquantitative comparison of normalized intensities for characteristic signatures of BPEA, i.e.,  $Br^-$ . In addition, the relative intensity for  $179^+$  for the latex L0 in Table 3 is not due to  $C_5H_8O_2^{79}Br^+$  ( $179^+$  is detected at  $m/z = 179.0975$  for L0, excluding any relation to BPEA), but the value was given to allow the reader to identify the relevance of the increase in normalized intensity for that specific signature (thus relevant for L2 and L3 but not for L1). It can then be concluded here that BPEA is significantly less detected for latex L1 compared to latexes L2 and L3. For the latter two latexes, similar values could be related to the very limited information depth of the ToF-SIMS technique. BPEA might be more incorporated in L3 than in L2, but the amount in the sample depth probed by ToF-SIMS was similar. As expected, for latexes L2 and L3, a more significant decrease in normalized intensity was observed for the core polymer characteristic peaks (especially  $C_4H_5O_2^-$ ), which is consistent with the larger introduction of BPEA at the surface of these latexes.

Prior to any polymerization from the surface, and in order to assess the accessibility of the surface anchored Br toward an ion exchange reaction with water-soluble species, the latex L3 was further subjected to a reaction with Cu(0) and  $CuCl_2$ /PMDETA (entry L3G0, Table 2). The change of Br signature to Cl one should show that activation of the alkyl bromide group of BPEA is possible and further confirm the appropriate location of BPEA. Figure 2g displays the ToF-SIMS spectrum in the negative mode for the latex L3G0, obtained by reacting the latex L3 with  $CuCl_2$ /PMDETA in the presence of Cu(0). The characteristic signatures for BPEA ( $^{79}Br^-$  but as well  $C_5H_8O_2^{79}Br^+$ ) are still detected but with a significantly lower normalized intensity (see Table 3). It was expected that peaks

similar to  $179^+/181^+$ , thus possibly  $C_5H_8O_2^{35}Cl^+$  and  $C_5H_8O_2^{37}Cl^+$ , could be detected, but they were not identified (data not illustrated). It can be due to the low  $CuCl_2$  concentration used in this experiment. Still, Cl was detected in the negative mode with both isotopes (and in the expected isotopic ratio): a peak at  $m/z = 34.970$  (corresponding to  $^{35}Cl^-$ ,  $m/z = 34.969$ ) and a peak at  $m/z = 36.967$  (corresponding to  $^{37}Cl^-$ ,  $m/z = 36.966$ ) in a higher level than the ubiquitous contamination. This confirmed an exchange reaction, most likely based on the radical process that is required for initiation and controlled propagation (based on the activation/deactivation equilibrium).

**Surface-Initiated Polymerization of NAM.** The successful introduction of BPEA and the accessibility of the alkyl bromide groups being confirmed, the latexes L1, L2, and L3 were further used as substrates for the surface-initiated polymerization of NAM in the presence of Cu(0),  $CuBr_2$ , and PMDETA. This monomer was selected as a good model for water-soluble neutral monomer, which can be easily characterized due to the amide group that is not present in the core monomers. The reactions were carried out at room temperature without purification and at high solids content of the initial latexes. The conditions are summarized in Table 2. The reagent concentrations were adapted from solution polymerizations performed in water (nonreported here) to avoid too fast polymerizations. Typically, the  $CuBr_2$ /BPEA molar ratios were in the 0.025–0.15 range, while the molar ratio PMDETA/ $CuBr_2$  was around 5. The conversion of NAM was monitored by  $^1H$  NMR spectroscopy in  $D_2O$ . In general, it appeared that most of the polymerizations reached a conversion plateau at rather high conversion values after 2–3 h reaction time (Figure 3).

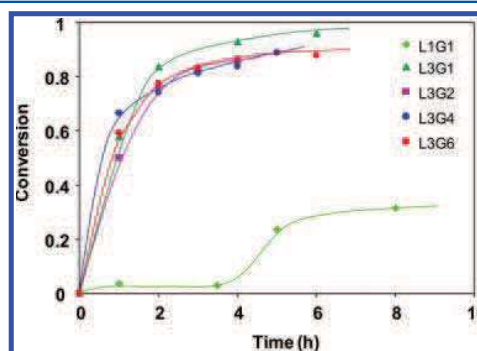


Figure 3. Conversion of NAM measured by  $^1H$  NMR analysis vs time for the Cu-mediated surface-initiated polymerizations of NAM from the latexes L1 and L3.

Even though all control experiments showed that there was no polymerization initiation from residual ACPA, or from other components of the catalytic system (see Table 2, control experiments), we still intended to confirm that the polymerization of NAM was initiated by the surface bromide groups, creating a covalently attached hairy polyNAM layer. For this purpose, the grafted latexes were dialyzed against water, dried, and analyzed first by FTIR and for one of them by ToF-SIMS. Besides the  $C=O$  band at  $1725\text{ cm}^{-1}$  (ester stretching vibration) that was observed on the FTIR spectra of the analyzed latexes (Figure 4), the band at  $1640\text{ cm}^{-1}$  typical of the amide group (amide I stretching vibration) was evidenced for the cleaned latexes L3G6, L3G1, and L3G3. These results

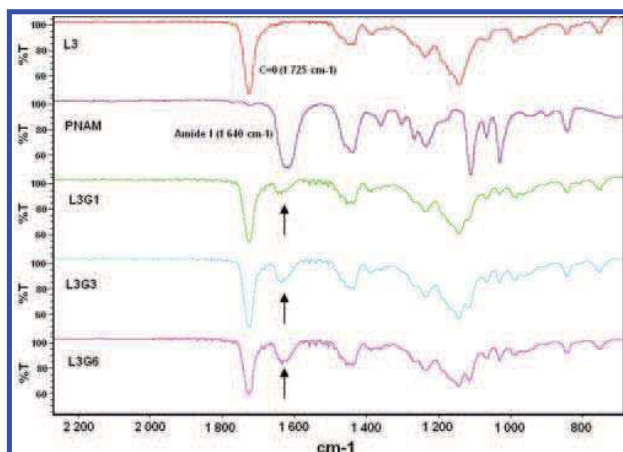


Figure 4. FTIR analysis of the latexes L3, L3G1, L3G3, and L3G6 cleaned by dialysis and dried and of polyNAM.

thus confirm the incorporation of polyNAM in the latex by a covalent bonding. The strong stability provided by the grafting of polyNAM chains (see following section) did not allow us to cleanly centrifuge the final grafted latex to determine the water-soluble content, which appeared to be very small on the basis of the NMR analysis performed on the collected serum.

The experimental conditions and the hydrophilic nature of NAM are in favor of the creation of a hydrophilic shell rather than polyNAM domains engulfed within the polymer core. ToF-SIMS analyses were performed on L3G1 grafted latex to confirm this assumption (see Figure 2 and Table 3). Figures 2d and 2h correspond to the spectra obtained on the latex L3G1 in the positive mode ( $m/z = 50-200$ ) and in the negative mode ( $m/z = 20-100$ ), respectively. Peaks characteristic to polyNAM are detected such as those at  $m/z = 26.004$  (corresponding to  $\text{CN}^-$ ,  $m/z = 26.003$ ),  $m/z = 42.007$  (corresponding to  $\text{CNO}^-$ ,  $m/z = 41.998$ ),  $m/z = 114.069$  (corresponding to  $\text{C}_5\text{H}_8\text{NO}_2^+$ ,  $m/z = 114.055$ ), and at  $m/z = 142.095$  (corresponding to  $\text{C}_7\text{H}_{12}\text{NO}_2^+$ ,  $m/z = 142.087$ ). This is confirmed by normalized intensity values in Table 3. The few N-based signatures already detected for L0, L3, and L3G0 are due to the use of ACPA as an initiator. Peaks characteristic of the core latex and Br are still detected (Figure 2d,h and Table 3). The normalized intensity values for core latex specific peaks significantly decreased, which illustrates a significant grafting of polyNAM at the surface. On the other hand, Br is still detected but not anymore the peaks specific to BPEA, i.e.,  $\text{C}_5\text{H}_8\text{O}_2^{79}\text{Br}^+$  and  $\text{C}_5\text{H}_8\text{O}_2^{81}\text{Br}^+$  (see Table 3). The normalized intensity for  $179^+$  is back to the value previously observed—and not corresponding to  $\text{C}_5\text{H}_8\text{O}_2^{79}\text{Br}^+$ —for the latex L0. This result is consistent with the polymerization mechanism in which chains are extended from BPEA units while maintaining a dormant Br end group. If  $\text{C}_5\text{H}_8\text{O}_2^{79}\text{Br}^+$  was as expected not detected anymore, no peak combining polyNAM and Br end group was however detected. The latex L3G1 should contain a low amount of polyNAM (see Figure 4), but this is not apparent in ToF-SIMS data. It should be reminded that the ToF-SIMS information depth is limited to the top surface where NAM polymerization is expected to start while FTIR information depth is larger, allowing the detection of the increase in the amount grafted.

Bulk and surface analyses thus confirmed the efficiency of the grafting reaction. The effect of the experimental conditions on the polymerization yield and kinetics was then examined from

the information displayed in Table 2 and in Figure 3. It first appeared that the polymerization was slow and the final NAM conversion was low at the lowest amount of BPEA (core latex L1). For higher BPEA concentrations (latexes L2 and L3), the grafting kinetics were faster but not significantly different from each other (see experiments L2G1 and L3G1 in Table 2). For both core latexes and irrespective of the added concentration of NAM, the final conversion was generally above  $\sim 80\%$  and sometimes higher than  $90\%$ . Thus, a minimum BPEA concentration was needed to ensure a high surface concentration (as suggested by the ToF-SIMS results) along with good accessibility of the bromide group at the surface. Upon polymerization of NAM, the hydrodynamic diameter of the particles determined by DLS increased (Table 2). When a narrow particle size distribution (dispersity below 0.1) was maintained, the final diameters reached values as high as  $140\text{ nm}$ , corresponding to a maximum hydrodynamic layer thickness of  $\sim 12\text{ nm}$ . In a few examples the final diameter was much higher (above  $170\text{ nm}$ ), but the dispersity was also high (above 0.1), indicating the presence of aggregates, most likely in very low concentration. In general, the core-shell latexes formed by grafting polyNAM from L2 and L3 remained very stable and became more viscous when the NAM/BPEA molar ratio was increased (see Table 2). Nevertheless, the viscosity values remained acceptable in most cases, i.e., below  $6\text{ mPa}\cdot\text{s}$ . Moreover, the latexes exhibited a blue color that was more or less intense depending on the experiments (the lower the Cu(II) absolute concentration, the lighter the color; see Table 2). In some examples a gel was obtained within short polymerization time and could not be diluted, indicating interparticle cross-linking via radical termination, which is not surprising at such high substrate concentration (i.e., short interparticle distance).

A series of grafting reactions were performed with the core latex L2 as a substrate and varying concentrations of NAM in the system, exhibiting an average molar ratio with respect to the overall BPEA of 4.1 (entry L2G1, Table 2), 20.5 (entries L2G2 and L2G3, Table 2), and 33.3 (entry L2G4, Table 2). The initiator and catalyst concentrations remained the same in all four experiments. Note that the relative proportion of NAM to BPEA was kept rather low, anticipating that the initiating efficiency of BPEA would not be  $100\%$ , as only part of it would be really accessible at the extreme surface. This corresponded to amounts of NAM from 5 up to 42 wt % with respect to the core polymer. Except for entry L2G2 (short reaction time), the final conversion decreased from  $100\%$  to  $71\%$  when the amount of NAM was increased. The overall amount of grafted polyNAM however increased from  $0.05\text{ g/g}_{\text{polymer}}$  for entry L2G1 to  $0.30\text{ g/g}_{\text{polymer}}$  for entry L2G4. The influence of the initial concentration of NAM on the final conversion is not very clear but might possibly be explained by competitive copper ions complexation between monomer and PMDETA.<sup>32</sup> The same trend was also observed for experiment L3G1 with the lowest concentration of NAM in comparison with the other grafting experiments from latex L3 (L3G2 to L3G6). With  $0.125\text{ g/g}_{\text{polymer}}$  of initial NAM, the final conversion was  $96\%$ , whereas it remained below  $90\%$  when NAM concentration was increased. The final particle diameter was larger when the amount of NAM was increased, and the particle size distribution became broader, indicating both the formation of a hydrophilic shell and the generation of aggregates via possible interparticle radical coupling reactions.



The effect of the concentration of the catalytic system was explored in grafting latex L3 with NAM in the presence of decreasing concentrations of PMDETA and CuBr<sub>2</sub> (entries L3G2, L3G4, and L3G5 in Table 2), while keeping a similar molar ratio between both and keeping the same amount of Cu(0) wire. When the PMDETA/CuBr<sub>2</sub> molar ratio was 0.5/0.1 (L3G2) or 0.2/0.05 (L3G4), the kinetics and the features of the grafted latex were similar. In contrast, when it was further decreased to 0.1/0.025 (L3G5) the reaction led to a gel. At such low deactivator content, the concentration of propagating radicals would be enhanced and would favor interparticle coupling reaction and the formation of gel. Eventually, the latex L3 was cleaned by dialysis before performing the grafting reaction in experiment L3G6 (Table 2). Although the polymerization of NAM was performed under diluted conditions, the results were very similar to the grafting reactions performed from raw latexes. This last result is a clear indication that residual initiator and surfactant do not interfere with the grafting process.

To conclude this part, robust conditions for an efficient Cu-mediated surface-initiated polymerization at room temperature were found from Br-functionalized latex particles that were not cleaned, i.e., in the presence of remaining radical initiator and SDS surfactant.

**Colloidal Stability of the Grafted Latexes.** In the previous section, we showed that core-shell latexes were obtained using surface-initiated polymerization of NAM. Such latexes coated by a neutral hydrophilic polymer may exhibit improved stability toward high ionic strength and freeze-thaw cycles. Demonstrating this improved stability would be an additional proof of the success of our grafting procedure. The corresponding data reported in Table 4 showed that, for all

**Table 4. Stability Tests to Freeze–Thaw Cycles and CaCl<sub>2</sub> Concentration of the Latexes L2 and L3 Grafted with PolyNAM**

entry	D from DLS before freezing (nm)/dispersity	D from DLS after 3 freeze–thaw cycles (nm)/dispersity	critical CaCl <sub>2</sub> conc (M)
L3	101/0.03	783/0.8	<0.0045
L2G1	105/0.03	112/0.06	0.0045
L2G3	210/0.30	193/0.25	>2.25
L2G4	270/0.3	235/0.3	>2.25
L3G1	140/0.04	146/0.05	>2.25
L3G1 <sup>a</sup>	145/0.05	150/0.08	>2.25
L3G2	119/0.06	113/0.03	>2.25
L3G3	140/0.03	147/0.002	>2.25
L3G4	130/0.05	180/0.08	>2.25
L3G6	260/0.2	230/0.24	>2.25

<sup>a</sup>Dialyzed latex.

grafted latexes, the stability to three freeze–thaw cycles was strongly improved since none of them underwent coagulation, while the nongrafted latex L3 did not remain stable. Similarly, an amazing stability of the grafted latexes under high CaCl<sub>2</sub> concentration (2.25 M) was shown (except for L2G1 with the lowest amount of grafted polymer). This is a strong evidence for the presence of the non ionic grafted polyNAM shell that protects the particles from irreversible aggregation.

## CONCLUSION

This article proposes, for the first time, robust conditions for grafting hydrophilic polymer chains using copper-mediated polymerization from concentrated bromide-functionalized latex particles, used “as synthesized” via classical emulsion polymerization. All steps were assessed very carefully by various analytical techniques, in particular ToF-SIMS. The latter evidenced the consumption of the initiating sites and the presence of a hydrophilic polymer layer at the particle surface. The grafting reaction was shown to be efficient from both the kinetic point of view and the final latex properties. For such a purpose, the main conditions to respect are (i) the need for sufficient Br surface concentration to maintain a fast reaction and high final conversion, (ii) the need for sufficient Cu(II) initial concentration to avoid gel formation, and (iii) the control of monomer/Br ratio to avoid too high viscosities. In the conditions studied, the grafted chains were not isolated, and it is thus impossible to conclude on their living character or on the control over their molar mass, which might be expected from an ATRP reaction. Although this was not the focus of this work, such a conclusion is of interest for fundamental understanding and should be studied further.

## AUTHOR INFORMATION

### Notes

The authors declare no competing financial interest.

## ACKNOWLEDGMENTS

We are grateful to Christina Laue and Antje Polenz from BASF for their technical work in the latex synthesis. Laura Autin and Philippe Cassagnau from the laboratory Ingénierie des Matériaux Polyme'res (IMP, UMR 5223, Villeurbanne) are acknowledged for their help in viscosity measurements. The electron microscopy analyses were performed at the CTμ (Centre Technologique des Microstructures of the University Claude Bernard Lyon 1), and we wish to thank the team for constant help and fruitful advice.

## REFERENCES

- (1) Barbey, R.; Lavanant, L.; Paripovic, D.; Schulwer, N.; Sugnaux, C.; Tugulu, S.; Klok, H. A. *Chem. Rev.* **2009**, *109*, 5437–5527.
- (2) Charleux, B.; D'Agosto, F.; Delaitre, G. *Adv. Polym. Sci.* **2010**, *233*, 125–183.
- (3) Cayre, O.J.; Chagneux, N.; Biggs, S. *Soft Matter* **2011**, *7*, 2211–2234.
- (4) Tsujii, Y.; Ohno, K.; Yamamoto, S.; Goto, A.; Fukuda, T. *Adv. Polym. Sci.* **2006**, *197*, 1–45.
- (5) Advincula, R. C. Brittain, W. J., Caster, K. C., Rühe, J., Eds. *Polymer Brushes*; Wiley-VCH: Weinheim, Germany, 2004.
- (6) Ayres, N. *Polym. Chem.* **2010**, *1*, 769–777.
- (7) Matyjaszewski, K.; Davis, T., Eds. *Handbook of Radical Polymerization*; John Wiley & Sons: Hoboken, NJ, 2002.
- (8) Fristrup, C. J.; Jankova, K.; Hvilsted, S. *Soft Matter* **2009**, *5*, 4623–4634.
- (9) Edmondson, S.; Osborne, V. L.; Huck, W. T. S. *Chem. Soc. Rev.* **2004**, *33*, 14–22.
- (10) Manuszak-Guerrini, M.; Charleux, B.; Vairon, J. P. *Macromol. Rapid Commun.* **2000**, *21*, 669–674.
- (11) Kizhakkedathu, J. N.; Brooks, D. E. *Macromolecules* **2003**, *36*, 591–598.
- (12) Kizhakkedathu, J. N.; Kumar, K. R.; Goodman, D.; Brooks, D. E. *Polymer* **2004**, *45*, 7471–7489.
- (13) Kizhakkedathu, J. N.; Norris-Jones, R.; Brooks, D. E. *Macromolecules* **2004**, *37*, 734–743.

- (14) Zhang, M.; Liu, L.; Wu, C.; Fu, G.; Zhao, H.; He, B. *Polymer* **2007**, *48*, 1989–1997.
- (15) Zhang, M.; Liu, L.; Wu, C.; Fu, G.; Zhao, H.; He, B. *J. Colloid Interface Sci.* **2006**, *301*, 85–91.
- (16) Mittal, V.; Matsko, N. B.; Butté, A.; Morbidelli, M. *Eur. Polym. J.* **2007**, *43*, 4868–4881.
- (17) Mittal, V.; Matsko, N. B.; Butté, A.; Morbidelli, M. *Polymer* **2007**, *48*, 2806–2817.
- (18) Min, K.; Hu, J. H.; Wang, C. C.; Elaissari, A. *J. Polym. Sci., Part A: Polym. Chem.* **2002**, *40*, 892–900.
- (19) Liu, Y. Y.; Chen, H.; Ishizu, K. *Langmuir* **2011**, *27*, 1168–1174.
- (20) Muñoz-Bonilla, A.; van Herk, A. M.; Heuts, J. P. A. *Polym. Chem.* **2010**, *1*, 624–627.
- (21) Jakubowski, W.; Matyjaszewski, K. *Macromolecules* **2005**, *38*, 4139–4146.
- (22) Magenau, A. J. D.; Kwak, Y.; Matyjaszewski, K. *Macromolecules* **2010**, *43*, 9682–9689.
- (23) Rosen, B. M.; Percec, V. *Chem. Rev.* **2009**, *109*, 5069–5119.
- (24) Zhang, Y.; Wang, Y.; Peng, C. H.; Zhong, M.; Zhu, W.; Konkolewicz, D.; Matyjaszewski, K. *Macromolecules* **2012**, *45*, 78–86.
- (25) Taniguchi, T.; Kasuya, M.; Kunisada, Y.; Miyai, T.; Nagasawa, H.; Nakahira, T. *Colloids Surf., B* **2009**, *71*, 194–199.
- (26) Matyjaszewski, K.; Gaynor, S. K.; Kulfan, A.; Podwika, M. *Macromolecules* **1997**, *30*, 5192–5194.
- (27) Poleunis, C.; Médard, N.; Bertrand, P. *Appl. Surf. Sci.* **2004**, *231*, 269–273.
- (28) Davies, M. C.; Lynn, R. A. P.; Davis, S. S.; Hearn, J.; Vickerman, J. C.; Paul, A. J. *J. Colloid Interface Sci.* **1993**, *161*, 83–90.
- (29) Davies, M. C.; Lynn, R. A. P.; Hearn, J.; Vickerman, J. C.; Paul, A. J.; Watts, J. F. *Langmuir* **1996**, *12*, 3866–3875.
- (30) Ihalainen, P.; Backfolk, K.; Sirvio, P.; Peltonen, J. *Colloids Surf., A* **2010**, *354*, 320–330.
- (31) Becker, J. S.; Dietze, H.-J. *Int. J. Mass Spectrom.* **2000**, *197*, 1–35.
- (32) Tang, W.; Kwak, Y.; Braunecker, W.; Tsarevsky, N. V.; Coote, M. L.; Matyjaszewski, K. *J. Am. Chem. Soc.* **2008**, *130*, 10702–10713.



**Poster Abstract**

**Efficient copper-mediated surface-initiated polymerization from raw polymer latex in water.**

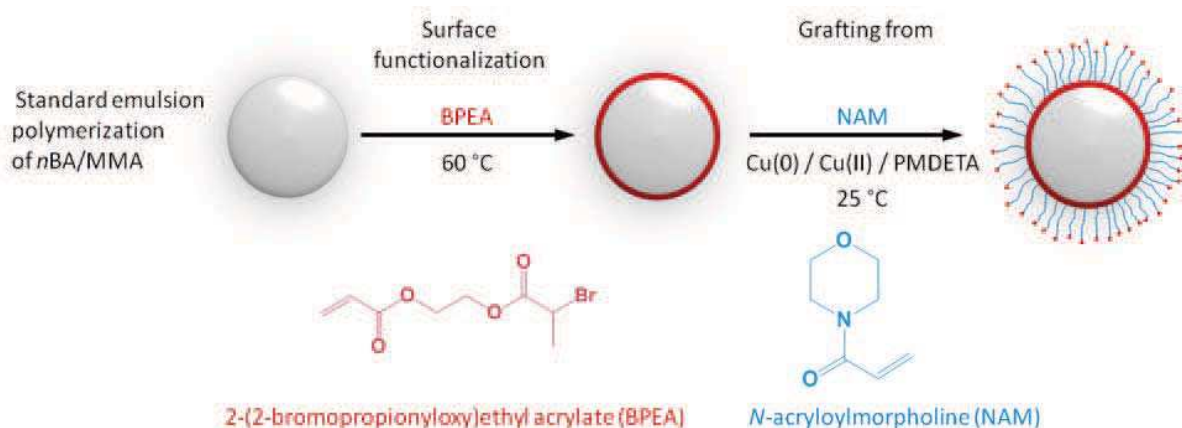
Virginie Chabrol,<sup>1\*</sup> Didier Léonard,<sup>3</sup> Matthias Zorn,<sup>2</sup> Bernd Reck,<sup>2</sup> Franck D'Agosto,<sup>1</sup>  
Bernadette Charleux<sup>1\*</sup>

<sup>1</sup>C2P2 (Chemistry, Catalysis, Polymers & Processes), Team LCPP, Université Claude Bernard-Lyon 1, CPE Lyon, CNRS, UMR 5265, Villeurbanne, France, <sup>2</sup>BASF SE, Ludwigshafen, Germany, <sup>3</sup>Université de Lyon, F 69622, Lyon, France. Institut des Sciences Analytiques, UMR 5280, Laboratoire des Sciences Analytiques, Bât. J. Raulin, Université Claude Bernard-Lyon 1, Villeurbanne, F-69622, France

\* [virginie.chabrol@lcpp.cpe.fr](mailto:virginie.chabrol@lcpp.cpe.fr); [bernadette.charleux@univ-lyon1.fr](mailto:bernadette.charleux@univ-lyon1.fr)

In the last years, there has been a growing interest in the “grafting from” methods with the development of controlled/living radical polymerization (CRP) techniques and more particularly atom transfer radical polymerization (ATRP).<sup>1</sup> Most studies were devoted to the grafting of polymer chains from inorganic surfaces, for instance silicon wafers or silica particles. Differently, polymer substrates have been much less studied. Core-shell particles with a hydrophobic polymer core and a hydrophilic polymer shell are the subject of many works<sup>2</sup> as they can find a wide range of applications. The idea to apply the “grafting from” technique to create such core-shell particles via surface-initiated ATRP (SI-ATRP) was first reported by Manuszak-Guerrini et al.<sup>3</sup> in 2000. The grafting strategy was to functionalize a crosslinked polystyrene latex with an inimer (i.e. a monomer bearing an alkyl halide group able to serve as an initiator in ATRP) at the particle surface and to activate it by a Cu(I) complex in the presence of a water-soluble monomer. Following this seminal work, other teams have used the same strategy to prepare core-shell particles by SI-ATRP.<sup>4,5,6</sup>

In this context, the aim of this work was to incorporate a hydrophilic polymer shell, poly(*N*-acryloylmorpholine), at the surface of polymer particles from emulsion polymerization by post-synthesis modification, using a “grafting from” approach based on aqueous copper-mediated radical polymerization (Scheme 1).



**Scheme 1: General principle of the Cu-mediated surface-initiated radical polymerization**

The starting latexes were synthesized via classical radical emulsion copolymerization of *n*-butyl acrylate and methyl methacrylate and were functionalized at their surface by a comonomer bearing a Br-functional group (the so-called inimer). The latter was introduced to play the role of the initiator in the grafting reaction, in the presence of the Cu(0)/CuBr<sub>2</sub>/PMDETA catalytic system. Since a few years, the use of copper metal has been particularly investigated because Cu(0) is easier to handle than Cu(I) or Cu(II) salts. If the mechanism of copper mediated polymerization is not fully understood and still under debates,<sup>7</sup> it offers a rather easy way to proceed and allows to decrease the amount of catalyst. Conditions in which the grafting step could be performed at room temperature, using high particle concentration in the presence of surfactant and initiator remaining from the emulsion polymerization were identified. The success of the functionalization and grafting steps was evaluated by ToF-SIMS (time-of-flight secondary ion mass spectrometry), by FTIR and by the final properties of the so-formed core-shell particles. It is the first time such grafting conditions have been applied with success from “real latexes”.

## References

- 1 Advincola, R. C.; Brittain, W. J.; Caster, K. C.; Rhe, J. (Eds.) *Polymer Brushes*, Wiley-VCH, Weinheim, Germany, **2004**
- 2 Charleux, B.; D’Agosto, F.; Delaittre, G. *Adv. Polym. Sci.* **2010**, 233, 125-183.
- 3 Manuszak-Guerrini, M.; Charleux, B.; and Vairon, J.P. *Macromol. Rapid Commun.* **2000**, 21, 669-674.
- 4 Kizhakkedathu, J.N.; Brooks, D.E. *Macromolecules* **2003**, 36, 591-598.
- 5 Zhang, M.; Liu L.; Wu C.; Fu G.; Zhao H.; He B. *Polymer* **2007**, 48, 1989-1997.
- 6 Mittal, V.; Matsko, N.B.; Butt, A.; Morbidelli, M. *Eur. Polym. J.* **2007**, 43, 4868-4881.
- 7 Zhang, Y.; Wang, Y.; Peng, C.H.; Zhong M.; Zhu, W.; Konkolewicz D.; Matyjaszewski, K. *Macromolecules* **2012**, 45, 78–86.

## Warwick 2012 - "The Polymer Conference"

### Poster Abstract

#### **Efficient metal-mediated surface-initiated polymerization from raw polymer latex in water.**

Virginie Chabrol, Didier Léonard, Matthias Zorn, Bernd Reck, Franck D'Agosto, Bernadette Charleux

The incorporation of a hydrophilic polymer shell at the surface of latex particles was studied using a grafting from approach based on aqueous copper-mediated radical polymerization. Latexes were synthesized via classical emulsion polymerization and functionalized at their surface with a Br-functional group which played the role of the initiator in the grafting reaction. Conditions under which the grafting could be performed at 25°C, using a real latex (no elimination of the surfactant and of the radical initiator), in the presence of  $\text{Cu}^0$ ,  $\text{CuBr}_2$  and PMDETA were identified.



[Home](#)[Account Info](#)[Help](#)ACS Publications  
High quality High impact.

**Title:** Transition Metal-Catalyzed Living Radical Polymerization: Toward Perfection in Catalysis and Precision Polymer Synthesis

Logged in as:  
Virginie CHABROL  
Account #:  
3000544287

**Author:** Makoto Ouchi et al.

[LOGOUT](#)

**Publication:** Chemical Reviews

**Publisher:** American Chemical Society

**Date:** Nov 1, 2009

Copyright © 2009, American Chemical Society

### PERMISSION/LICENSE IS GRANTED FOR YOUR ORDER AT NO CHARGE

This type of permission/license, instead of the standard Terms & Conditions, is sent to you because no fee is being charged for your order. Please note the following:

- Permission is granted for your request in both print and electronic formats, and translations.
- If figures and/or tables were requested, they may be adapted or used in part.
- Please print this page for your records and send a copy of it to your publisher/graduate school.
- Appropriate credit for the requested material should be given as follows: "Reprinted (adapted) with permission from (COMPLETE REFERENCE CITATION). Copyright (YEAR) American Chemical Society." Insert appropriate information in place of the capitalized words.
- One-time permission is granted only for the use specified in your request. No additional uses are granted (such as derivative works or other editions). For any other uses, please submit a new request.

[BACK](#)[CLOSE WINDOW](#)

Copyright © 2012 [Copyright Clearance Center, Inc.](#) All Rights Reserved. [Privacy statement.](#)  
Comments? We would like to hear from you. E-mail us at [customercare@copyright.com](mailto:customercare@copyright.com)



**RightsLink®**[Home](#)[Account Info](#)[Help](#)

**Title:** Understanding Atom Transfer Radical Polymerization: Effect of Ligand and Initiator Structures on the Equilibrium Constants

Logged in as:  
Virginie CHABROL  
Account #:  
3000544287

**Author:** Wei Tang et al.

[LOGOUT](#)

**Publication:** Journal of the American Chemical Society

**Publisher:** American Chemical Society

**Date:** Aug 1, 2008

Copyright © 2008, American Chemical Society

### PERMISSION/LICENSE IS GRANTED FOR YOUR ORDER AT NO CHARGE

This type of permission/license, instead of the standard Terms & Conditions, is sent to you because no fee is being charged for your order. Please note the following:

- Permission is granted for your request in both print and electronic formats, and translations.
- If figures and/or tables were requested, they may be adapted or used in part.
- Please print this page for your records and send a copy of it to your publisher/graduate school.
- Appropriate credit for the requested material should be given as follows: "Reprinted (adapted) with permission from (COMPLETE REFERENCE CITATION). Copyright (YEAR) American Chemical Society." Insert appropriate information in place of the capitalized words.
- One-time permission is granted only for the use specified in your request. No additional uses are granted (such as derivative works or other editions). For any other uses, please submit a new request.

[BACK](#)[CLOSE WINDOW](#)

Copyright © 2012 [Copyright Clearance Center, Inc.](#) All Rights Reserved. [Privacy statement.](#)  
Comments? We would like to hear from you. E-mail us at [customercare@copyright.com](mailto:customercare@copyright.com)

[Home](#)[Account Info](#)[Help](#)**Title:**

Ab Initio Evaluation of the Thermodynamic and Electrochemical Properties of Alkyl Halides and Radicals and Their Mechanistic Implications for Atom Transfer Radical Polymerization

Logged in as:

Virginie CHABROL

Account #:

3000544287

[LOGOUT](#)**Author:**

Ching Yeh Lin et al.

**Publication:**

Journal of the American Chemical Society

**Publisher:**

American Chemical Society

**Date:**

Sep 1, 2008

Copyright © 2008, American Chemical Society

### PERMISSION/LICENSE IS GRANTED FOR YOUR ORDER AT NO CHARGE

This type of permission/license, instead of the standard Terms & Conditions, is sent to you because no fee is being charged for your order. Please note the following:

- Permission is granted for your request in both print and electronic formats, and translations.
- If figures and/or tables were requested, they may be adapted or used in part.
- Please print this page for your records and send a copy of it to your publisher/graduate school.
- Appropriate credit for the requested material should be given as follows: "Reprinted (adapted) with permission from (COMPLETE REFERENCE CITATION). Copyright (YEAR) American Chemical Society." Insert appropriate information in place of the capitalized words.
- One-time permission is granted only for the use specified in your request. No additional uses are granted (such as derivative works or other editions). For any other uses, please submit a new request.

[BACK](#)[CLOSE WINDOW](#)

Copyright © 2012 [Copyright Clearance Center, Inc.](#) All Rights Reserved. [Privacy statement.](#)  
Comments? We would like to hear from you. E-mail us at [customercare@copyright.com](mailto:customercare@copyright.com)

[My Orders](#)[My Library](#)[My Profile](#)

Welcome virginie.chabrol@etu.univ-lyon1.fr

[Log out](#) | [Help](#)[Home](#) > [My Orders](#) > [View Your RightsLink Orders](#)

## License Details

This is a License Agreement between Virginie CHABROL ("You") and John Wiley and Sons ("John Wiley and Sons"). The license consists of your order details, the terms and conditions provided by John Wiley and Sons, and the [payment terms and conditions](#).

[Get the printable license.](#)

<a href="#">License Number</a>	2931970928121
<a href="#">License date</a>	Jun 18, 2012
<a href="#">Licensed content publisher</a>	John Wiley and Sons
<a href="#">Licensed content publication</a>	Journal of Polymer Science Part A: Polymer Chemistry
<a href="#">Licensed content title</a>	Environmentally benign atom transfer radical polymerization: Towards "green" processes and materials
<a href="#">Licensed content author</a>	Nicolay V. Tsarevsky, Krzysztof Matyjaszewski
<a href="#">Licensed content date</a>	Jul 28, 2006
<a href="#">Start page</a>	5098
<a href="#">End page</a>	5112
<a href="#">Type of use</a>	Dissertation/Thesis
<a href="#">Requestor type</a>	University/Academic
<a href="#">Format</a>	Print and electronic
<a href="#">Portion</a>	Figure/table
<a href="#">Number of figures/tables</a>	2
<a href="#">Original Wiley figure/table number(s)</a>	schema 2 figure 3
<a href="#">Will you be translating?</a>	No
<a href="#">Order reference number</a>	None
<b>Total</b>	<b>0.00 USD</b>

[← Back](#)

Copyright © 2012 [Copyright Clearance Center, Inc.](#) All Rights Reserved. [Privacy statement](#) . Comments? We would like to hear from you. E-mail us at [customercare@copyright.com](mailto:customercare@copyright.com)



# RightsLink®

[Home](#)[Account Info](#)[Help](#)

**Book:** Polyelectrolytes and Polyzwitterions

**Chapter:** Controlled Synthesis of Polymers with Ionic or Ionizable Groups Using Atom Transfer Radical Polymerization

**Author:** Tsarevsky Nicolay V., Matyjaszewski Krzysztof

**Publisher:** American Chemical Society

**Date:** Jul 6, 2006

Logged in as:  
Virginie CHABROL  
Account #:  
3000544287

[LOGOUT](#)

Copyright © 2006, American Chemical Society

## PERMISSION/LICENSE IS GRANTED FOR YOUR ORDER AT NO CHARGE

This type of permission/license, instead of the standard Terms & Conditions, is sent to you because no fee is being charged for your order. Please note the following:

- Permission is granted for your request in both print and electronic formats, and translations.
- If figures and/or tables were requested, they may be adapted or used in part.
- Please print this page for your records and send a copy of it to your publisher/graduate school.
- Appropriate credit for the requested material should be given as follows: "Reprinted (adapted) with permission from (COMPLETE REFERENCE CITATION). Copyright (YEAR) American Chemical Society." Insert appropriate information in place of the capitalized words.
- One-time permission is granted only for the use specified in your request. No additional uses are granted (such as derivative works or other editions). For any other uses, please submit a new request.

[BACK](#)[CLOSE WINDOW](#)

Copyright © 2012 [Copyright Clearance Center, Inc.](#) All Rights Reserved. [Privacy statement.](#)  
Comments? We would like to hear from you. E-mail us at [customercare@copyright.com](mailto:customercare@copyright.com)



# RightsLink®

[Home](#)[Account Info](#)[Help](#)

**Title:** Polymer Brushes via Surface-Initiated Controlled Radical Polymerization: Synthesis, Characterization, Properties, and Applications

Logged in as:  
Virginie CHABROL  
Account #:  
3000544287

[LOGOUT](#)

**Author:** Raphael Barbey et al.  
**Publication:** Chemical Reviews  
**Publisher:** American Chemical Society  
**Date:** Nov 1, 2009

Copyright © 2009, American Chemical Society

## PERMISSION/LICENSE IS GRANTED FOR YOUR ORDER AT NO CHARGE

This type of permission/license, instead of the standard Terms & Conditions, is sent to you because no fee is being charged for your order. Please note the following:

- Permission is granted for your request in both print and electronic formats, and translations.
- If figures and/or tables were requested, they may be adapted or used in part.
- Please print this page for your records and send a copy of it to your publisher/graduate school.
- Appropriate credit for the requested material should be given as follows: "Reprinted (adapted) with permission from (COMPLETE REFERENCE CITATION). Copyright (YEAR) American Chemical Society." Insert appropriate information in place of the capitalized words.
- One-time permission is granted only for the use specified in your request. No additional uses are granted (such as derivative works or other editions). For any other uses, please submit a new request.

[BACK](#)[CLOSE WINDOW](#)

Copyright © 2012 [Copyright Clearance Center, Inc.](#) All Rights Reserved. [Privacy statement.](#)  
Comments? We would like to hear from you. E-mail us at [customercare@copyright.com](mailto:customercare@copyright.com)

**RightsLink**®[Home](#)[Account Info](#)[Help](#)**ACS Publications**  
High quality. High impact.**Title:** Direct Molar Mass Determination of Self-Assembled Amphiphilic Block Copolymer Nanoobjects Using Electrospray-Charge Detection Mass SpectrometryLogged in as:  
Virginie CHABROL  
Account #:  
3000544287[LOGOUT](#)**Author:** Tristan Doussineau, Cong Yu Bao, Rodolphe Antoine, Philippe Dugourd, Wenjing Zhang, Franck D'Agosto, and Bernadette Charleux**Publication:** ACS Macro Letters**Publisher:** American Chemical Society**Date:** Mar 1, 2012

Copyright © 2012, American Chemical Society

**PERMISSION/LICENSE IS GRANTED FOR YOUR ORDER AT NO CHARGE**

This type of permission/license, instead of the standard Terms & Conditions, is sent to you because no fee is being charged for your order. Please note the following:

- Permission is granted for your request in both print and electronic formats, and translations.
- If figures and/or tables were requested, they may be adapted or used in part.
- Please print this page for your records and send a copy of it to your publisher/graduate school.
- Appropriate credit for the requested material should be given as follows: "Reprinted (adapted) with permission from (COMPLETE REFERENCE CITATION). Copyright (YEAR) American Chemical Society." Insert appropriate information in place of the capitalized words.
- One-time permission is granted only for the use specified in your request. No additional uses are granted (such as derivative works or other editions). For any other uses, please submit a new request.

[BACK](#)[CLOSE WINDOW](#)

Copyright © 2012 [Copyright Clearance Center, Inc.](#) All Rights Reserved. [Privacy statement.](#)  
Comments? We would like to hear from you. E-mail us at [customercare@copyright.com](mailto:customercare@copyright.com)









## **Functionalized latex particles as substrates for metal mediated radical polymerization**

*The incorporation of a hydrophilic polymer shell at the surface of latex particles was studied using a "grafting from" approach based on aqueous metal-mediated radical polymerization. Latexes were synthesized via classical emulsion polymerization and functionalized at their surface by a comonomer bearing a Br-functional group (the so-called inimer), which played the role of the initiator in the grafting reaction. Conditions under which the grafting could be performed at 25°C, using a real latex (no elimination of the surfactant and of the radical initiator), in the presence of CuBr<sub>2</sub>, N,N,N',N'',N''-pentamethyldiethylenetriamine (PMDETA) and zero valent metal, in particular Cu(0), were identified. The success of the functionalization and grafting steps was evaluated by ToF-SIMS (time-of-flight secondary ion mass spectrometry), by FT-IR and by the final properties of the so-formed core-shell particles.*

*Keyword: Grafting from, Core-shell particle, Emulsion polymerization, Metal mediated polymerization*

## **Greffage par polymérisation radicalaire par transfert d'atome d'une écorce hydrophile à la surface de particules de latex fonctionnalisées**

*Le sujet de cette thèse consiste à incorporer une couronne de polymère hydrophile à la surface de particules de latex par amorçage et croissance en utilisant la polymérisation radicalaire contrôlée par transfert d'atome induite par les métaux. Les particules de latex, obtenues par polymérisation radicalaire en émulsion ont été fonctionnalisées avec un « inimère », monomère comportant une fonction halogénée capable de jouer le rôle d'amorceur dans l'étape de greffage. Cette étape de greffage a ensuite été effectuée en présence de CuBr<sub>2</sub>, PMDETA et d'un métal à valence zéro tel que le cuivre, à température ambiante à partir de latex non post-purifiés (présence de tensio-actif et d'amorceur résiduels et à taux de solide élevés). Au cours du processus, l'incorporation de l'inimère et de la couronne hydrophile a été vérifiée par ToF-SIMS (time-of-flight secondary ion mass spectrometry), par FTIR et par l'étude des propriétés colloïdales des latex greffés.*

*Mots Clés : Greffage à partir de, Particule cœur-écorce, polymérisation en émulsion, Polymérisation radicalaire par transfert d'atome induite par les métaux*